Mechanistic Studies on Transition Metal Complex Catalysed Homogeneous Hydrogenation.

A thesis submitted to the

Board of the Faculty of Physical Sciences

in partial fulfilment of the

requirements for the degree of

Doctor of Philosophy

of the

University of Oxford

by

Uma Devi Sharma

St. John's College

Oxford

Michaelmas Term

1996

RADCLIFFE SCIENCE LIBRARY OXFORD
DEPOSITED
17 MAR 1997
THESIS

Aslib Abstract

Mechanistic Studies on Transition Metal Complex Catalysed Homogeneous Hydrogenation

Uma Devi Sharma

St. John's College

D. Phil

Michaelmas 1996

The development of systems capable of catalysing the reduction of unsaturated bonds with very high selectivities is one of the greatest successes of asymmetric catalysis. The mechanism by which rhodium complexes catalyse alkene hydrogenation has been effectively established through a combination of kinetic studies and isolation and characterisation of the intermediates in solution. It was hoped to elucidate the corresponding ruthenium catalysed mechanism using similar techniques.

Following the synthesis of a selection of ruthenium catalysts, their activity towards the reduction of a selection of dehydroamino acid derivatives at ambient temperature and pressure was investigated. Having successfully tested out the activity of these catalysts, NMR studies were initiated in order to observe and characterise intermediates in the catalytic cycle.

Considerable effort was put into the NMR studies, the systems were looked at under both argon and hydrogen, but although some substrate containing species were observed, it was found to be effectively impossible to break into the catalytic cycle and observe intermediate species using NMR techniques. Electrospray mass spectrometry investigations yielded more successful results, though still no hydrogen containing intermediates were observed.

However, it was possible to make a detailed kinetic study of several ruthenium catalyst / substrate systems by looking at the dependence of reaction rate on classic variables such as hydrogen pressure, catalyst concentration and substrate concentration. The combined results of electrospray experiments, kinetic analyses and kinetic modelling using computer packages enabled a possible mechanistic pathway to be proposed.

Acknowledgements

I would like to thank:

St. John's College, Oxford for generously providing financial assistance which enabled me to come back to Oxford and participate in the end-of-DPhil talks.

The DP staff.

Dr George Fleet for his friendship, guidance and advice over the last seven years.

Dr Luet Wong for his friendship and advice over the last six years and for Friday dinner hours last year.

My friends and colleagues.

My family and the cats.

Abbreviations

Acac	acetylacetonato
Ac	acetyl
^{o}An	2- methoxyphenyl
Ar	aryl
BINAP	(R)-2,2'-bis(diphenylphosphino)-1,1'-binaphthyl
^{t}Bu	*tertiary* butyl
C	celcius
COD	1,5-cyclooctadiene
CHIRAPHOS	(2R,3R)-bis-(diphenylphosphino)butane
DAST	diethylaminosulphur trifluoride
DIPAMP	(S,S)-1,2-bis-(*ortho*anisylphenylphosphino)ethane
DIPHOS	1,2-bis-(diphenylphosphino)ethane
DPPF	1,1'-bis(diphenylphosphino)ferrocene
DUPHOS	1,2-bis((2R,5R)-2,5-dimethylphospholano)benzene
DMA	N,N-dimethylacetamide
Et	ethyl
ee	enantiomeric excess
g	grammes

GIT	gear iterator
h	hours
Hz	hertz
IR	infra - red
mac	Z-Methyl-2-acetylamino-3-phenylpropenoate
Me	methyl
min	minutes
ml	millilitres
mmol	millimoles
m.p.	melting point
NBD	bicyclo[2.2.1]hepta-2,5-diene
NMR	nuclear magnetic resonance
NOE	nuclear Overhauser effect
OXPAMP	(S)-(2-methoxyphenyl)-P-phenyl-P-(2'-diphenylphosphino) ethylphosphine
PROPAPHOS	(R)-1,2-bis-(diphenylphosphino)propane
PROPHOS	(R)-1,2-bis-(diphenylphosphino)propane
Ph	phenyl
ppm	parts per million
t.l.c.	thin layer chromatography

Contents

	Page
Introduction	
Rhodium Chemistry	1
Ruthenium Chemistry	16
Directed Hydrogenation	27
Project Aims	28
Results and Discussion	
Rhodium Chemistry	30
Binding constants from NMR studies, analysis of kinetic data and further investigations of methyl-2-acetamido acrylate	31
A comparison, using NMR techniques, of substrate binding to Rh(DIPAMP)(NBD)TfO and Rh(OXPAMP)(NBD)TfO	49
Attempts to observe the dihydride intermediate	57
Investigations into the rhodium complex catalysed reduction of carbonyl compounds	66
Ruthenium Chemistry	69
Catalyst Syntheses	70
Preliminary investigations into the catalytic activity of the ruthenium complexes towards the reduction of simple dehydroamino acid derivatives	80
Binding Studies	86

Modifications to Heiser's Catalyst 95

RU(DPPF)(allyl)(acac) 104

Kinetics 115

Directed Hydrogenation 132

Experimental 134

References 167

Appendix 1 172

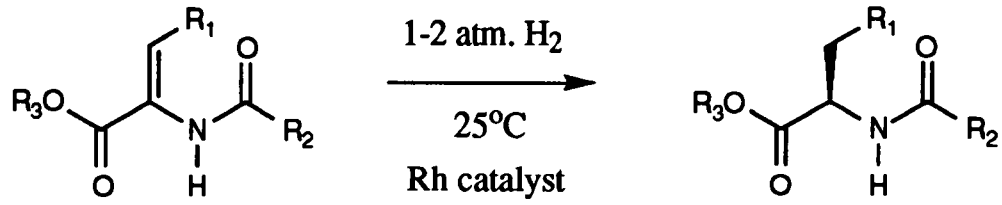
Appendix 2 173

Introduction

Rhodium chemistry

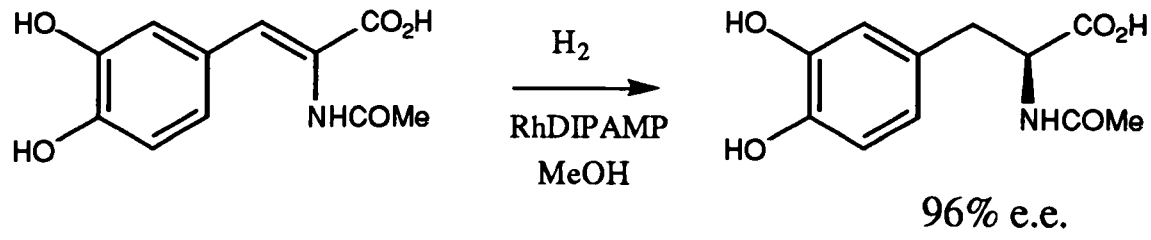
One of the most impressive achievements in organotransition metal chemistry to date is the development of highly selective asymmetric catalysts used for enantioselective epoxidation[1], dihydroxylation[2], alkene isomerisation[3] and alkene hydrogenation[4].

In 1968, Horner[5] and Knowles[6] discovered that prochiral olefins could be hydrogenated enantioselectively, under very mild conditions, using rhodium complexes of the Wilkinson catalyst type[7] containing optically active phosphine ligands (***Scheme 1***). Enzyme-like enantioselectivity and catalytic activity (enantioselectivities greater than 95% and limiting rates approaching 17 000 catalyst turnovers/s) can be achieved using such catalysts for the hydrogenation of dehydroamino acid derivatives (enamides).



Scheme 1: *the extraordinarily mild conditions and the ability to hydrogenate enamides with high enantioselectivity aroused great interest in homogeneous hydrogenation around the world*

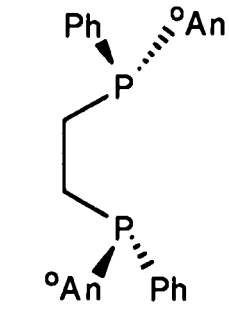
The industrial production of L-DOPA[8], a drug active against Parkinson's disease, is an example of the practical utility of this synthetic method (***Scheme II***).



Scheme II: *a breakthrough in using this chemistry came with the development of L-DOPA, active against Parkinson's disease, in the mid 1970's*

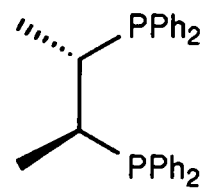
Enamides have established themselves as standard substrates for testing new ligand systems[9] and the ligands found to give the best results in enantioselectivity are chelating bisphosphines [9c,10,11], some of which are shown in ***Figure 1***.

The chiral centre can be the coordinating phosphorus atom (**1, 5, *Figure 1***) or, more commonly, a backbone carbon atom[9c,12] (**2, 3, *Figure 1***) and all successful ligands have two aromatic rings on each phosphorus atom. The majority of bisphosphines form five or seven membered chelate rings with rhodium[12], five membered chelates providing the greater number of highly selective catalytic systems[9c].



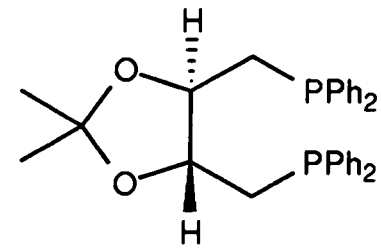
(R,R)-DIPAMP

1



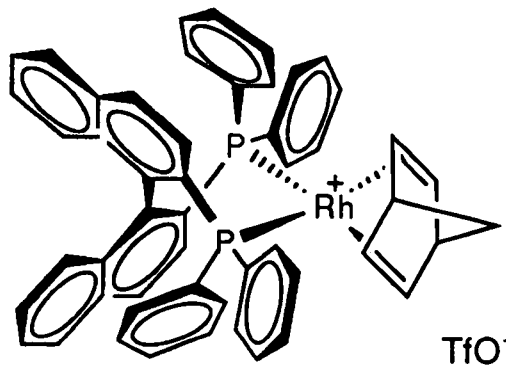
(S,S)-CHIRAPHOS

2

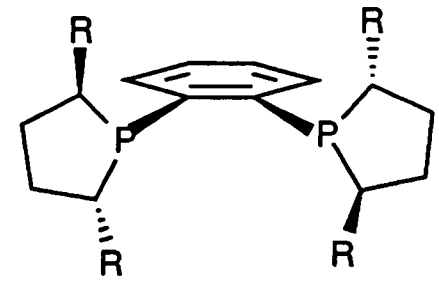


(R,R)-DIOP

3



4



DUPHOS

R = Me, Et, Pr, ^{i}Pr

5

Figure 1: *the highest enantioselectivities in rhodium catalysed homogeneous hydrogenation are obtained with chelating bisphosphines that form 5 or 7 membered rings*

It has been found that in moving from five to seven-membered chelates, the strength of binding of the enamide to the metal centre falls and the overall rate of hydrogenation increases[12]. One possible explanation for this is that the increasing flexibility associated with a bigger chelate ring size facilitates attainment of the favoured transition state geometries of the various reaction steps. However chelate rings with eight or more members seem too flexible for effective chirality transfer.

Five and seven-membered chelate rings are non-planar. A consequence of this is that the phenyl groups attached to the phosphorus atoms are either equatorial or axial; 'face-exposed' or 'edge-exposed'. Five membered chelates have an alternating edge-face-edge-

face array of arene rings attached to the phosphorus atoms[12] (**4, *Figure 1***). It is generally believed that this chiral array of phenyl rings serves as the chiral template that is responsible for the enantioface recognition and selection by the catalyst.

Investigations into substrate requirements for high enantioselectivities[10] found that the range of possible substrates that can be used is very small.

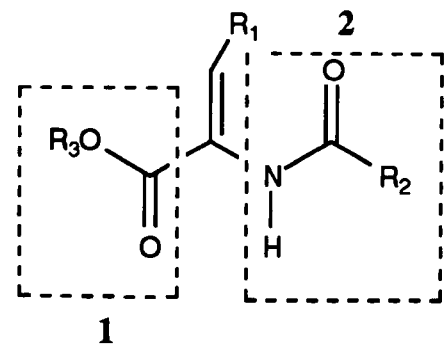


Figure 2: *although rhodium bisphosphine catalytic hydrogenation is one of the most elegant methods for synthesising chiral compounds in high optical yields, the variety of possible olefins is very limited*

Systematic studies have shown that R_1 (***Figure 2***) can be alkyl, aryl, or hydrogen; the vinylic hydrogen cannot be substituted by any other group; functional group **1** must have electron withdrawing character[13] *eg* carboxylate, carbonyl, cyano and functional group **2** must possess a β–carbonyl substituent as, during complexation to rhodium, a chelate with both the alkene and carbonyl bound to the metal is formed[9b,10,14] (***Figure 3***).

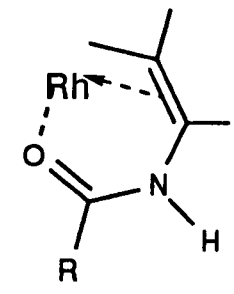
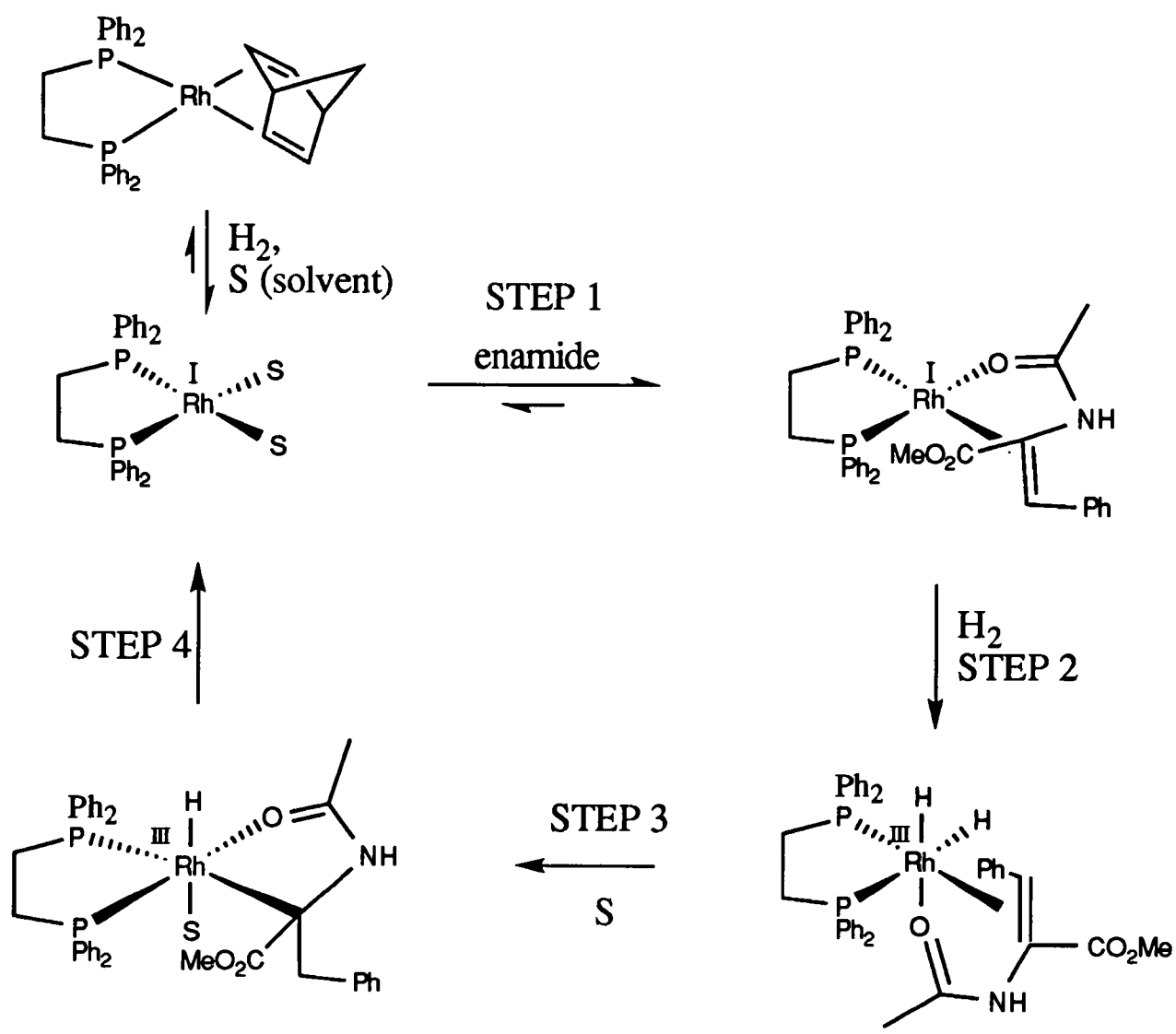


Figure 3: *the initially formed enamide complex is a chelate involving the alkene and carbonyl moieties of the enamide*

The Z isomer is hydrogenated faster and more selectively than its E counterpart[9b,10,14], though catalysts derived from the DUPHOS series of ligands (**5**, ***Figure 1***) can successfully hydrogenate both E and Z enamides[15]. In some of the best cases, the enantiomeric excess is close to 99%, the reaction is rapid at normal or slightly elevated

hydrogen pressures and the catalyst can frequently permit 10^3-10^5 turnovers before deactivation. E isomers bind weakly and isomerise to the Z isomer in the presence of catalyst[15].

The accepted reaction mechanism has been defined through careful kinetics carried out by Halpern[16] and characterisation of reactive intermediates in solution using NMR techniques by Brown[17], most of the work being carried out using the chiral ligand DIPAMP (**1**, ***Figure 1***). The currently accepted pathway is shown in ***Scheme III***:



Scheme III*: extensive investigation into the mechanism of rhodium complex catalysed homogeneous hydrogenation has yielded the pathway above as the most favoured route*

Before the catalytic cycle begins, the diene coordinated to the rhodium becomes saturated on the uptake of hydrogen and is substituted by solvent molecules, producing the solvated complex[12,18]. For the achiral case (using *eg* DIPHOS -bis(1,2 diphenylphosphino)ethane- as the ligand) the mechanism can be divided into four steps:

Step 1: Formation of an enamide complex.

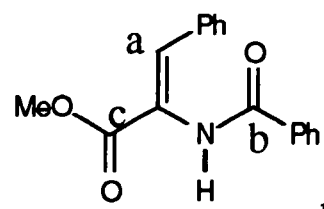
Step 2: Oxidative addition of hydrogen.

Step 3: Hydrogen transfer to an sp^2 carbon atom, leading to an alkylrhodium intermediate.

Step 4: Reductive elimination of the amino acid derivative.

For the enantioselective variant, where a chiral catalyst is used, each intermediate in the mechanistic cycle is present in two diastereomeric forms. The stereochemistry of the product is determined by the primary complexation of the substrate to the catalyst but the extent of the enantioselectivity is determined by the oxidative addition of hydrogen, as discussed below[16,19,20]. Various experiments have been carried out to verify the existence of postulated intermediates in the mechanism:

Step 1: NMR (^{31}P, ^{13}C, ^{1}H) and X-Ray analysis of [Rh(MAC)DIPHOS]BF_4 (MAC=Z-methyl-2-acetylamino-3-phenylpropenoate) showed that coordination to rhodium occurs through the carbonyl and alkene (η^2)[9b,21]. Brown[9b] obtained ^{13}C NMR spectra of isotopically enriched enamide complexes (***Figure 4***) using catalysts containing the ligands DIPHOS and DIPAMP. A change in the chemical shift of a moiety compared with its chemical shift in the free enamide was indicative of that moiety being bound to the metal centre. Both the amide and alkene labelled carbons displayed a change in chemical shift, but the carboxyl carbonyl was essentially unshifted.



^{13}C label at a, b or c

Figure 4: *changes in the chemical shift of ^{13}C labelled enamides points towards the shifted carbon being involved in the complexation to rhodium*

One DIPAMP enamide complex (***Figure 5***) has also been characterised crystallographically[22].

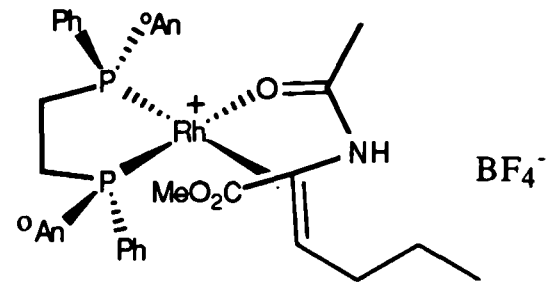
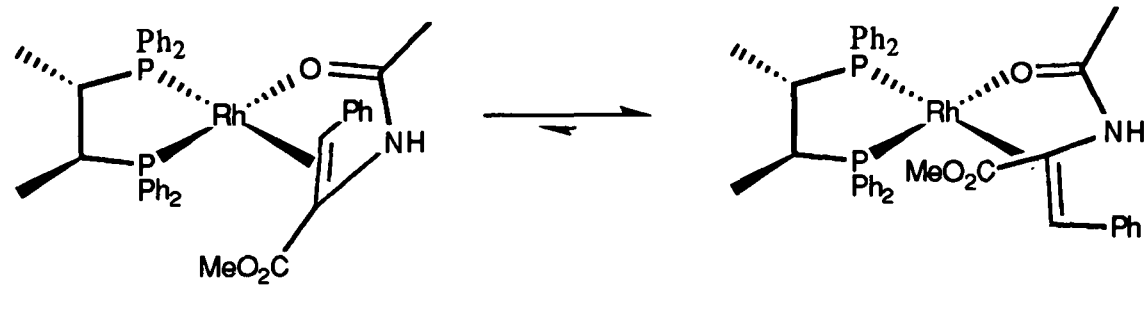


Figure 5: *X-Ray crystal structures give an indication of the solution structure of intermediates in the catalytic cycle*

DANTE magnetisation transfer techniques[17] demonstrated that the enamide complex is in rapid equilibrium with the methanol solvate complex and, for the chiral case, both major and minor diastereomers are in rapid equilibrium with one another on the timescale of hydrogen addition (***Scheme IV***).



Scheme IV*: two diastereomeric intermediates are formed between an enamide and a chiral catalyst with C2 symmetry. One is more favoured on considering steric interactions between the ester and aryl rings on the phosphorus*

Molecular mechanics show the major diastereomer to be favoured on steric grounds, considering interactions between the carboxylate group and one of the phosphorus aryl substituents, but this modelling does not include solvent or entropic considerations. Recent work[23] using ^{103}Rh NMR chemical shift values demonstrates an electronic difference between the diastereomers which might account for their relative stabilities.

Von Phillipsborn's NMR work[24], using the system below (***Figure 6***), gives evidence (in support of Brown's DANTE work[17]) that diastereomeric interconversion occurs *via* both inter- and intramolecular ligand exchange processes and not exclusively by complete dissociation of the substrate followed by readdition to the opposite enantiotopic olefin

face. The primary step for both processes is rate determining dissociation of the olefin end of the enamide. This can then be followed by:

1) reattachment

2) rotation of the olefin moiety and reattachment, thus leading to the other diastereomer

3) complete dissociation (the observation of solvent effects on both rates and enantioselectivities means that solvent participation might occur).

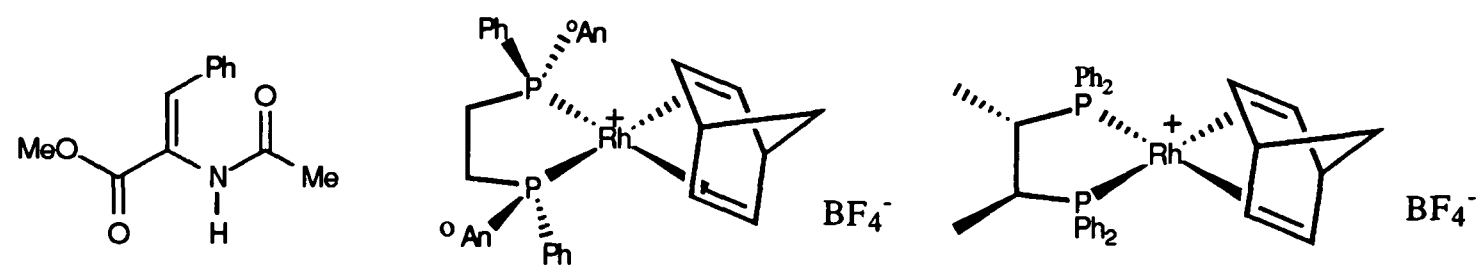


Figure 6: *using (^{31}P,^{31}P)-{^{1}H} 2D EXSY NMR techniques for various mixing times, von Phillipsborn was able to observe diastereomeric interconversion for the enamide complexes formed from the system above*

Studies using DIPAMP as the ligand (chosen because both diastereomers can be observed and thus both diastereomeric pathways can be monitored) show that it is actually the minor diastereomer which reacts faster with hydrogen and leads to the predominant hydrogenated isomer[10]. Cooling the solutions to about -35°C freezes out the interconversion of the diastereomeric adducts such that their reaction with hydrogen can be separately and directly observed. Molecular mechanics have explained this in terms of steric interactions; on hydrogen addition, as the complex shifts from square planar towards octahedral coordination, steric interactions increase for the major diastereomer, but with the minor diastereomer the process occurs without substantial opposition. Thus, the minor diastereomer is more reactive towards the addition of hydrogen.

Von Phillipsborn's ^{103}Rh NMR shift work suggests the hydrogen addition step might be electronically controlled, however. For several enamides, *para* substituents on the phenyl ring attached to the alkene had marked effects on the rhodium chemical shift; electron donating substituents shielded the rhodium nucleus whilst electron withdrawing groups deshielded the rhodium. Changing the ester or amide substituents had little effect on the

rhodium chemical shift. Using various chiral catalysts, the major diastereomer was found to be more shielded than the minor *ie* there was a consistent electronic difference at rhodium between the diastereomers. By comparison with theories examining how ligand electronic factors control regio- and stereoselectivity of hydrogen addition to d^8 square planar complexes[30], it was decided that hydrogen addition parallel to the metal-oxygen bond (π donor ligand) would destabilise the five-coordinate transition state, whereas addition parallel to the metal-olefin bond (donor/acceptor ligand) would be favoured (***Figure 7***). Von Phillipsborn suggests the major diastereomer to be more shielded due to the enamide ligand acting as a better electron donor *via* both the olefin and amide moieties. Increased shielding of rhodium (as in the case of the major diastereomer) appears to indicate stronger bonding of the substrate, which renders the metal less reactive towards adding another ligand.

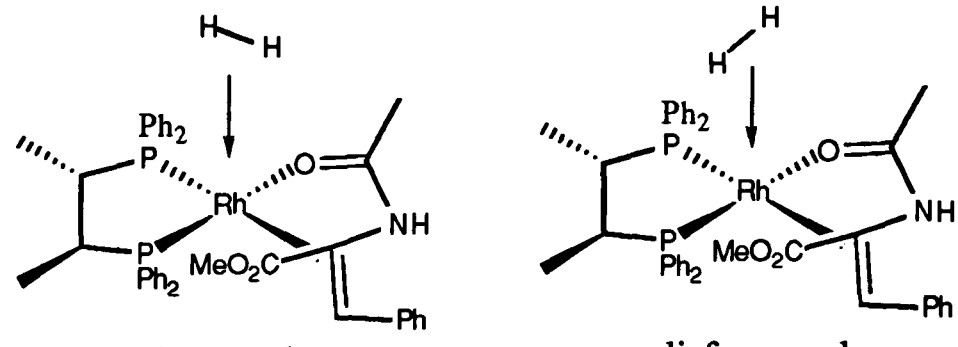


Figure 7: *hydrogen addition to an enamide complex would be expected to proceed more favourably if the hydrogen added parallel to the metal-olefin bond (donor/acceptor ligand)*

Taken together, molecular mechanics, NOE analyses of solution structures and X-Ray crystallography provide a very self-consistent set of structures for these intermediates.

Step 2: Under ambient conditions, oxidative addition of hydrogen is the turnover limiting step of the catalytic cycle. If this addition was reversible, then a *para* enriched hydrogen sample would equilibrate to a mixture of *para* and the thermodynamically favoured *ortho* forms of hydrogen on exposure to rhodium enamide complexes. Using DIPHOS and DIPAMP as the ligands on rhodium, Brown monitored any *ortho/para* equilibration during the addition of *para* enriched hydrogen to enamides by laser Raman spectroscopy[25a]. No equilibration occurred until reduction was complete; the lack of

ortho/para hydrogen interconversion *during* hydrogenation indicates that hydrogen addition is irreversible (in contrast to Wilkinson's catalyst).

Other significant work using *para*hydrogen has been carried out by Eisenberg[25b] and is based on the fact that NMR signal enhancement of several orders of magnitude can be observed with *in situ* ^1H NMR if the two hydrogen atoms of *para*hydrogen are transferred into magnetically inequivalent positions with retention of their singlet spin correlation. This increase in NMR sensitivity has allowed the detection, for the first time, of several metal dihydride complexes (*eg* $Rh(H_2)(olefin)(PPh_3)_2Cl$) which were previously present at concentrations too low for detection by normal methods. It is also possible to obtain hydrogenation rate constants and Eisenberg's values for enamide reductions closely match those of Halpern's[16,25b].

The rapidity of the two subsequent steps under ambient conditions means that only the substrate bonding and oxidative addition steps need to be considered in describing the kinetics for the two diastereomeric pathways. Indeed, as described above, the enantioselectivity is not controlled by the relative stabilities of the diastereomers, but by the energy difference between the diastereomeric transition states for hydrogen addition. As the pressure of hydrogen increases or the temperature falls, the enantioselectivity is expected to fall, as a result of diminished conversion of the major into the minor diastereomer[16].

At higher pressures of hydrogen, the rate of hydrogen addition is increased. This is accompanied by a simultaneous relative decrease in diastereomeric interconversion and hence a fall in enantiomeric excess. The temperature dependence of enantioselectivity is a result of the dissociation of the major diastereomer having a larger enthalpy of activation than the value for the process of hydrogen addition. At lower temperatures, the diastereomeric interconversion is 'frozen' and the major diastereomer has a higher probability of reacting with hydrogen, leading to an increased production of the minor hydrogenation product.

The lowered enantiomeric excesses obtained at high hydrogen pressures can be offset by higher reaction temperatures[16]. Fortunately, the higher temperature has little influence on enantiomeric excess in the low pressure limit and leads to higher rates due to

i) an increase in the magnitude of all rate constants

ii) extending the low pressure limit, where reaction rate is first order with respect to hydrogen pressure, to higher pressures.

Formation of an intermediate dihydride seems highly likely by analogy with the well recognised oxidative addition reactions of hydrogen with other Rh^{I} and related d^{8} complexes (Ir^{II})[10]. The continued failure to intercept the dihydride apparently reflects its very rapid transfer to the alkyl hydride (Step 3). Such a dihydride would show substantial deviation from perfect octahedral symmetry and the potential energy of the system would increase on moving from four to six coordination (due to an increase in steric crowding). Recent work[26] casts doubt on the existence of a six-coordinate dihydride intermediate. In theory, four isomers could arise for each diastereomer on hydrogen addition, corresponding to addition from above and below the coordination plane; along the metal-olefin axis or along the metal-carbonyl axis (***Figure 8***). Previous (crude) molecular mechanics concluded that only one trajectory was viable on steric grounds. Landis claims[26] that his refined molecular mechanics show no real hindrance to hydrogen approach and that the energy difference between the isomers is sufficiently small to make the distinction between various hydrogen addition modes difficult. Thus, it is argued that the failure to observe dihydride intermediates cannot be attributed to unfavourable changes in steric energies.

Landis' molecular mechanics suggest metal dihydride complexes are *not* appropriate models for the transition state for oxidative addition of hydrogen and he suggests that non-classical metal hydride complexes might be possible candidates (these would not differ much in energy from the classical dihydrides, as shown by the existence of both types of hydride in closely related complexes)[27]. Another alternative is concerted H-H rupture and M-H, C-H bond formation.

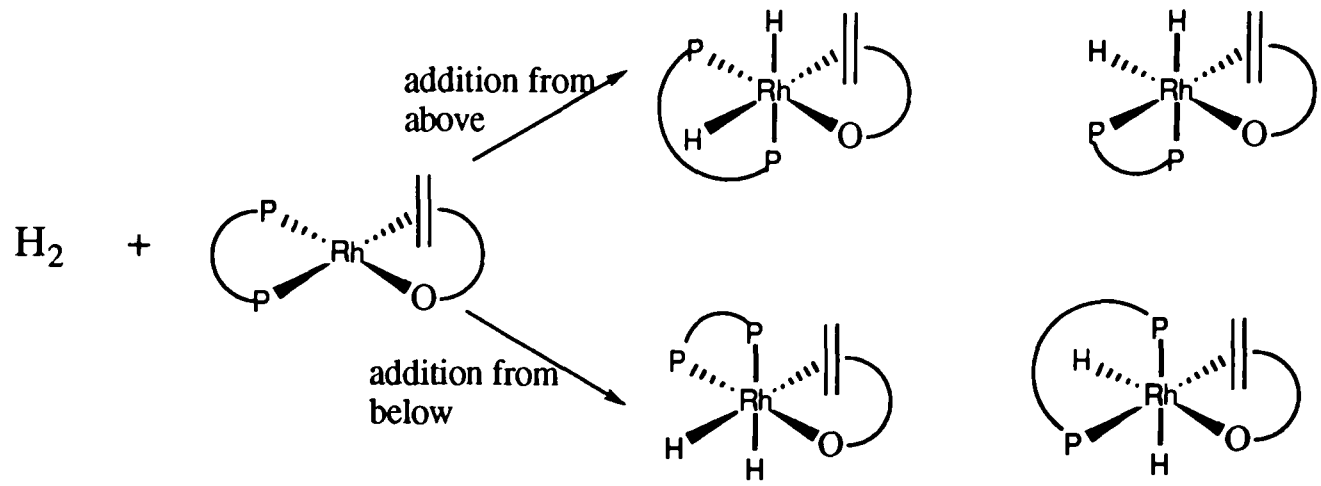


***Figure 8**: in theory four isomers can be formed by the cis additon of hydrogen to square planar rhodium enamide complexes*

Step 3: Transfer of a hydrogen atom to the alkene is irreversible and very fast, so there is no observable accumulation of the alkyl hydride intermediate under ambient conditions[20,21,28]. However, below -40°C, this step becomes rate determining due to its high activation energy and this allows the alkyl hydride to be intercepted and characterised[19,28]. The alkyl hydride shown below (***Figure 9***) exhibited a ^1H resonance at -20.9 ppm for the Rh-H proton (ddd, $J_{P_B\text{-}H}$=36 Hz, $J_{Rh\text{-}H}$=27 Hz, $J_{P_A\text{-}H}$= 14 Hz) at -78°C[28]. Further information on the structure of such intermediates has also been obtained from studies on more stable iridium analogues[29,30] (*eg* IrCl(CO)(DIPHOS)).

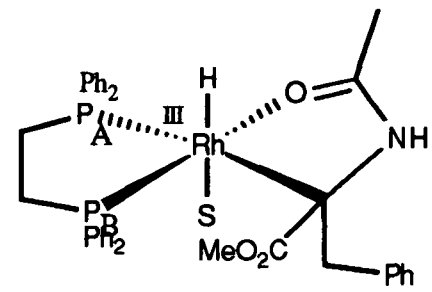


***Figure 9:** at low temperatures the concentration of alkyl hydride accumulates, allowing the interception and characterisation of this intermediate*

Tracer experiments using deuterium showed addition to be stereospecifically *cis*. These experiments, along with a lack of any isotopic scrambling, supported the irreversibility of this step. NMR spectral experiments using enamides containing 50% ^{13}C label at C_α showed hydrogen transfer on insertion to occur to the β–carbon of the alkene bond while the α–carbon becomes bonded to the rhodium[28]: ^{13}C NMR at -78°C showed labelled C_α to be coupled to both phosphorus atoms and rhodium ($J_{P_A\text{-}^{13}C}$=84 Hz, $J_{Rh\text{-}^{13}C}$=21 Hz, $J_{P_B\text{-}^{13}C}$=4 Hz).

Halpern also proved that only *one* solvent molecule was coordinated to the rhodium by carrying out a ^{31}P NMR monitored titration using MeCN - the change in the spectrum upon incremental additions of MeCN was noted[28]. It was found that exactly one equivalent of MeCN was required. Proof that MeCN was actually coordinated to rhodium was obtained by using $MeC^{13}N$. ^{1}H NMR showed a ^{15}N-H coupling (J= 29 Hz) whilst ^{31}P NMR showed an absence of any ^{31}P-^{15}N coupling, indicating that the nitrogen was not *trans* to a phosphorus atom *ie* the proton and nitrogen containing solvent were *trans* to each other.

Using the system in ***Figure 10***, the formation of the alkyl hydride was monitored by ^{31}P NMR at 220K. It was found that the alkyl hydride is formed at the expense of the minor diastereomer[19] - these peaks disappeared to be replaced by new peaks corresponding to alkyl hydride.

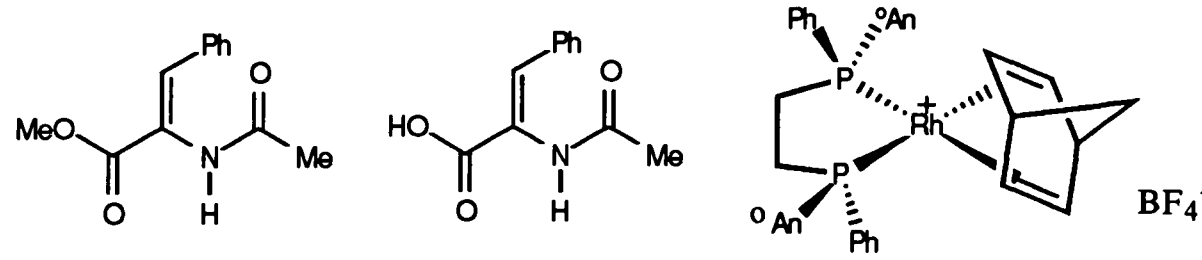


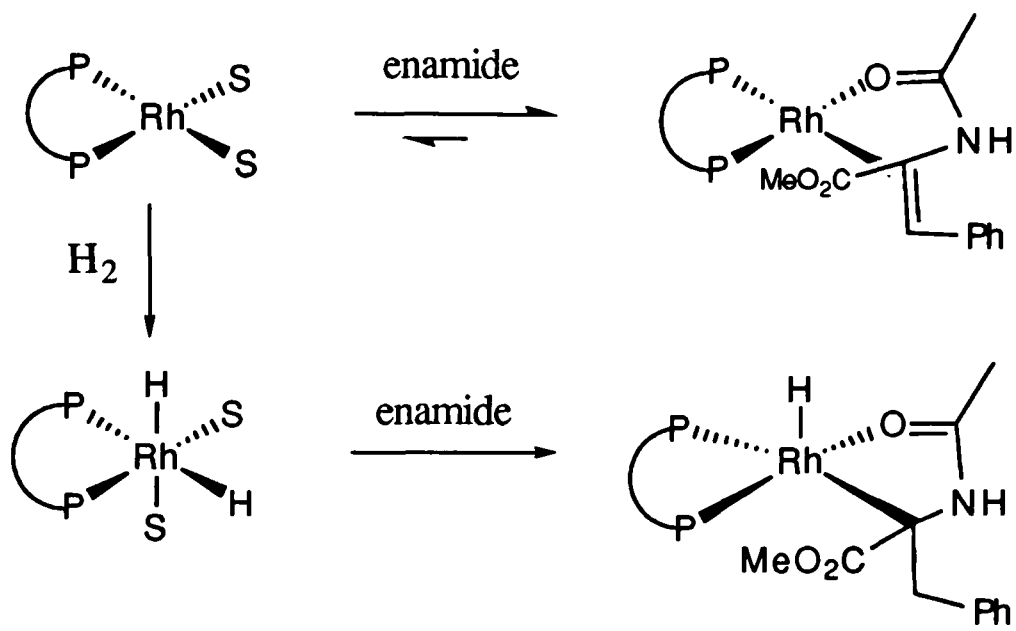
Figure 10: *at 220K the minor diastereomer for the above system is present to the extent of approximately 30% by ^{31}P NMR. When the system is exposed to hydrogen, it is the minor diastereomer which disappears to be replaced by alkyl hydride peaks*

Step 4: This step is rapid and irreversible. Its irreversibility follows from the lack of reactivity of the hydrogenated product.

The aim of the writer's Part II project[31] was to investigate the legitimacy of the accepted mechanism. Although there is substantial evidence for the structure of the enamide complex and for the addition of hydrogen being irreversible and *cis*, there is no proof that the order of steps 1 and 2 is correct.

A kinetically indistinguishable alternative would involve sequential addition of hydrogen and the enamide. This would require dissociation of the enamide complex which initially forms so that a dihydride could be created (***Scheme V***).

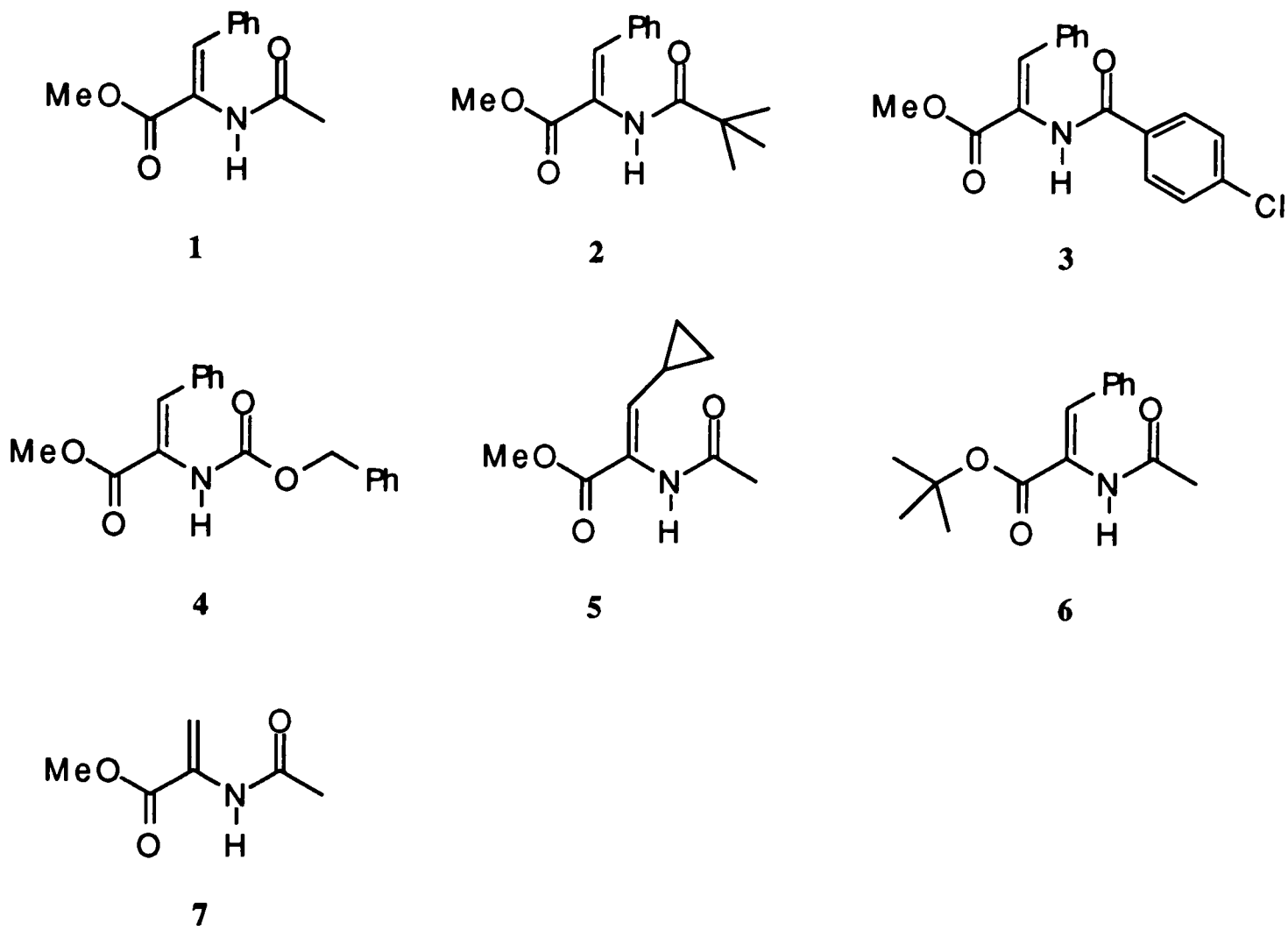
Intermediate situations could also exist; *eg* partial dissociation of the enamide complex could occur (as in the interconversion of diastereomeric enamide complexes) to obtain unsaturation at the metal centre, thus enabling hydrogen to add.



***Scheme V**: alternative mechanisms, with the same kinetic form, require the initially formed enamide complex to dissociate fully or partially to allow a dihydride to form*

Experiments were devised to distinguish between these pathways. The rates of hydrogenation of various enamide substrates were to be compared with the binding constants for formation of their enamide complexes. If the mechanism involved dissociation or partial dissociation of the enamide complex, as in the alternatives above, then substrates which bound more strongly to the metal would be expected to exhibit lower rates of hydrogenation, whereas if the accepted mechanism was correct, there would be no real correlation between the reaction rates and binding constants. As the enamides bind to the metal through their alkene and carboxamido groups, a range of enamides was synthesised with different substituents on and hence different basicities of the alkene and amide carbonyl double bonds (***Figure 11***).

The results obtained showed no correlation between reaction rates and binding constants. This was taken to mean that the enamide is already attached to the metal when hydrogen adds (reactions following a mechanism with Steps 1 and 2 reversed would be expected to show an inverse correlation between binding strengths and hydrogenation rates due to the need for the initially formed enamide complex to dissociate from the rhodium before hydrogen adds).



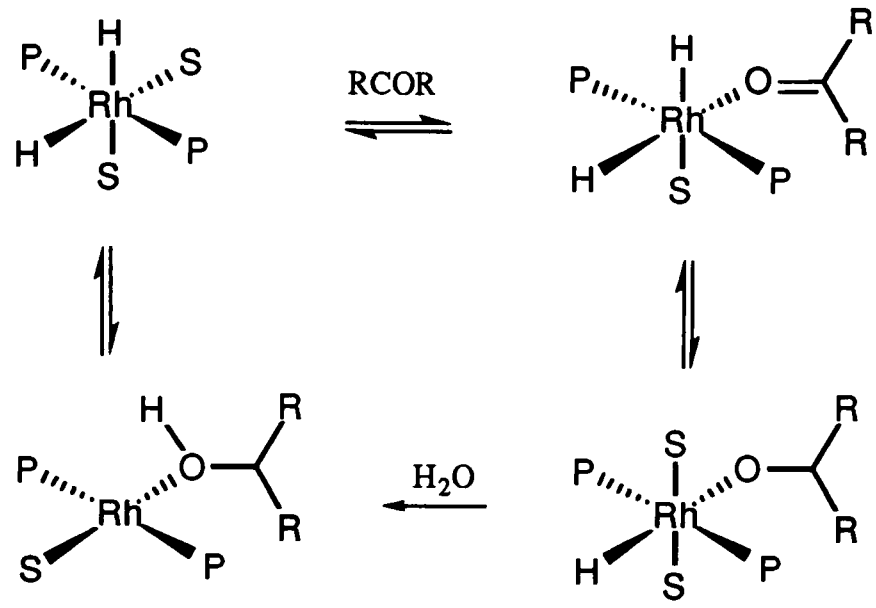
1 2 3 4 5 6 7

Figure 11: *changing the amide and alkene substituents alters the electron density associated with the moieties and hence the strength with which the enamides bind to the metal*

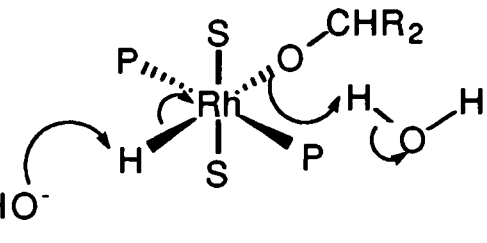
One of the enamides, methyl-2-acetamido acrylate (**7, *Figure 11***), appeared to be following a more complex mechanism than the other substrates. Its hydrogenation data indicated that it was weakly bound to rhodium, in contrast to the value of its binding constant obtained from ^{31}P NMR. Further investigations indicated apparent second order kinetics with respect to the enamide. The most probable mechanism corresponding to this rate law was thought to be one consisting of two competing pathways, one of which required a second molecule of enamide to dissociate one of the chelating phosphorus atoms from the metal. The existence of a second species in the reaction mixture was also in keeping with the ^{31}P NMR experiments which showed line broadening, indicating a dynamic system and the existence of two interchanging species.

The first reports of rhodium catalysed reduction of *ketones* were by Schrock and Osborn in 1970[32]. Their catalytically active species was $[Rh(PR_3)_3(MeOH)_2]^+$ and a promotion of the rate of reaction was observed on the addition of small quantities of water.

Deuterium studies and the facile reduction of ketones (such as acetophenone) lacking α hydrogen atoms indicated that the enol form did not play a significant role in the catalytic cycle. They proposed the following mechanism, ***Scheme VI.***



water and ROH could aid the final step in the following way:

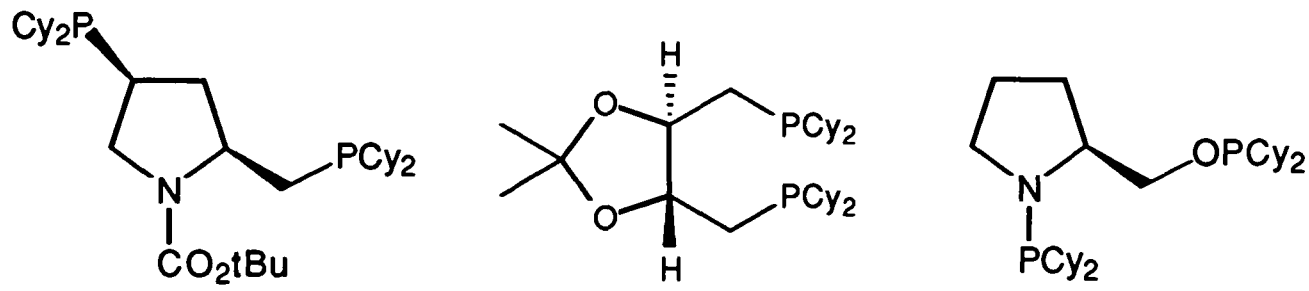


Scheme VI*: Schrock and Osborn's mechanism for ketone hydrogenation involved a stepwise hydride migration of the carbonyl followed by a proton transfer step, aided by water*

In general, catalysts employed for the reduction of olefins have been found to exhibit limited activity when used to hydrogenate ketones. The catalytic activity of rhodium (I) has been markedly improved by using electron donating, fully alkylated phosphines to increase the electron density at the metal centre. The more the electron density of rhodium is increased, the more the interaction with any substrate is enhanced by accelerating the oxidative addition and making coordination/chelation to the metal centre more rigid, resulting in high enantioselectivity.

Ligands such as those shown in ***Figure 12*** yield rhodium catalysts capable of reducing ketones (especially α dicarbonyl compounds) quickly and effectively under one

atmosphere of hydrogen[33]. The decarbonylation trend of rhodium (I) species is apparently suppressed by chelating diphosphines.



Cy = cyclohexyl

Figure 12: *alkylated phosphines are effective chiral auxiliary ligands for the asymmetric hydrogenation of prochiral ketones*

The mechanism of rhodium catalysed hydrogenation has not been investigated thoroughly. A starting point is to assume that the mechanism of asymmetric hydrogenation of olefins could also apply to that of ketones. As with olefins, two possible routes are favoured[34a]. The hydride route involves oxidative addition of hydrogen followed by substrate coordination and subsequent intramolecular hydride migration leading to the hydrido-alkoxo species. In the preferred ketone route, formation of a ketone complex is followed by oxidative addition of hydrogen (***Scheme VII***).

Tani isolated a ketoamide rhodium (I) complex at low temperature[34a] (as observed by ^{31}P NMR) and in the absence of any X-ray data, the intermediate was tentatively assigned the structure shown in ***Figure 13***. Others have since repeated this work[34b].

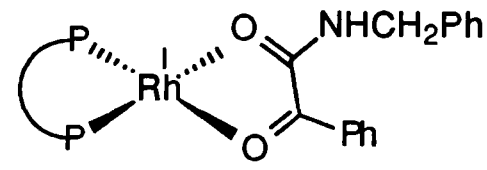
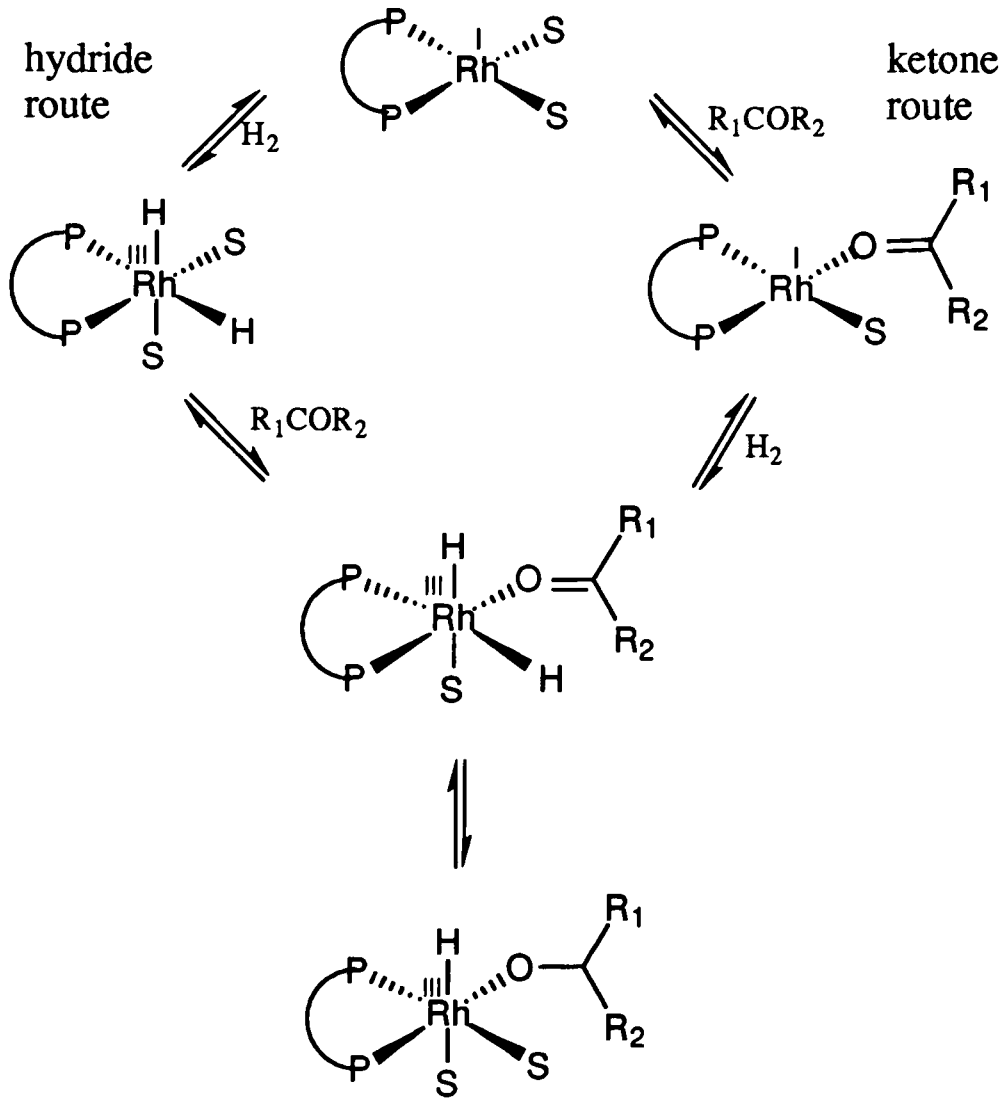


Figure 13: *the thermally unstable intermediate formed on the addition of diketones to activated rhodium catalysts is believed to have the above structure*

Ruthenium chemistry

Enantioselective hydrogenations using ruthenium catalysts were of marginal interest until the development of Noyori's atropisomerically chiral BINAP ligand (2,2-bis(diphenylphosphino)-1,1-binaphthyl) in the 1980's[35] (***Figure 14***).



***Scheme VII**: the reaction scheme for ketone reduction could proceed through two possible routes, of which the ketone route is the preferred pathway*

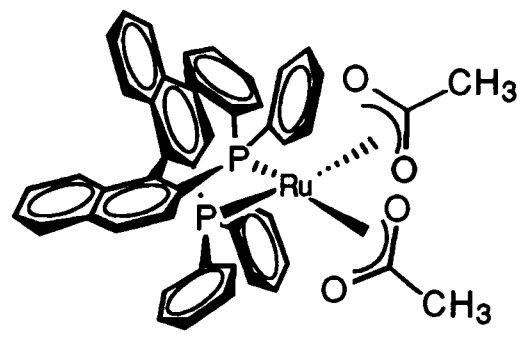


***Figure 14**: the monopolistic position of Rh(I) as a catalyst for asymmetric hydrogenation was challenged on the introduction of Ru BINAP catalysts. The versatility and enantioselectivity of ruthenium's applications now overshadows rhodium*

The drawback of ruthenium based catalysts is that they require high pressures and sometimes elevated temperatures; therefore their best field of application is where rhodium catalysts do not excel *eg* reduction of carbonyl compounds. Ruthenium catalysts are very effective for the reduction of ketones which bear a potential metal binding group, especially β-ketoesters (*vide infra*).

Ruthenium is generally inferior to rhodium for the asymmetric hydrogenation of dehydroamino acid derivatives; however it is capable of catalysing the reduction of a much wider range of functional alkenes lacking the acylamino moiety. A notable case is the reduction of more hindered alkenes[36], ***Figure 15***.

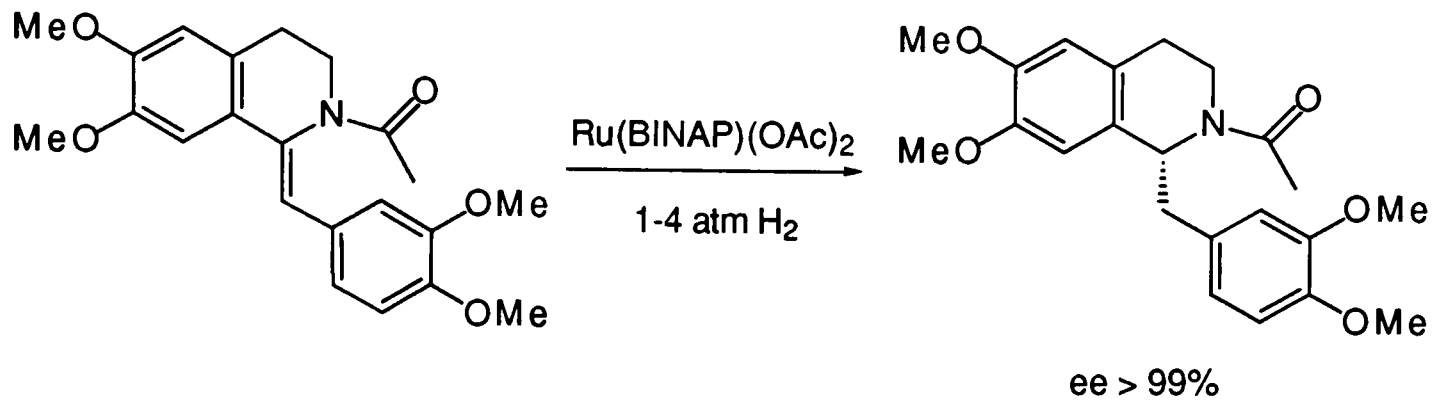


Figure 15: *1-benzylated tetrahydroisoquinolines are key intermediates for the synthesis of a variety of isoquinoline alkaloids; the development of an efficient asymmetric synthesis of such compounds is highly desirable. Note that the corresponding rhodium catalysed hydrogenation proceeds with a lower optical yield (≈ 75%).*

An examination of reductions of the same substrate using the same ligands on the metal centre (usually BINAP) allows a comparison of ruthenium and rhodium catalysed asymmetric hydrogenations. The following points emerge:

(i) For the hand of rhodium catalyst which, on reduction, yields the R product, the corresponding ruthenium catalyst gives the S enantiomer, often with greater optical efficiency.

(ii) For cases where rhodium complexes are ineffective, the configuration of the hydrogenated product from ruthenium catalysis cannot be related to the configuration of the reagent or catalyst; no general predictions can be made.

(iii) In rhodium catalysis, several ligands yield products in high enantiomeric excess. In ruthenium catalysed hydrogenation however, only BINAP and related bisphosphine ligands are highly effective. Four main types of ruthenium catalysts are used (***Figure 16***).

(iv) With ruthenium catalysed reductions, the configuration of the product for a series of related alkenes can depend on the substitution pattern about the double bond.

These points indicate a mechanistic divergence between the two metals.

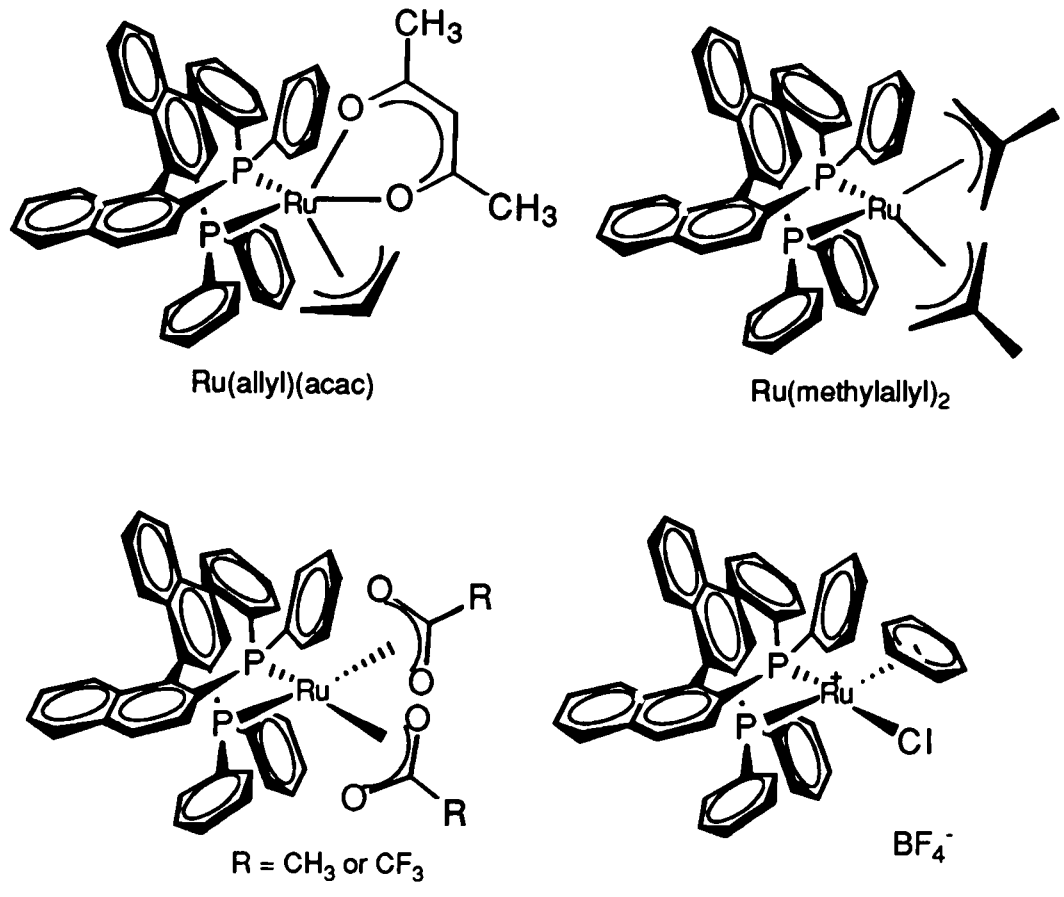
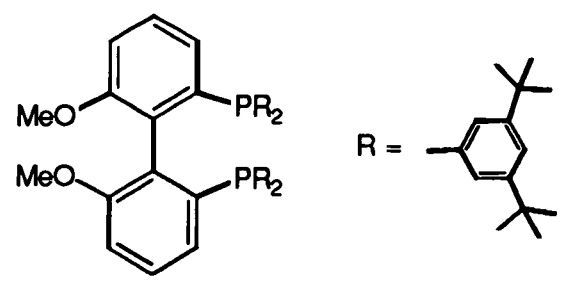


Figure 16: *most successful ruthenium catalysts employ BINAP and its analogues as the ligands on the metal*

Mechanistic detail on the ruthenium aided catalytic cycle is very sparse. Parallel investigations in the case of rhodium were aided by the fact that the resting state of the catalyst appears to contain an olefin bound to rhodium; thus the catalytic cycle and the interconversion of reaction intermediates could be followed by NMR. Much less is known about the nature of reactive intermediates in ruthenium chemistry, as the eighteen electron ruthenium diacetate complexes normally used do not appear to complex reversibly with olefins (*vide infra*). A stable hydrogen-containing solvate complex of composition [RuH(isopropanol)$_2$**1**]BF_4 (**1** as shown below) has been isolated as a red crystalline solid. Its structure has been determined by X-Ray diffraction and is best described as a distorted square pyramid[37a]. The relatively air stable complex is as effective as [Ru(OAc)$_2$**1**] towards pyrone hydrogenation and is consequently either an intermediate in the hydrogenation cycle, or it reacts to form an active species.



1

The most extensive mechanistic work to date has been carried out by Halpern[37] on tiglic acid (***Figure 17***). He obtained a rate law which indicated product inhibition and an inverse dependence of rate on initial substrate concentration:

$$k_{obs} = \frac{2k[Ru]_{tot}[H_2]}{[S]_o + [P]_o}$$

The following mechanism, involving heterolytic cleavage of hydrogen, was proposed (***Scheme VIII***). Entry to the catalytic cycle is effected by the rapid displacement of one acetate ligand in $Ru(BINAP)(OAc)_2$ by tiglic acid.

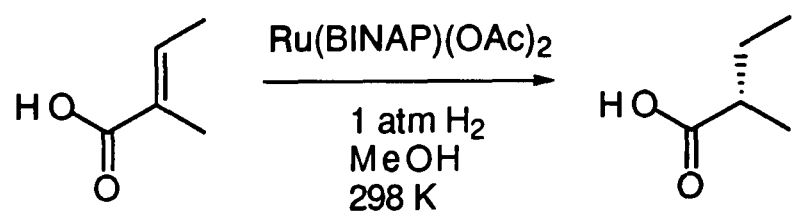


Figure 17: *investigations of the reduction of tiglic acid have led to a preliminary insight into the mechanism of ruthenium catalysed asymmetric hydrogenation*

NMR evidence points to one acetate group always being bound to the metal; no evidence was found to suggest the alkene bond is coordinated to the metal. Halpern concluded that 'if coordination of the alkene to ruthenium is, as generally believed, a prerequisite to insertion, then such coordination must occur *after* reaction with hydrogen.'

If the five membered alkylruthenium chelate is a true intermediate, deuteration should lead to the incorporation of one deuterium atom (β to the acid, ***Figure 18***) in the product, as the second deuterium atom would be pooled with exchangeable solvent protons. Experiments carried out on a variety of carboxylic acids support this result.

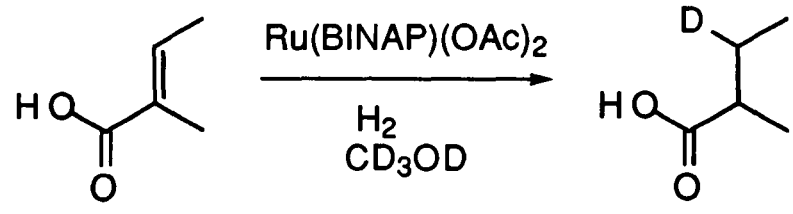
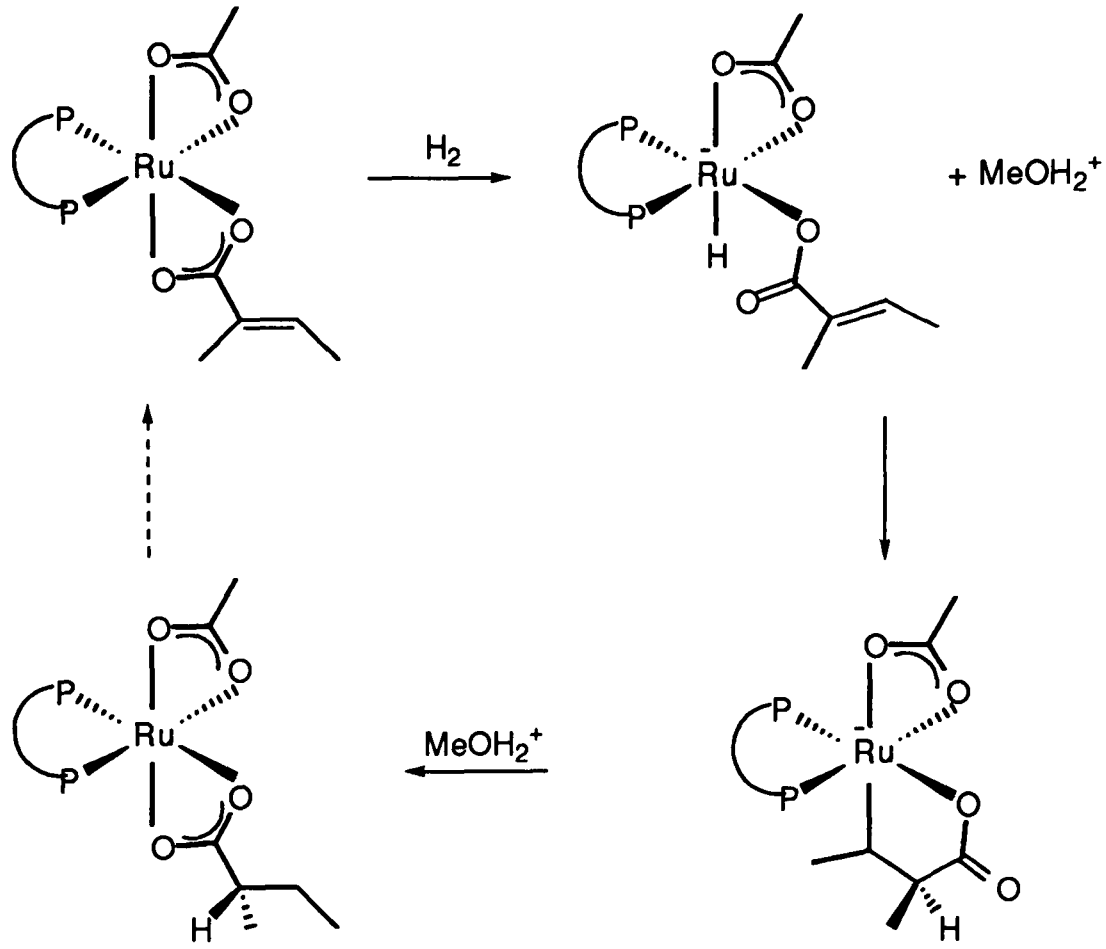


Figure 18: *the reduction above was carried out to investigate the position of deuterium incorporation into the product. Deuterium addition was found to be both regio- and stereoselective*

Results such as that in ***Figure 18*** show a lack of significant deuterium incorporation at the α position, rule out substantial hydrogen/deuterium exchange between hydrogen and the solvent prior to reaction with substrate and also imply that hydrogen/deuterium exchange between the ruthenium hydride intermediate and solvent, prior to insertion of the alkene bond, must be comparatively slow.



Scheme VIII: *Halpern's proposed mechanism for the reduction of tiglic acid involves heterolytic cleavage of hydrogen and does not show the alkene directly coordinated to ruthenium*

The alkylruthenium chelate complex is finally transformed into product by proton transfer to ruthenium, followed by RH elimination.

Halpern found that while the addition of strong base had no effect on the kinetics of the reaction (a process such as $RCO_2H + OH^- \rightarrow RCO_2^- + H_2O$ would be expected to occur), the addition of more than one equivalent of trifluoromethanesulphonic acid with respect to catalyst concentration completely suppressed hydrogenations. He suggests that the acid might protonate the catalyst to give rise to cationic species which apparently are not active catalysts for hydrogenations. Indeed, the addition of base reversed the inhibition by acid.

The stringency of the requirement for heterolytic hydrogen cleavage in Halpern's mechanism has recently been questioned[38]. Brown argues that identical results to those obtained in the deuterium labelling experiments would arise from an intermediate dihydride or dideuteride which transferred only one atom to the coordinated substrate. If the resultant alkyl hydride then had sufficient lifetime (and fast exchange rate) to allow essentially complete exchange of Ru-H with solvent O-H before elimination, the product would be regioselectively monodeuterated and the reaction would have followed a pathway avoiding heterolytic cleavage, in line with the rhodium mechanism. Evidence to support this proposal is found in the rhodium catalysed reduction of dehydroamino acids in water; the product is that of formal HD addition with exchange occurring at the rhodium alkyl hydride stage[39].

Brown analysed the deuterium content in the reduced products from ***Figure 19*** using both H_2/MeOD and D_2/MeOH systems[38]. A consistent pattern emerged with both hydrogen atoms undergoing isotopic exchange with the solvent to a similar extent. This implies that with Brown's catalyst the exchange process precedes any transfer of hydrogen to coordinated substrate. These results do not require heterolytic cleavage of hydrogen and therefore do *not* lend support to Halpern's ionic mechanism which, if general, should be neither substrate nor ligand specific.

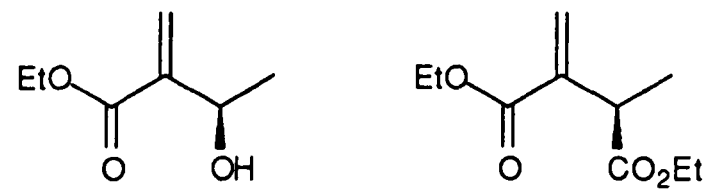


Figure 19: *reduction of the above alkenes was carried out under various conditions. The deuterium distribution in the products was analysed*

Noyori[40] has carried out deuterations which show that addition across the double bond occurs with *cis* stereochemistry, ***Figure 20***.

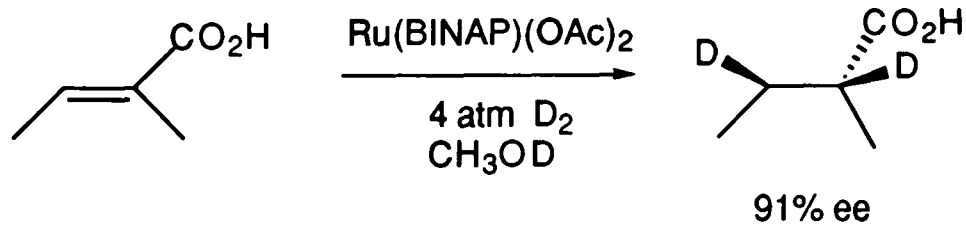


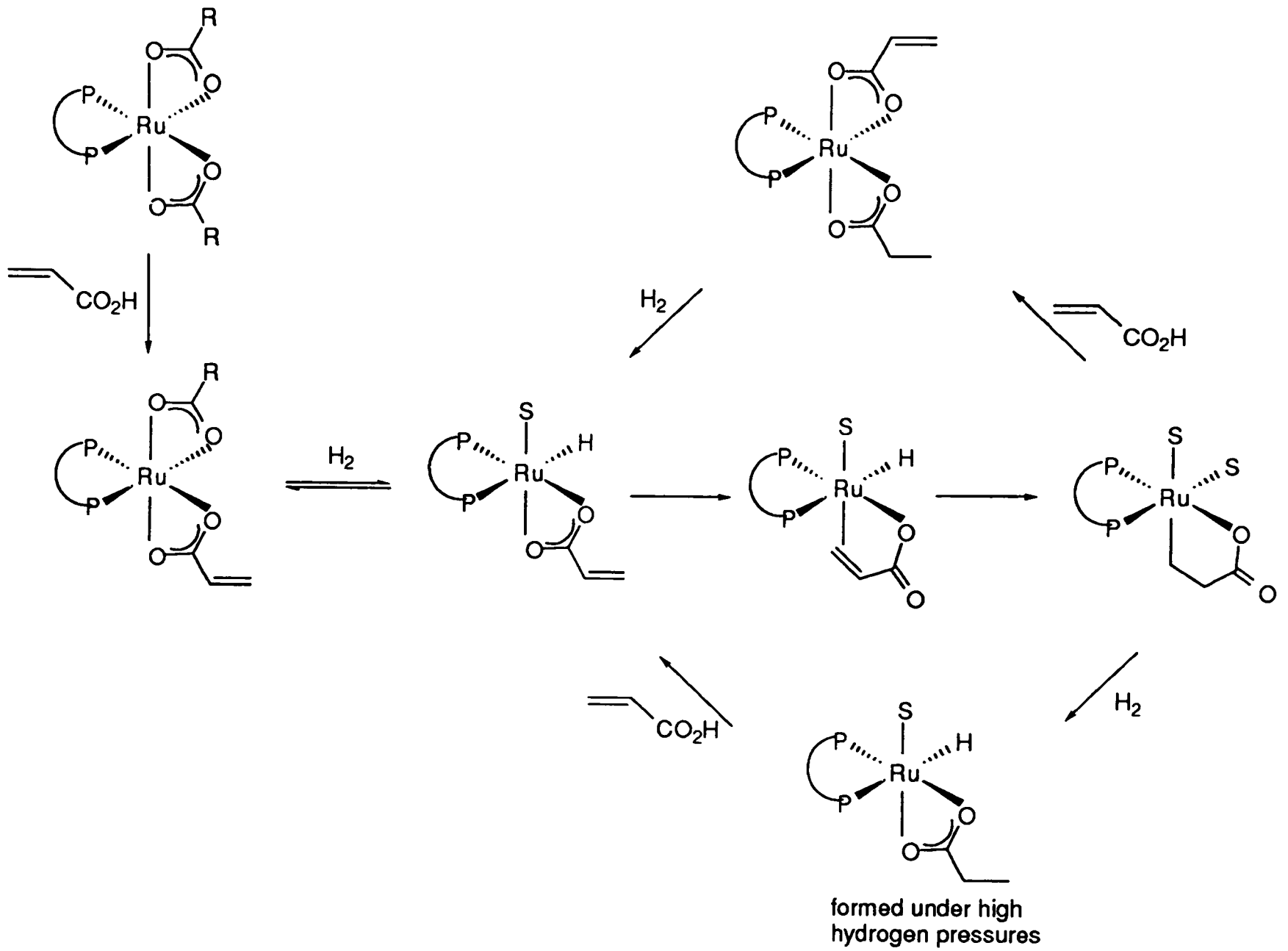
Figure 20: *examination of the stereochemistry of ruthenium catalysed hydrogenation indicates* cis *addition across the olefinic bond*

Examination of the reaction of various unsaturated carboxylic acids with deuterium in MeOH and with hydrogen in MeOD showed, in keeping with Halpern's results, hydrogens to be introduced at positions α to the carboxylic acids whilst protons from the solvent were incorporated β. As expected, increasing the hydrogen pressure increased the extent of incorporation of gaseous hydrogen at the β position.

These observations are in keeping with a mechanism involving monohydride complexes and five membered alkylruthenium chelates. Noyori proposes the mechanism below (***Scheme IX***) which involves the addition of two hydrogen atoms to the olefinic face in a *cis* fashion from different sources (hydrogen and solvent, or two different hydrogen molecules).

It is noteworthy that attempts to observe the formation of a ruthenium hydride species, by reacting $Ru(BINAP)(OAc)_2$ with hydrogen, failed.

Both Halpern and Noyori's mechanisms involve heterolytic hydrogen activation, leading to a non-pairwise addition of hydrogen to the substrates reduced. As with his rhodium work, Eisenberg has observed *para*hydrogen induced polarisation (PHIP) during the $Ru(BINAP)(OAc)_2$ catalysed reduction of a number of aprotic substrates such as arylacrylates[40b]. Since PHIP requires pairwise addition of hydrogen, its occurrence calls into question the applicability of the proposed mechanisms for all substrates. However, scrambling of hydrogen and deuterium is not promoted by $Ru(BINAP)(OAc)_2$ in CD_2Cl_2 exept in the presence of added acid; these results are consistent with a pairwise activation of hydrogen in aprotic media and heterolytic splitting of hydrogen in the presence of acid.



Scheme IX: *Noyori's proposed mechanism for the reduction of acrylic acids involves monohydride complexes and five membered alkyl rhodium chelates*

Ruthenium is superior to all other transition metals in its ability to catalyse the enantioselective hydrogenation of prochiral carbonyl compounds. Hardly any mechanistic work exists on this subject.

Simple ketones only yield products with high enantioselectivity when they contain a secondary binding group in proximity to the carbonyl, enabling the formation of a chelate involving the metal centre, ***Figure 21***. Unlike the case with olefins, all reductions of carbonyls follow a single stereochemical pattern and the configuration of the product can be related back to that of the catalyst[41].

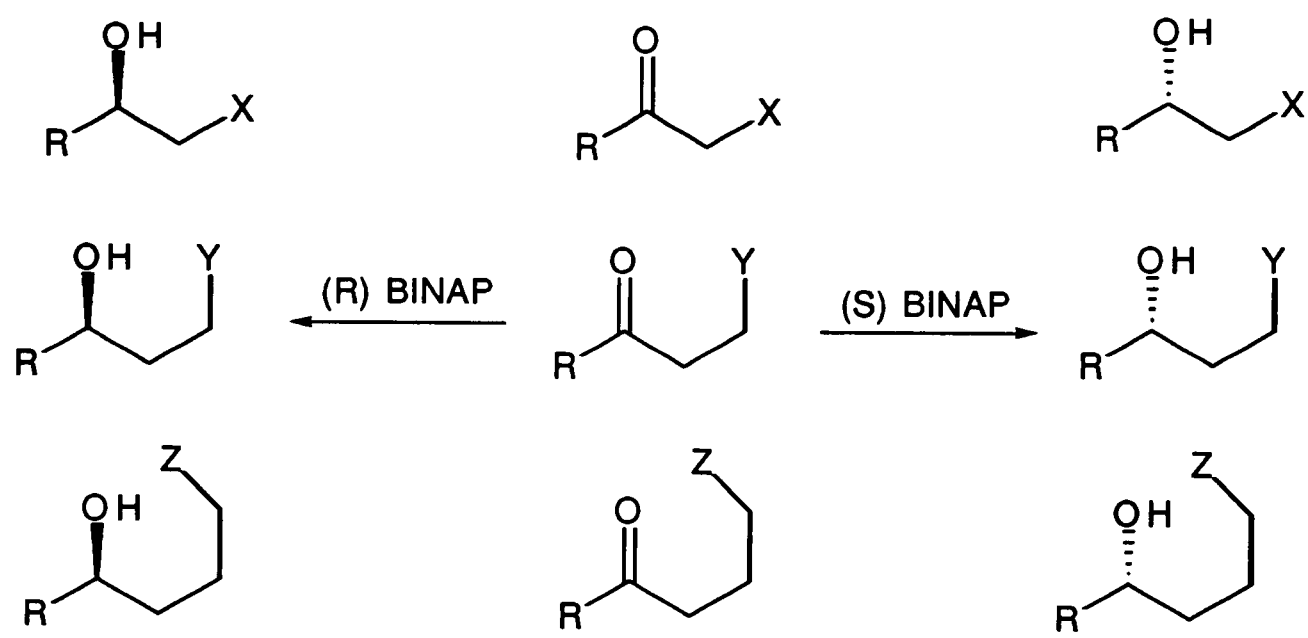


Figure 21: *functionalised ketones can be reduced using Ru(BINAP)(OAc)$_2$ or ruthenium halogen containing complexes. The key factor in the stereodifferentiation is the simultaneous coordination of the carbonyl oxygen and the heteroatom to ruthenium making a 5 to 7 membered chelate ring*

The best results are obtained using halogen containing catalysts of the type (BINAP)RuBr$_2$, presumably Br$^-$ is better displaced from ruthenium than AcO$^-$. Enantiomeric excesses approach 100% for the reduction of β ketoesters[42]. In the presence of trace amounts of strong acid, the asymmetric hydrogenation of β ketoesters (using [Ru(BINAP)Cl$_2$]$_2$NEt$_3$) has been found to proceed at low temperatures and readily attainable pressures (40°C, 30 psi H$_2$)[43]. The effect of acid is reversed on the addition of triethylamine.

Noyori has recently been able to effectively hydrogenate simple aromatic ketones lacking any heteroatom to anchor the ruthenium metal[44]. Impressive turnover frequencies

(defined as the number of moles of product per mol catalyst per hour) have been obtained using a $RuCl_2(BINAP)(dmf)_n$ / diamine / KOH / ^iPrOH system. Interestingly, β ketoesters themselves are inert under these reaction conditions.

Two very useful aspects of ruthenium catalysed carbonyl reduction are dynamic kinetic resolution and double asymmetric induction. Kinetic resolution is a process in which one of the enantiomeric constituents of a racemate is more readily transformed into a product than is the other. In ordinary kinetic resolution the maximum yield of one enantiomer is 50% and the enantiomeric excess is affected by the extent of the conversion.

In dynamic kinetic resolution a racemate can be converted to one major stereoisomer, hence the chemical yield may be 100% and the enantiomeric excess is independent of conversion, ***Figure 22***.

The ruthenium BINAP catalysed hydrogenation of certain optically labile α substituted β ketoesters proceeds with dynamic kinetic resolution to afford one of the four possible stereoisomeric hydoxy esters in > 90% yield[45]. Three conditions must be satisfied for this to occur:

(i) racemisation of the ketoester substituent must be sufficiently faster than hydrogenation

(ii) facial discrimination by the chiral catalyst must be excellent

(iii) the structure of functional groups of substituents must allow for a clear distinction between the stabilities of *syn* and *anti* transition states in the stereodetermining step. (The chirality of the BINAP ligand controls the facial selectivity at the carbonyl function, whereas constraints in the substituents determine the relative reactivities of the enantiomers)

Thus, in theory, a racemic starting material can be converted in 100% yield to a single chiral product possessing stereodefined *vicinal* asymmetric centres.

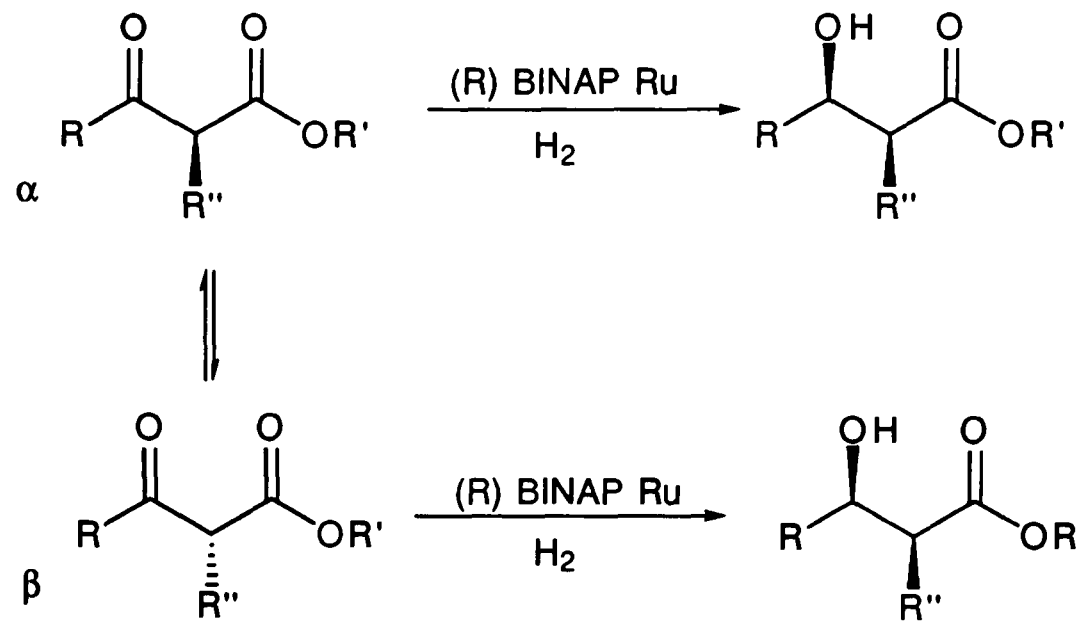


Figure 22: *if the rate of racemisation between α and β is rapid with respect to the rate of hydrogenation, then when the rates of reaction of α and β with hydrogen are substantially different, hydrogenation will form* one *isomer selectively from the four possible stereoisomeric hydroxy esters*

Double asymmetic induction is aided by intramolecular chirality transfer, ***Figure 23***. The stereogenic centre installed in the ketone in ***Figure 23*** causes a unique asymmetric induction such that the ratio of (R,R) to *meso* (R,S) in the final product diol is 99:1[46]. Most of the minor (S) enantiomer produced in the first step (0.75%) is removed by conversion to the *meso* diol. Double asymmetric induction allows facile access to key components of pepstatin and its analogues, potent aspartic proteinase inhibitors.

Directed Hydrogenation

Stereoselectivity can be achieved through *substrate* control in cases where a polar functional group (usually OH but also, in the case of rhodium, CO_2R, NHCOR and SOR) is present at a stereogenic centre α to an electron deficient double bond[4], ***Figure 24***.

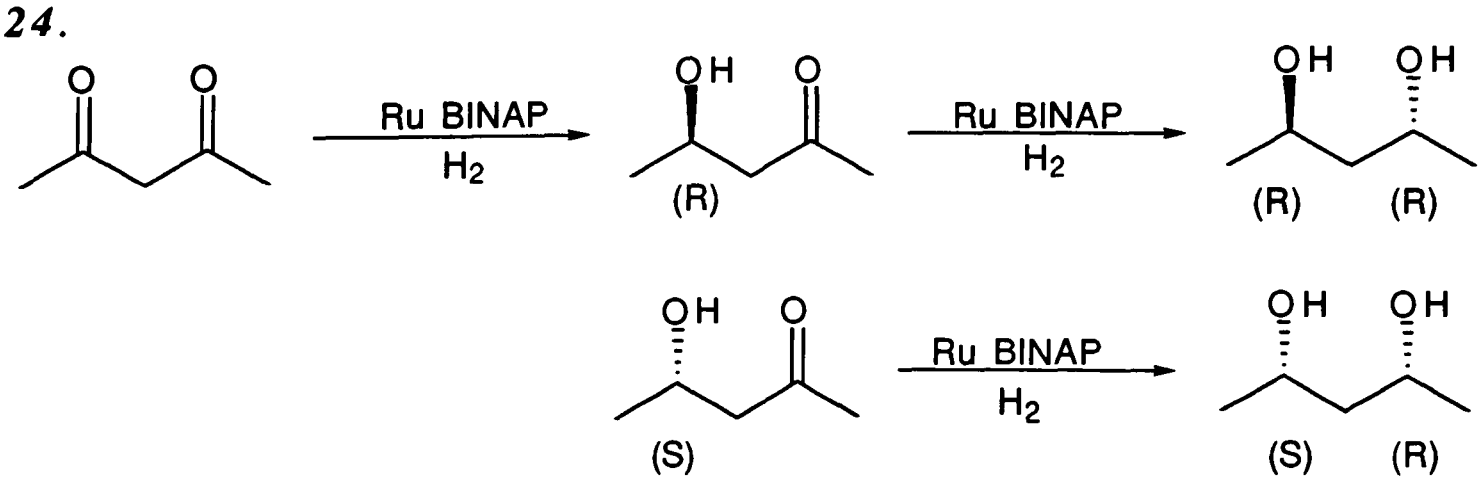


Figure 23: *double asymmetric induction in the ruthenium catalysed hydrogenation of β diketones yields predominantly one out of four possible diols*

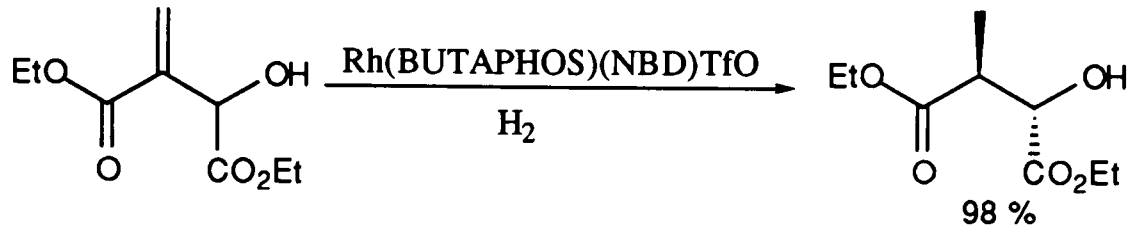


Figure 24: *in homogeneous directed hydrogenation, a polar functional group in proximity to an alkene binds to the metal centre and controls the delivery of hydrogen preferentially to one face of the olefin, on consideration of steric constraints*

A chelate complex involving the alkene, directing group and the metal centre is formed, the *anti* stereoselectivity is rationalised by formation of a chelate with steric interacions minimised[47].

If an asymmetric catalyst is used to carry out a reduction, then diastereoselective hydrogenation is accompanied by kinetic resolution of a racemic reactant[48]. Thus a simple route to enantiomerically pure compounds exists (***Figure 25***).

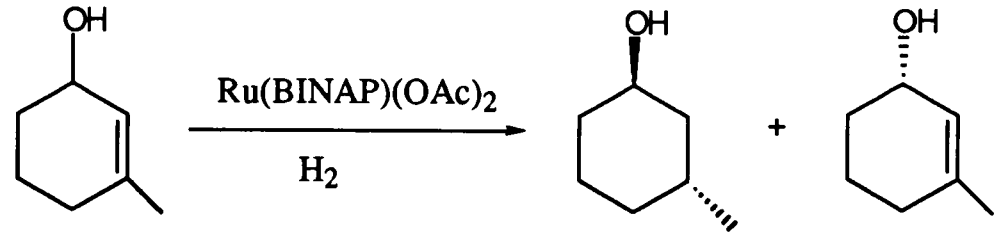


Figure 25: *enantiomers are hydrogenated at different rates, allowing for their kinetic resolution. Only OH is effective in ruthenium directed homogeneous hydrogenation*

Ruthenium catalysts behave similarly to cationic rhodium catalysts in terms of stereoselectivity, relative reactivity of different reactants and in the discrimination between directing groups.

Project Aims

The initial aims of this project were to gain an insight into the mechanism of ketone reduction and make inroads into the ruthenium catalysed alkene hydrogenation cycle using a combination of kinetics and NMR techniques. As the work developed however, the emphasis shifted towards ruthenium work and it will be seen that investigations into ruthenium catalysed alkene reductions form the crux of this thesis.

It was decided that ketone reduction would best be investigated using rhodium catalysts, due to the much milder conditions required (generally 1-2 atm hydrogen). Ruthenium catalysed reductions were also, for convenience, to be conducted at atmospheric pressure. The best substrates to use under such conditions would be dehydroamino acid derivatives. Some further work on rhodium catalysed alkene reduction was also to be carried out.

Results and Discussion

Rhodium chemistry

It was initially envisaged that work using rhodium catalysts would focus on establishing the mechanism by which ketones undergo hydrogenation. In addition, attempts would be made to 'tie up' the few remaining loose ends in the mechanism of rhodium complex catalysed alkene reduction.

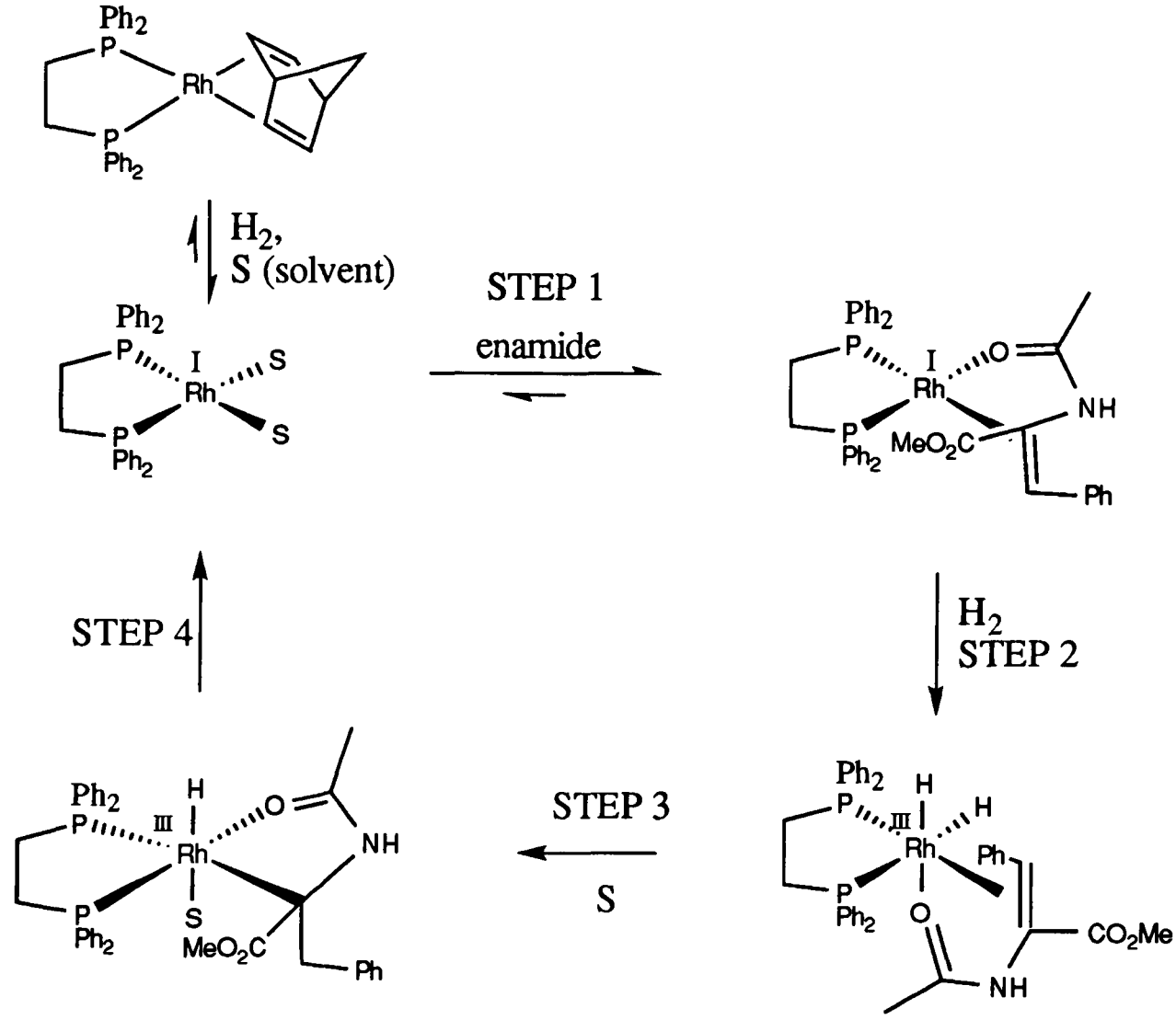
The work contained in this chapter covers five areas:

- a description of the methods developed in the writer's part II project[31] for determining the binding constant of a complex using NMR techniques. The obtention of accurate rate constants for intermediate steps in the mechanistic cycle using kinetic modelling techniques will also be described. These modelling packages allow the development of postulated mechanisms, once accurate kinetic data has been obtained experimentally.
- further investigations into the mechanism by which methyl-2-acetamido acrylate (p14, introduction) undergoes hydrogenation.
- an investigation, using NMR binding studies, into the role of the *ortho*methoxy groups in DIPAMP during the catalytic cycle for alkene reduction. This investigation was carried out by comparing DIPAMP with the non C2 symmetric ligand OXPAMP (*vide infra*) and constitutes the most significant part of the rhodium work discussed in this chapter.
- attempts to observe the elusive dihydride intermediate in the alkene mechanistic cycle (the intermediate from step 2, ***Scheme 1***, p4, introduction).
- a brief summary of initial investigations into the rhodium complex catalysed reduction of carbonyl compounds.

The methods by which these rate and binding constants were obtained will be illustrated during the explanation of continued investigations into the mechanism of the rhodium complex catalysed reduction of methyl-2-acetamido acrylate.

Binding constants from NMR studies, analysis of kinetic data and further investigations of methyl-2-acetamido acrylate

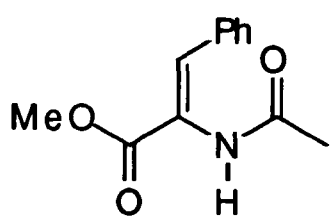
As mentioned in the introduction, previous work[31] had investigated the legitimacy of the widely accepted mechanism for rhodium complex catalysed alkene reduction (***Scheme X***). The investigations were carried out by correlating the rates of hydrogenation of various enamides with the binding constants for formation of their enamide complexes.



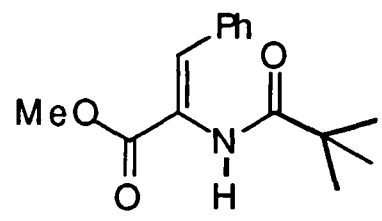
***Scheme X**: extensive investigation into the mechanism of rhodium complex catalysed homogeneous hydrogenation has yielded the pathway above as the most favoured route*

Using the substrates depicted in ***Figure 26***, values were obtained for binding constants for the formation of enamide complexes (Step 1, ***Scheme X***) and rate constants for the addition of hydrogen to those enamide complexes. Methyl-2-acetamido acrylate (**4, *Figure 26***) appeared to be following a more complex mechanism than the other substrates. Its hydrogenation data indicated that it was weakly bound to rhodium, in contrast to the value of its binding constant obtained from ^{31}P NMR. Further investigations indicated apparent second order kinetics with respect to the enamide. The

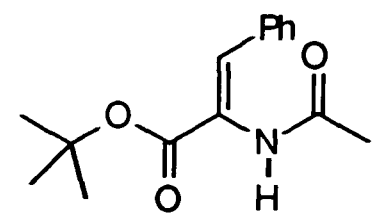
most probable mechanism corresponding to this rate law was thought to be one consisting of two competing pathways, one of which required a second molecule of enamide to dissociate one of the chelating phosphorus atoms from the metal. The existence of a second species in the reaction mixture was also in keeping with the ^{31}P NMR experiments which showed line broadening, indicating a dynamic system and the existence of two interchanging species.



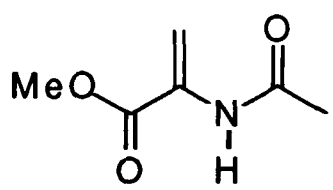
1, mac



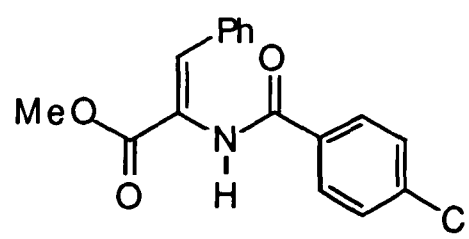
2



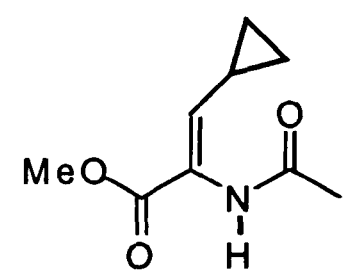
3



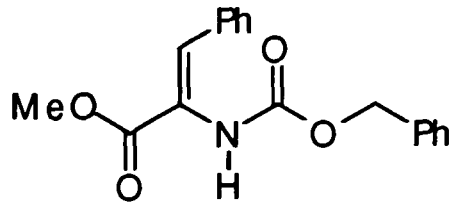
4



5



6



7

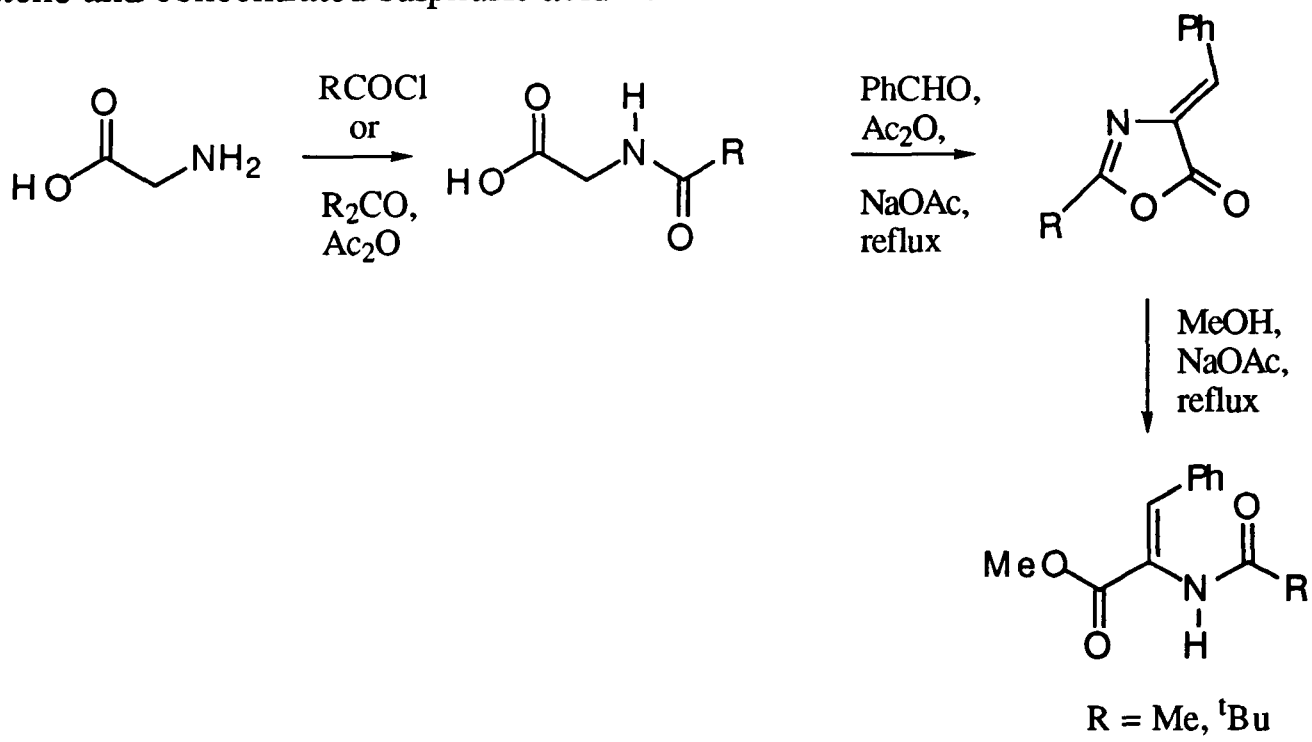
***Figure 26**: changing the amide and alkene substituents alters the electron density associated with the moieties and hence the strength with which the enamides bind to the metal*

The anomaly observed in the reduction of the acrylate could possibly have been an artefact introduced on using a chiral catalyst. It could have been due to the effect of extraneous oxygen in the system being magnified at very low catalyst concentrations, or it could have just been an artefact of PROPHOS. Attempts were made to try and clarify the mechanism by which this substrate underwent hydrogenation.

Investigations required the strength of binding of enamides to the catalyst to be compared with their rates of hydrogenation. Hence substrates were chosen on the basis that they

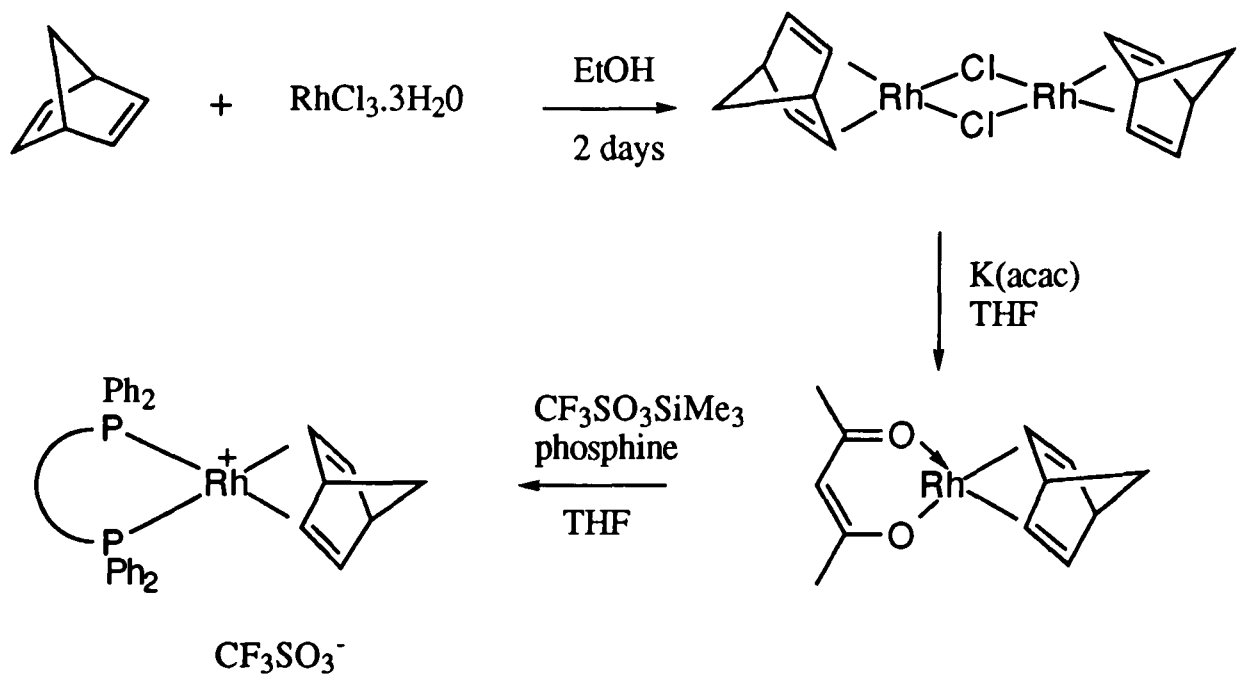
should have significantly different electron density at the alkene and carbonyl double bonds and so have considerably different binding constants. The substrates used in these studies are shown above (**1**, **2**, **3** and **4**, ***Figure 26***). Substrates **1** and **2** showed varying basicity of the amide carbonyl. The *tert*-butyl amide, **2**, was known to dissociate more slowly from rhodium than the reference methyl amide, **1**[17] (the *tert*-butyl group is more electron donating than methyl and so would be expected to increase electron density at the carbonyl group). Comparing the commercially available acrylate, **4** with MAC, **1**, would look at the effect of changing the electron density of the alkene double bond. Substrate **3** varied the ester group (compared with MAC) and was known to be a weaker binder than **1**[17], presumably due to the steric bulk of the *tert*-butyl group.

The acrylate itself is a commercially available compound. Two of the other enamides used in this work (**1** and **2**) were prepared using the Erlenmeyer oxazolone synthesis[49], followed by cleavage with methanol (***Scheme XI***). The Z oxazolone was always formed and its cleavage to the enamide produced the desired Z isomer. Substrate **3** was simply prepared by esterification of Z-2-acetylamino-3-phenylpropanoic acid using isobutene and concentrated sulphuric acid[23].



Scheme XI: *mac and the ^{t}Bu amide were prepared using the Erlenmeyer oxazolone synthesis*

The catalysts were prepared using a general method developed by Brown[50], ***Scheme XII***.



Scheme XII: *the general method for preparing ionic rhodium bisphosphine complexes*

The need for very accurate data in the kinetics experiments meant that a system isolated from fluctuations in temperature and pressure was required. To this end a constant volume apparatus, illustrated below[50], was used.

The apparatus consisted of a double-walled Schlenk tube which had its outer jacket connected to a thermostatted circulating water-bath. The side-arm was attached to a short length of Teflon tubing and then a ring of steel tubing connected the assembly to a small gas cylinder and a transducer, with isolating taps. This section of the apparatus was immersed in the constant-temperature bath. The transducer was connected to an amplifier and through that to a PC; the pressure was measured at pre-defined intervals (usually 5s) and *pt* data stored in tabular form by means of a programme[51], $ADDH_2$. The programme was based on an interrupt driven routine whose frequency could be altered by the operator. The routine received a reading of the amplified voltage output from the pressure transducer and converted it into a pressure by means of a calibration factor. The changing pressure-time dependence was displayed graphically on the computer screen.

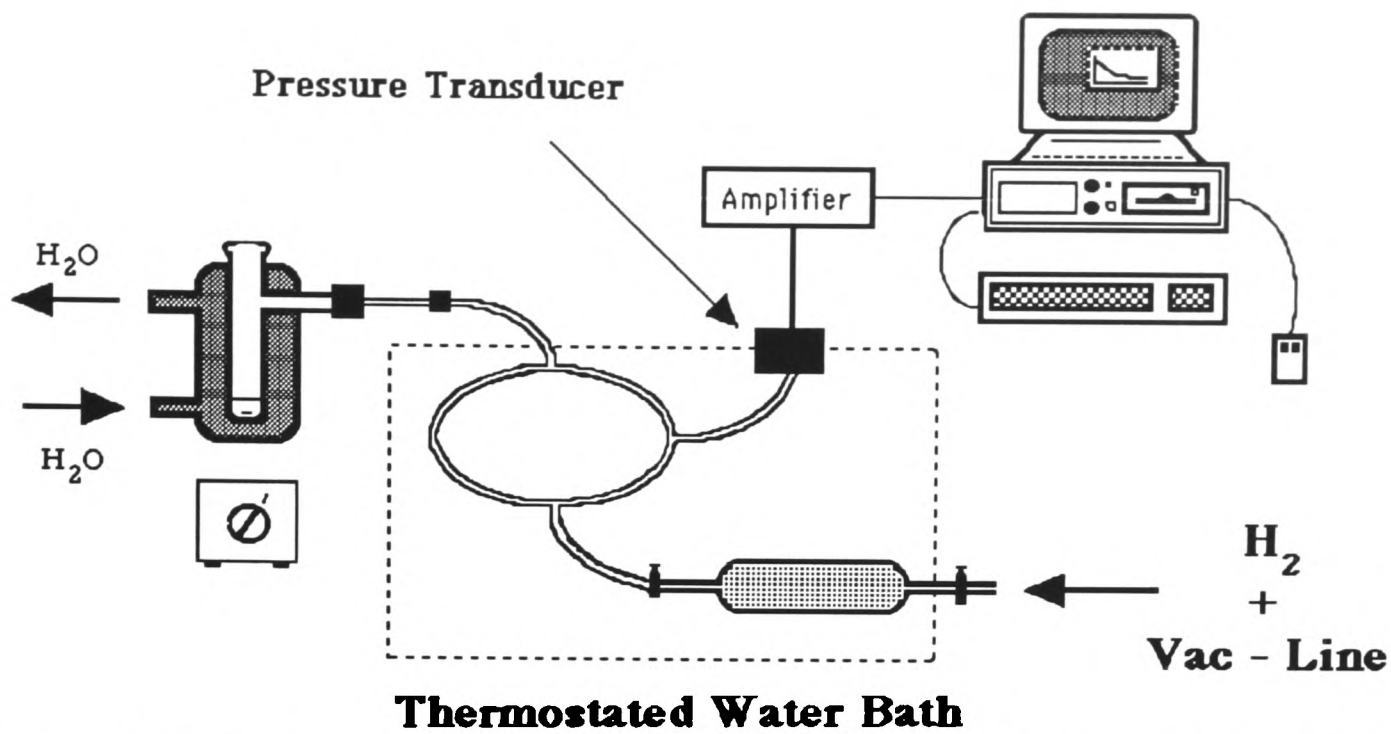


Figure 27: *reductions were performed in a constant volume apparatus linked to a computer*

So that the only variable during hydrogenations was the substrate being reduced, the following were all kept constant:

i) the 500 µl syringe used *ie* the total volume of the solution

ii) the bottle of HPLC methanol

iii) the temperature (normally at 25°C)

iv) the pressure (at 1600 mbar)

v) the stirring speed (preset on the mechanical stirrer)

vi) the batch of catalyst used

vii) the substrate concentration (at 0.1M).

Hydrogenations were carried out in batches of five so that consistent results could be obtained for each substrate. The batches used different amounts of catalyst (usually between 0.5 and 2.5 mol%).

General method for hydrogenations using the constant volume apparatus.

A stock solution of substrate (0.5 mmol) in degassed methanol (2.5 ml) and a stock solution of catalyst (10 µmol) in degassed methanol (2.0 ml) were prepared and then 500 µl substrate solution (0.1 mmol), a known volume of catalyst solution (usually between 0.5 and 2.5 mol%) and enough degassed methanol to make the total volume up to 1.0 ml

were placed in the reaction vessel of the constant volume apparatus (***Figure 27***) under a stream of argon. The reaction vessel was cooled to -78°C (CO_2/acetone) and the apparatus was evacuated to below 0.1 mbar. It was then filled with argon to a pressure of approximately 1100 mbar and the freeze-pump-thaw technique was repeated a further five times before the entire apparatus was filled with hydrogen to a pressure of approximately 1000 mbar.

The reaction mixture was then subjected to another six freeze-pump-thaw degas cycles using hydrogen in place of argon and at the end of the final cycle the hydrogen pressure was set to approximately 150 mbar below the required pressure (*ie* usually set to 1450 mbar) and the apparatus sealed.

The reaction vessel was warmed to the required temperature (25°C or 0°C) and kept at that temperature with the aid of a water circulator fitted with a thermostat. When the pressure in the apparatus had stabilised to within 0.5 mbar (over approximately a 2 min period), a magnetic stirrer, which was preset to a constant speed, was placed under the reaction vessel and sampling of the reaction vessel pressure (at 5s intervals) was commenced with the computer programme $ADDH_2$. Sampling was continued until the pressure in the reaction vessel had stabilised to within 0.5 mbar.

The hydrogenation procedure was then repeated a further four times for each substrate, using different catalyst concentrations.

In order to obtain kinetic data that could be used for quantitative analysis, hydrogenations had to be conducted away from the diffusion limit, where the rate of hydrogenation was mass-transport limited[52]. For 0.1 mmol substrate, this corresponded to a reaction time of about 120s. The form of the *pt* plot obtained on hydrogenation was a primary indication of the strength of binding between the substrate and catalyst. If binding was very strong, the rate was essentially invariant over most of the hydrogenation (pseudo zero order), resulting in a sharp 'elbow' in the *pt* plot on completion of the reaction. If the binding was weak the rate decayed exponentially, resembling first order behaviour (***Figure 29***).

This could be explained by saying that binding to the catalyst was now reversible and as the substrate concentration was reduced, so too was the proportion of reactive species.

Hydrogenations of the acrylate using the catalyst [Rh(NBD)(DIPHOS)]$^+$TfO$^-$ (**A**, ***Figure 28***) were very fast and at the diffusion limit unless very low catalyst concentrations were employed[31]. In an attempt to slow the system down, reductions were performed using the catalysts [Rh(NBD)(PROPHOS)]$^+$TfO$^-$ and [Rh(NBD)(CHIRAPHOS)]$^+$TfO$^-$ (**B** and **C**, ***Figure 28***). All reductions were performed in the constant volume apparatus using the general method described above. Hydrogenations were slowed down but were still very fast compared with other simple enamides: reactions using catalyst concentrations greater than 0.5 mol % were diffusion controlled (***Figure 29***). The initially pale orange solutions remained pale yellow after hydrogen activation and throughout the reaction *ie* unlike most enamides, this substrate did not exhibit any colour changes to indicate complex formation or completion of hydrogenations. For comparison, enamides **1** and **3** (***Figure 26***) were also reduced using [Rh(NBD)(PROPHOS)]$^+$TfO$^-$ (***Figure 30***). The initially pale orange solutions went blood red on hydrogen activation, indicating the formation of an enamide complex (Step 1, ***Scheme X***) and on completion of the reduction process, the solution was pale yellow.

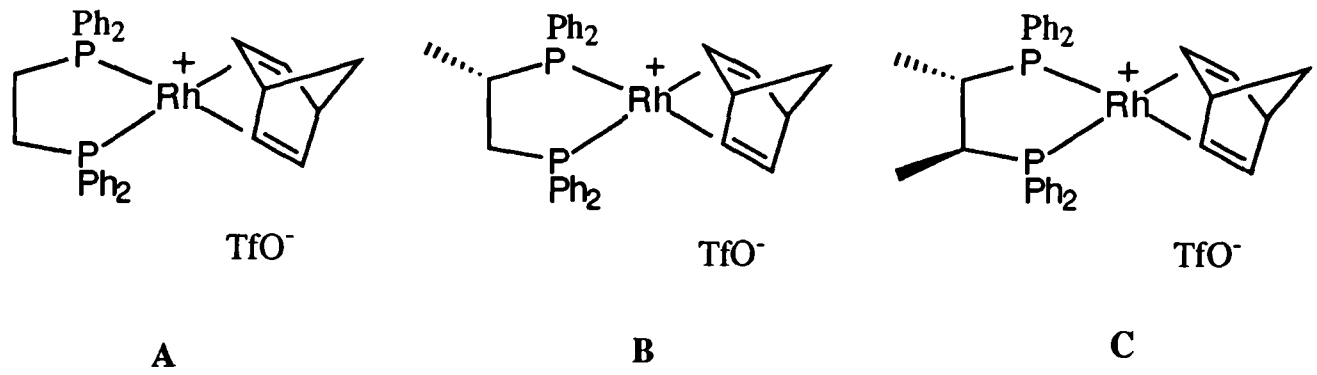


Figure 28: *all three of the catalysts above were used in investigations into the mechanism by which the acrylate underwent hydrogenations*

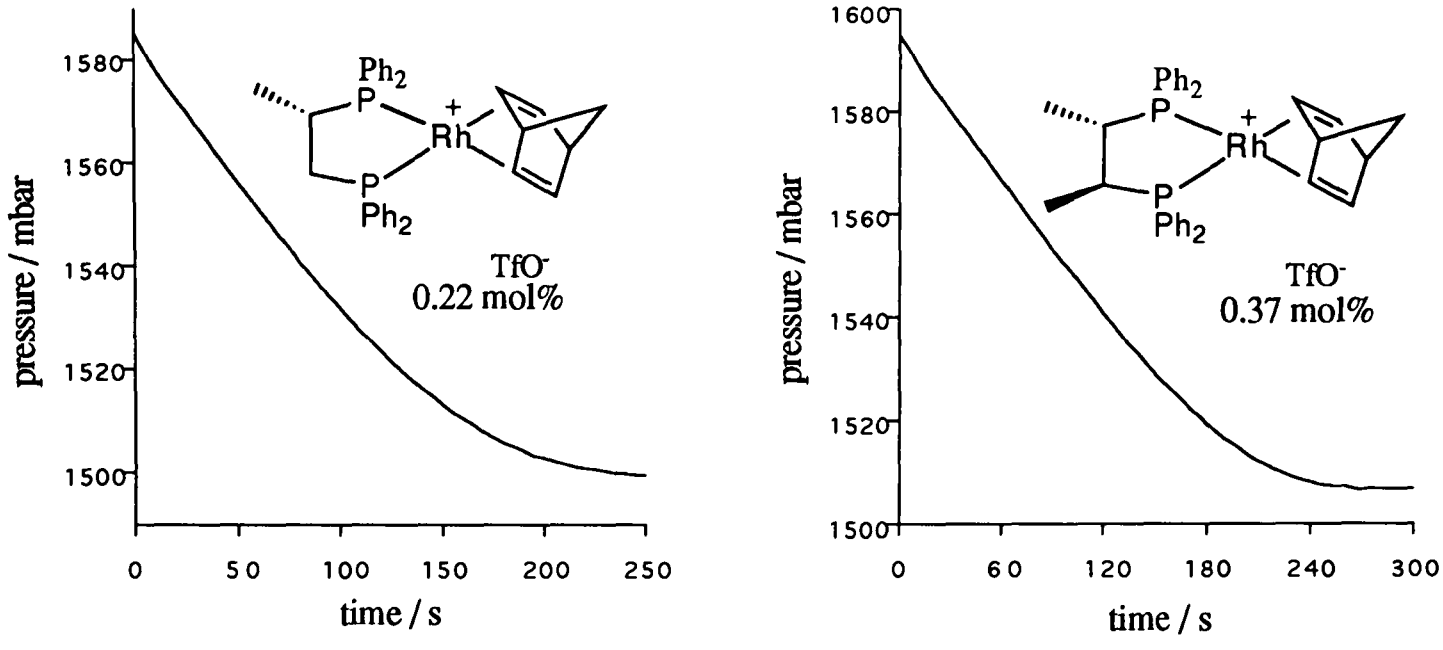


Figure 29: *reductions of the acrylate were still very fast when using rhodium prophos and rhodium chiraphos*

Kinetic data had indicated that methyl-2-acetamido acrylate was weakly bound to rhodium, as shown by the curvature observed in its hydrogenation plots. Binding studies were next carried out to determine how strongly the enamides were complexed to rhodium.

Binding constants for the formation of enamide complexes were to be calculated from ^{31}P NMR spectra taken of the complexes at the temperature of hydrogenation *ie* 298K. Samples were prepared under argon and their phosphorus spectra taken as soon as possible after preparation.

General method for preparation of enamide complexes.

Samples of the bisphosphine rhodium (I) methanol solvate complex were prepared by dissolving the bisphosphine rhodium(I) bicyclo[2.2.1]-heptadiene trifluoromethane sulphonate (10 μmol) in dry, degassed methanol (300 μl) in a 5 mm NMR tube. The solution was then cooled to -78°C, degassed by three vacuum/argon cycles and the NMR tube finally filled with hydrogen. Next, the solution was 'whirlimixed' to aid hydrogenation of the complex, which was indicated by a colour change from dark orange to pale yellow. For quantitative studies, it was essential that all the bicyclo[2.2.1]-

heptadiene was reduced *ie* that catalyst activation was complete, else binding constants could not be obtained. The atmosphere in the NMR tube was then replaced with argon after freezing the solution and a solution of the enamide (usually 30 μmol) or a mixture of two enamides (usually 15 μmol of each) in dry, degassed methanol (300 μl) was added to the tube, resulting in the formation of an enamide complex (usually deep red). ^{31}P NMR spectra were then obtained at 25°C or 0°C as required on a Bruker AMX500 at 202.46 MHz. Before pulsing was begun, the NMR tube was allowed to equilibrate for 10 min inside the probe.

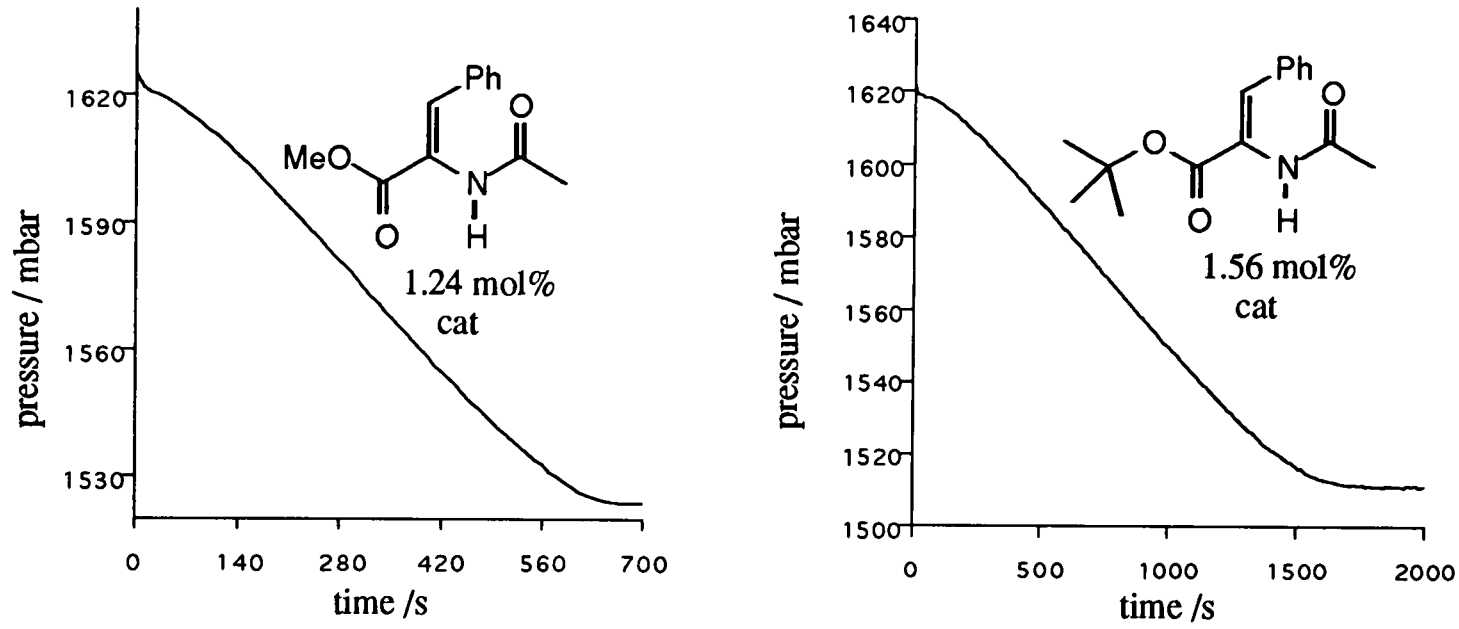


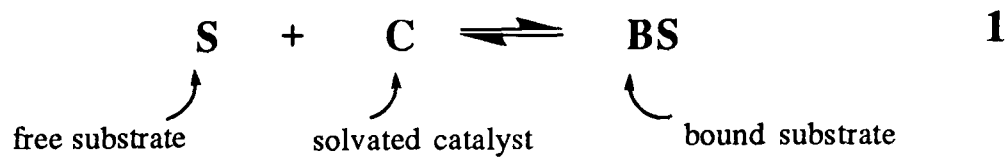
Figure 30: *rhodium prophos was also used to catalyse the reduction of mac and the ^{t}Bu ester*

Using three molar equivalents of substrate drove the equilibrium **1**, below, to the right and so the only phosphorus containing species present was the enamide complex. Spectra in this case consisted of two sets of double doublets for each of the major and minor diastereomers which arose from the two inequivalent phosphorus atoms: each phosphorus atom coupled to the rhodium (large coupling) and was then coupled to the other phosphorus (smaller coupling). Mixtures of two substrates gave eight double doublets, whose relative intensities gave an indication of their relative binding strengths. Non C2 symmetric catalysts such as [Rh(NBD)(PROPHOS)]TfO also gave rise to spectra containing eight double doublets due to the existence of twice as many diastereomers.

An absolute value for the binding constant of one substrate was needed. Once this was known, mixtures of this reference substrate and the other substrates could be looked at, leading to relative values of binding constants as compared with the reference substrate. To get relative binding constants, both enamide complexes needed to be visible in the ^{31}P spectra to an extent that accurate integration of their signals could be performed. Also, no solvate could be present. Thus initally 1:1 mixtures of substrates were prepared using 15 μmol each substrate and 10 μmol catalyst. The excess substrate drove the equilibrium to the right and ensured no solvate peaks, as all the catalyst was present in the form of enamide complexes. If, due to vastly differing K values, only one substrate was observed in the mixture, the 1:1 ratio was varied until peaks corresponding to the enamide complex of the weaker binder also appeared.

From these relative values, absolute values for the binding constants of the other substrates could be obtained, once the absolute value of the reference substrate was known. MAC was usually picked as the reference substrate.

The equilibrium under consideration was:



1

for which

$$K = \frac{[BS]}{[S][C]}$$

and both [S] and [BS] could be calculated. For mixtures of substrates in the absence of solvate

$$\frac{K_2}{K_1} = \frac{[BS_2][S_1]}{[BS_1][S_2]}$$

where K_1 refers to the reference substrate.

So when working with relative values, only the equilibrium concentrations of the substrates and enamide complexes needed to be known. The initial concentrations of the

substrates were known and so the equilibrium concentrations were worked out by difference, knowing the amount of substrate bound to the catalyst. The equilibrium concentrations of the enamide complexes were determined by integration of the peaks in the ^{31}P NMR spectrum.

To work out the absolute value of the equilibrium constant of the reference substrate, [C] could not be zero *ie* some solvate complex had to be present. Spectra were run on 1:1 solutions of the reference substrate and catalyst so that an equilibrium existed in which there was a chance of observing the solvate.

For the equilibrium **1**, [BS] and [C] were obtained from the ^{31}P spectrum and [S] was $[S]_{initial}$ - [BS]. Hence a value for K_{BIND} was obtained for the reference substrate. For the runs on mixtures of substrates, integration of the peaks in the phosphorus spectra led to a ratio of the concentrations of the two bound enamides. Knowing the initial concentrations of the substrates, a ratio of the equilibrium amounts of substrates was obtained and hence binding constants were obtained using the above equation.

If the phosphorus atoms of the enamide and solvate complexes had different relaxation rates, their peak intensities in the ^{31}P NMR spectra would be altered by this difference and integration of the peaks would not be representative of the relative concentrations of the species present. Previous work had tested the validity of using signal integration as a direct indication of equilibrium concentrations by acquiring spectra with different delay periods and carrying out measurements of longitudinal relaxation times, T_1, using an inversion recovery technique[31]. The differing delay period exercise showed no changes in peak intensities, indicating an absence of intensity anomalies due to relaxation differences between the complexes (Appendix 1). The T_1 experiment also showed the differences in the relaxation rates of the phosphorus atoms was not marked.

The spectra obtained were proton decoupled. The advantage of this was that coupling often reduces the available signal/noise ratio and so it proves advantageous to acquire spectra with splittings due to proton coupling removed (spectra would also be

considerably simplified). An undecoupled spectrum of an enamide complex was obtained and compared with a decoupled spectrum to check that the relative intensities of the peaks was the same in both cases *ie* to check that the improvement in the signal/noise ratio on moving to the decoupled case was uniform. No change in intensity was observed.

These investigations justified using the relative intensities of the peaks in the ^{31}P NMR spectra as a direct indication of the relative concentrations of the enamide complexes.

Absolute values of binding constants using Rh(PROPHOS) were obtained from ^{31}P NMR spectra (***Figures 31, 32*** and ***33***) and are listed in the table below (***Table 1***). ***Figure 31*** shows both pairs of major and minor diastereomers which exist in the Mac/PROPHOS system. In the case of the ^{t}butyl ester however, only the major diastereomers were observed (***Figure 32***). The complex derived from methyl-2-acetamido acrylate was actually dynamic at the reaction temperature of 25°C (***Figure 33***). The dynamic nature displayed in binding studies by the acrylate / PROPHOS system was investigated further by carrying out variable temperature ^{31}P NMR experiments on a sample containing a five fold excess of acrylate over catalyst. Cooling the system down to -70°C froze out the dynamic exchange and the spectrum obtained showed that both major and minor diastereomers were present in equal amounts (***Figure 33***). ***Figure 33*** shows that the species present a 298K did not correspond to a 'straightforward' enamide complex. The P_4 analogue of PROPHOS (***Figure 34***) was synthesised in order to obtain its ^{31}P NMR and rule out its presence in the binding studies spectra.

(unless otherwise stated, all the spectra shown in figures were obtained on the AMX 500 MHz; 202.46 MHz for ^{31}P NMR and samples were run in CD_3OD)

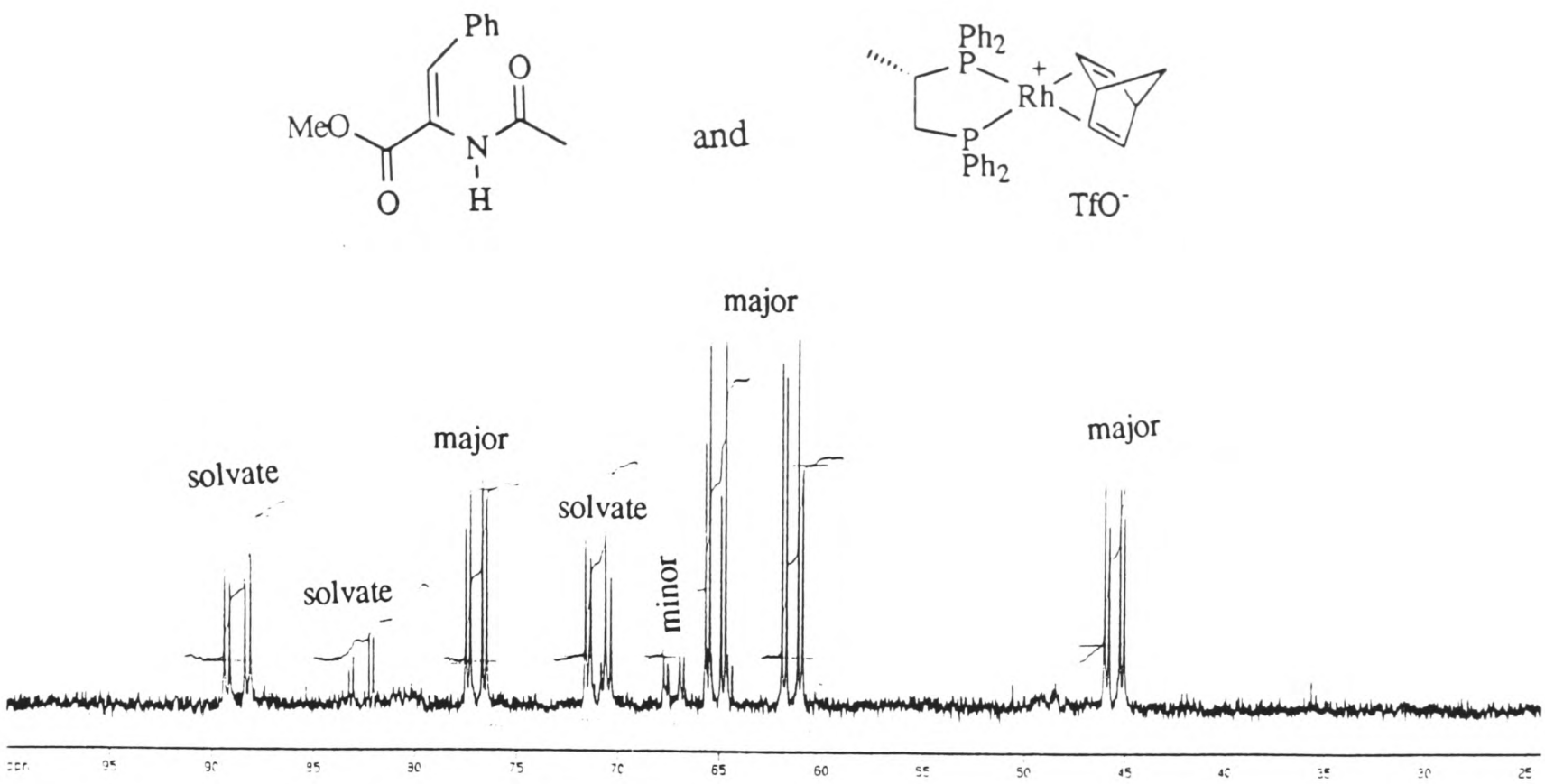


Figure 31: *both major and minor diastereomers were observable using the mac/propos system*

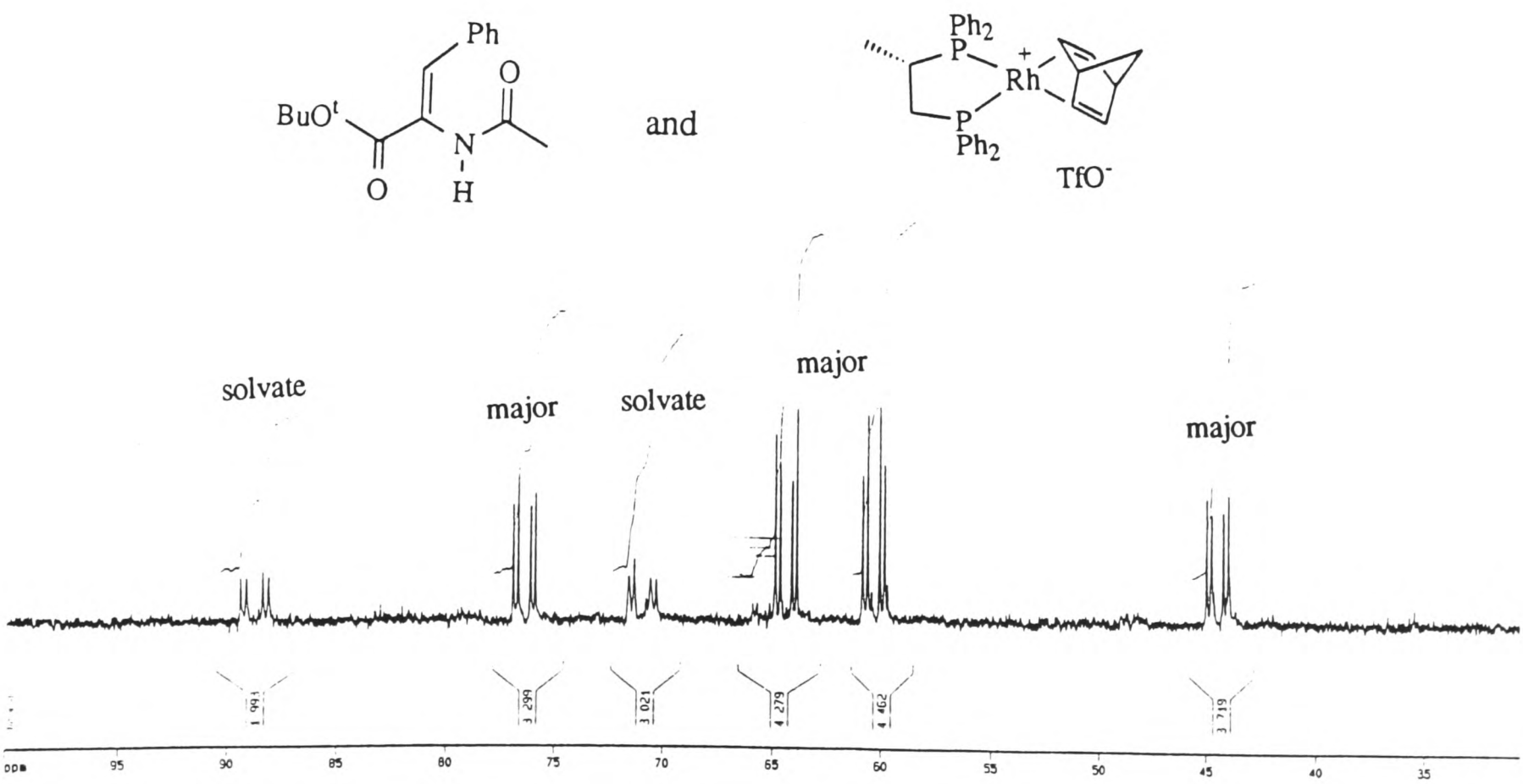


Figure 32: *only the major diastereomers were seen using the ^{t}Bu ester/prophos system*

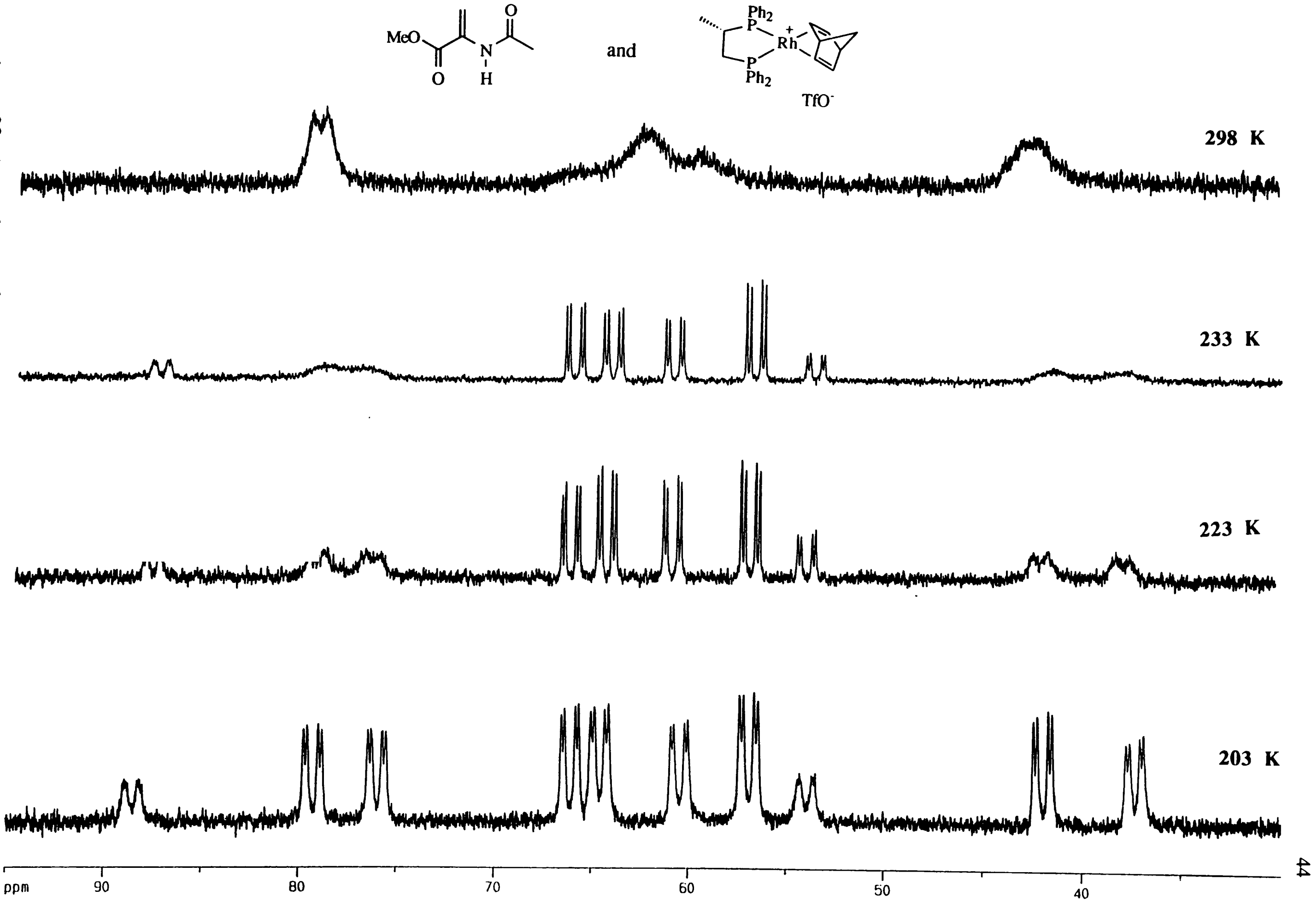


Figure 33: *the acrylate/prophos system was dynamic at room temperature. When cooled down to 203K, the dynamic exchange was frozen out*

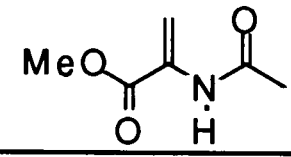
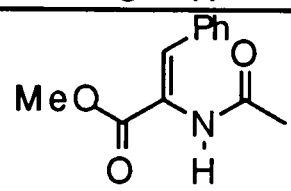
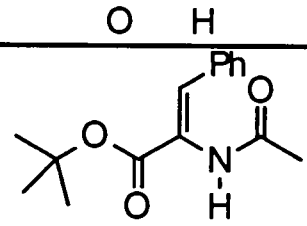
Enamide	K_{BIND} / mol^{-1} l
	850
	1750
	2700

Table I: *binding constants for the formation of enamide complexes to prophos*

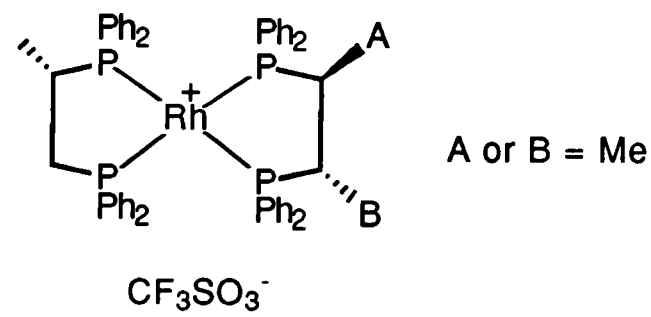


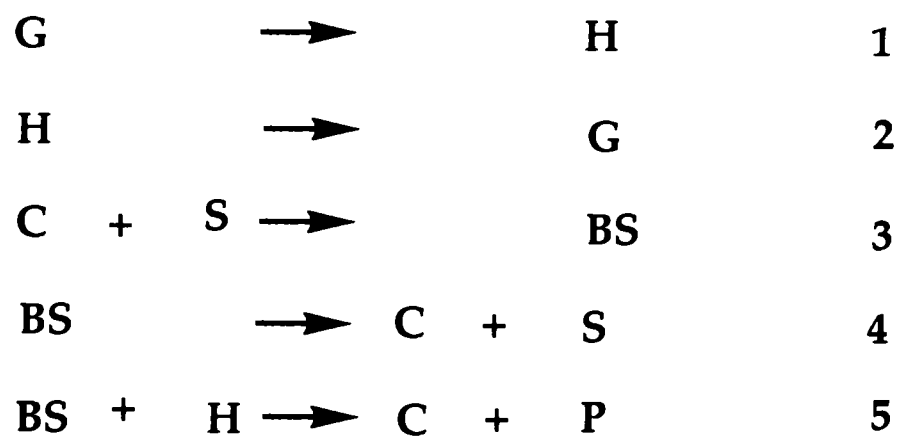
Figure 34: *^{31}P NMR of the P_4 analogue of prophos ruled out its presence in the acryalte/prophos VT study*

The kinetic data was then analysed by numerical integration programmes which allowed simulation of the data against proposed catalytic pathways. A disadvantage of working at constant volume was that the rate equation became very hard to solve because the changing hydrogen pressure meant the steady-state approximation was invalid. Analysing the data by numerical integration methods allowed the changing pressure to be easily incorporated into the mechanistic model used in the simulation. Two programmes were used to analyse the data[53]:

i) GEAR- a simulation programme that integrated a given set of equations to give species concentrations as a function of time

ii) GIT- a programme used to fit a reaction model to a set, or sets, of data.

The model first used in analysis (***Scheme XIII***) was based on the currently accepted reaction mechanism (***Scheme X***).



Scheme XIII: *the model corresponding to the currently accepted mechanism for rhodium complex catalysed enamide reduction using an achiral catalyst*

Equations **1** and **2** referred to the gas-liquid interfacial transfer. **G** was equivalent to the solution concentration if all the hydrogen gas in the apparatus was dissolved in the solvent present and **H** was the actual concentration of the solution. A value for **G** was obtained following calibration of the total volume of the apparatus against a mercury barometer[51] (the total volume was found to be 17.8 ml). Knowing that the saturation solubility of hydrogen in methanol is 4.01×10^{-3} M at 1 atm hydrogen pressure and 25°C[54], a value for k_1/k_2 of 172.32 was derived[51]. k_1 and k_2 were then determined by using the numerical iterator GIT on data obtained from diffusion rate experiments, varying k_1 and k_2 but keeping their ratio constant at 172.32. Values obtained[31] were $k_1 = 0.963 \times 10^{-3}\ s^{-1}$, $k_2 = 0.166\ s^{-1}$.

Equations **3** and **4** corresponded to the formation of the enamide complex **BS** from catalyst **C** and substrate **S**. The absolute value of k_3 needed to be much greater than the other rate constants in order to prevent the complexation step from becoming rate determining. Values for k_3 and k_4 were decided on the basis that k_3/k_4 was equal to K_{BIND}. k_3 and k_4 were varied in conjunction with k_5 during the kinetic analysis, keeping their ratio fixed at K_{BIND}, until the best fit to the model was obtained for each set of data.

Equation **5** represented the transfer of hydrogen to the substrate, the whole process having been condensed into one step leading to product **P**. K_5 was varied in the analysis to produce the best fit to the model for a given data set. ***Scheme XIII*** was modified when using chiral catalysts by allowing for the formation of major and minor

diastereomers of the enaimde complex, their interconversion and subsequent independent reaction with hydrogen.

Kinetic analysis and modelling

Data from hydrogenations was stored as *pt* data using the programme $ADDH_2$[51]. ITR files were then created using the computer programmme MAKEITR[54]. This file contained initial concentrations of the model species together with the experimental data, which was converted into concentrations of product with time. The files were then reduced in size to about fifty points by removing points from the less important straight-line region of the plots, whilst keeping all the data which corresponded to the curved region of the plots.

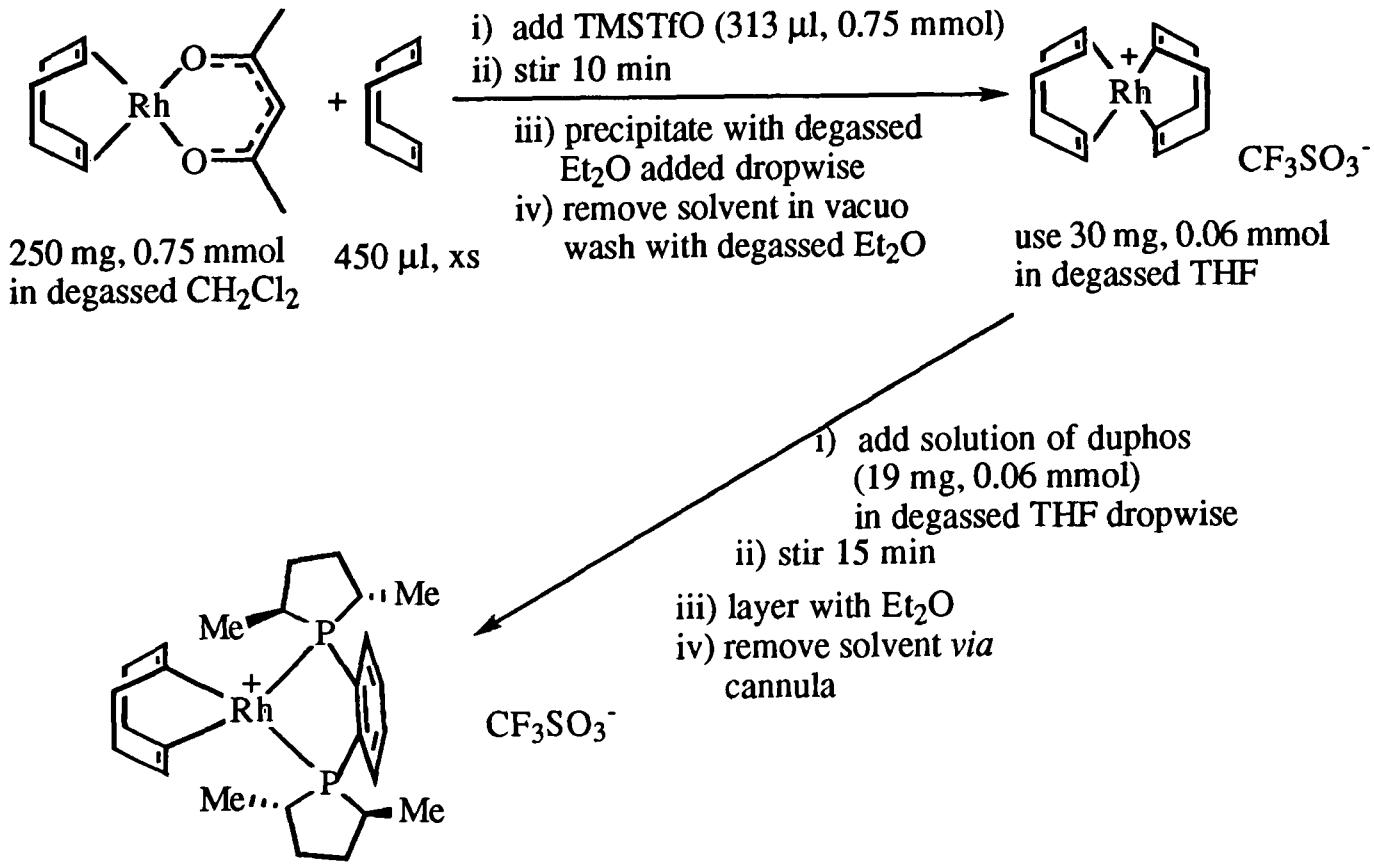
Next the modelling programme GIT was run, using a GEAR file containing the model rate constants (with k_3, k_4 and k_5 marked as variable and the ratio of k_3 to k_4 fixed at K_{BIND}) for each of the runs from the set of five obtained from hydrogenating each substrate. GIT modelled the experimental data against the theoretical data and gave a value for the optimum deviation between the two. The best values for the rate constants were found by initially guessing their values and running GIT. Guesses were deliberately set low because the iterating programme altered rate constants by a percentage of their value and thus a larger change in these constants could be achieved. This allowed the programme to 'escape' from local minima. GIT was allowed to optimise the variable rate constants to produce a best fit and the value for the average deviation was noted. The process was then repeated with different initial values for the variable rate constants until the lowest average deviation was obtained. Values of k_5 were then obtained for the sets of data combined, keeping k_3 and k_4 constant and iterating on k_5 only.

Modelling of the kinetic and binding data obtained using Rh(PROPHOS) showed the currently accepted mechanism (***Scheme X***) to fit for substrates **1** and **3**, ***Figure 26***. (For the enantioselective variant, where a chiral catalyst is used, each intermediate in the mechanistic cycle (***Scheme X***) is present in two diastereomeric forms; the model shown in ***Scheme XIII*** was modified to allow for this). However, the data obtained for

methyl-2-acetamido acrylate did not fit this mechanism. It did not exactly fit a mechanism involving a second molecule of enamide (as discussed on p14) in the rate determining step either.

Further attempts to find models that fitted the kinetic data obtained on this substrate were unsuccessful; the anomalous nature of this substrate could not be explained. It was hoped that catalyst systems using this substrate might be used to isolate the elusive intermediate resulting from oxidative addition of hydrogen to the metal (Step 2, ***Scheme X***) due to the speed with which this intermediate underwent hydrogenations (*vide infra*).

Kinetic studies on alkene hydrogenation catalysed by the rhodium catalysts of Burke's recently developed DUPHOS ligands[15] were also carried out in order to determine the mechanisms by which they operate and the strength with which they bind enamides. The catalyst was synthesised from $Rh(COD)_2TfO$[15] (***Scheme XIV***) and obtained as a bright orange powder, δ_P(202.46 MHz, CD_3OD) 77.6 ppm, d, J = 148.4 Hz.



Scheme XIV: *the synthesis of Burke's DUPHOS range of catalysts*

Pt plots showed the methyl DUPHOS/mac system to be a weakly bound system, ***Figure 35***. Plots were sigmoidal due to the longer activation period for the removal of COD compared with NBD[55]. The solution was pale yellow throughout the hydrogenation -

there were no colour changes corresponding to complex formation. Reactions were very fast and were diffusion controlled at catalyst concentrations greater than 1 mol%. The weak binding of the substrate was verified by binding studies (***Figure 36***) which led to a value for K_{BIND} of 1000 mol^{-1} l. Binding studies carried out on the DUPHOS/acrylate system showed it to be much less dynamic than the PROPHOS/acrylate system, even at 25°C (***Figure 37***). Kinetic modelling of the DUPHOS/mac system led to a rate constant of 2150 $mol^{-1}ls^{-1}$ and showed that this catalyst followed the accepted hydrogenation mechanism involving sequential addition of enamide and hydrogen to the metal.

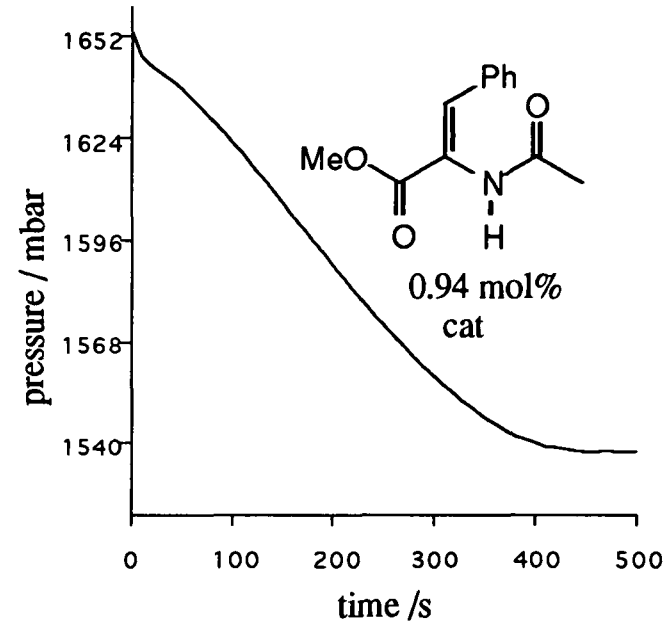


Figure 35: *plots for the rhodium duphos catalysed reduction of mac indicated that the substrate was a weakly bound system*

A comparison, using NMR techniques, of substrate binding to Rh(DIPAMP)(NBD)TfO and Rh(OXPAMP)(NBD)TfO

DIPAMP (**A**, ***Figure 38***) is one of the few bisphosphine ligands containing stereogenic phosphorus atoms rather than chirality in the chelate backbone. The role of the *ortho*methoxy phenyl groups in DIPAMP during its rhodium complex catalysed hydrogenation of alkenes requires clarification[56]. Studies on analogous iridium complexes indicated that the methoxy group is ligated during the catalytic cycle[57a] but it is not clear how this influences the stereoselectivity. In order to investigate the role of the methoxy groups futher, Brown synthesised OXPAMP (**B**, ***Figure 38***), a ligand containing only one methoxy group[58].

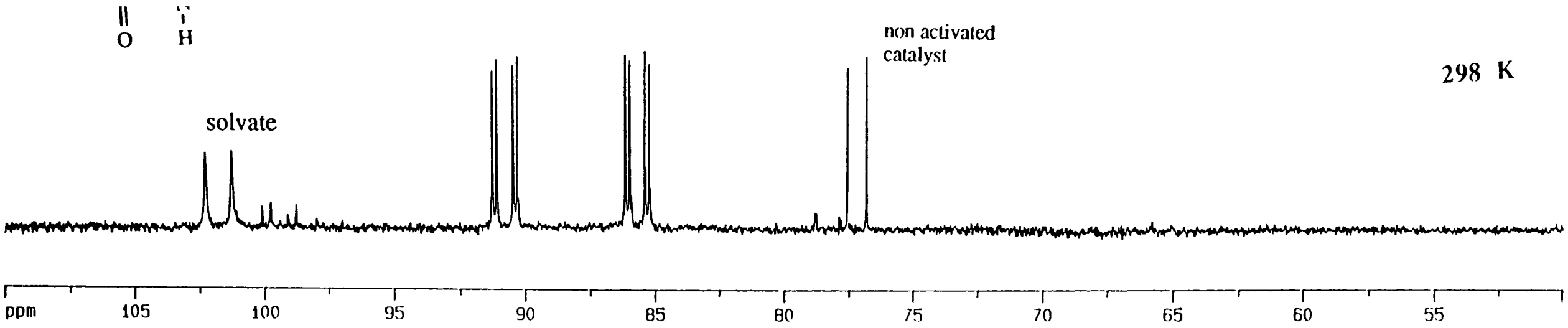


Figure 36: *an absolute value of the binding constant for the mac/duphos complex was obtained from* ^{31}P *NMR*

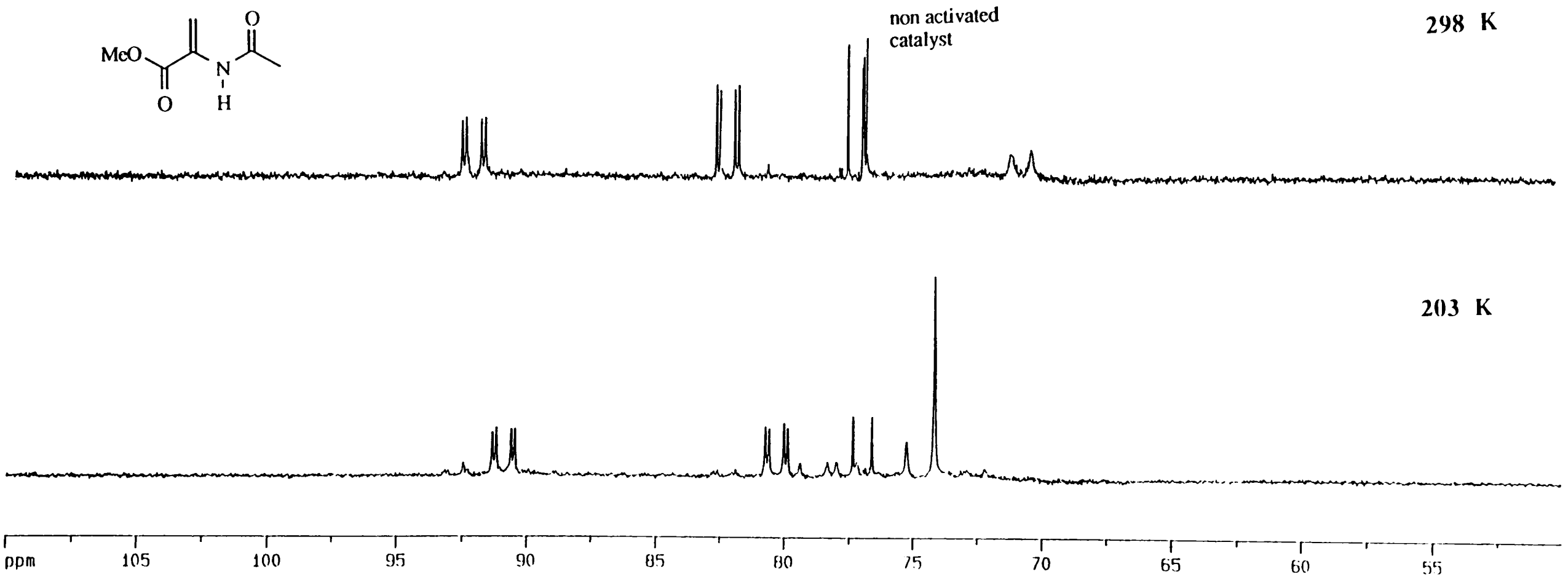


Figure 37: *the acrylate/duphos system was only slightly dynamic at 298K*

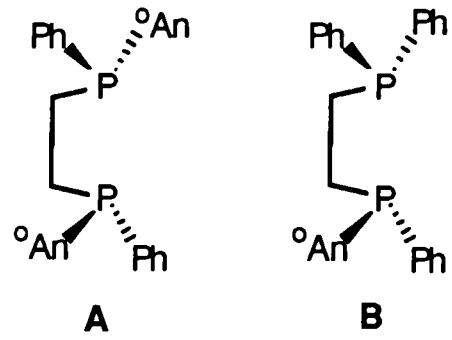


Figure 38: *oxpamp was synthesised in order to clarify the role of the methoxy groups in dipamp during rhodium catalysed reductions*

OXPAMP was to be used in direct comparisons with the C2 symmetric DIPAMP in asymmetric hydrogenation. As in the case with the non C2 symmetric ligand PROPHOS (p43), four enamide complexes (two major, two minor) result from this catalyst and enamides. ^{13}C NMR EXSY studies using labelled mac and Rh(OXPAMP)(NBD)TfO (***Figure 39***) allowed the distinction between inter- and intra-molecular dissociation mechanisms during major/minor enamide complex conversion (p6, introduction)[59].

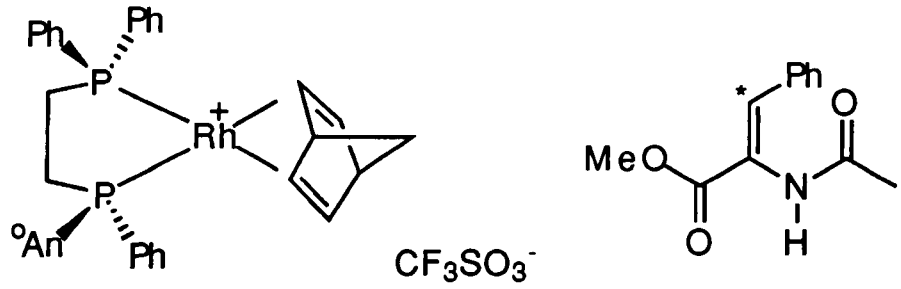


Figure 39: *inter- and intra-molecular dissociation mechanisms for the enamide complexes formed from the system above were distinguished using ^{13}C NMR EXSY studies*

The results of the EXSY experiments pointed to the dominance of the *intra*molecular exchange process. Also, observation by ^{1}H NMR of the alkyl hydride intermediate at 233K showed the formation of only *one* alkyl hydride occurs, with the methoxy group *trans* to the amide group, ***Figure 40***[59].

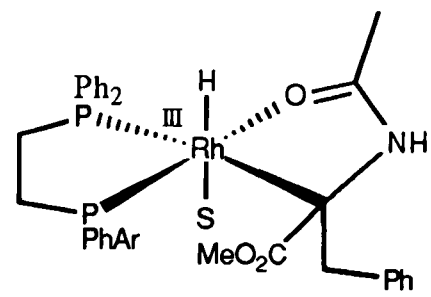


Figure 40: *only one alkyl hydride intermediate is formed between Rh(OXPAMP)(NBD)TfO and mac*

It was decided to conduct a direct comparison between the rhodium complexes of OXPAMP and DIPAMP in terms of binding constants for enamide complex formation and also to attempt to obtain rate constants for the exchange processes interconverting the different structures in solution. Investigations were conducted using a strong binder (^{t}butyl amide) and a weak binder (^{t}butyl ester, ***Figure 41***). Previous DANTE work[17] on Rh(DIPAMP)(NBD)TfO indicated that the ^{t}butyl amide (***Figure 41***) was very slow to dissociate from rhodium whilst the ^{t}butyl ester interconverted its major and minor enamide complexes, *via* a predominantly intramolecular mechanism, with a rate constant of 8.30 s^{-1} at 301K.

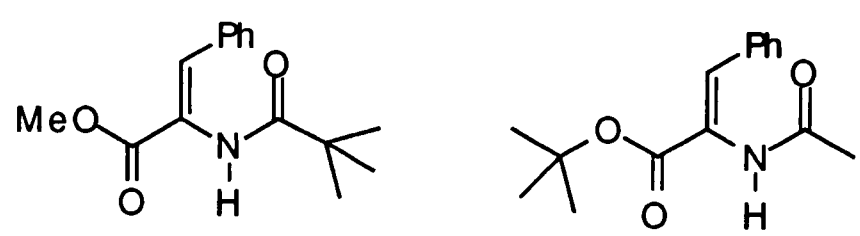
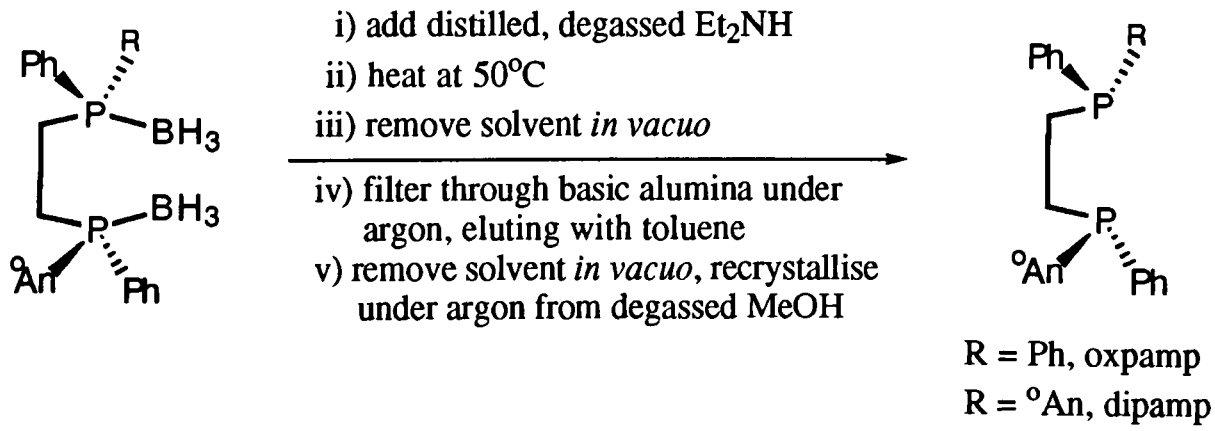


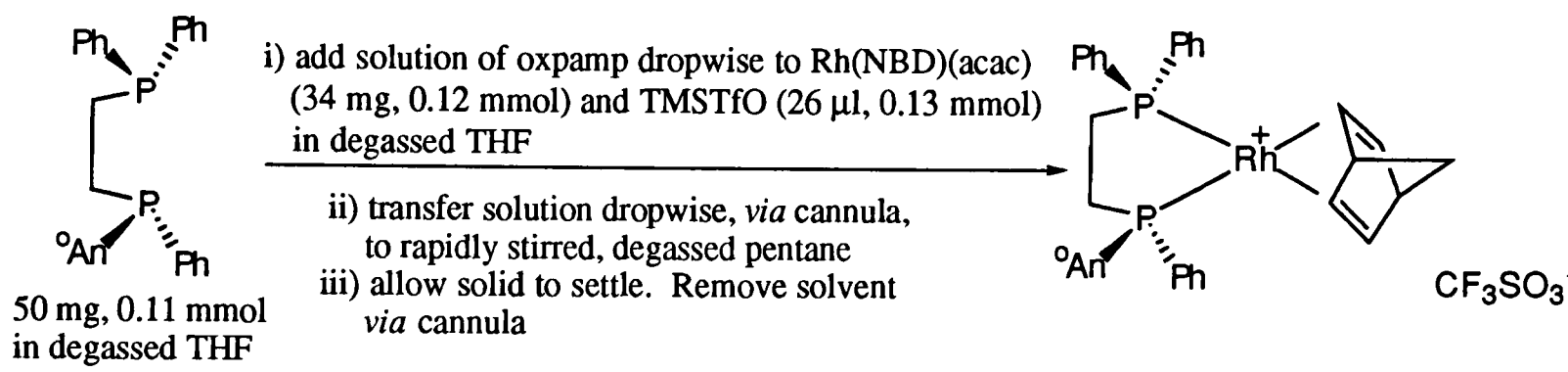
Figure 41: *inversion experiments were conducted using two substrates with very different binding strengths to rhodium*

DIPAMP and OXPAMP were obtained from stocks of the boronated precursor by heating in distilled, degassed diethylamine followed by filtration through alumina and recrystallisation from methanol under argon[60, 58], ***Scheme XV***. Rh(DIPAMP)(NBD)TfO was then prepared from Rh(NBD)(acac) in the usual way (p34), yielding the product as an orange powder (δ_P, 202.46 MHz, CD_3OD 51.0 ppm, d, $J_{P\text{-}Rh}$ = 158.7 Hz).



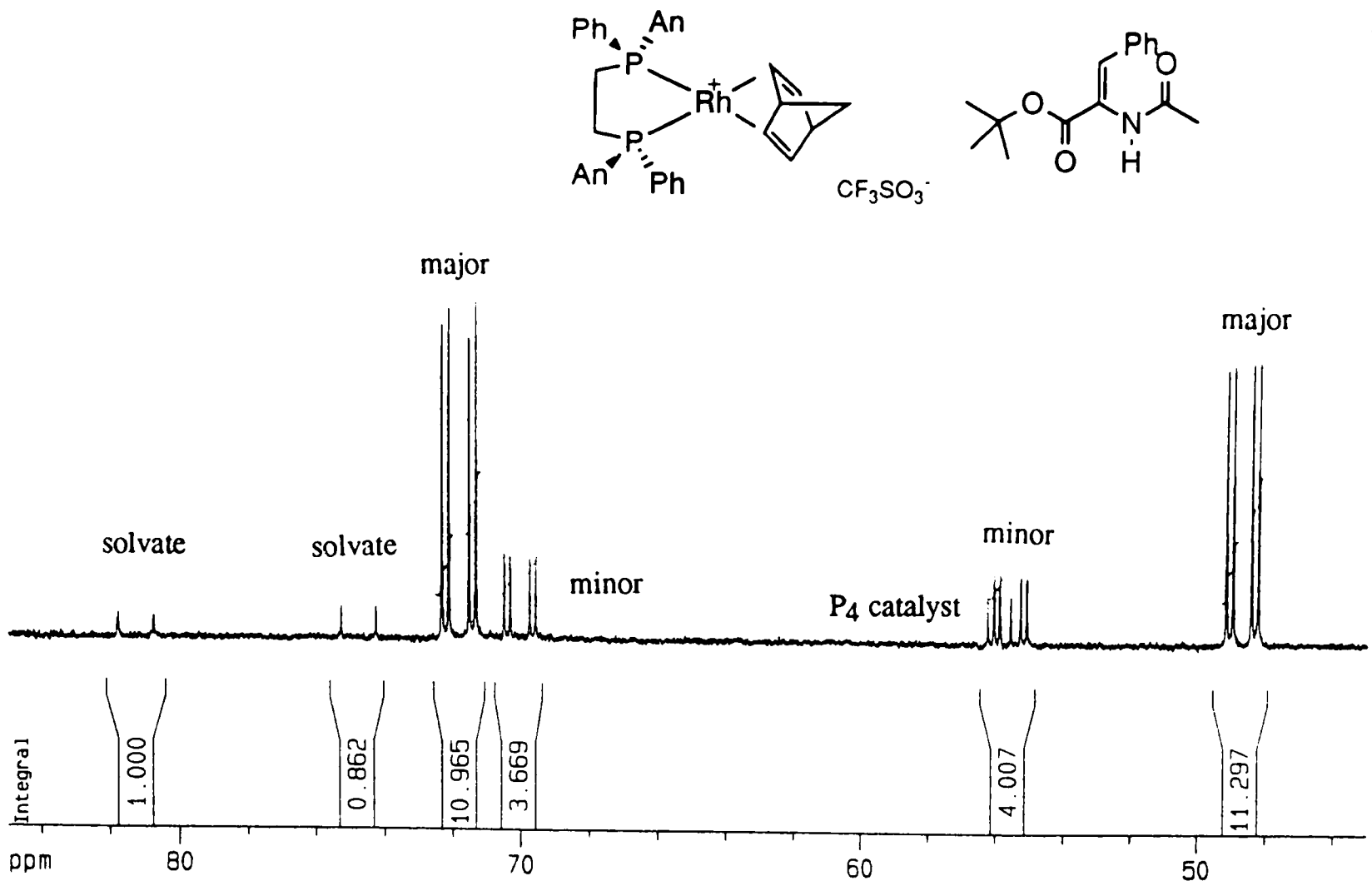
Scheme XV: *the preparation of oxpamp and dipamp from their boronated precursors*

The synthesis of *pure* samples of Rh(OXPAMP)(NBD)TfO was slightly more problematic. Recrystallisation of impure samples was hindered by the fact that the catalyst was prone to 'oiling out', rather than precipitating out slowly. Pure catalyst samples were eventually obtained by a dropwise addition of the phosphine to the activated rhodium species, thus minimising the formation of any P_4 catalyst and any other side products, ***Scheme XVI***. The product was obtained as a bright orange solid (δ_P 202.46 MHz, CD_3OD, 56.5 and 51.3 ppm, dd, $J_{P\text{-}Rh}$ = 158.3 Hz, $J_{P\text{-}P}$ = 29.7 Hz).



Scheme XVI: *pure samples of Rh(OXPAMP)(NBD)TfO were only obtained on dropwise addition of the phosphine to the rhodium complex*

Binding constants for the formation of dark red enamide complexes using these catalysts were obtained in the manner described previously (p38). For both catalysts, an absolute value of the binding constant for complex formation using the *t*butyl ester was obtained but studies involving the *t*butyl amide required mixed binding studies to be performed due to the stronger binding of this substrate resulting in the absence of observable solvate peaks, ***Figure 42***. It was noted that with both catalysts, activation resulted in the formation of small amounts of P_4 catalyst, even though the samples of non activated catalyst were free of such contaminants, as shown by ^{31}P NMR. Also, in the case of [Rh(NBD)(OXPAMP)]TfO, the minor diastereomer was present in a significant amount (compared with [Rh(NBD)(DIPAMP)]TfO) and the peaks due to solvated catalyst appeared as a broad doublet rather than two distinct double doublets. This latter fact was either due to a dynamic solvate species or coincidental chemical shifts for the two double doublets. The binding constants obtained from preliminary studies are tabulated below, ***Table II***.



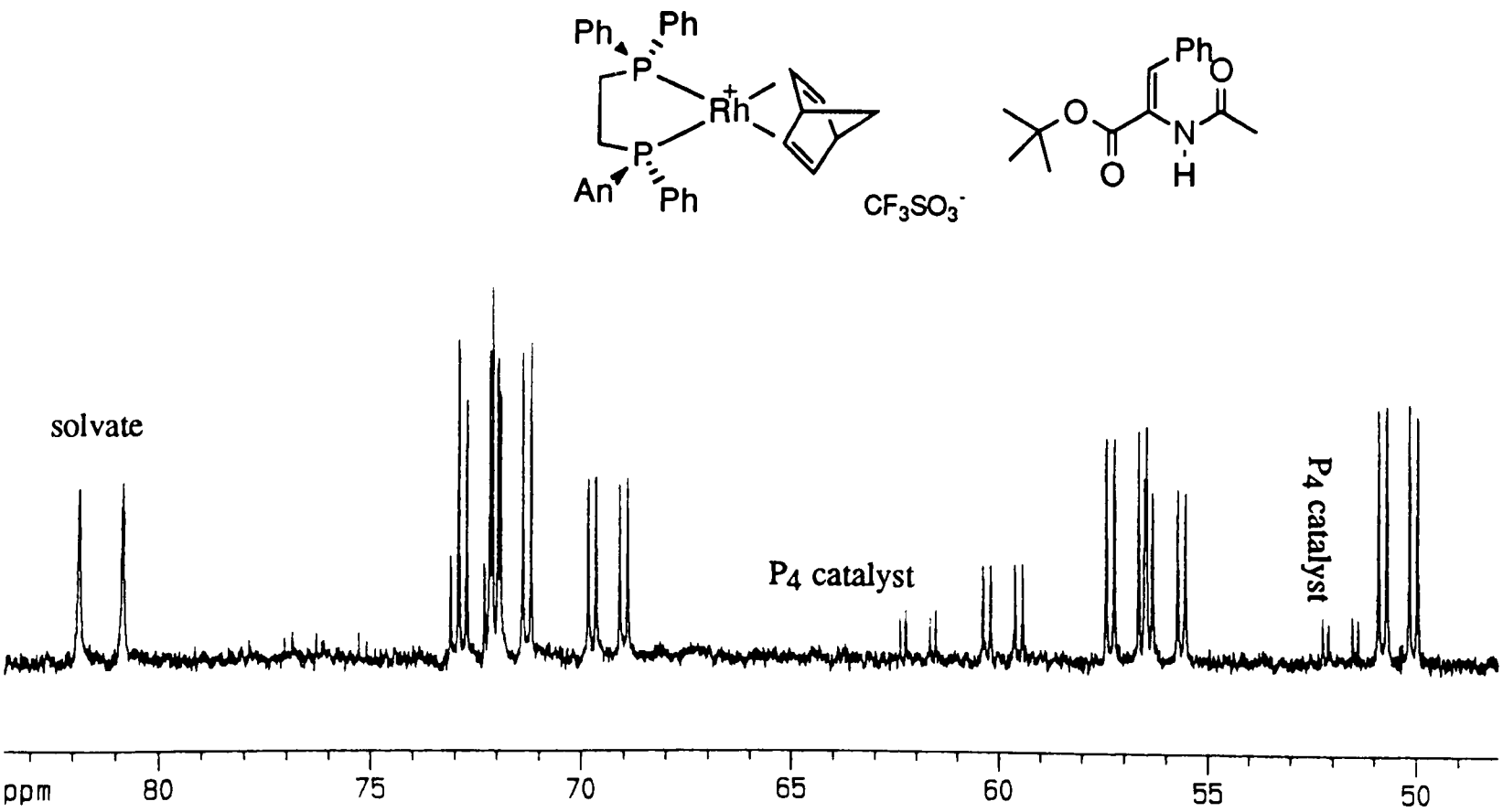


***Figure 42**: binding studies carried out on Rh(DIPAMP) and Rh(OXPAMP)*

Catalyst	Substrate	K_{BIND} / mol^{-1} l
Rh(DIPAMP)(NBD)TfO	butyl amide	2900
Rh(DIPAMP)(NBD)TfO	butyl ester	2500
Rh(OXPAMP)(NBD)TfO	butyl amide	3500
Rh(OXPAMP)(NBD)TfO	butyl ester	1500

Table II: *binding constants obtained from preliminary ^{31}P NMR studies*

The first point of interest is that both the butyl ester and amide appear to have comparable binding with each of the catalysts used. This contrasts with previous studies on [Rh(NBD)(DIPHOS)]TfO which showed the amide to bind twenty times more strongly than the ester[31].

Also, the binding of each substrate to both [Rh(NBD)(OXPAMP)]TfO and [Rh(NBD)(DIPAMP)]TfO is of the same order of magnitude, indicating the presence or absence of methoxy groups on the phenyl rings is not important with respect to binding properties. Others[57b] have suggested that the role of the methoxy groups may be steric rather than a coordinative interaction; *ortho*ethyl analogues of DIPAMP yield enantiomeric excesses almost as high as those obtained with rhodium DIPAMP catalysts.

NMR exchange experiments were also carried out on samples of the enamide complex prepared under argon in CD_3OD. Between 20 and 30 mg catalyst was dissolved in 300 µl distilled, degassed CD_3OD and activated by 'whirlimixing' under hydrogen. The hydrogen atmosphere was then replaced with argon and one equivalent of enamide in 300µl CD_3OD was added to the NMR tube under argon.

The NMR tube was then transferred to the NMR probe (202.46 MHz) which was preset to the required temperature (310K or 300K). A standard ^{31}P NMR spectrum was first obtained before any inversion experiments.

The inversion experiments were conducted by applying a selective 180 pulse (produced by a Q3 pulse of 40 ms supplied from a homebuilt pulse shaper unit) to the desired

doublet, followed by a variable time delay, τ, to allow any exchange to occur. A non selective 90 pulse was next applied in order to excite the whole spectum and the data was recorded using 160 scans per experiment.

The process was then repeated with varying increasing time delays for up to seventeen more acquisitions. The whole set of spectra was plotted out in blocked form (*vide infra*), thus allowing immediate observation of transfers in signal intensity. Changes in the intensity of any doublet other than the one which had been irradiated indicated that exchange was occurring between the sites concerned.

In the case of the C2 symmetric DIPAMP catalyst, any exchange was a two site process and analysis of the NMR data (*via* integration of the doublets concerned or by recording the relative peak intensities) followed by plotting changes in intensity against time resulted in a visual indication of the rates of transfer of magnetisation and hence the rates of exchange. As found previously in Brown's DANTE work[17], the *t*butyl amide was bound too strongly for any changes in its spectrum to be observable at the temperature of acquisition. The *t*butyl ester however did show exchange (***Figure 43***) and an analysis of the NMR data showed the initial rate of intensity change to be greater for the intramolecular exchange process (plot 2, ***Figure 43***), in keeping with previous DANTE work.

The situation was more complicated with Rh(OXPAMP)(NBD)TfO due to the catalyst being non C2 symmetric and the existence of four enamide complexes. The interpretation of any resultant four site exchange was liable to be very complicated. An NMR programme was devised to enable sequential excitation of one of the doublets corresponding to each of the four signals due to the four enamide complexes. The results obtained using the *t*butyl ester conducted at 310K are illustrated below (***Figure 44***).

The changes in signal intensity were relatively slight (intensity plots, ***Figure 44***). This, coupled with the fact that kinetic analysis of the NMR data would be very complicated, led to the conclusion that a quantitative analysis of the intensity/time plots would not bear

fruitful results. The intensity/time plots did however indicate that exchange appears to occur between one major diastereomer and its corresponding minor diastereomer and not between the two major diastereomers or the two minor diastereomers.

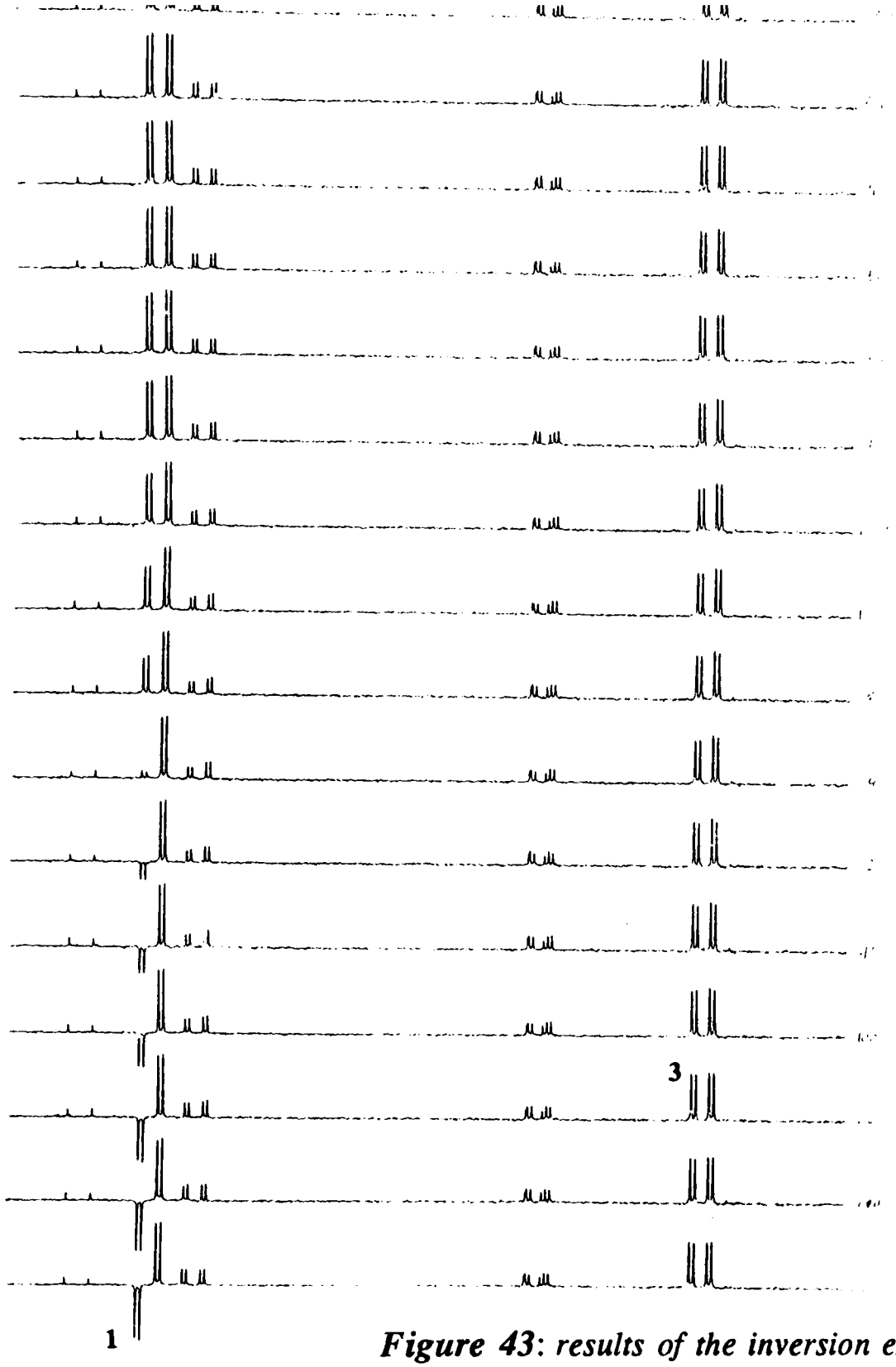
The initial rates of exchange appeared to be faster than in the case of the DIPAMP system. The separate signals in the OXPAMP experiment did not appear to exchange at significantly different rates from one another, thus indicating once more that the methoxy groups were not playing a significant role in substrate binding to this catalyst.

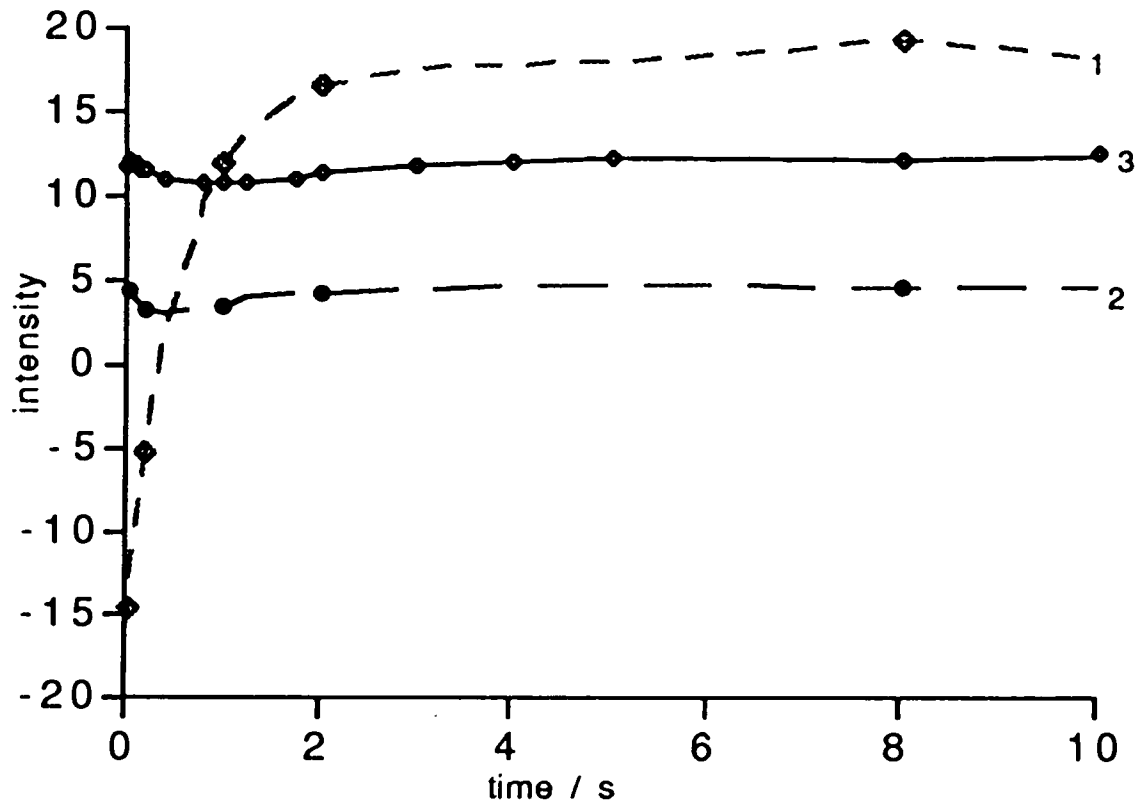
In conclusion, the work contained in this section does not appear to indicate that the methoxy groups in DIPAMP are ligated to such an extent that they influence binding of the substrate to the metal centre during the catalytic cycle; though the binding constants came from preliminary work that would need to be reconfirmed several times before being considered conclusive.

Attempts to observe the dihydride intermediate

As discussed in the introduction, although the mechanism of rhodium complex catalysed hydrogenation has been extensively studied, the intermediate corresponding to oxidative addition of hydrogen to the metal (the product from Step 2, ***Scheme XVII***) has never been observed. The chances of observing this intermediate are greatest in a catalyst / substrate system which exhibits very fast hydrogenation rates. Methyl DUPHOS catalysed hydrogenations had been found to be diffusion controlled as low as catalyst concentrations of 1 mol % and methyl - 2 - acetamido acrylate had been found to be a substrate which underwent very rapid hydrogenations (p48). Thus, it was decided to attempt observations of the dihydride using this acrylate / DUPHOS system (***Figure 45***).

Initial attempts were carried out by flushing NMR tubes containing enamide solutions (previously prepared under argon using a five molar excess of substrate over catalyst) with hydrogen at -90°C (dry ice / Et_2O / N_2) and agitating the tube gently to aid diffusion of the gas into solution. Using an excess of substrate over catalyst made it possible to





note: only a selection of the points plotted
are indicated by the graphing package

***Figure 43**: results of the inversion experiment carried out on Rh(DIPAMP)(NBD)TfO and the ^{t}butyl ester. The graph shows the intensity changes of affected signals for varying time delays*

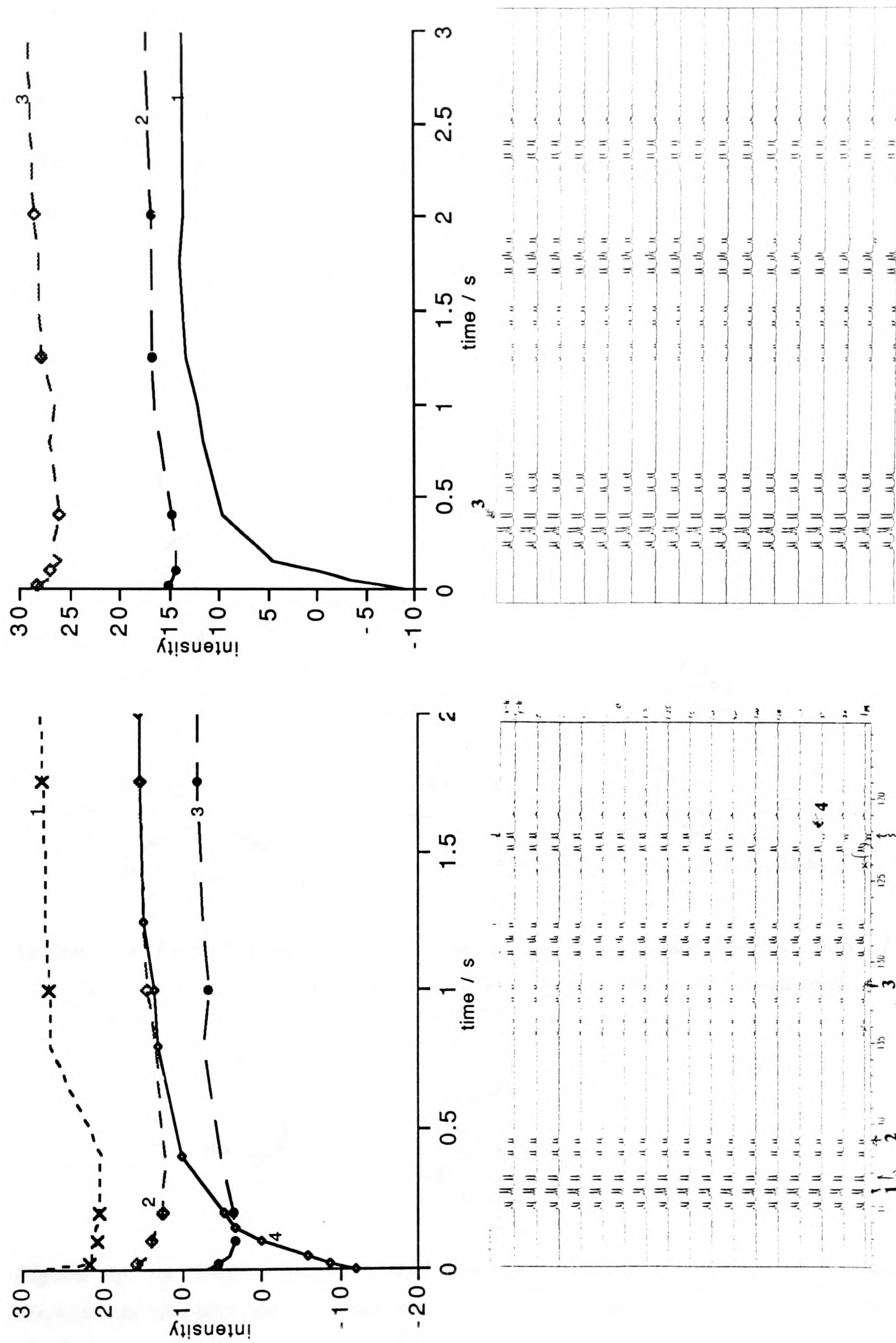
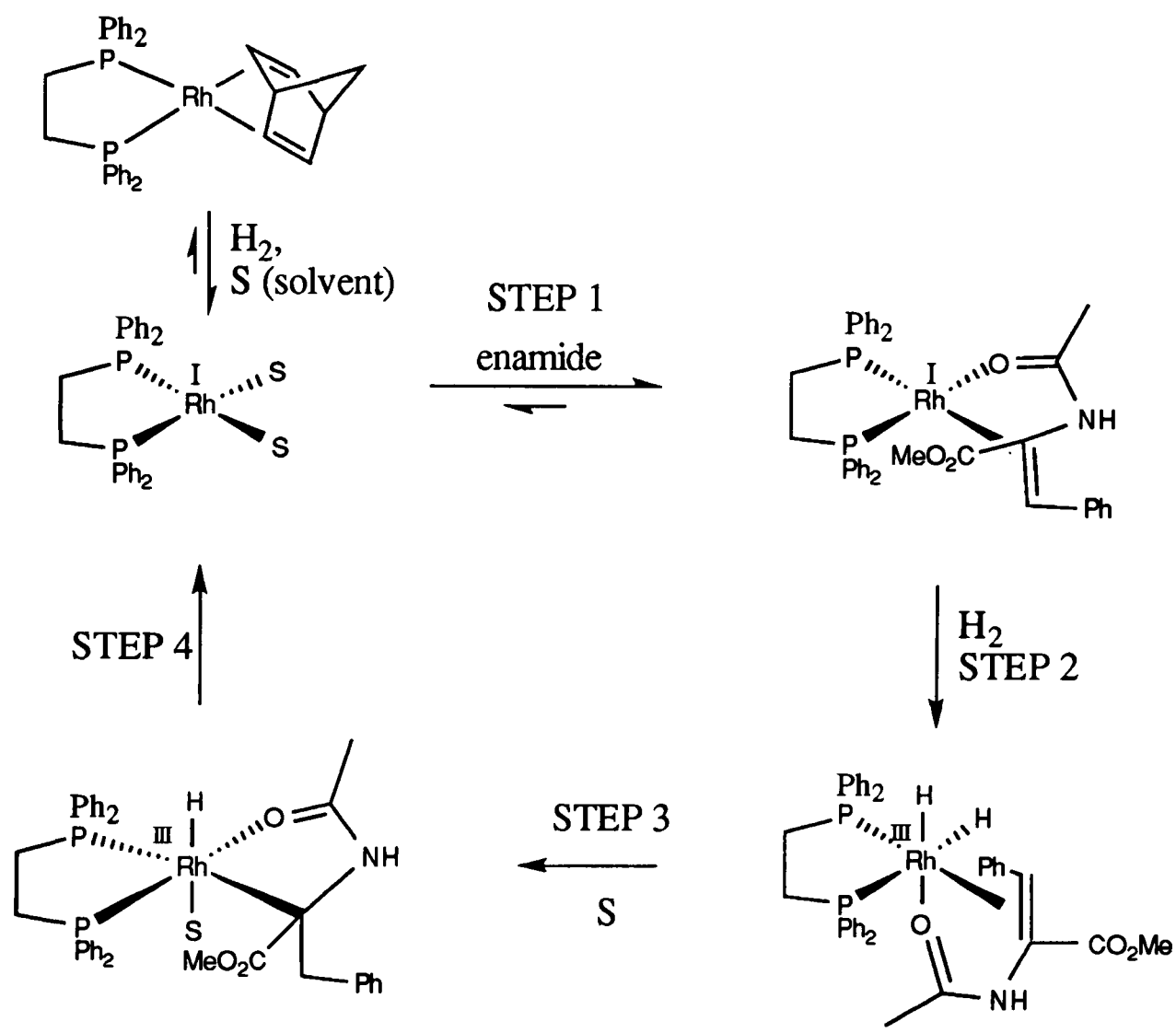


***Figure 44**: results of the inversion experiment carried out on Rh(OXPAMP)(NBD)TfO and the ^{t}butyl ester. The graph shows the intensity changes of affected signals for varying time*

allow for some hydrogenation of the substrate occurring. The tubes were kept at -90°C and then transferred as quickly as possible to the NMR machine (Bruker AMX 500 MHz) whose probe had been previously cooled to -80°C. ^{31}P NMR spectra were then obtained in blocks of 800 scans. No colour change was observed on placing the enamide solution under a hydrogen atmosphere; nor was there any significant change from the ^{31}P spectra obtained from binding studies under argon (p50).



Scheme XVII *extensive investigation into the mechanism of rhodium complex catalysed homogeneous hydrogenation has yielded the pathway above as the most favoured route*

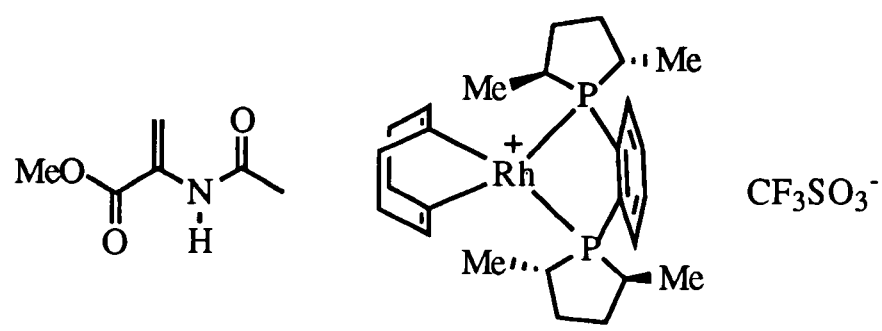


Figure 45: *the Rh(DUPHOS)(NBD)TfO catalysed reduction of methyl-2-acetamido acrylate was very fast and could therefore be useful in attempts to observe the rhodium dihydride*

A problem with using 5 mm NMR tubes is that diffusion of hydrogen gas into the solution becomes the rate limiting factor and thus the concentration of hydrogen in solution can be very low. It was hoped to overcome this problem by presaturating the solutions with hydrogen: a solution of rhodium solvate was prepared and kept under hydrogen in the NMR tube and then a solution of the enamide (in the minimum amount of deuterated methanol) was added to the tube. The NMR tube was then flushed with hydrogen again and transferred to the previously cooled NMR probe. Samples prepared in this way still showed no observable trace of dihydride. Warming the solution up to -65°C did not lead to any changes in the NMR spectra.

Next, attempts were carried out using the rhodium catlayst of the achiral ligand 1,3 bis(diphenylphosphino)propane (***Figure 46***), prepared according to Brown's method[50] and obtained as a bright orange solid δ_P (202.46 MHz, CD_3OD) 12.8 ppm, d, J_{Rh-P} = 149 Hz. Reductions using this ligand would be expected to be very fast, due to the larger chelate ring. The spectra obtained in NMR investigations would also be simpler using an achiral ligand.

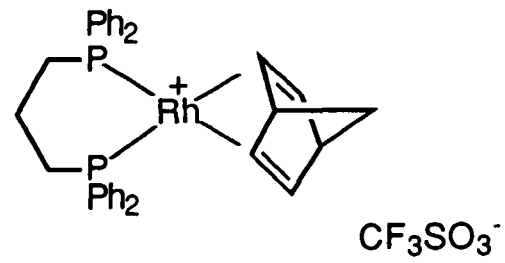
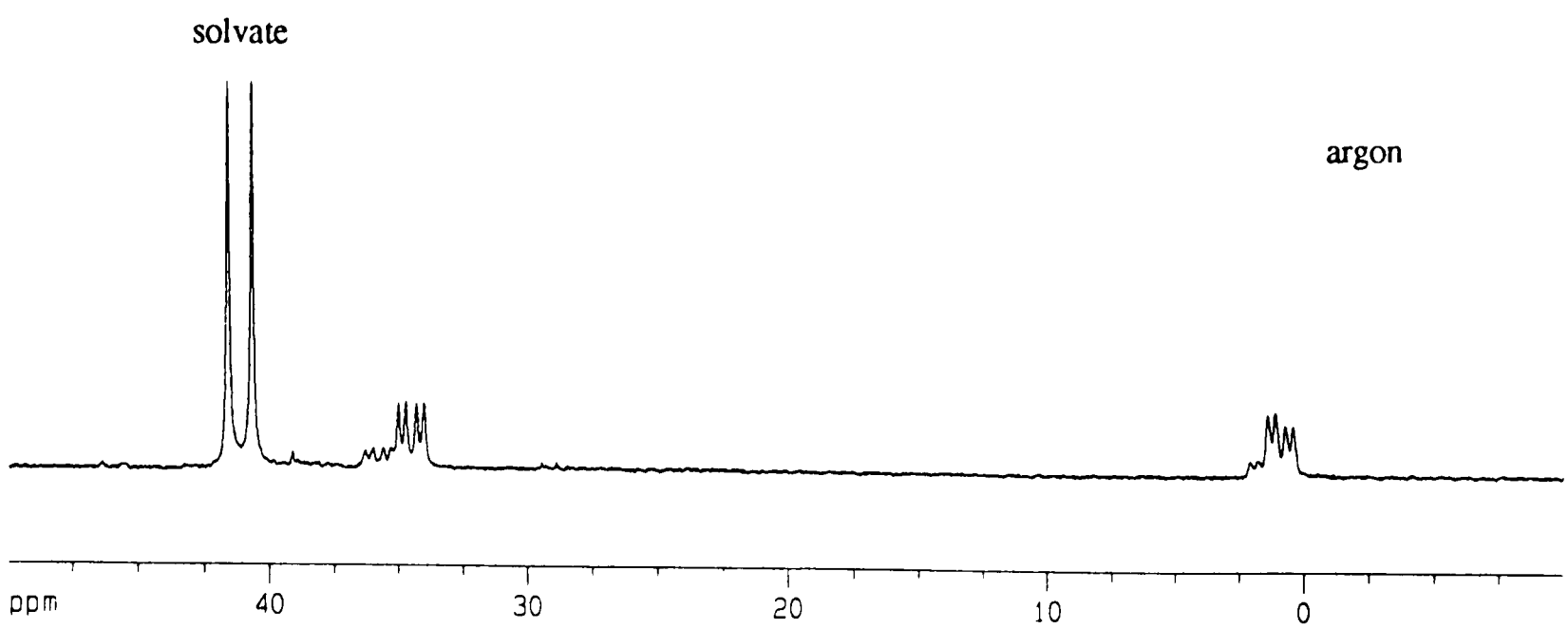


Figure 46: *the rhodium catalyst formed from 1,3-bis(diphenylphosphino)propane catalyses very fast enamide reductions*

^{31}P NMR spectra were obtained on samples prepared by presaturating the catalyst solution with hydrogen before the addition of a five molar excess of acrylate. The initially orange solution went paler on hydrogen activation but no colour change indicative of complex formation was observed on addition of the acrylate to the NMR tube. A spectrum acquired at 298K revealed a solvate species (δ 40.6, d, J_{Rh-P} = 190.9 Hz) and two double doublets corresponding to the enamide complex (δ 31.9, 5.8, J_{Rh-P} = 143.8 Hz, J_{P-P} = 63.2 Hz). Spectra acquired at -80°C (***Figure 47***) showed the peaks due to solvate, two double doublets corresponding to enamide complex and two smaller double



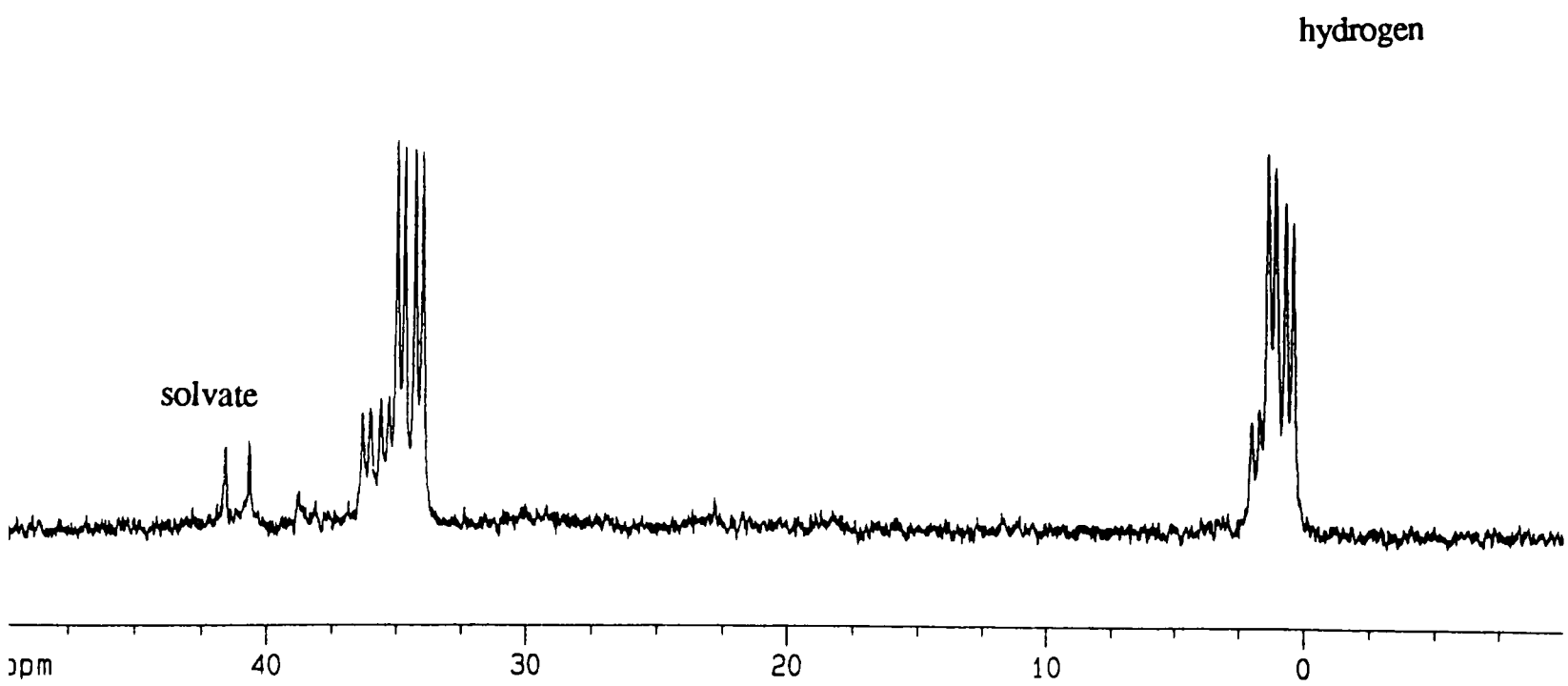


Figure 47: *different conformations of the chelate ring in Rh(PROPAPHOS)(NBD)TfO were frozen out at -80°C*

doublets with coupling constants similar to those of the larger double doublets (J = 59 Hz). Peaks corresponding to hydride species would be expected to have coupling constants in the region of 100 Hz. It was thought that the smaller intensity peaks were due to different conformations of the six membered ligand chelate being frozen out at -80°C, rather than peaks corresponding to a dihydride species; this was confirmed experimentally by conducting a normal binding study under argon on this system at -80°C (***Figure 47***).

Another possible system that exhibited fast hydrogenations was that of PROPHOS and methyl - 2 - acetamido acrylate (***Figure 48***), previously shown to be dynamic down to -80°C (p44). It was hoped that ^{31}P spectra of solutions of this system prepared under a hydrogen atmosphere would show the double doublets corresponding to the minor diastereomer disappearing as the hydrogenation proceeded.

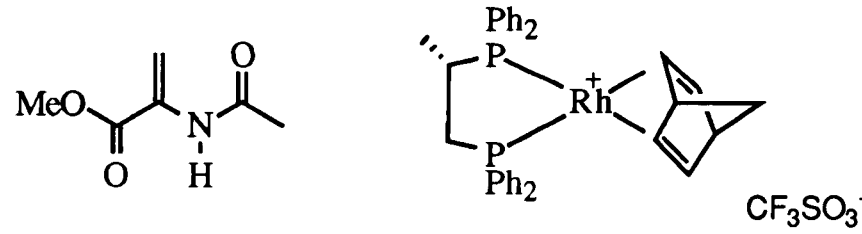


Figure 48: *the final system used to attempt to observe the dihydride was the prophos/acrylate combination*

The experiment was conducted in two ways. Firstly, experiment A, a sample was monitored immediately after preparation with each acquisition lasting 1500 scans. Secondly, experiment B, a sample was prepared and left for three hours (under hydrogen) before acquisition was begun, to allow some catalytic turnover ot occur. At -80°C, spectra obtained essentially resembled those of binding studies conducted under argon (***Figure 49***). Warming the sample from experiment A up to -50°C showed a change in intensity of one of the double doublets at the expense of formation of a broad dynamic peak (***Figure 49***), corresponding to the species with that double doublet carrying the flux of the catalysis. Warming up the sample from experiment B to -50°C showed the change in intensity of the signals to be more marked than in experiment A (***Figure 49***). Coupling constants of the new signals equalled 89.5 Hz, which is

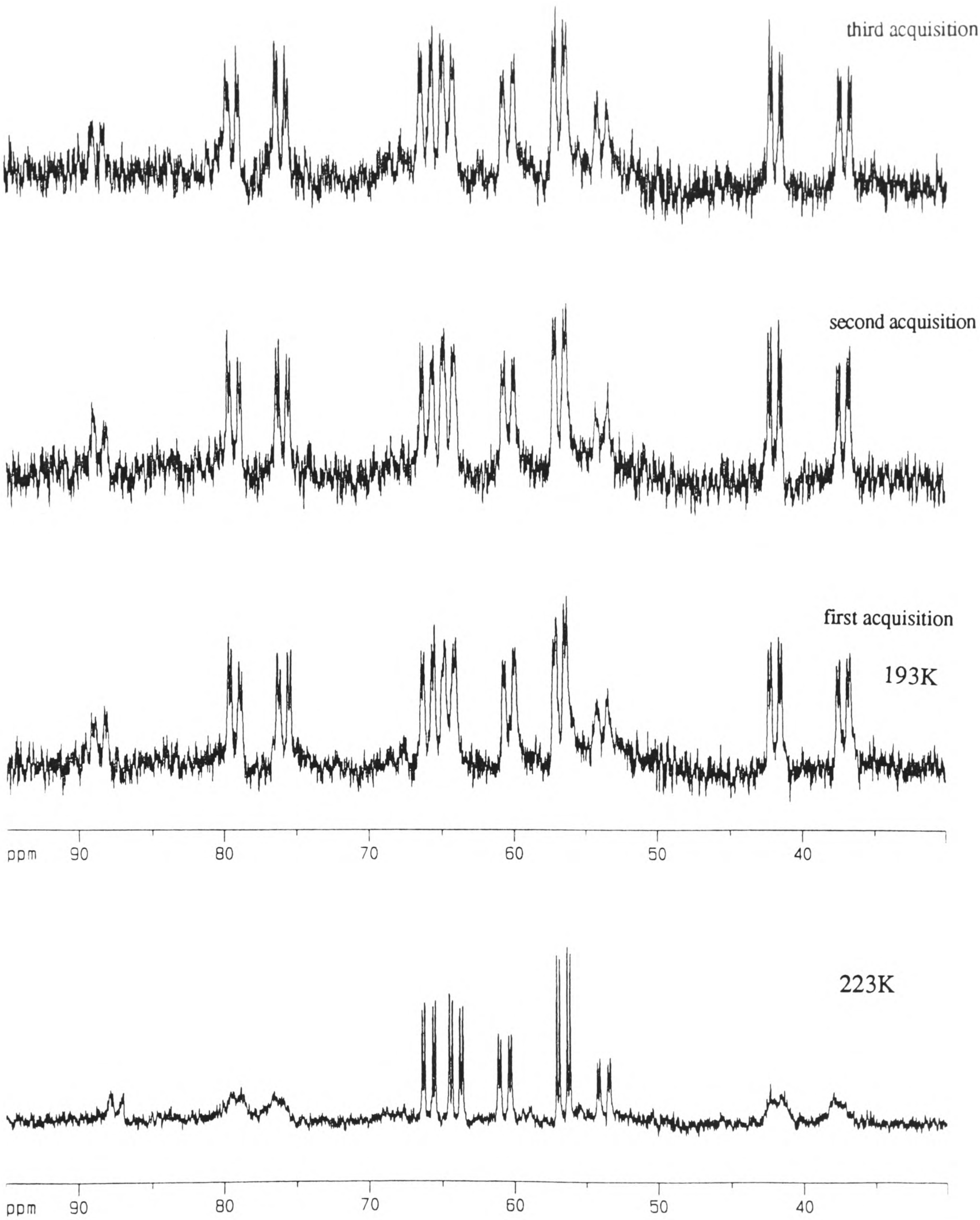


Figure 49: *the prophos/acrylate system exhibited peaks corresponding to the alkyl hydride but no traces of the dihydride were observed*

indicative of the alkyl hydride (product from Step 3, ***Scheme XVII***) rather then the intermediate dihydride *ie* once again the dihydride was proving elusive.

It was possible that the main reason why attempts to observe the dihydride were unsuccessful was due to the concentration of hydrogen in solution not being high enough. With 5mm NMR tubes, not only is it difficult to get enough hydrogen into the solution to then consider it saturated, but also the dead volume in the tube above the solution is so small that it is almost impossible to get a high enough hydrogen concentration to ensure efficient diffusion of hydrogen across the gas/liquid interface. One way of improving this situation is to use 8mm NMR tubes in the Bruker 250 MHz spectrometer.

Repeating the PROPHOS/acrylate experiment on the Bruker AM 250 MHz spectrometer using an 8 mm NMR tube which had been left under a hydrogen atmosphere at -80°C for five hours before acquisition was begun at -50°C, once again failed to yield peaks in the ^{31}P NMR corresponding to the intermediate dihydride. It had been hoped that using a wider bore NMR tube would enable any traces of the intermediate to be observed more easily as the concentration of hydrogen in solution was now greater than in the case of 5 mm tubes.

The final attempt to observe the dihydride worked on the premise that the chances of it being intercepted might be greater if the system was looked at as soon as the substrate had gone into solution under hydrogen. The reaction was carried out on the Bruker AM 250 (101.23 MHz, CD_3OD) using 8 mm NMR tubes. The catalyst solution was presaturated with hydrogen by repeated 'whirlimixing' under hydrogen and then excess acrylate was added as a solid. The system was degassed with hydrogen once more before being allowed to stand until the acrylate began to dissolve. As soon as it had almost gone into solution, the NMR tube was transferred to the precooled probe and acquisition was begun at 266K. Blocked spectra showed peaks due to the solvate and enamide complexes, but no evidence of any dihydride was seen.

With time, the solvate peaks diminished in intensity, in accordance with more of the substrate going into solution and forming the enamide complex. The system was then warmed up to 246K in order to try and force turnover to begin and thus enable any dihydride to be trapped. However, there was still no trace of any species that might correspond to a dihydride intermediate. A ^1H NMR of the sample was later obtained and showed only reduced substrate, thus indicating that the hydrogen concentration in solution *had* been sufficiently high to allow catalytic turnover.

It had been hoped to repeat the experiments at elevated hydrogen pressures at a later date.

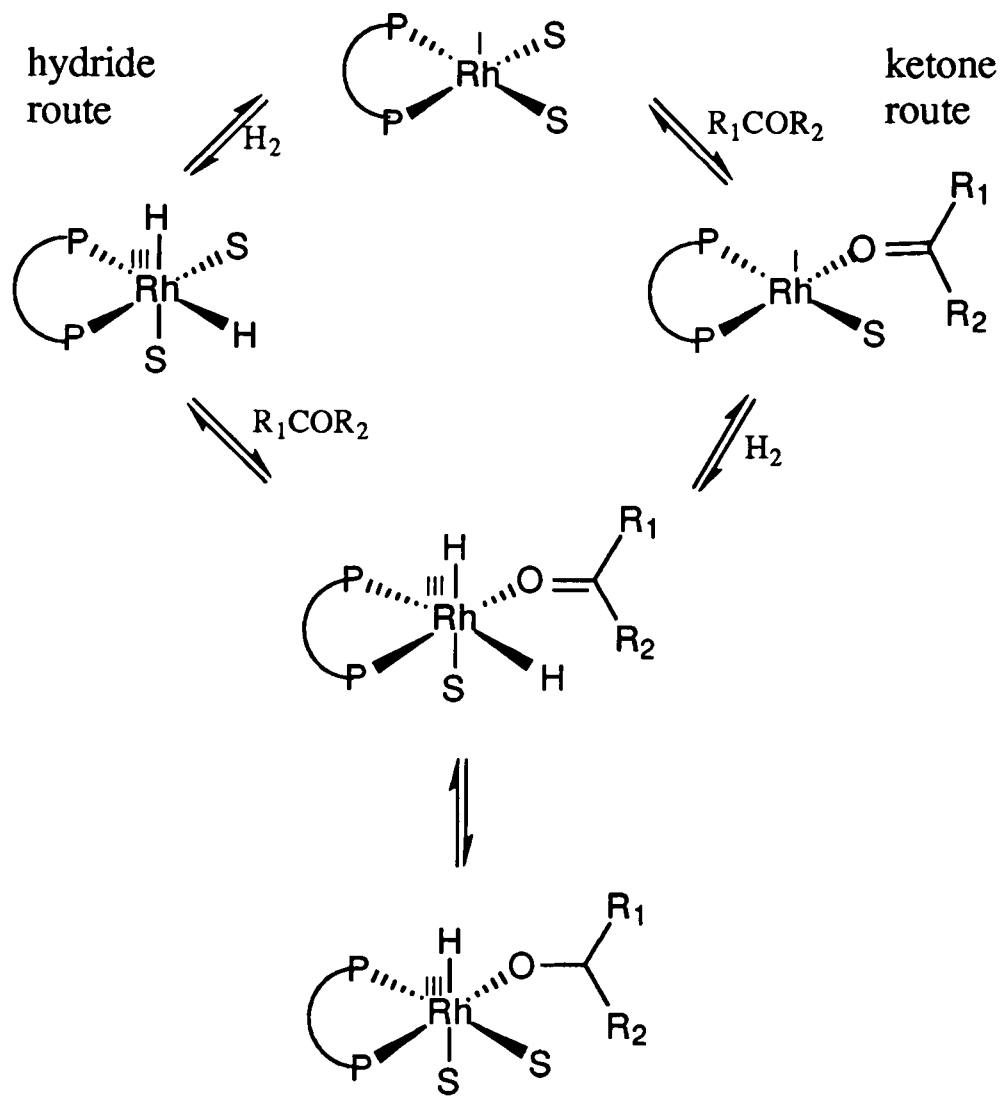
Investigations into the rhodium complex catalysed reduction of carbonyl compounds

Little mechanistic work has been carried out in the area of metal complex catalysed reduction of ketones, as mentioned in the introduction. This area was the next focus of attention. It was hoped to propose a mechanism by combining kinetic studies on hydrogenations with the isolation and characterisation of intermediates in the reaction (using, for example, NMR and electrospray techniques). By comparison with alkene hydrogenation, the two pathways to be considered were the hydride and ketone route (***Scheme XVIII***). The usage of basic alkyl diphosphine ligands enables hydrogenations to be carried out at atmospheric pressure and ambient temperature[33,34b], though the alkyl groups render both the free ligand and the resultant rhodium catalyst much more air sensitive than their aromatic counterparts.

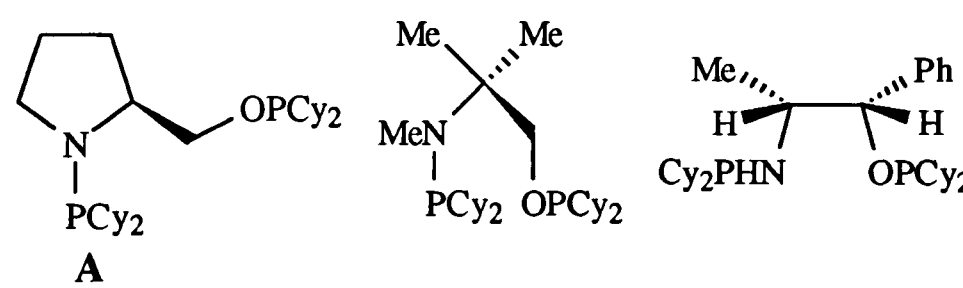
Recent work by Mortreux and Petit[61] utilises chiral aminophosphine-phosphinite ligands (AMPP) such as those shown in ***Figure 50***. The ligands are readily prepared by the action of R_2PCl on cheap and readily available optically active amino alcohols. Generally, the cyclic more rigid derivatives are favoured ligands for asymmetric hydrogenation, due to the higher enantiomeric excesses they afford.

Due to the constraints of the apparatus to be used (a maximum working pressure of two atmospheres of hydrogen), the extensive work previously carried out by Mortreux[34b,61]

and the high turnover observed using AMPP ligands, the ligand chosen for mechanistic studies (also favoured by Mortreux and Petit) was the cypronop ligand, **A**, ***Figure 50***. Following the synthesis of the air sensitive ligand[61] and catalyst[50] [Rh(NBD)CyProNOP]$^+$TfO$^-$, hydrogenations were carried out to investigate the effects of solvent, temperature and added base (triethylamine) on reaction rates.



Scheme XVIII: *the reaction scheme for ketone reduction could proceed through two possible routes, of which the ketone route is the preferred pathway*



A

Cy = cyclohexyl

Figure 50: *AMPP ligands are easily produced from cheap, readily available optically active amino alcohols*

Preliminary hydrogenations were carried out on simple, commercially available ketones (such as benzil) to get an idea of the effect on reaction rates of changing the conditions

under which reductions were carried out. All reactions were performed in the constant volume apparatus.

Initial investigations carried out on the reduction of ketones using the catalyst [Rh(NBD)CyProNOP]$^{+}$TfO^{-} used a catalyst which was not completely pure. Whilst satisfactory for catalytic work, the system was not pure enough for quantitative kinetic studies. Attempts to purify both the ligand and the rhodium catalyst were hampered by the extreme sensitivity of the N-P bond under mild acid conditions.

In the absence of a catalytic system pure enough to be used for quantitative studies on ketone hydrogenation and in view of the interesting developing results in ruthenium work (*vide infra*), this area of work was not pursued further.

Ruthenium chemistry

As mentioned previously (p18), four major classes of ruthenium catalyst have been reported to be successful in the hydrogenation of alkene and carbonyl double bonds. They are Genet's Ru(methylallyl)$_2$ catalysts[63], Noyori's Ru(acetate)$_2$[35], cationic Ru complexes of the type [RuX(BINAP)(arene)]Y[64] the Ru(allyl)(acac) or Ru(allyl)(facac) systems developed by Brown[38] (***Figure 51***). The first ruthenium complex to be used as an effective hydrogenation catalyst towards enamides was Ru(BINAP)Cl$_2$.NEt$_3$. This catalyst was superseded by the development of Noyori's Ru(BINAP)(OAc)$_2$ catalyst and the related bis(trifluoroacetate) analogue, though it still remains the catalyst of choice when considering carbonyl reductions. [RuX(BINAP)(arene)]Y is also an effective catalyst towards the reduction of carbonyl groups and is more conveniently prepared than Ru(BINAP)Cl$_2$.NEt$_3$ (*vide infra*). In general only BINAP and related bisphosphine ligands are highly effective in terms of both yields and enantiomeric excesses, though Burke's DUPHOS ligands and Cesarotti's biheteroaryls lead to impressive enantiomeric excesses on the reduction of carbonyl groups[62].

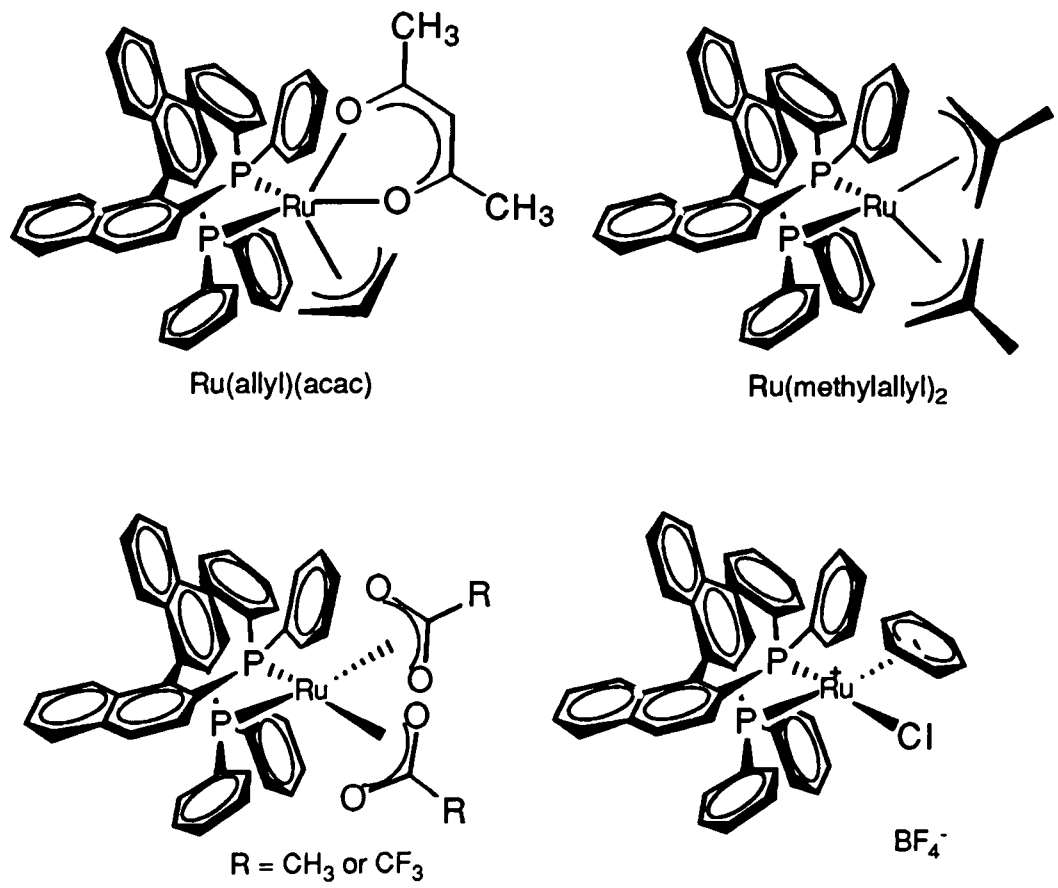


Figure 51: *most successful ruthenium catalysts employ BINAP and its analogues as the ligands on the metal*

Very little investigative work has been carried out on the mechanism of ruthenium catalysed hydrogenation[37,40]. In order to probe the catalytic pathway, it was decided to synthesise the ruthenium BINAP catalysts corresponding to the four catalytic systems above. Hydrogenations and investigations into the identity of reaction intermediates would then be carried out to see whether reactions catalysed by the different systems proceeded through common intermediates. The experimental protocols followed in this investigation were determined by those found to be successful in the analogous rhodium case *ie* a combination of kinetic analysis and NMR characterisation of intermediates in the catalytic cycle.

The majority of ruthenium complex catalysed reductions require both high temperatures and elevated pressures. One type of substrate that can be reduced at ambient temperature and pressure is the simple dehydroamino acid derivative used in the investigation of rhodium complex catalysed alkene reductions. Thus, for convenience, this class of substrates was also picked for ruthenium complex catalysed investigative work.

The straightforward synthesis of these substrates has been described previously (p34). Having obtained samples of the substrates required for this work, synthesis of the ruthenium BINAP catalysts was envisaged using standard organometallic techniques, bearing in mind the fact that ruthenium complexes are considerably more air sensitive than rhodium catalysts and the requirement of *pure* catalysts for the obtention of quantitative, meaningful results.

Catalyst syntheses

Brown's Ru(BINAP)(allyl)(acac) catalyst was prepared by refluxing BINAP and (η^4-bicyclo[2.2.1]hepta-2,5-dienyl(η^3-2-propenyl)acetylacetonatoRu^{II} in toluene overnight[38]. The (η^4-bicyclo[2.2.1]hepta-2,5-dienyl(η^3-2-propenyl)acetylacetonatoRu^{II} itself was prepared as shown in ***Scheme XIX***. Note that ruthenium complexes are much more prone to oxidation than rhodium complexes. All solvents were therefore freshly distilled and thoroughly degassed and all the manipulations in ***Scheme XIX*** after formation of

the Ru^{II} polymer were carried out on a vacuum line under argon using standard techniques and glassware[65,66]. Glass stoppers were used rather than subaseals and reactions were carried out in the minimum amount of solvent in the smallest size of appropriate glassware. All ruthenium intermediates and all of the catalysts were stored under argon in the fridge and were indefinitely stable when kept this way (monitiored by ^{31}P NMR).

Having obtained the Ruacac precursor, the reflux to obtain Ru(BINAP)(allyl)(acac) was performed under argon (***Scheme XX***). Removal of the solvent *in vacuo* and washing with degassed pentane yielded the product as a yellow powder δ_P(202.46 MHz, toluene) 64.4(d, J = 37 Hz), 37.2(d, J = 37 Hz). Chiraltiy exists at the ruthenium in this class of catalysts. If the ligand precursor is achiral (such as in the DPPF analogue - *vide infra*), a racemate is formed and ^{31}P NMR reveals a single AB quartet. If, as in this case, an optically active bisphosphine is used then two diastereomeric complexes result and depending on the diastereomeric ratio, two AB quartets may be observed in the ^{31}P NMR. Using BINAP as the ligand the diastereomeric ratio appeared to be 10:1 at 101.23 MHz. This catalyst requires activation before being used in hydrogenation reactions[38]. Activation is carried out by adding two equivalents of trimethylsilyltrifluoromethane sulphonate to the ruthenium catalyst in dichloromethane, stirring for fifteen minutes and then removing the solvent *in vacuo* to leave a yellow oil which is finally dissolved in the solvent required for reduction (usually methanol). The active catalyst is believed to have the form shown in ***Figure 52***. NMR (^{31}P and ^{19}F) and electrospray mass spectrometry investigations[38] indicated that the allyl group drops off, on activation, to be replaced by the triflate, which is possibly chelate coordinated but labile. In dilute methanol (the conditions of the electrospray mass spectrometry probe) the TfO^- dissociates, giving the molecular ion shown in ***Figure 52***.

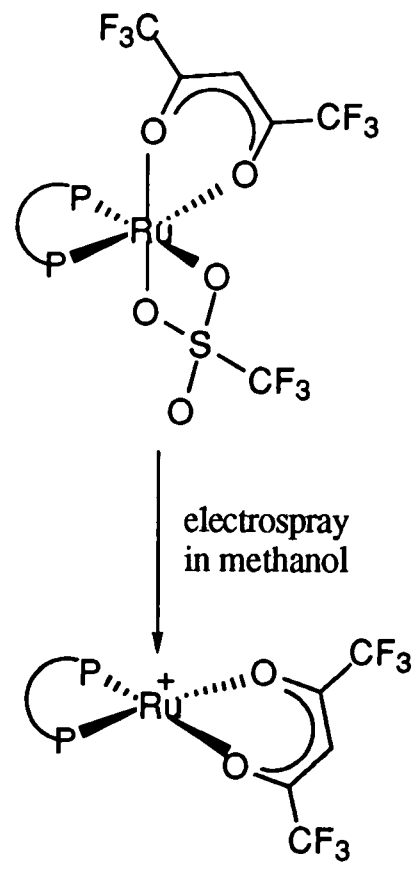
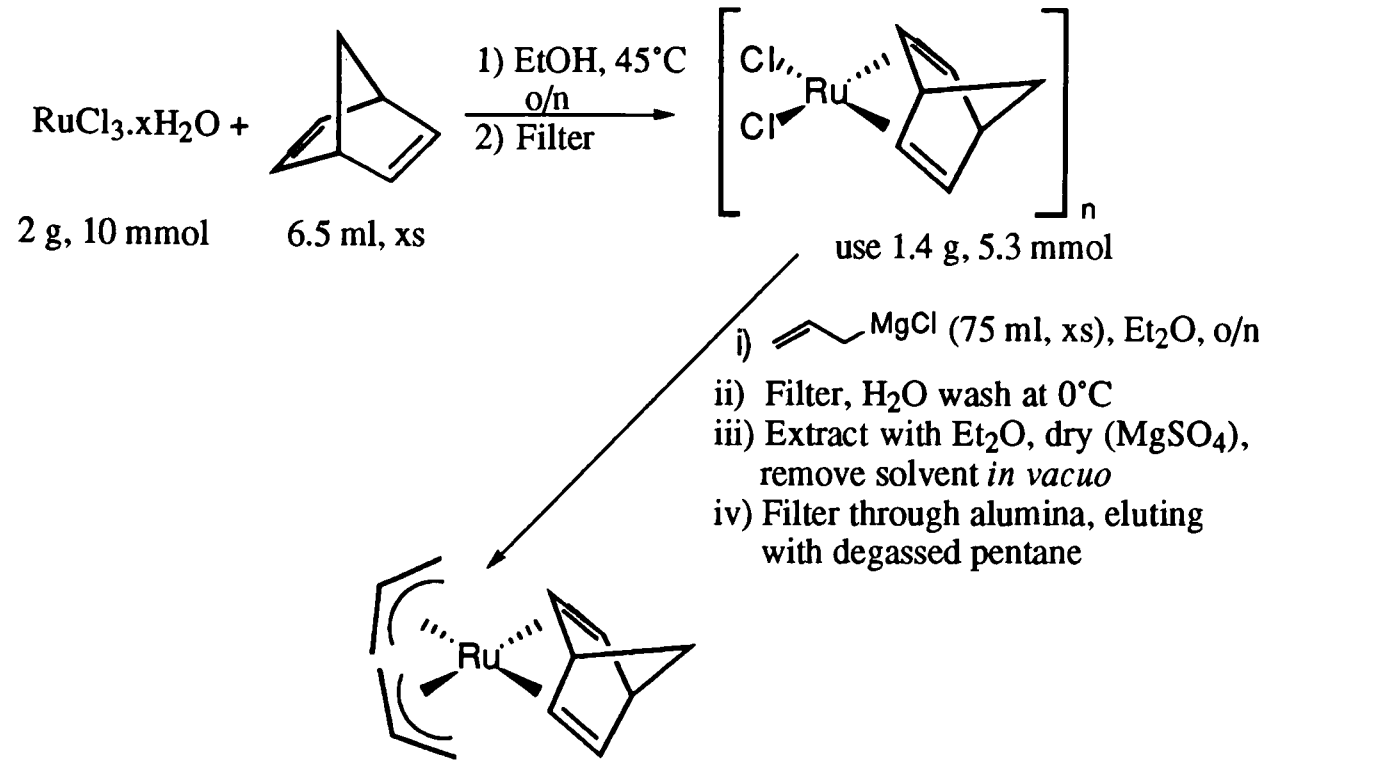


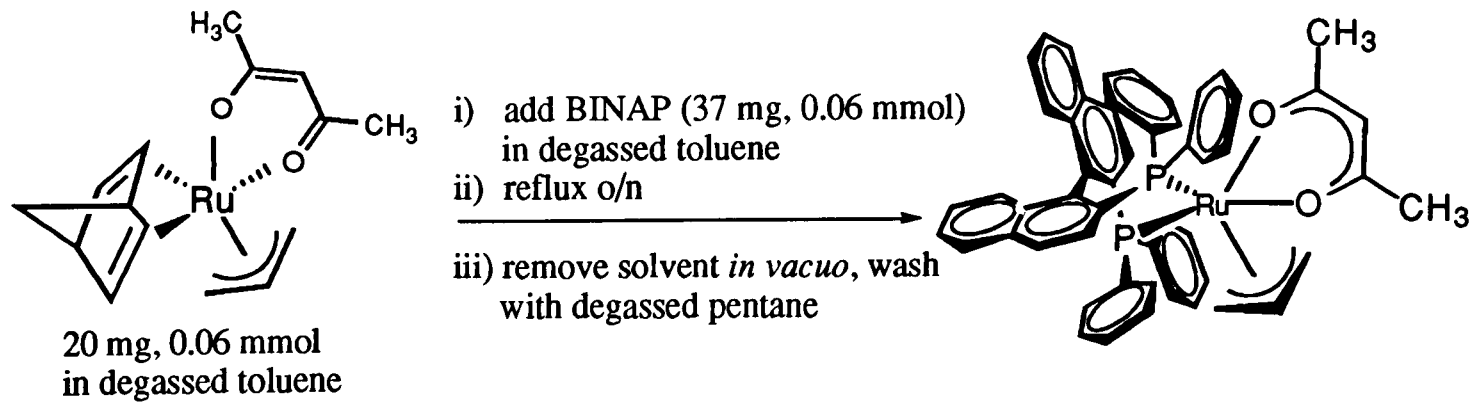
Figure 52: *Brown's ruthenium catalysts require activation by TMSTfO to become active catalysts towards alkene reduction.*

The next catalyst to be synthesised was Genet's bis(methylallyl). Initial attempts were made using the bis(allyl) system prepared as shown in ***Scheme XXI***. Ruthenium bis(allyl)(bicyclo[2.2.1]hepta-2,5-dienyl) and BINAP were stirred under argon at 100°C for five hours in accordance with the literature procedure[63]. Very little product was observed (by ^{31}P NMR, 101.23 MHz) and the reaction mixture contained mostly starting material (δ -14.3 ppm). The reaction was repeated in an 8 mm NMR tube and monitored by ^{31}P NMR (101.23 MHz, using an external lock, D_2O, in a 10 mm NMR tube jacket). After 48 hours two doublets at 70.2 ppm and 58.2 ppm (J = 52 Hz) were observable in the NMR, along with a peak corresponding to unreacted BINAP. The starting material peak diminished over the next three days to show, by ^{31}P NMR, a 66% conversion to product but the reaction was not a clean one, as observed by the NMR. Using excess ligand to try and drive the reaction to completion did not result in better yields or a cleaner reaction. Genet himself claims[63] that 'most of these ruthenium(II) complexes were isolated in an analytically pure state except BINAP'.

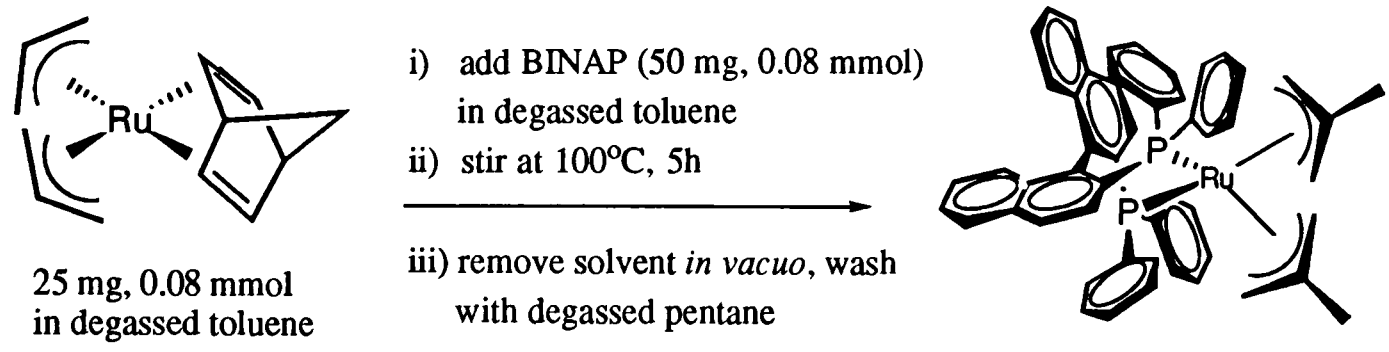


* prepared from Ph_3COH, propionic anhydride and $HBF_4.Me_2O$.
Stored under argon in the fridge

***Scheme XIX**: the synthesis of Ru(acac)(allyl) involves several air sensitive stages*



***Scheme XX:** a variety of phosphines will chelate to this ruthenium precursor, on refluxing the mixture in THF or toluene*



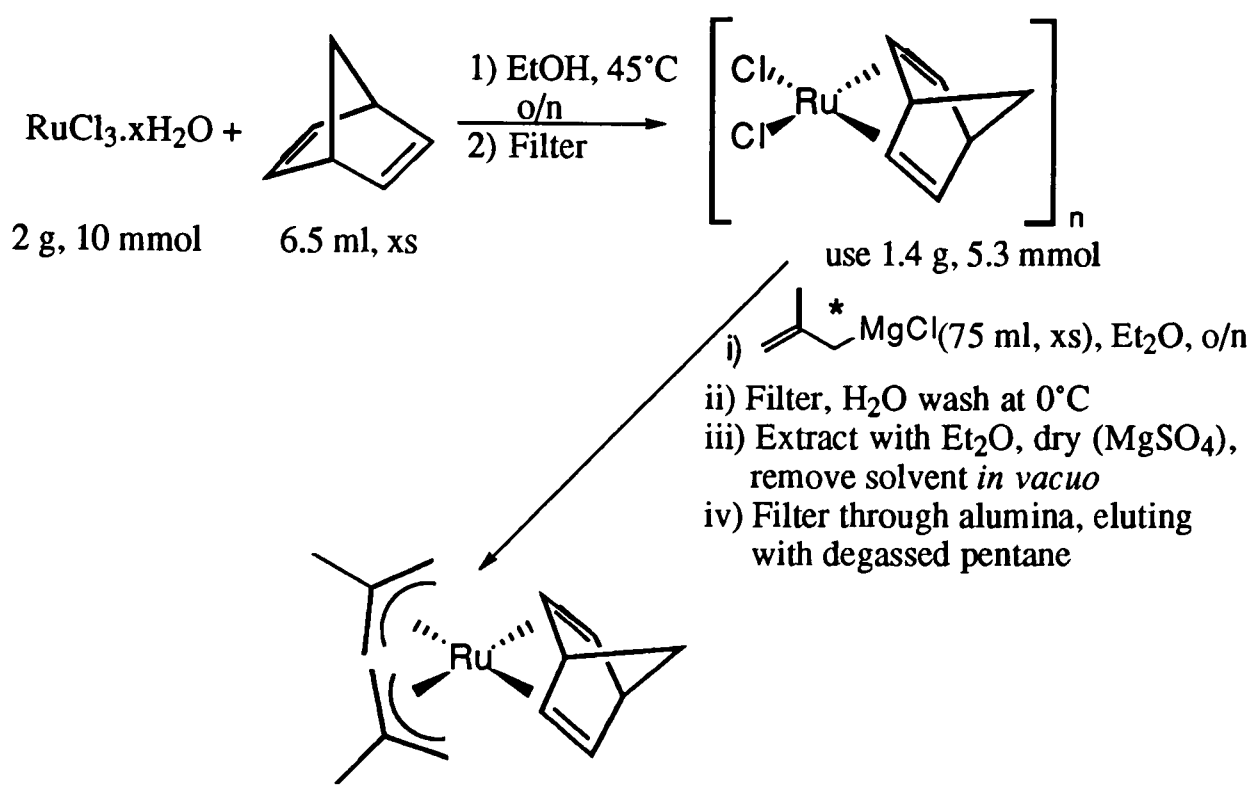
Scheme XXI: *problems were encountered in trying to reproduce Genet's catalyst synthesis*

Attempts to reflux the red/brown reaction mixture led to a much messier NMR. Purification of the product by recrystallisation under argon using dichloromethane/pentane (distilled and degassed) were unsuccessful. Conducting columns under argon (eluting with ethyl acetate) enabled the species showing two doublets in its ^{31}P NMR to be obtained. However the literature claims that the methyl allyl system leads to a product with a chemical shift at 40 ppm which is a singlet. Either Genet's results were wrong, a dimeric ruthenium species had been formed containing two distinct types of phosphorus atoms that coupled to each other or, when forming the bis(allyl) product, the phosphorus atoms were inequivalent due to the allyl groups being coordinated to the ruthenium differently (*eg* one allyl group could be sideways on). Investigations into the actual structure of the species by electrospray mass spectrometry revealed a peak of mass 741 which corresponded to $[(M+H)^+$-2(allyl) + O] and an unidentified peak at 858.

It is possible that Genet initially tried his catalyst synthesis with $Ru(allyl)_2(nbd)$ and, failing to get clean reactions, moved onto the methylallyl complex. Thus, it was decided to move onto a synthesis starting with the methylallyl ruthenium species. This ruthenium precursor was prepared according to ***Scheme XXII***.

The reaction mixture was stirred at 100°C and monitored by ^{31}P NMR once more. A peak at 42.4 ppm was observable after 12 hours, though after several days two doublets at 58.3 ppm and 70.2 ppm (J = 50.2 Hz) could also be seen. These grew in intensity with respect to the reported peak at roughly 40 ppm over the next few days. The refluxed

reaction mixture was once more a much dirtier reaction than the reaction stirred at 100°C. Purification attempts were unsuccessful. Failure to obtain this catalyst pure meant that the system was of no further use in quantitative investigations into the ruthenium catalysed alkene reduction mechanism.



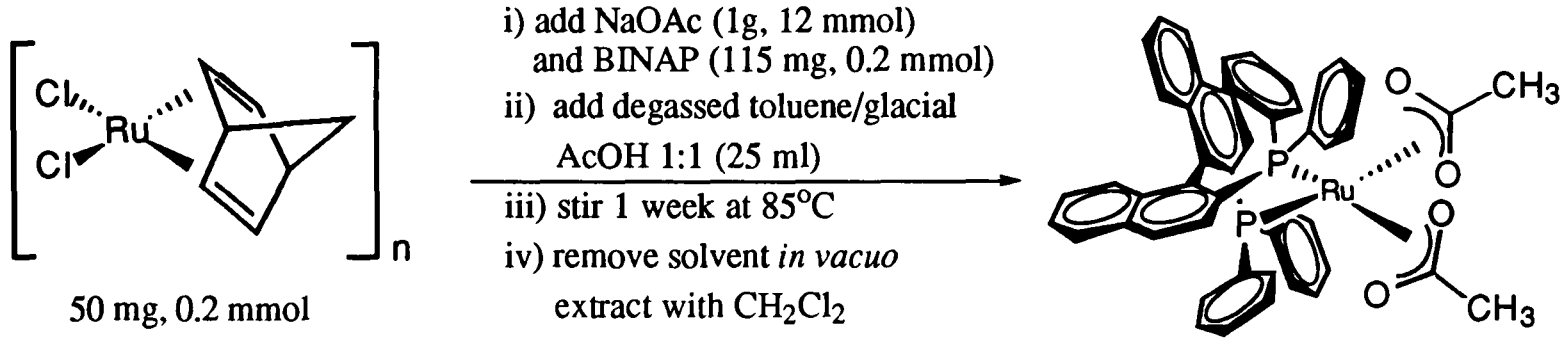
* MgCl prepared from allylchloride and Mg following the dry stir method of magnesium activation[67]

Scheme XXII: *the preparation of ruthenium bis(allyl)(bicyclo[2.2.1]hepta-2,5-dienyl)*

Noyori's $Ru(BINAP)(OAc)_2$ catalyst (***Scheme XXII***) is highly air sensitive and notoriously difficult to prepare pure, especially following Noyori's own method without access to a glovebox[35]. In the absence of a glovebox, it was decided to avoid Noyori's synthesis and look for alternative, facile routes to this catalyst. The first synthesis of this catalyst to be attempted was one recently published by Chan[68] and shown below (***Scheme XXIII***).

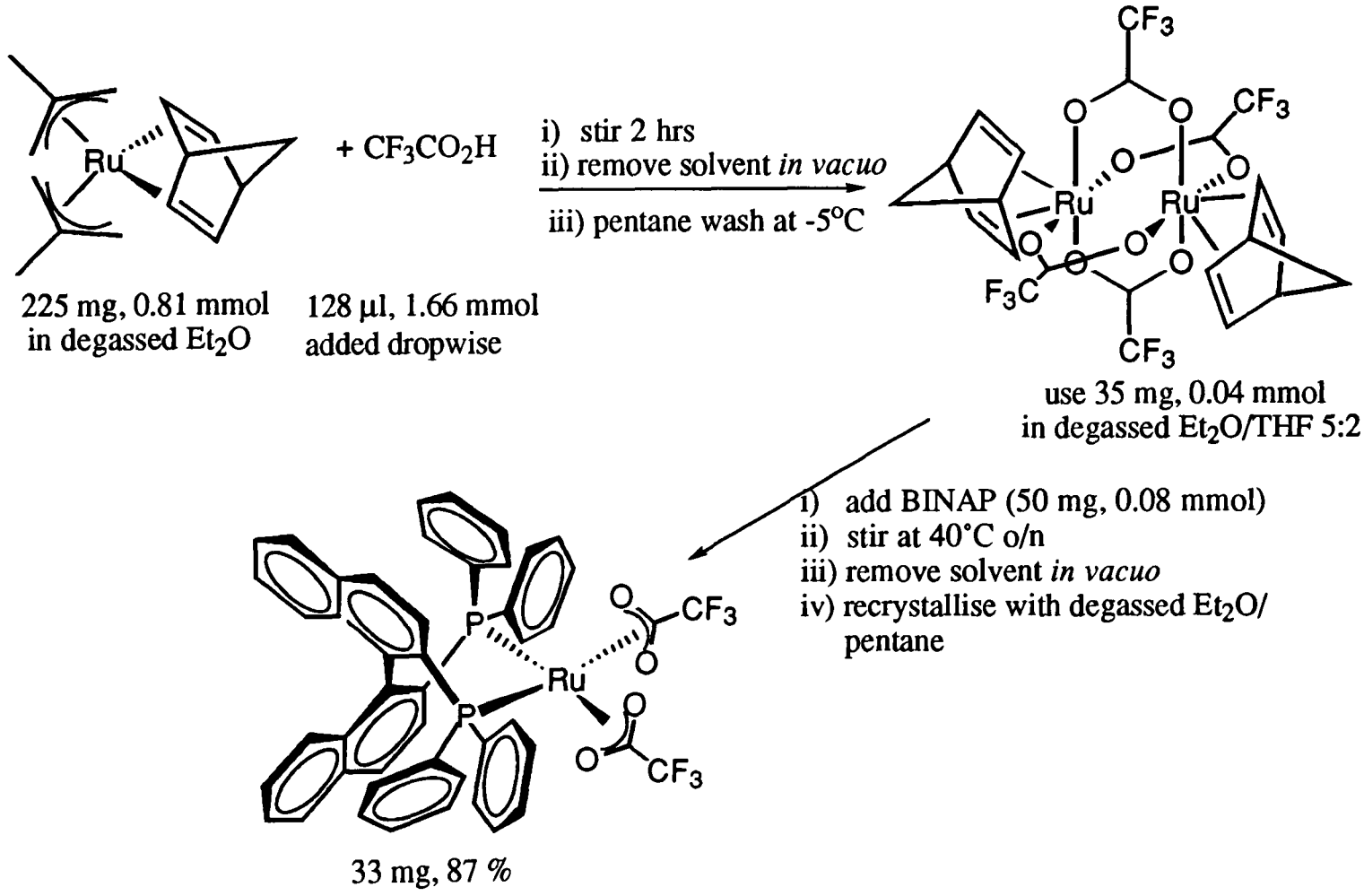
After stirring the reagents under argon for a week at 85°C, the solvent was removed from the dark brown suspension and the residue was extracted with degassed dichloromethane. Solvent removal yielded a light brown solid which had a ^{31}P NMR (101.23 MHz, CH_2Cl_2) that was not completely clean, though the major peak was a singlet at 65.84 ppm corresponding the required product. This method of preparing $Ru(BINAP)(OAc)_2$

did not lead to batches of catalyst pure enough for quantitative kinetic studies or descriptive NMR work.

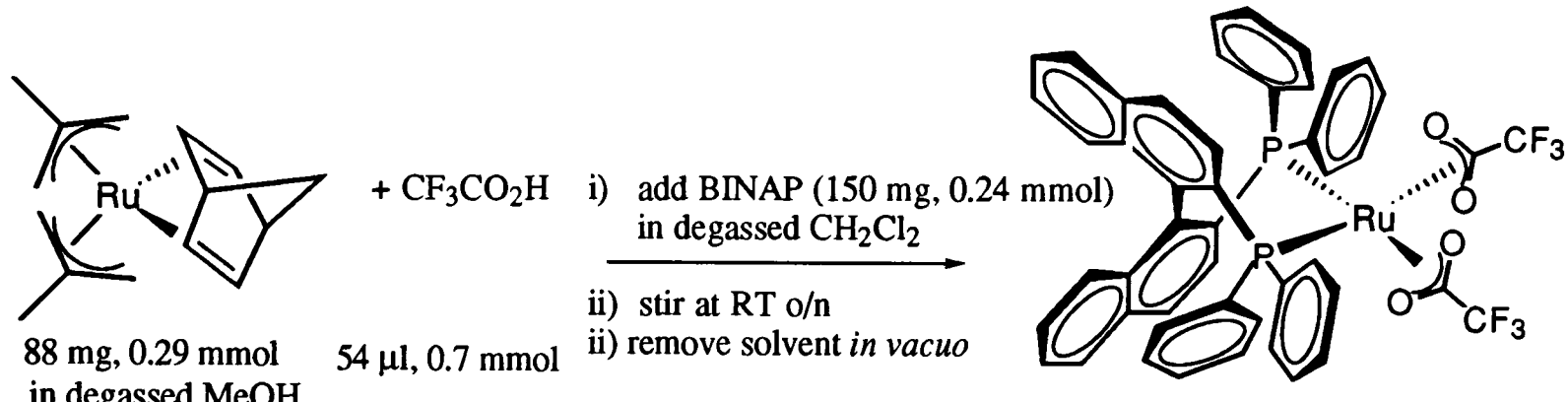


Scheme XXIII: *Chan claims to have found a simple, one pot route to pure batches of Noyori's catalyst. However, his results could not be reproduced*

The next synthesis to be attempted was Heiser's[69] which would yield both the bis acetate and the bis trifluoroacetate. The air sensitive trifluoroacetate can be obtained in two ways, both of which were attempted to compare purity of the product and ease of preparation (***Scheme XXIV***, ***Scheme XXV***).



Scheme XXIV: *Heiser's catalyst can be prepared by a two stage procedure passing through a dimeric ruthenium intermediate*



Scheme XXV: *the one pot route to Heiser's catalyst is higher yielding and more convenient than the two step procedure in* ***Scheme XXIV***

Both methods led to pure samples of trifluoroacetate as a pale yellow powder δ_P(202.46 MHz, $CDCl_3$) 57.5 ppm, but the one pot, one stage method shown in ***Scheme XXV*** was chosen for future syntheses of this catalyst, from the point of view of convenience.

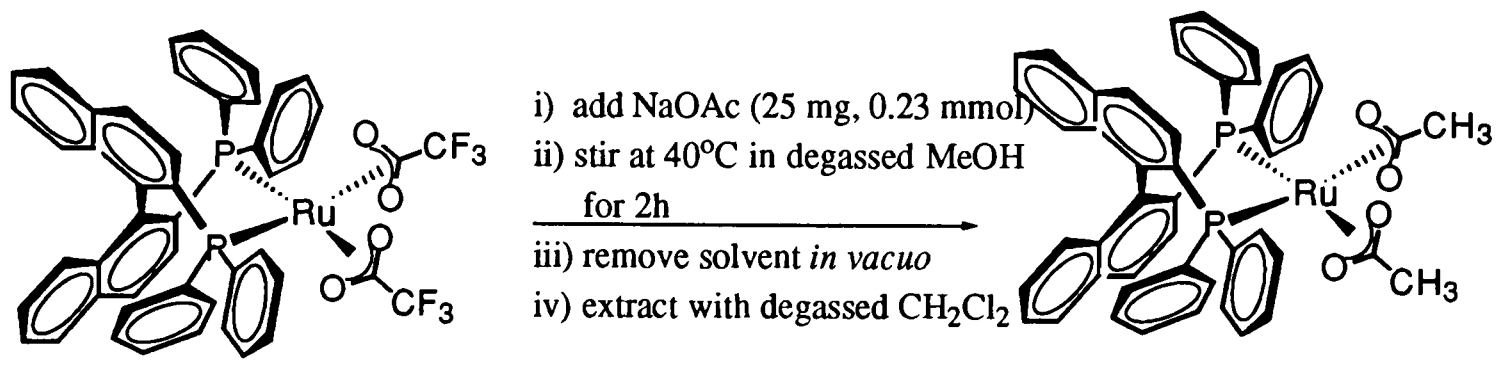
Note that the product was extremely sensitive to traces of water (even in $CDCl_3$) and on contact with water, water bridged dimeric species were formed (two different species δ 51.3, 54.3, 54.4 and 64.2 ppm, all d, J = 48.4 Hz). As a result of this fact, all solvents used in the catalyst synthesis and later in hydrogenation reactions were freshly distilled and degassed to ensure complete removal of both water and air. The $CDCl_3$ used in the obtention of NMR spectra was also freshly distilled and degassed. Adding trifluoroacetic anhydride to solutions containing bridged dimeric species resulted in reconversion of the bridged species into the trifluoroacetate monomer, though the resulting catalytic mixture was less active than legitimately pure catalyst samples (*vide infra*).

Noyori's catalyst was isolated as a pure pale yellow powder (δ_P 202.46 MHz, $CDCl_3$ 65.84 ppm) from Heiser's catalyst as shown in ***Scheme XXVI*** below.

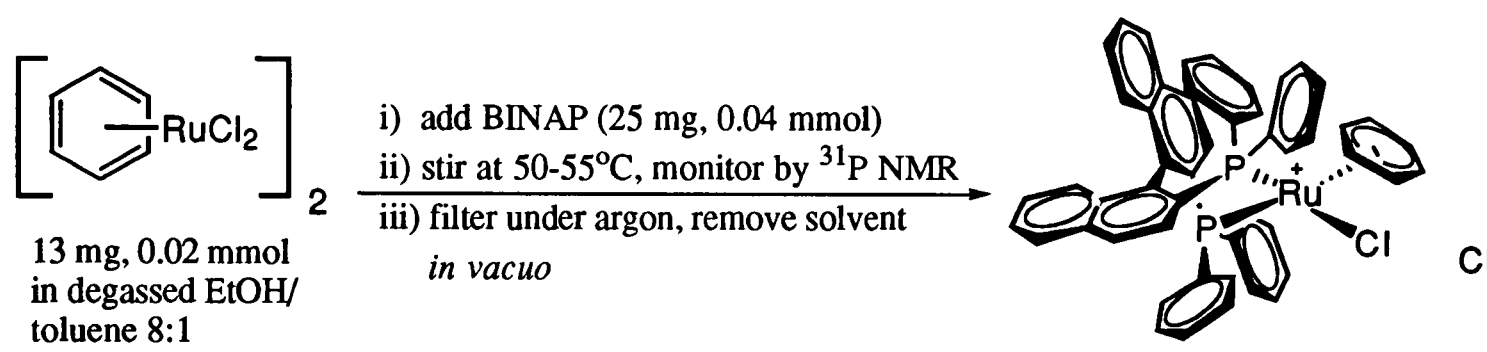
Obtaining a pure sample of the ionic ruthenium catalyst (***Figure 51***) proved slightly troublesome. Takaya's synthesis[64] stirred the reagents under argon at 50-55°C for 45 min before filtration and removal of the solvent *in vacuo*, ***Scheme XXVII***.

Following this method led to a species which contained two smaller doublets in addition to those corresponding to the required product (δ_P (101.23 MHz, $CDCl_3$) 31.0,

39.1(major d, J = 63 Hz) and 55.4, 60.3 (minor d, J = 42 Hz)). The yield was also very low.



Scheme XXVI: *reacting pure samples of Heiser's catalyst with NaOAc results in pure batches of Noyori's catalyst*



Scheme XXVII:*it was not possible to obtain completely pure samples of the above ionic ruthenium catlayst*

In an attempt to improve the yield, the reaction was repeated but this time the mixture was heated overnight. Unfortunately, ^{31}P NMR showed no trace of the required product and instead showed the doublets at 55.4 and 60.3 (the minor product in the 45 min stir reaction) along with a dominating singlet at 48 ppm.

Thus, it was decided to monitor the reaction by ^{31}P NMR. A mixture of benzeneruthenium (II) chloride dimer (13 mg, 0.02 mmol) and (R)-2,2'-bis(diphenylphosphino)-1,1'-binaphthyl (25 mg, 0.04 mmol) was placed in an 8 mm NMR tube and degassed. An 8:1 mixture of distilled, degassed ethanol and toluene (2.8:0.3 ml) was added *via* cannula and the contents of the NMR tube were heated at 50-55°C in blocks of 15 min. Every 15 min, the NMR tube was allowed to cool, placed in a 10 mm NMR tube with D_2O in the interannular space and a ^{31}P NMR was obtained (101.23 MHz). Product was apparent after the first acquisition. The process was

continued until the first traces of impurity started to form (doublets at 55.4, 60.3 J=42 Hz which appeared after 1.5h). The solution was then filtered through a celite pad and the solvent removed *in vacuo* to yield the product as a brown powder.

Preliminary investigations into the catalytic activity of the ruthenium complexes towards the reduction of simple dehydroamino acid derivatives

Having obtained pure samples of most of the catalysts, preliminary hydrogenations were next carried out in order to determine whether the catalysts *were* in fact active towards the reduction of the chosen substrates under the reaction conditions employed (ambient temperature and pressure). A substrate commonly used in ruthenium catalysed hydrogenations is 2 - acetyl - 6,7 - dimethoxy - 1 - methylene - 1,2,3,4 - tetrahydroisoquinoline[36], **1**, ***Figure 53***.

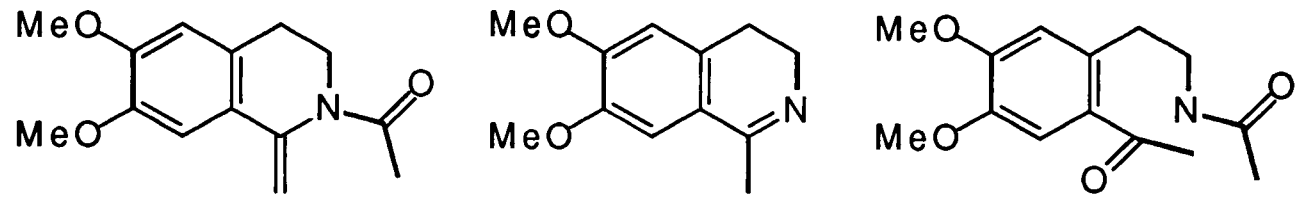


Figure 53: *compounds 1 and 3 are both readily obtained from compound 2*

Reduction of **1**, followed by deacetylation affords salsolidine, a compound with important physiological properties. The ruthenium catalysed reduction pathway is the best asymmetric syntheses of salsolidine. **1** was synthesised from 6,7 - dimethoxy - 1-methyl - 3,4 - dihydroisoquinoline (**2**, ***Figure 53***) by treating **2** with a 1:1 mixture of acetic anhydride and pyridine and heating (from which water had been rigorously excluded) at 95°C for thirty minutes[70]. Removal of the solvent *in vacuo* followed by dilution with ethyl acetate and removal of solvent again left yellow/brown crystals which were recrystallised from ethyl acetate to yield **1** as white crystals. The product was very moisture sensitive, especially in the presence of trace amounts of acid. Any water present during either the synthesis of **1** or its recrystallisation, led to almost exclusive production of the ring opened product **3**, ***Figure 53***.

All hydrogenations were carried out in methanol in the constant volume apparatus at 25°C and an initial pressure of 1.5 atmospheres. Distilled, degassed methanol was used as the solvent and reductions were carried out using the general method previously described. A catalyst loading of 2.5 mol% was initially used and was decreased as required if

reactions appeared diffusion controlled. Each catalyst was tested for its activity in hydrogenating the five enamides below, ***Figure 54***.

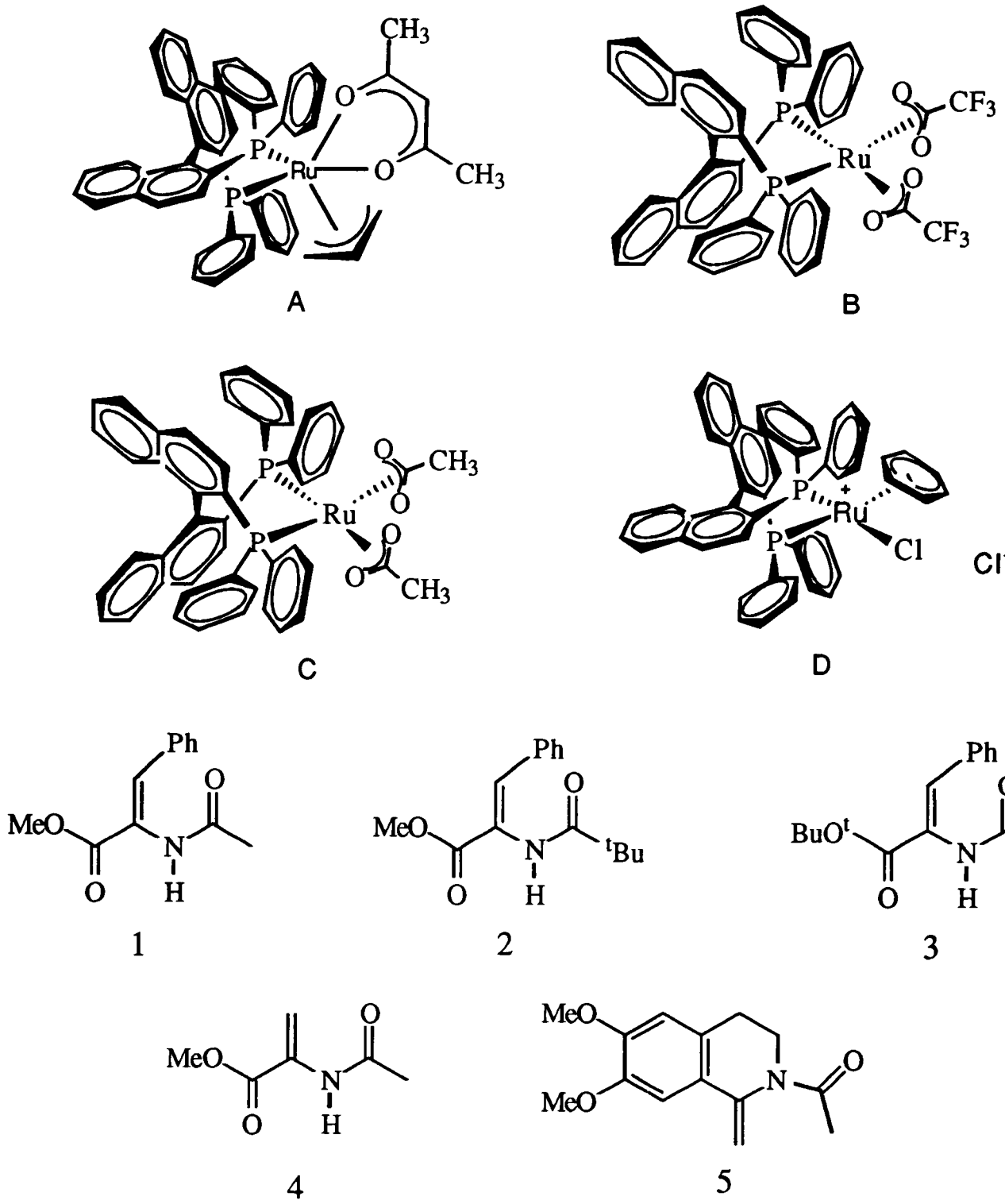


Figure 54: *four different catalyst systems were used to catalyse the reduction of the five enamides shown above*

It has already been mentioned that Brown's Ru(BINAP)(allyl)(acac) (**A**, ***Figure 54***) requires activation before being used in hydrogenation reactions[38]. Activation was carried out by adding two equivalents of trimethylsilyl trifluoromethanesulphonate to the yellow ruthenium catalyst in dichloromethane, stirring the resultant orange solution for fifteen minutes and then removing the solvent *in vacuo* to leave a yellow oil which was then dissolved in methanol.

Reductions using this catalyst system produced the pressure / time plots below (***Figure 55***). All solutions were pale yellow before, during and after hydrogenations *ie* unlike its rhodium analogues, this catalyst did not undergo any colour changes to indicate its own activation or any formation of a complex involving the metal and the enamide. This catalyst was found to be ineffective in the reduction of the ^{t}butyl amide **3**, ***Figure 54***. The isoquinoline enamide (**5**, ***Figure 54***) was 93% reduced.

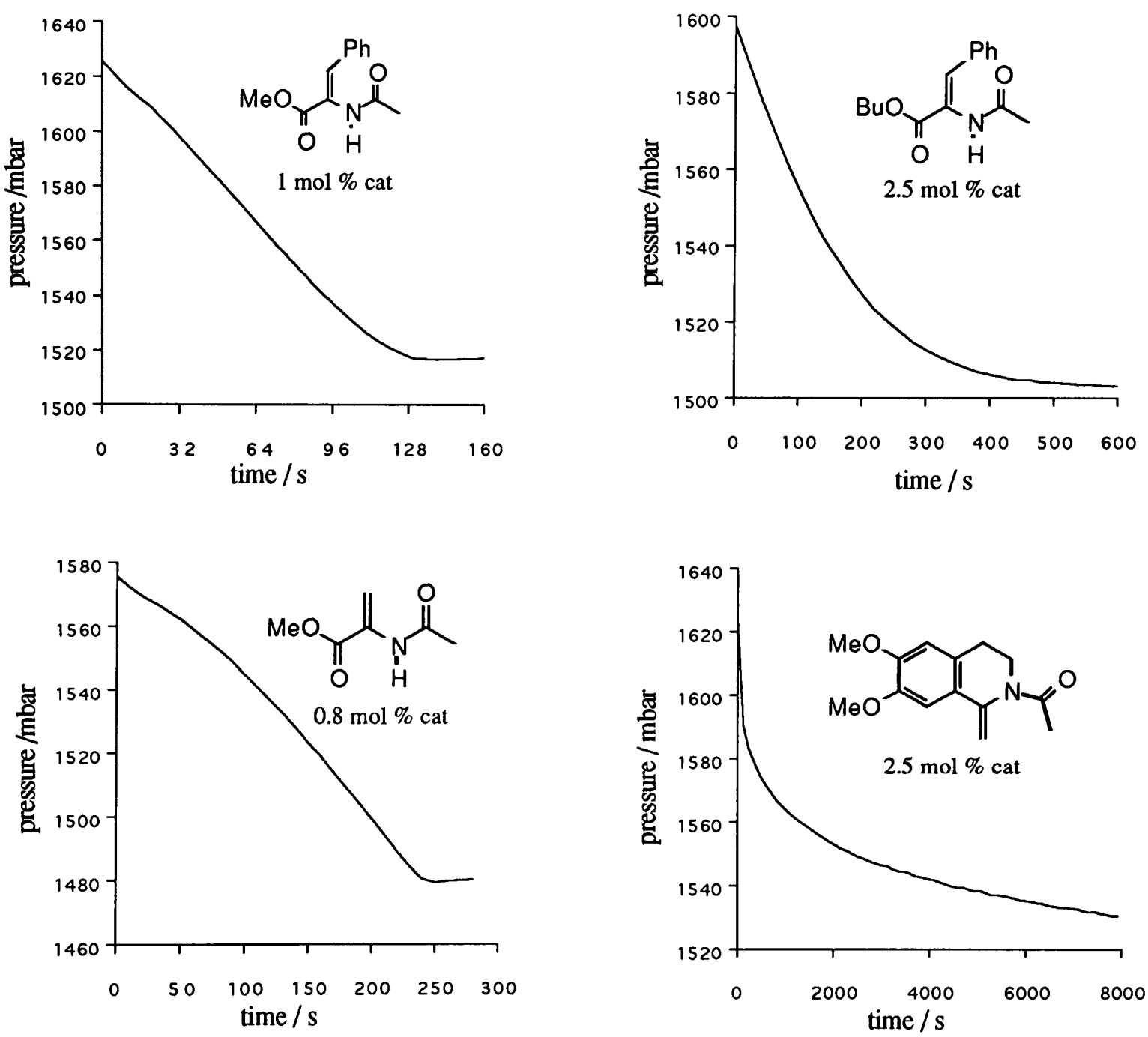


Figure 55: *Brown's catalyst effectively reduced four of the five enamides it was tested on*

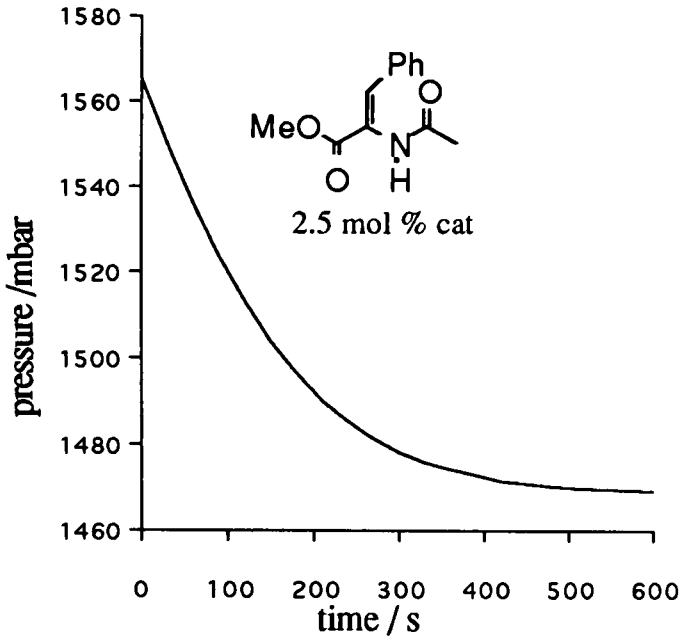
The next catalyst system to be tested out was Heiser's (**B**, ***Figure 54***). Like catalyst **A**, usage of this catalyst led to quick reaction times (though in the case of mac, reaction occurred after a short induction period of up to 100s). All five substrates tested were completely reduced using the trifluoroacetate catalyst (***Figure 56***). As mentioned

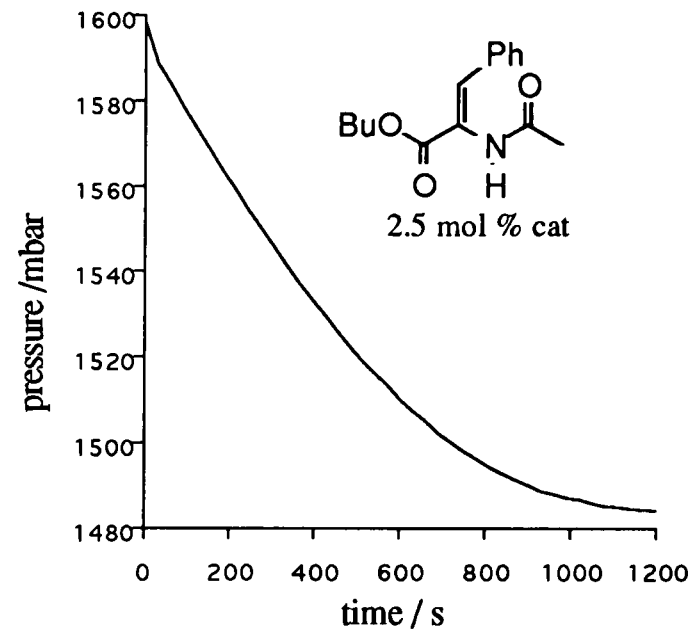
previously, this catalyst was very moisture sensitive and water bridged dimeric species were formed in the presence of trace amounts of water. Adding degassed trifluoroacetic anhydride to such catalyst solutions resulted in pure ^{31}P NMR spectra. Hydrogenations using samples of catalyst treated in this way were found to be twice as slow as reductions performed using legitimately pure batches of catalyst *ie* trifluoroacetic anhydride or the acid it produced inhibited the reduction of enamides. Once again, there were no colour changes during these hydrogenations. All solutions were pale yellow throughout the reduction process.

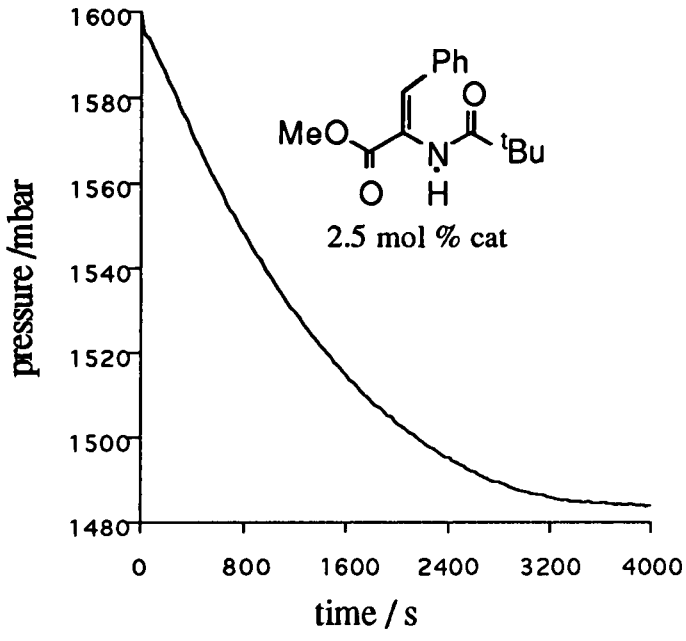
Noyori's bis(acetate) (**C**, ***Figure 54***) did not reduce any of the substrates under the conditions described above. All solutions were pale yellow - no colour changes corresponding to catalyst activation were observed. It was planned to eventually test the catalyst out again at elevated pressures.

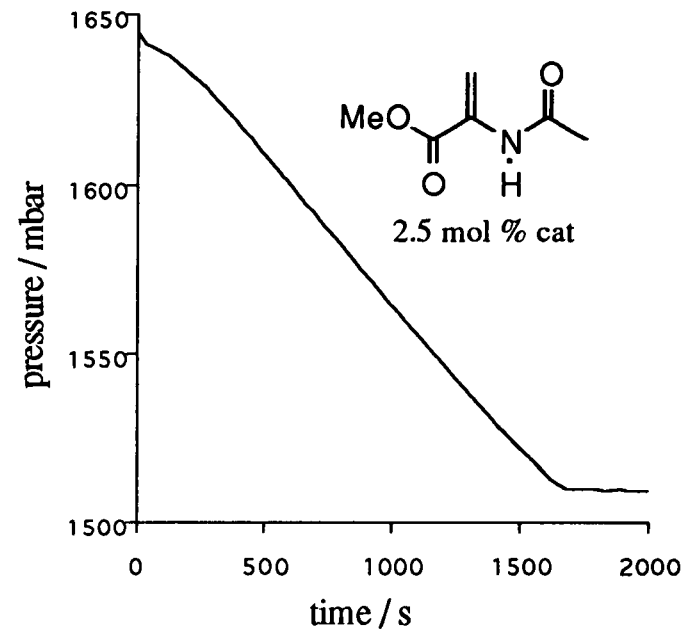
Finally the ionic catalyst (**D**, ***Figure 54***) was found to hydrogenate some of the substrates at longer reaction times than previously tested catalysts. Once again, all solutions were pale yellow at all stages - no colour changes corresponding to catalyst activation were observed. Neither the *t*-butyl amide nor the *t*-butyl ester could be reduced to any significant extent (8-10%), ***Figure 57.***

The pressure/time data obtained from these hydrogenations was next analysed by the numerical integtation programmes GEAR and GIT[53]. The model used in the preliminary analysis was a very simple one based on an achiral system *ie* formation of only one intermediate in the catalytic cycle was considered and the possibility of major and minor diastereomers was ignored. This enabled approximate values of rate constants and binding constants to be obtained for these systems. The results obtained are shown below (***Table III***). NMR studies were next carried out to obtain real indications of binding constants and also intercept intermediates in the catalytic cycle. If the values of K_{BIND} obtained from NMR studies differed widely from those obtained through modelling studies, it would be possible to infer that the species turning over in the catalytic cycle were *not* the same as the species being observed in the NMR experiments.









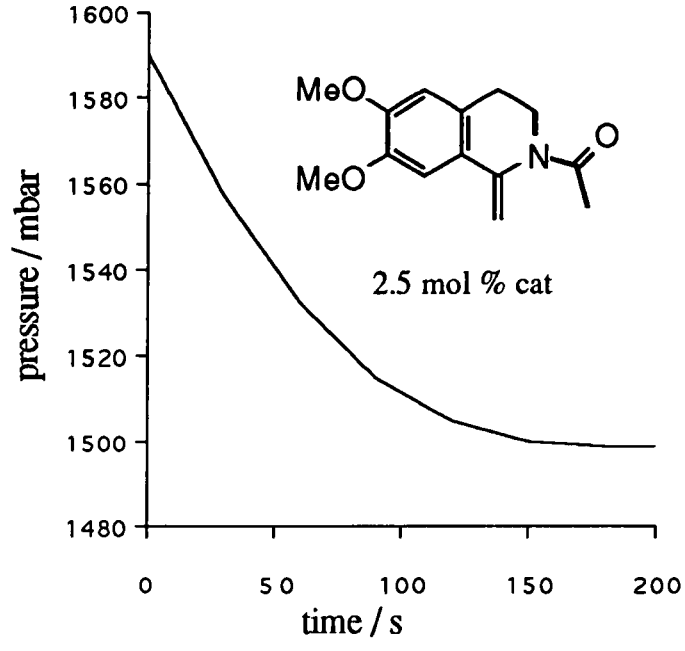
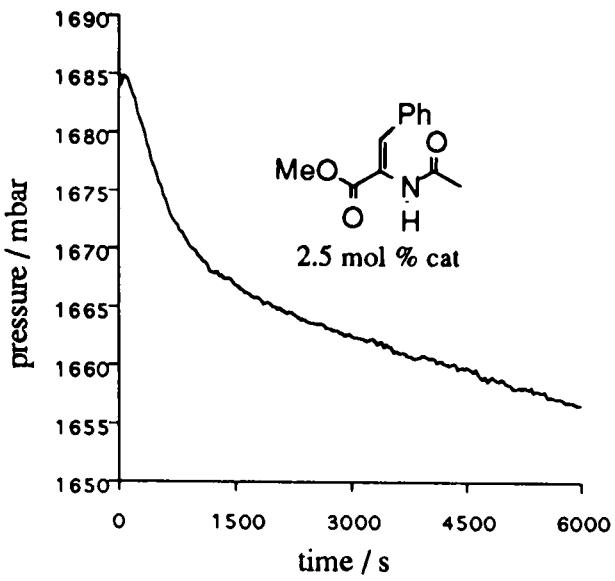
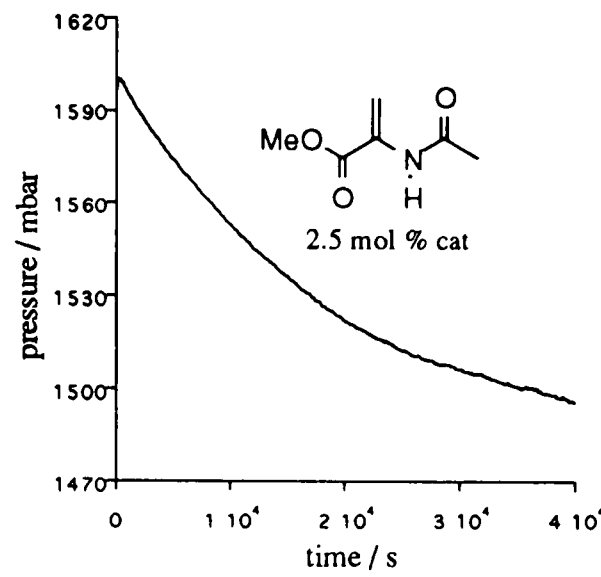
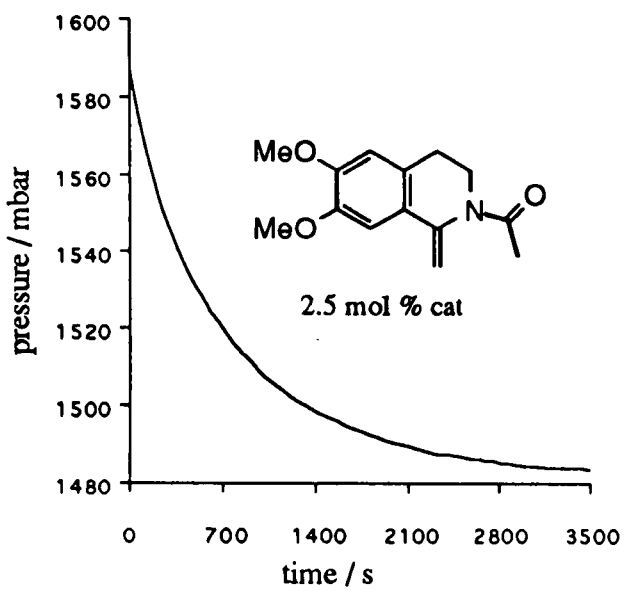


Figure 56: *Heiser's catalyst reduced all five enamides employed*







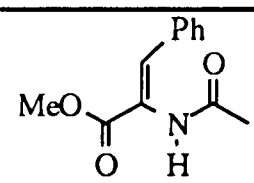
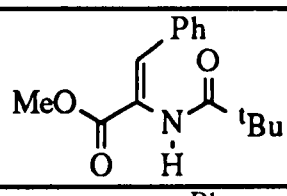
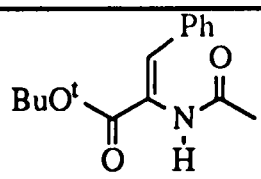
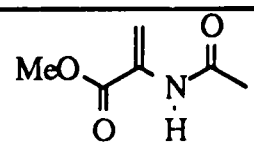
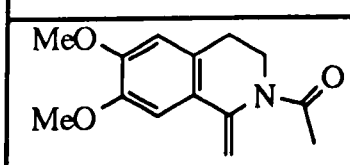
	Catalyst A	Catalyst B	Catalyst D
	K_{BIND} = 840 k = 282 mol^{-1} l s^{-1}	K_{BIND} = 9 k = 100 mol^{-1} l s^{-1}	K_{BIND} = 0.4 k = 105 mol^{-1} l s^{-1}
		K_{BIND} = 7 M^{-1} k = 140 mol^{-1} l s^{-1}	
	K_{BIND} = 5 k = 150 mol^{-1} l s^{-1}	K_{BIND} = 11 k = 25 mol^{-1} l s^{-1}	
	K_{BIND} = 80 300 k = 74 mol^{-1} l s^{-1}	K_{BIND} = 50 890 k = 3.72 mol^{-1} l s^{-1}	K_{BIND} = 0.02 k = 111 mol^{-1} l s^{-1}
		K_{BIND} = 577 k = 8 mol^{-1} l s^{-1}	K_{BIND} = 0.2 k = 591 mol^{-1} l s^{-1}

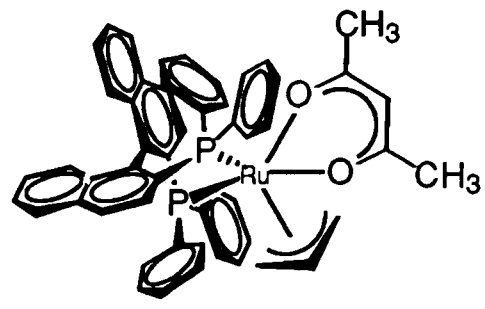
Figure 57: *reductions using the ionic catalyst were much slower compared with other catalysts*

Table III: *preliminary modelling of kinetic data led to the rate and binding constants shown above*

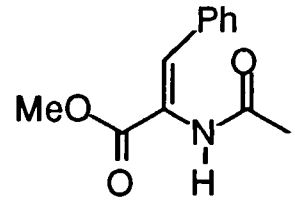
Binding studies

Having tested out the catalytic activity of previously synthesised ruthenium catalysts towards the hydrogenation of simple dehydroamino acid derivatives, binding studies were initiated in order to observe and characterise intermediates in the catalytic cycle. It has already been mentioned that mechanistic detail for alkene reductions following a ruthenium catalysed pathway is very sparse. Parallel investigations using rhodium were aided by the fact that the resting state in the catalytic cycle contains the olefin bound to rhodium; thus the catalytic cycle and the interconversion of reaction intermediates could be followed by NMR.

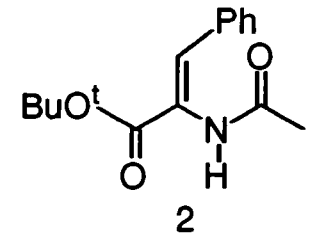
The literature does not contain any significant NMR work carried out using ruthenium chemistry. Attempts to observe the formation of a ruthenium hydride species by reacting $Ru(BINAP)(OAc)_2$ with hydrogen are reported to have failed[40]. NMR studies were performed under argon using 600 µl freshly distilled, degassed CD_3OD. Samples were prepared according to the general method described earlier. The first system to be investigated was that shown below (***Figure 58***).



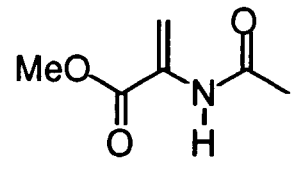
Ru(BINAP)(allyl)(acac)



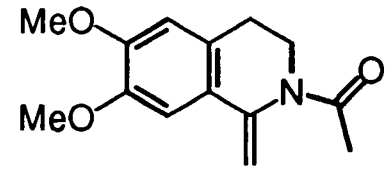
1



2



3



4

Figure 58: *preliminary binding studies were performed on Brown's catalyst and the four enamides it had been found to be capable of reducing*

Initially, the activation of the catalyst under argon was monitored by ^{31}P NMR 202.46 MHz, degassed CD_3OD) in a control experiment. The double doublets of the unactivated catalyst (δ 64.5, 37.2 ppm, J = 37 Hz) were replaced, on activation by TMSTfO, by dynamic peaks at room temperature. Cooling down to 233K resulted in two double doublets corresponding to major and minor diastereomers of the activated catalyst δ 65.7, 50.4 ppm (d, J = 41.0 Hz) and 62.3, 44.4 ppm (d, J = 42.5 Hz), ***Figure 59***.

In rhodium chemistry, cooling samples down to about 233K freezes out the interconversion of the diastereomeric enamide complexes such that their reaction with hydrogen can be separately and directly observed[10]. By analogy with rhodium chemistry, ruthenium binding samples were cooled down to 233K, as well as being observed at the hydrogenation reaction temperature of 298K.

NMR samples for binding studies were prepared under argon by taking 5μmol (4 mg) of activated catalyst in 300μl distilled and degassed CD_3OD and then adding between ten and fifteen equivalents of enamide (in 300μl CD_3OD) to the catalyst at -78°C under argon. A large excess of enamide was used in the hope of driving any potentially unfavourable equilibrium for the formation of an enamide complex to the right. With the exception of enamide **4**, no colour changes were observed on addition of enamide solutions to the catalyst *ie* in contrast to rhodium chemistry, there was no visual indication of any complex formation.

Enamide **1** gave rise to a spectrum at 233K which showed the presence of both major and minor diastereomers (***Figure 60***). The system was dynamic at 298K. Both the alkene and carbonyl moities of the enamide appeared bound to the metal: peaks at high chemical shift corresponded to the phosphorus atom *trans* to the carbonyl oxygen of the enamide and the peaks at lower chemical shift corresponded to the phosphorus atom *trans* to the enamide double bond. Chemical shifts and coupling constants are tabulated below, ***Table IV***.

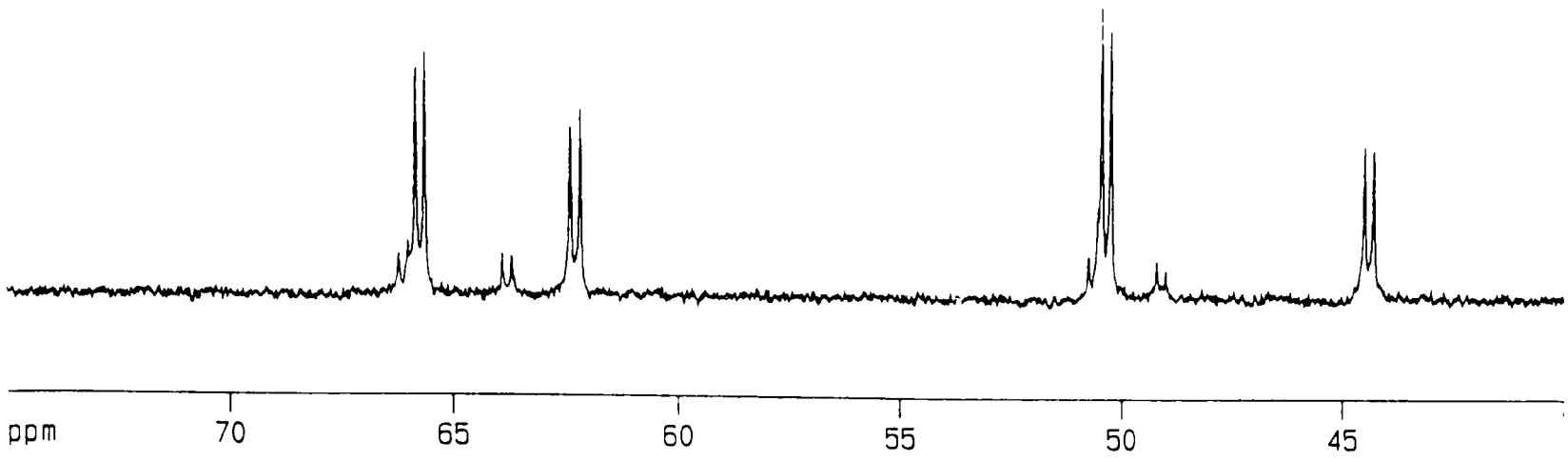


Figure 59: *treating Ru(BINAP)(allyl)(acac) with TMSTfO resulted in the above ^{31}P spectrum at 233K*

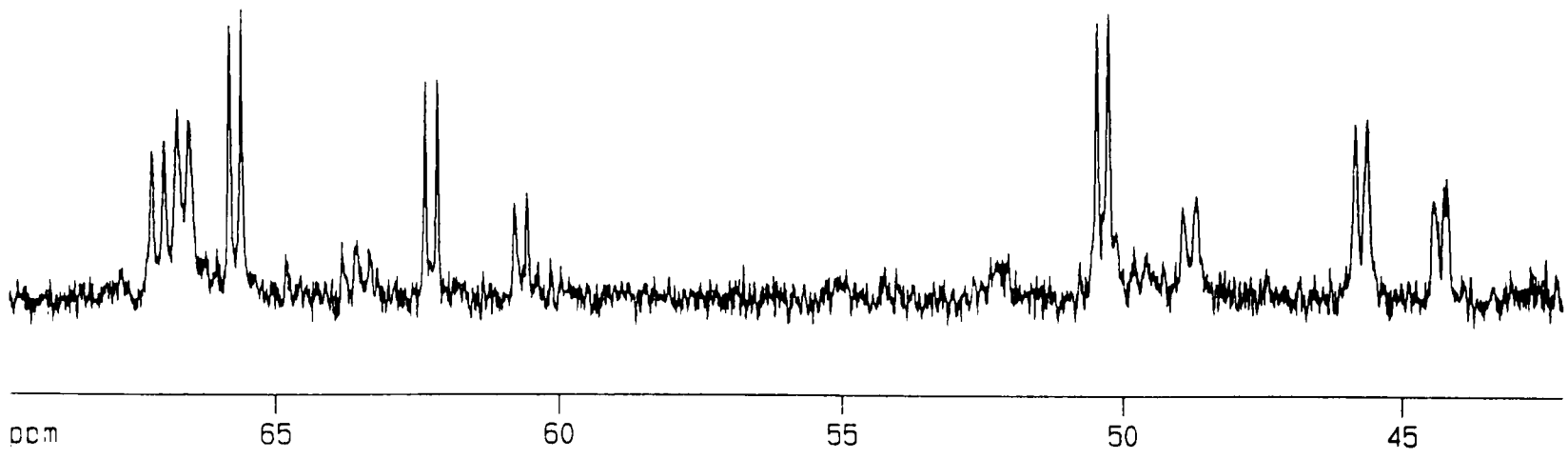


Figure 60: *binding studies performed on mac showed the presence of both major and minor diastereomers*

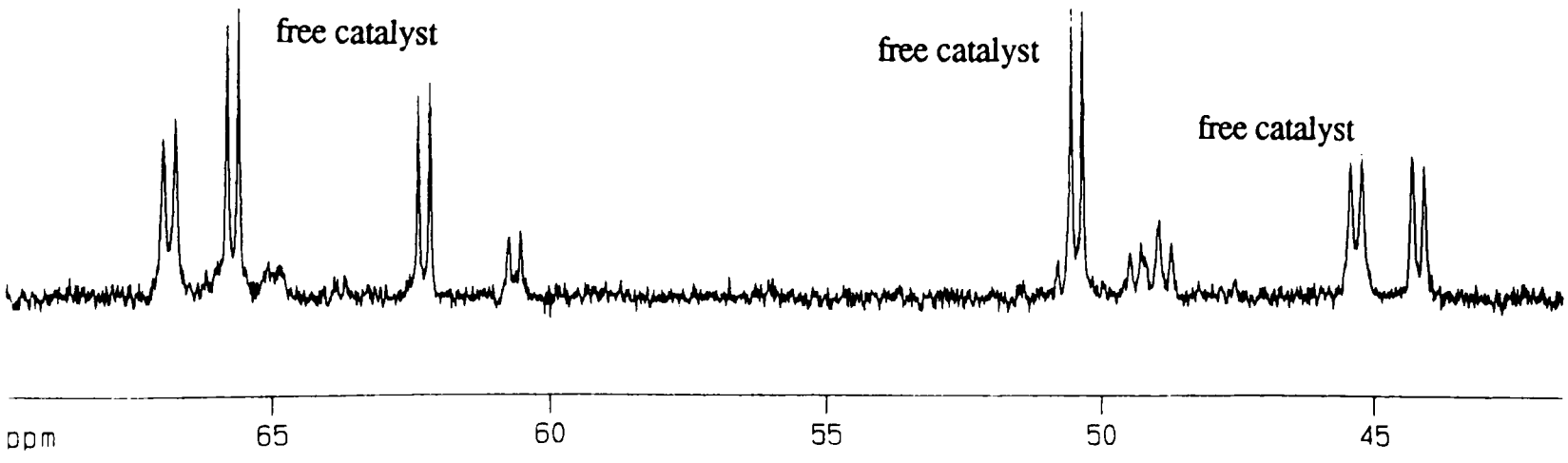


Figure 61: *using the ^{t}butyl ester led to spectra containing only the major diastereomer*

Only the major diastereomer was observed in the case of enamide **2** at 233K. Once again, the system was dynamic at 298K (***Figure 61***).

The spectrum from enamide **3** was dynamic at room temperature and was not clean enough to provide any real information at 233K.

Finally, enamide **4** at 233K appeared to give rise to a species with two alkene moities bound to the metal, along with a small amount of carbonyl and enamide bound species (***Figure 62***). The intitially yellow catalyst solution went dark red on the addition of excess enamide. At 298K, only an AB quartet with a severe roof effect was observed. Note, the absence of any free catalyst in these spectra was an indication of the great magnitude of the binding constant of this enamide.

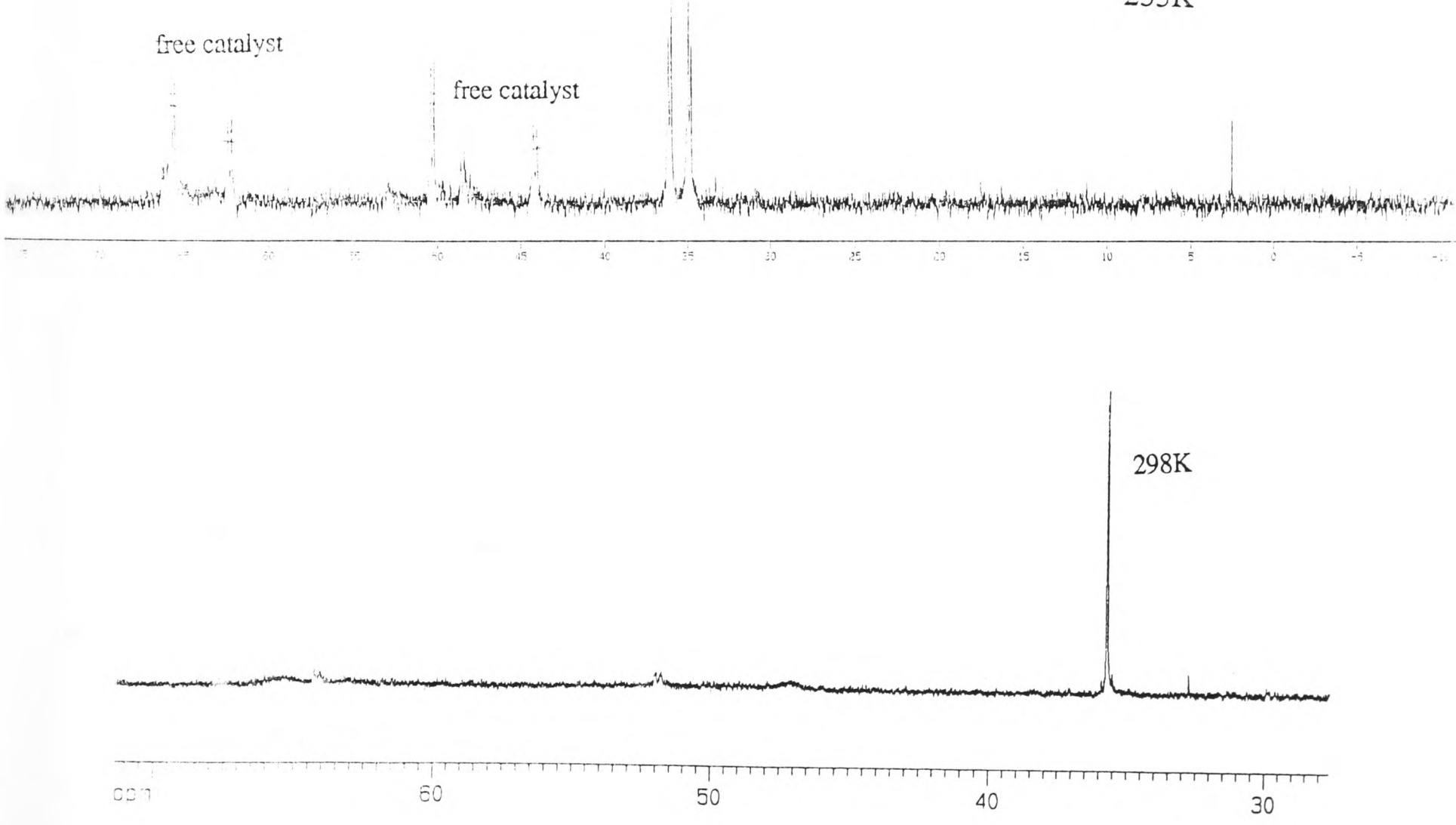


Figure 62: two molecules of the isoquinoline derivative appeared to be bound to this catalyst

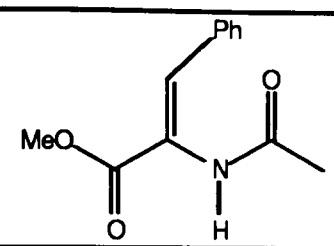
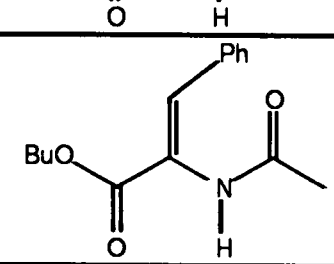
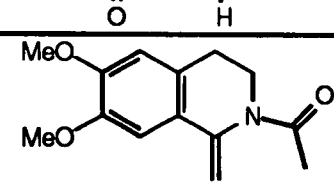
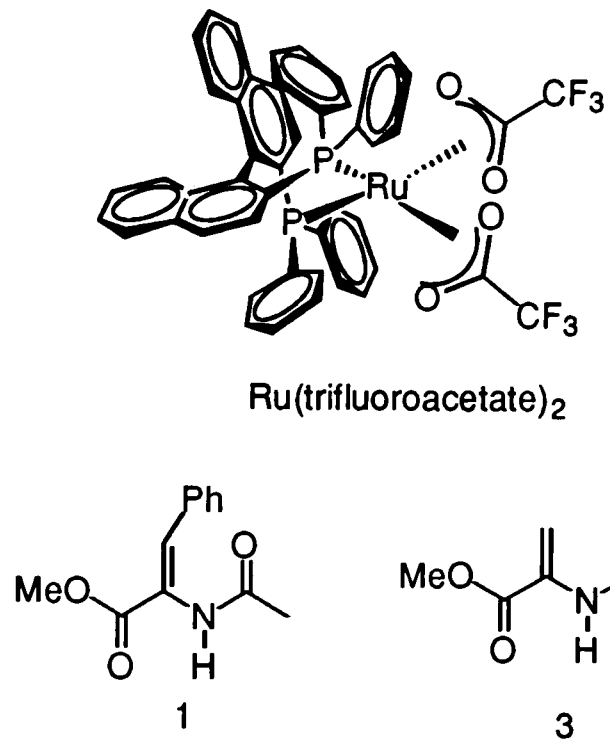
Substrate	Signals	δ / ppm	J / Hz
none	doublets	65,7, 50.3 52.3, 44.4	41.0 42.5
	doublets	67.1, 45.7 66.6, 48.7	43.5 40.3
	doublets	66.9, 45.3	40.3
	doublets	36.2, 34.9	35.9

Table IV: *^{31}P NMR data for samples of Brown's catalyst with enamides, acquired under argon at 233K*

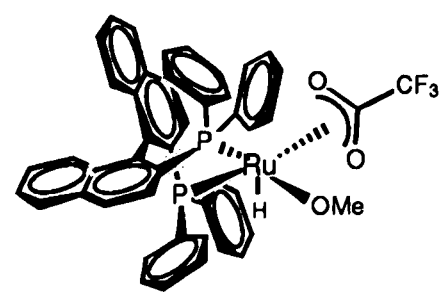
Binding studies involving Heiser's catalyst (***Figure 63***) were also carried out. On cooling samples of the catalyst alone (in distilled, degassed CD_3OD), the singlet observed at 298K (δ 57.7ppm) was found to be accompanied by a lower intensity double doublet at temperatures lower than 233K (δ 62.0, 56.6 ppm, J = 45 Hz). At temperatures higher than 253K, this double doublet was dynamic. Two possible species that could give rise to the double doublet were a hydride species (hydrogen having come from the solvent) or, more likely, a dimeric species with solvent bridges (***Figure 64***).

^1H NMR at 233K ruled out the possibility of a hydride species by the lack of a signal in the region 0 to -30 ppm. When a 1:1 mixture of enamide **3** and the catalyst (prepared in the same way as described above for samples of Brown's catalyst) was looked at under argon, only peaks corresponding to free catalyst were observed. The system was warmed up to 298K and an excess of substrate was added, but still no peaks corresponding to complexed enamide could be seen. There were no colour changes corresponding to complex formation.



Ru(trifluoroacetate)$_2$

***Figure 63**: initial binding studies using Heiser's catalyst concentrated on using two of the five possible enamides*



hydride species

***Figure 64:** a hydride species would contain inequivalent phosphorus atoms and give rise to an AB quartet in its ^{31}P NMR spectrum*

It was possible that entry into the catalytic cycle required preactivation by hydrogen and that that was the reason why binding studies under argon had been unsuccessful. By ananlogy with rhodium chemistry, a 5 mm NMR tube containing the catalyst in 300 µl degassed CD_3OD was 'whirlimixed' for five minutes under hydrogen. The solution remained pale yellow throughout. The hydrogen atmosphere was then replaced with argon and a solution of enamide in 300 µl degassed CD_3OD was added to the NMR tube. No change in the colour of the solution or the phosporus spectrum was observed.

Next, a 1:1 mixture formed under *hydrogen* was examined. An NMR tube containing CD_3OD and the enamide was whirlimixed and degassed with hydrogen many times over a period of half an hour, in the hope of saturating the solution with hydrogen. Then a solution of catalyst in the minimum amount of CD_3OD was added and the system was

degassed again and kept at 183K overnight, under a hydrogen atmosphere, to allow some catalytic turnover to occur. Any alkylhydride or ruthenium hydride intermediates were likely to be stable only at very low temperatures, therefore the next day, the sample was monitored by ^{31}P NMR at temperatures between 193K and 243K, warming up by 10K each time. Still no species other than free catalyst was observed.

Nor were any new species seen when a five molar excess of enamide over catalyst was used and the system under hydrogen investigated again (between 193K and 233K), though the intensity of the double doublet was noticed to have increased appreciably with respect to the singlet.

The enamide used was then changed, in the hope that a bound species might be seen. Using enamide **3**, a 1:1 mixture of enamide and catalyst under hydrogen was looked at between 233K and 298K warming up by 10K each time. The same results as above were obtained *ie* the only peaks in the spectrum were due to free catalyst. Adding excess enamide to a catalyst solution (under argon) at 298K could not force the equilibrium to the right either and no complexed enamide appeared to be present.

Finally, it was decided to conduct binding studies using a basic amide, N,N-dimethyl acetamide, DMA (***Figure 65***). This amide is a more basic entity than methanol, so if the double doublet observed at low temperature did correspond to a dimer with bridging solvent molecules, the addition of the more basic amide would be expected to break up these dimers and hence lead to a change in the NMR spectrum. As in the case with enamide **3**, to keep the experimental technique employed consistent, the catalyst was 'activated' by whirlimixing under hydrogen before the addition of DMA. A change in the NMR spectrum was indeed observed (***Figure 66***) on a 1:1 mixture of amide and catalyst looked at under argon. At 233K, two doublets were observed in addition to a peak corresponding to free BINAP (δ 60.1, 55.7, d, J = 44.5 Hz). It was possible that DMA was effecting decompsition of the catalyst to some extent; at 298K essentially only a peak corresponding to free phosphine was observed.

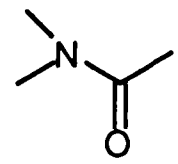


Figure 65: *N,N dimethylacetamide was added to Heiser's catalyst to see if basic amide moieties did indeed bind to the ruthenium*

It is puzzling that the amide functions of the enamides previously used in binding investigations did not yield similar results to the N,N-dimethyl acetamide experiment. Electrospray mass spectrometry of the intermediate formed between the catalyst and DMA showed a peak at 811 corresponding to $(RuP_2DMA)^+$.

It was next decided to attempt to monitor, by ^{31}P NMR (202.46 MHz), an *in situ* hydrogenation using this catalyst at 298K. Firstly, the catalyst alone was looked at at 298K. Its spectrum consisted of a singlet at 57.7 ppm *ie* there was no change from its appearance under argon. The fact that the catalyst spectrum did not change on exposure to hydrogen indicated that preactivation of the catalyst by hydrogen before the addition of enamide was *not* necessary and this had not been the reason for failure to observe any signs of bound enamide species.

A series of blocked spectra were next run on an NMR tube containing an excess of enamide **3** over catalyst under hydrogen. A 5 mm NMR tube containing the catalyst in 500 µl degassed CD_3OD was 'whirlimixed' and degassed under hydrogen several times in the hope of saturating the solution with hydrogen. This sample was sealed and used to shim the NMR probe. Then, the enamide (in 100 µl CD_3OD) was syringed into the NMR tube, the system was sealed and shaken up and acquisition was immediately commenced. The spectra showed the presence of new peaks between 50 and 65 ppm and the intensity of the singlet corresponding to free catalyst was seen to decrease with time. However the spectra were not very informative. It has been hoped to repeat this investigation under high pressure conditions.

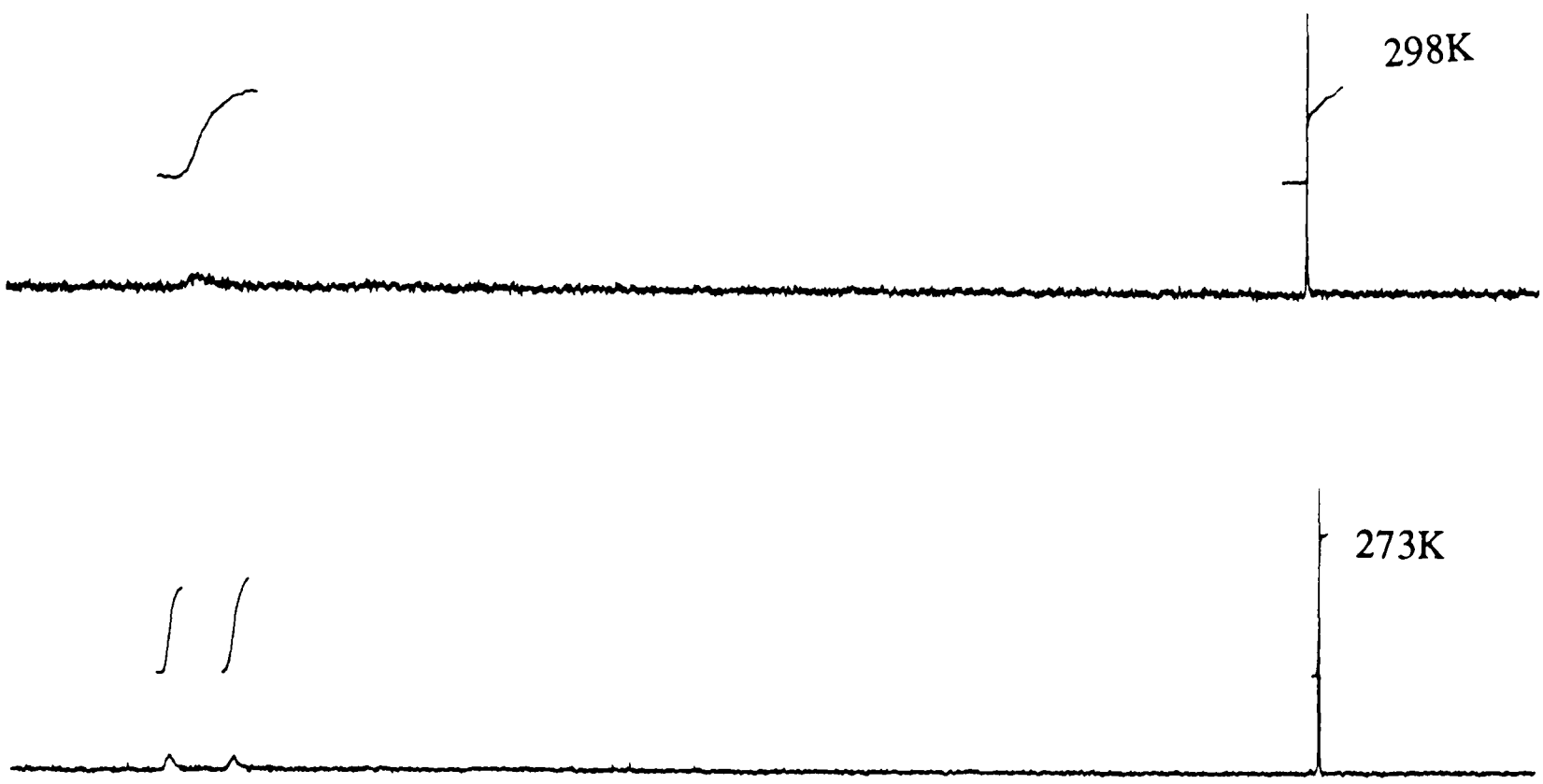


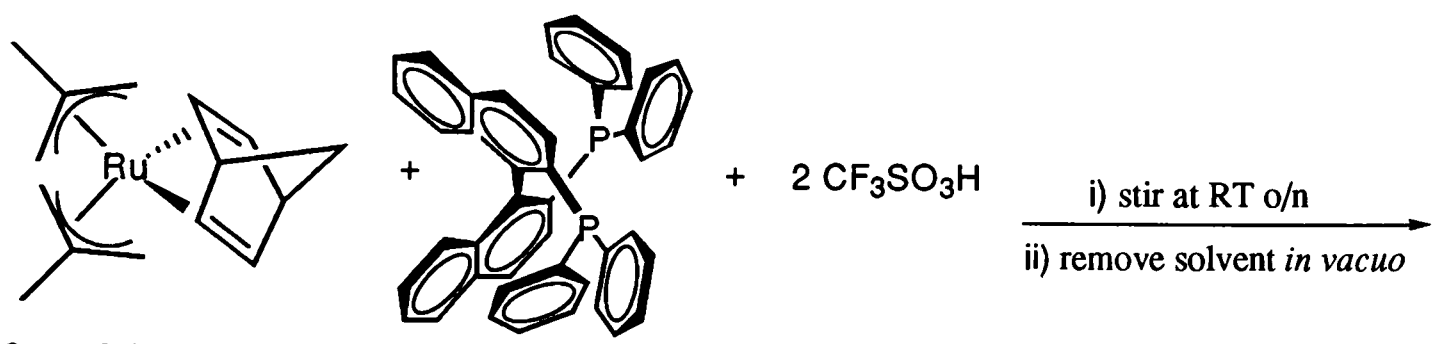
***Figure 66**: binding studies on N,N-dimethyl acetamide*

Modifications to heiser's catalyst

A sterically encumbered catalyst environment can impede tight binding of a substrate (leading to low enantiomeric excesses) or even shut down catalysis completely. One reason for the lack of success in observing bound enamide species with Heiser's catalyst could be that the trifluoroacetate groups sterically impede the enamide's approach towards the metal centre. Thus, it was decided to try and modify the catalyst's structure by replacing one or both of the trifluoroacetate groups. The synthesis of two new catalysts was envisaged. It has already been explained (p71) how Brown's Ru(BINAP)(allyl)(acac) catalyst is inactive towards hydrogenation until activated by the addition of TMSTfO. By analogy, the Heiser catalyst was treated with TMSTfO. It was expected that the TMSTfO would react with trifluoroacetic acid produced to form the silylated acid, whilst the triflate groups would replace the trifluoroacetate groups. The more labile triflate groups would hopefully facilitate the approach of an enamide to bind to the metal centre.

The reaction to form the catalyst, **catalyst 1**, was carried out in an NMR tube in freshly distilled, degassed $CDCl_3$ and monitored by ^{31}P NMR (202.46 MHz). The initially yellow coloured solution of Heiser's catalyst immediately turned dark red on the addition of an excess of TMSTfO. The NMR showed four broad signals (δ 81.4, 75.9, 7.4, 0.8 ppm in a 1:8:8:1 ratio) and one narrow singlet (δ 54.3 ppm). When the reaction was carried out using exactly two equivalents of TMSTfO, it was found that there were two broad peaks in the ^{31}P NMR spectrum, δ 75.1 and 7.9 ppm, which were accompanied by an intense singlet at -2.1 ppm. The high field peaks probably corresponded to ruthenium dimers. Removal of the solvent *in vacuo* left a dark red oil which was stored under argon in the fridge. The exact structure of this catalyst is unknown; the results of electrospray mass spectrometry investigations revealed peaks at 889 and 873 as the major species corresponding to $[RuP_2TfO]^+$ and $[RuP_2TfO + O\}^+$.

The second modified catalyst, **catalyst 2**, to be synthesised followed Heiser's method[69], but included the addition of triflic acid instead of trifluoroacetic acid (***Scheme XXVIII***).



Scheme XXVIII: *replacing the trifluoroacetate groups in Heiser's catalyst with trifluoromethane sulphonate groups would hopefully lead to a more labile catalyst*

Once again, the reaction was carried out in an NMR tube and monitored by ^{31}P NMR (101.23 MHz). BINAP in the minimum amount of distilled, degassed dichloromethane was added, *via* cannula, to an NMR tube containing the ruthenium precursor, degassed methanol and two equivalents of triflic acid. The initially yellow solution turned dark red immediately and ^{31}P NMR showed the existence of two pairs of double doublets (δ 74.5, 1.5 ppm, J = 52 Hz and δ 38.7, 37.6 ppm, J = 34 Hz). Once again, the exact structure of this catalyst is unknown, electrospray mass spectrometry investigations revealed peaks at 889 and 873 as the major species corresponding to $[RuP_2TfO]^+$ and $[RuP_2TfO + O\}^+$.

The catalytic activity of these two new catalysts towards hydrogenations and binding studies was next investigated.

Both catalysts were tested out in hydrogenation reactions and their binding properties were also investigated (202.46 MHz). It had been hoped that the catalysts would contain labile functionalities and hence approach of the enamide to the metal centre (not observed at all with Heiser's catalyst) would be facilitated. Hydrogenations and binding studies were performed in the normal fashion with due care exercised to avoid the presence of all moisture and air. Binding studies were performed under argon, with no exposure to hydrogen for 'preactivation', using both one equivalent and an excess of substrate with

respect to catalyst. Hydrogenations used 2.5 mol % catalyst. Solutions in both the kinetic and NMR studies were orange/red before, during and after 'reaction' *ie* at no stage was there any visual evidence of complex formation or catalytic turnover. The results are tabulated below (***Table V***). From the table, it is apparent that the two catalysts gave rise to similar spectra in their binding studies (except when using mac, substrate **1**), yet as hydrogenation catalysts, **catalyst 2** was a very poor catalyst whilst **catalyst 1** gave rise to some acceptable results (notably with substrates **1** and **3**). It was decided that this could point to the fact that the species observed in the ^{31}P NMR had nothing to do with the catalytic cycle.

To clarify whether these substrates were bound through the alkene or not, binding studies were carried out using the basic amide N,N-dimethyl acetamide and also using labelled mac (followed by ^{13}C NMR in the case of labelled mac). Investigations used both modifications of Heiser's catalyst and Ru(BINAP)(allyl)(acac).

Catalyst 2 with N,N-dimethyl acetamide gave rise to a spectrum which was dynamic at 233K and sharpened up at 298K. No peaks in the expected 'enamide' region (less than 50 ppm) were observed at 233K. Other than the lack of signals in the enamide region, the spectrum was not very informative.

The spectrum from Brown's Ru(BINAP)(allyl)(acac) with N,N-dimethyl acetamide (***Figure 67***) was confusing at 233K (extra peaks, J = 43 Hz, possibly arising from two

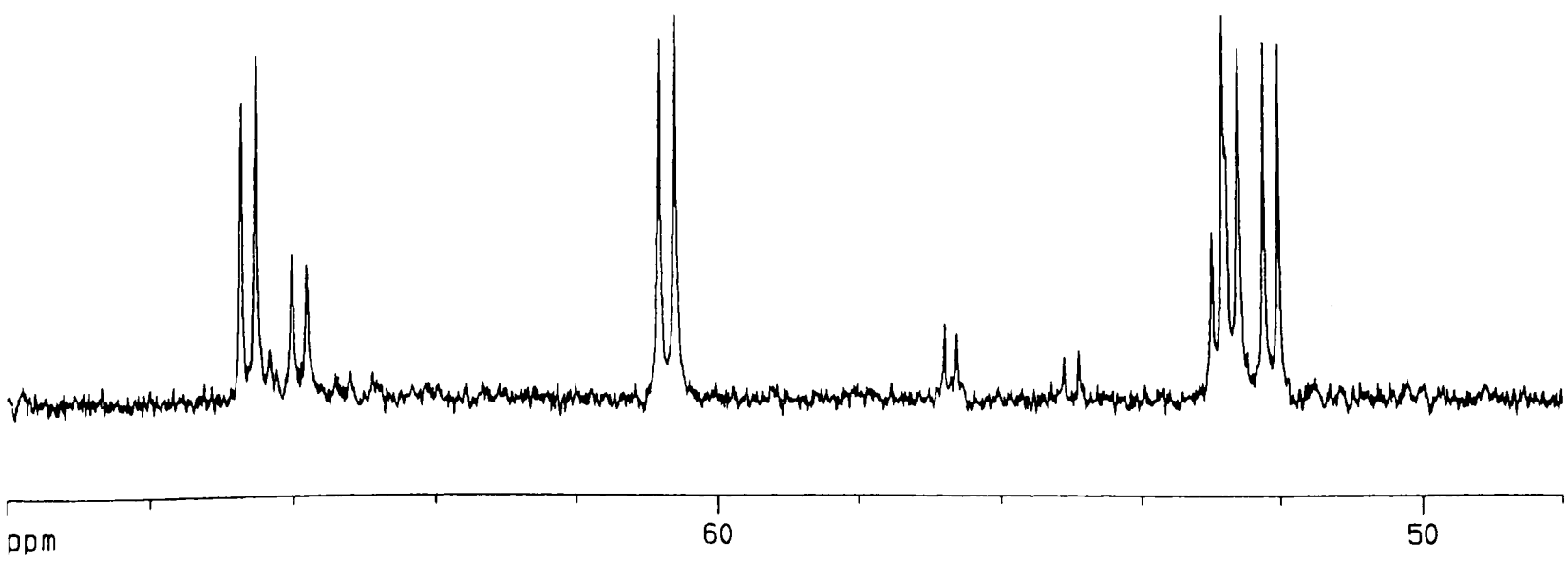


Figure 67: *extra peaks were observed in the spectrum from Ru(BINAP)(allyl)(acac) and N,N-dimethyl acetamide*

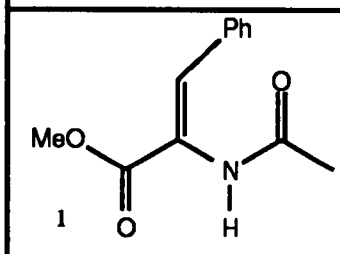
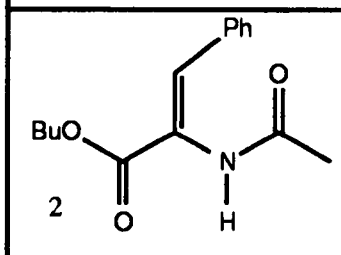
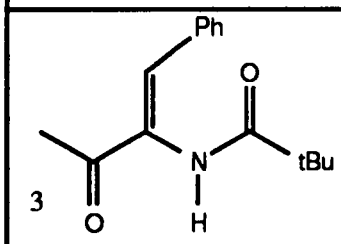
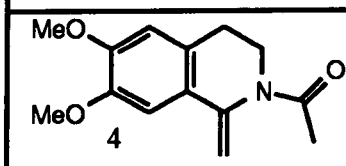
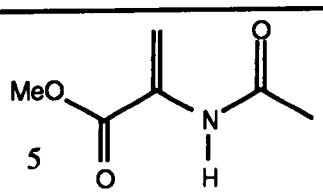
substrate	hydrogenations		binding studies	
	catalyst 1	catalyst 2	catalyst 1	catalyst 2
none			233K d at 82.2, 75.4 ppm, J 51Hz 298K br s at 81.9, 75.7, 7.4, 0.9 ppm	233K d at 82.2, 75.9 ppm, J 51Hz 298K d at 74.6, 38.6, 37.5, 1.5 ppm
 1	100 % reduction	60 % reduction	233K d at 66.9, 66.3ppm, J 45 Hz 298K d at 51.6, 51.4 ppm	233, 298K d at 52.0, 51.9 ppm J 35 Hz
 2	69 % reduction	6 % reduction	233, 298K d at 52.3, 51.3 ppm J 44 Hz	233, 298K d at 52.3, 51.3 ppm J 44 Hz
 3	100 % reduction (diff control)	28 % reduction	233K d at 65.3, 64.8 ppm J 48 Hz 298K br s at 40 ppm	233K d at 65.6, 65.1 ppm J 45 Hz 298K br s at 40 ppm
 4	63 % reduction	no reduction	233K no binding observed under H_2	233, 298K br s at 63.0, 30.0 ppm
 5	69 % reduction	49 % reduction	233, 298K messy	233, 298K messy

Table V: *a comparison of the activity of catalysts 1 and 2 towards hydrogenation and binding studies*

Using labelled mac (***Figure 68***), it was hoped that the chemical shift of the labelled carbon would change due to the shielding influence experienced on coordination to ruthenium. Thus conclusive proof that the alkene was bound to the metal would be obtained. The results are shown in ***Table VI***.

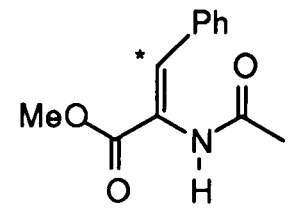


Figure 68: *the usage of labelled mac alllowed binding studies to be followed by* ^{13}C *NMR*

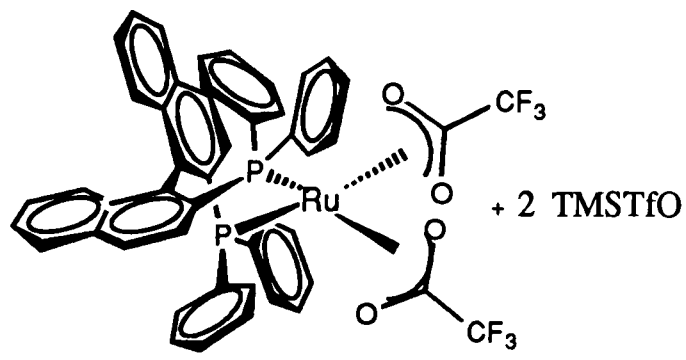
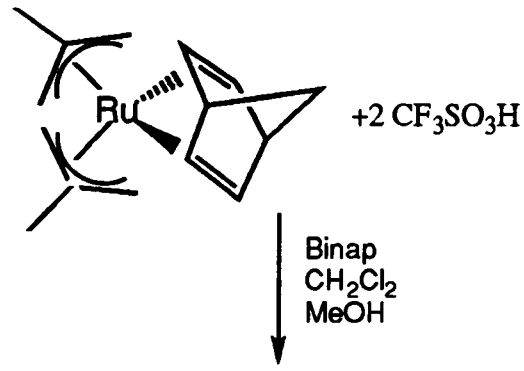
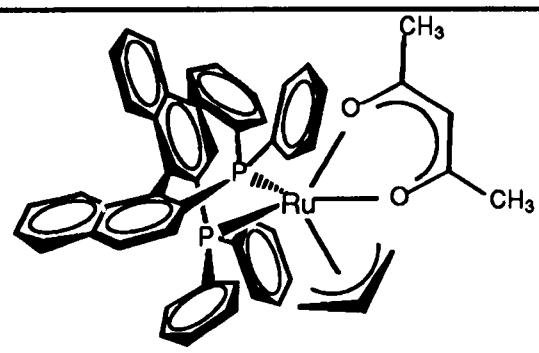
 catalyst 1	using 3 mol eq. mac, at 233K the major peak in ^{13}C NMR was at 134 ppm (free substrate). There was a tiny amount of the 'complexed' peak at 125 ppm, ratio 10:1. Note ^{31}P NMR did not show any free catalyst, therefore the ratio of complexed mac was expected to be higher. At 298K the ratio was 10:0.4.
 catalyst 2	using 3 mol eq. mac, at 233K the major peak in ^{13}C NMR was at 134 ppm (free substrate). There was a tiny amount of the 'complexed' peak at 125 ppm. At 298K the peak corresponding to complexed mac was even smaller.
 catalyst 3	using 3 mol eq. mac, at 233K the major peak in ^{13}C NMR was at 134 ppm (free substrate). There was a tiny amount of the 'complexed' peak at 125 ppm. At 298K the peak corresponding to complexed mac was even smaller.

Table VI: *NMR studies failed to indicate that labelled mac was coordinated to any of the three catalysts used*

The results from ***Table VI*** indicate that with all three catalysts the ruthenium was biting onto the oxygen and the alkene was getting nowhere near the metal centre.

In case these systems required activation of some sort with hydrogen before the catalytic cycle could truly begin, binding studies were next carried out under hydrogen.

When an NMR tube containing catalyst **1** in degassed CD_3OD was whirlimixed under hydrogen no colour changes were observed and two singlets at 83.4 and 69.1 ppm were observed in the phosphorus spectrum (202.46 MHz) at 233K. By 183K the singlets were two broad peaks at 82.0 and 71.2 ppm. ^1H NMR showed there to be no peaks in the region below 0 ppm, thus no metal hydride had been formed. Binding studies were carried out on all three substrates shown in ***Figure 69*** at temperatures between 193K and 233K (increasing the temperature by 10K each time). In all cases no colour changes were observed and the only peaks observed in the phosphorus were those corresponding to 'free' catalyst *ie* there was no evidence at all of any enamide being bound.

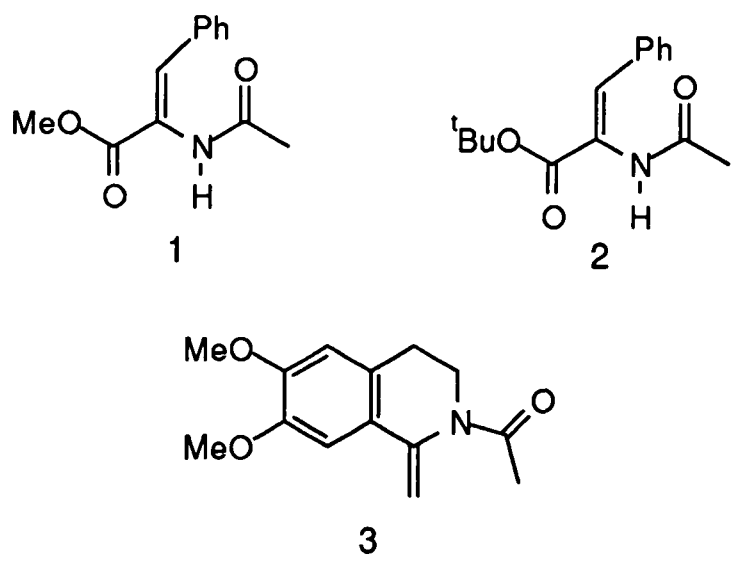
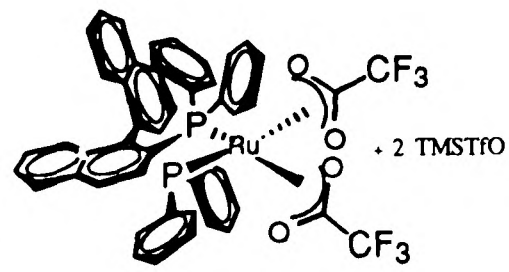
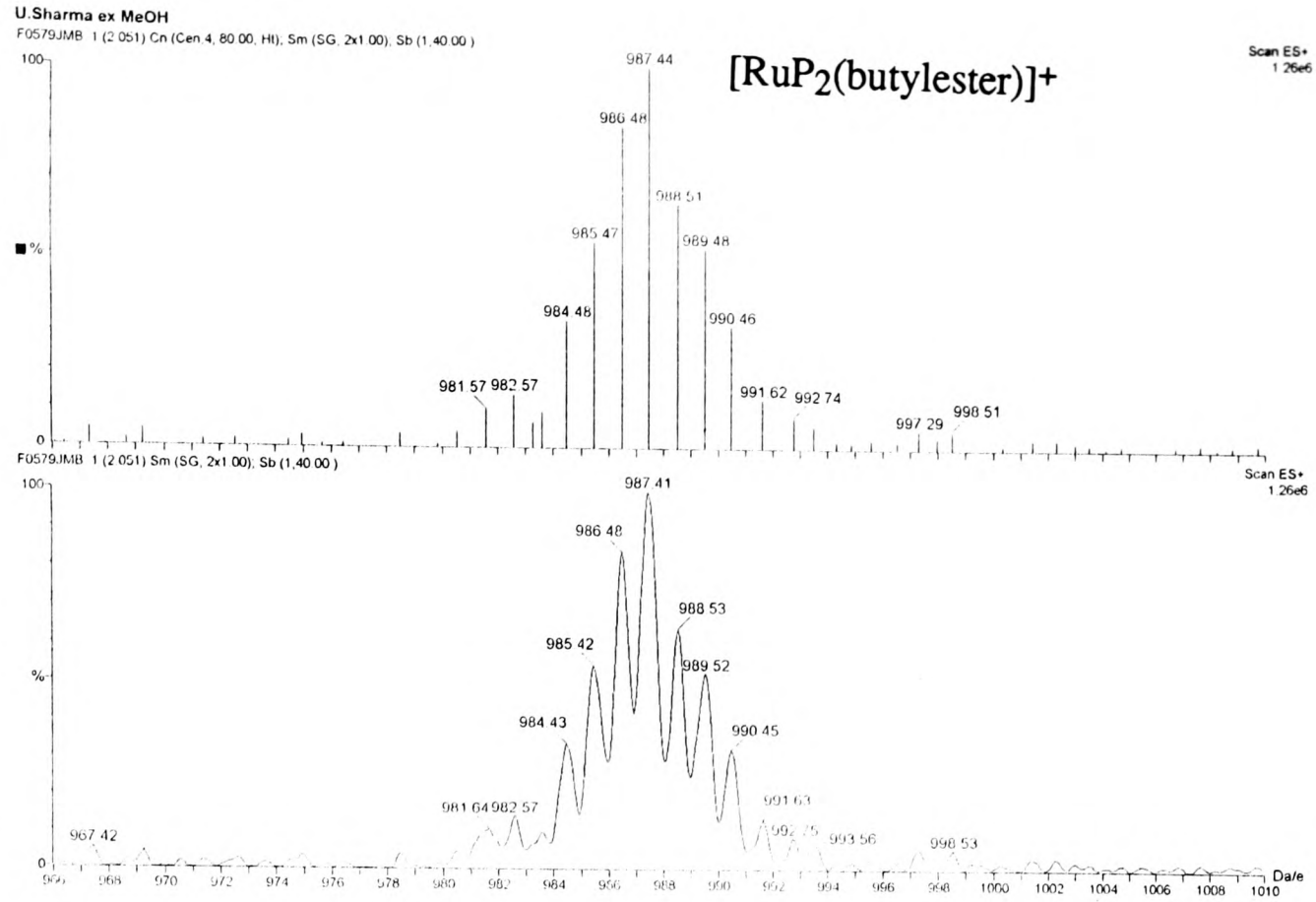


Figure 69: *substrates used in binding studies under hydrogen*

Electrospray mass spectrometry was next carried out on mixtures, formed under argon, of catalysts **1** and **2** with various enamides and N,N-dimethyl acetamide. They showed the existence of an intermediate in which the trifluoroacetate group(s) had been displaced and the substrate had bound, probably through its oxygen as ruthenium is a much more oxophilic centre than rhodium. Peaks corresponding to $[RuP_2substrate]^+$ were consistently observed, ***Figure 70***.

The conclusion drawn from the results obtained so far was that with all the catalysts used, the alkene moiety of the enamides was never bound to the metal. It could be due to the





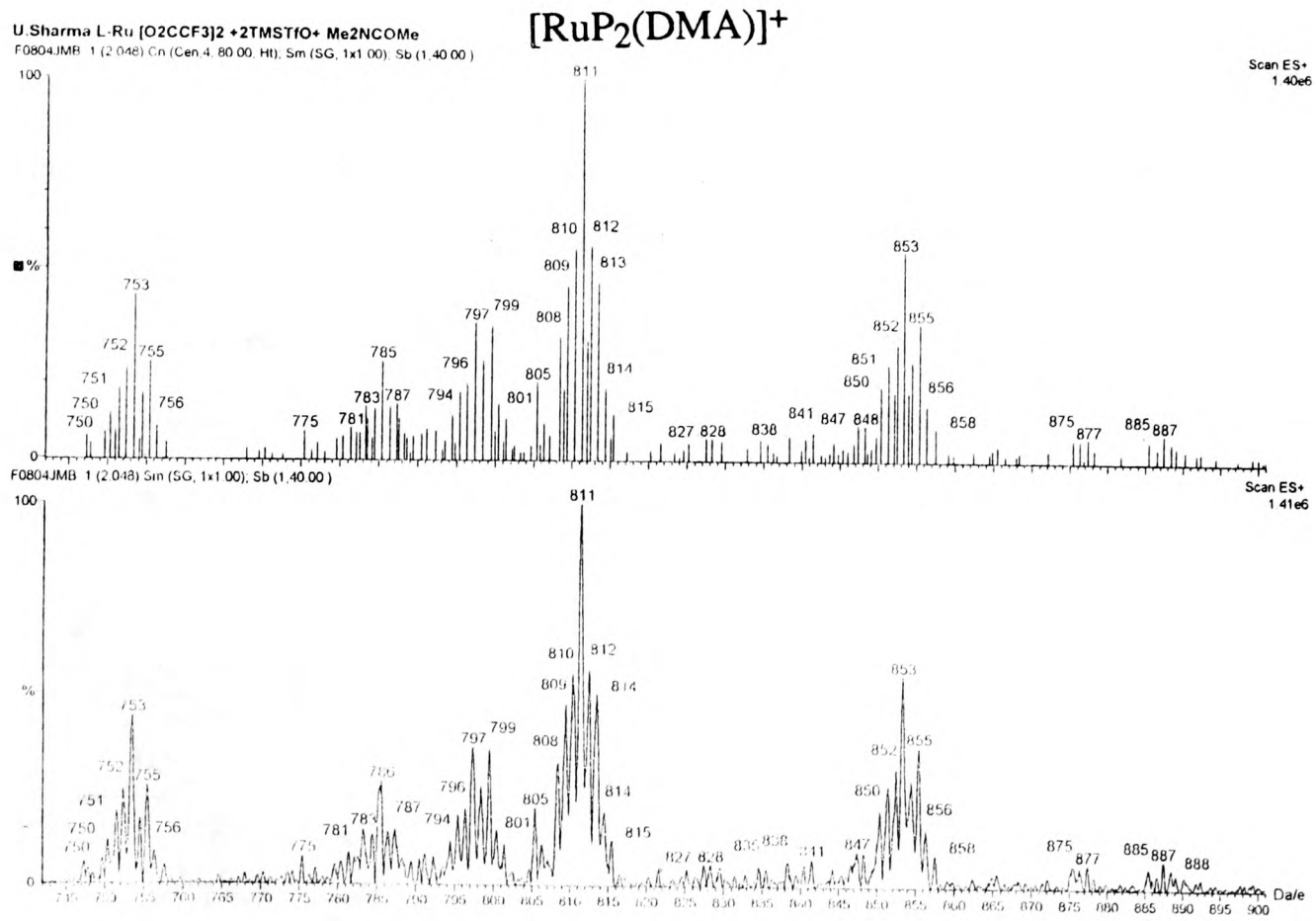
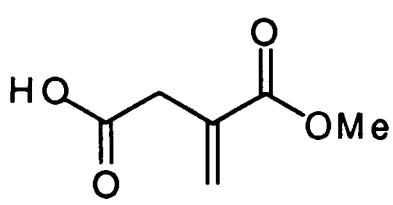


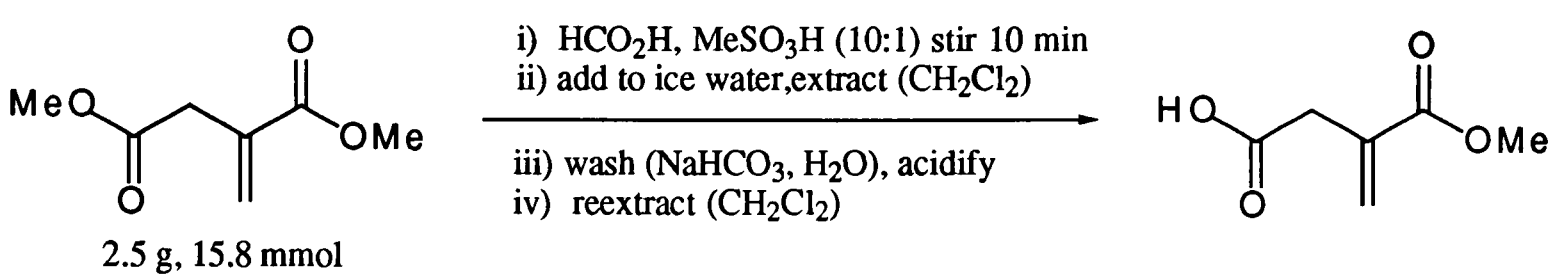
***Figure 70**: electrospray investigations carried out on these catalysts consistently produced peaks corresponding to [RuP2sub]+*

intermediate where the alkene was coordinated to the ruthenium being so transient that it was impossible to trap, or it could be due to alkene approach towards the metal centre being impeded by other bulky groups around the ruthenium atom.

In order to overcome the problem of getting the alkene in place, it was decided to try using a tethered alkene which was already linked to one of the ligands attached to the metal centre and hence more likely to approach the ruthenium atom.

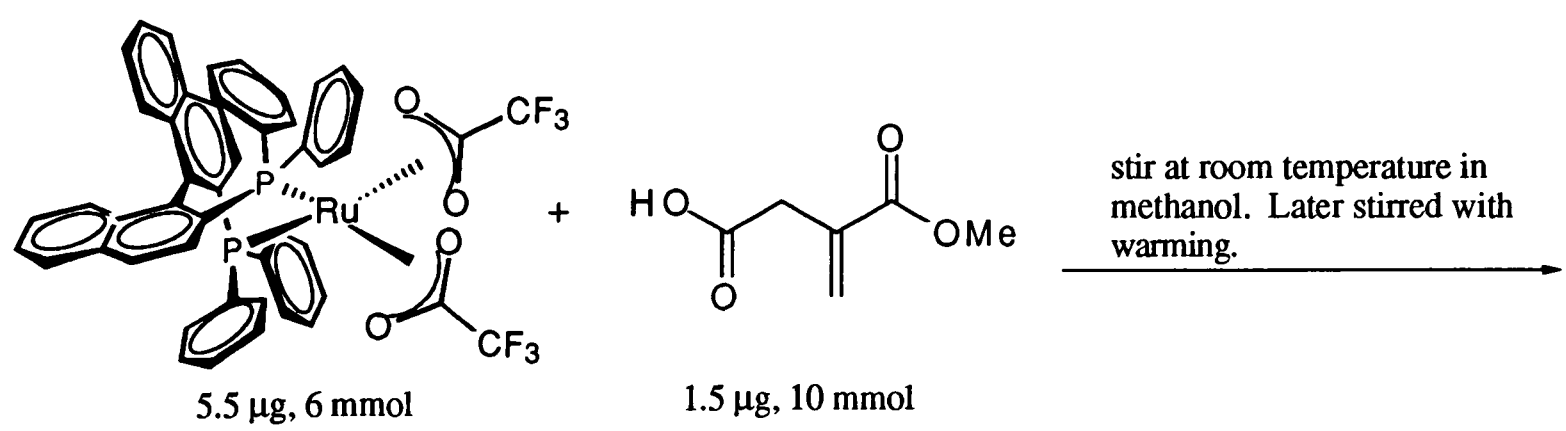


was the tether of choice. This compound was prepared in the following way[71] (***Scheme XXIX***).

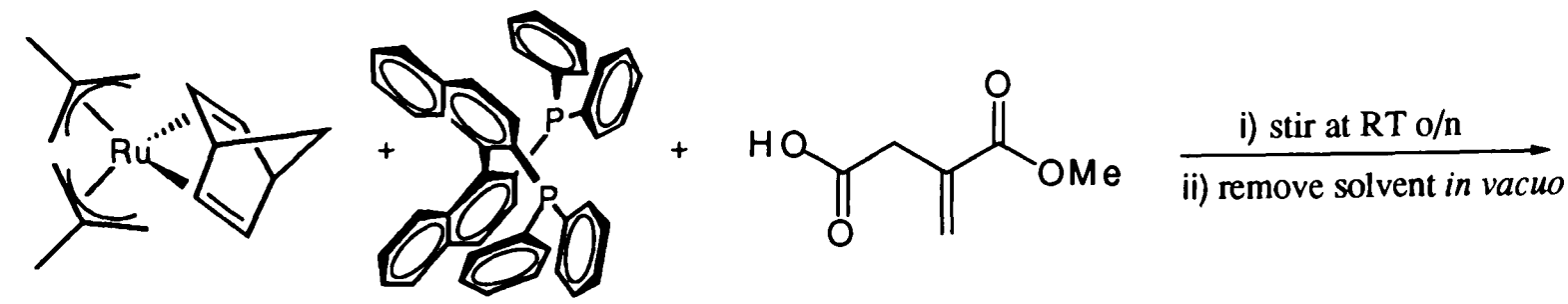


Scheme XXIX: *an alkene that was also capable of complexing to the metal through its carboxylate function was synthesised*

Synthesis of an appropriate ruthenium catalyst was attempted in two ways. Firstly an *in situ* approach starting with Heiser's catalyst was attempted (***Scheme XXX***) and a synthesis following Heiser's method[69] was also carried out (***Scheme XXXI***). The *in situ* approach was monitored by ^{31}P NMR (202.46 MHz). Heiser's catalyst and the carboxylic acid were stirred under argon in distilled, degassed methanol and later, when no reaction was occurring, the yellow solution was warmed and monitored every few hours by NMR. Both attempted syntheses proved unsuccessful.



Scheme XXX: *an in situ attempt to complex the carboxylic acid to Heiser's catalyst failed*



6 mg, 20 μmol in degassed methanol

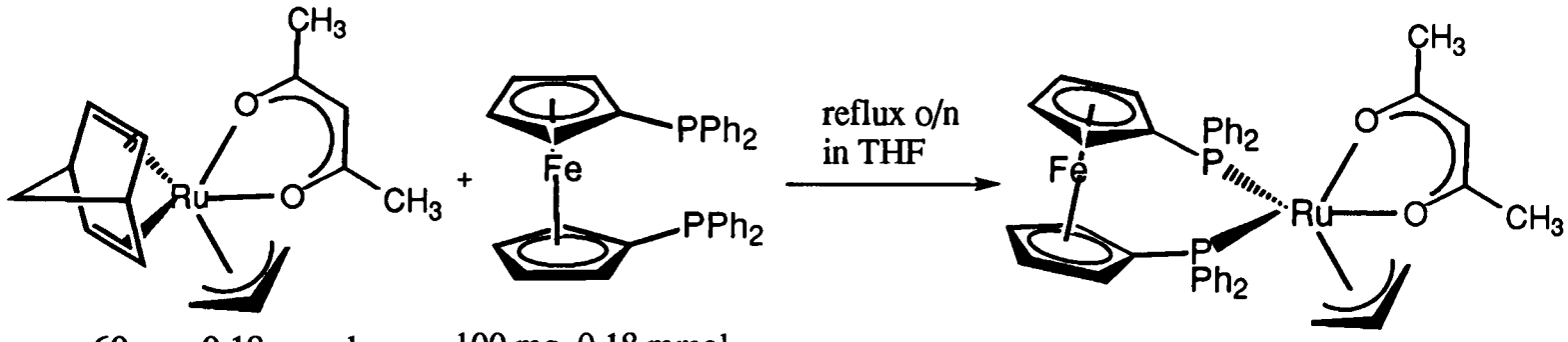
12.4 mg, 20 μmol in degassed CH_2Cl_2

2.9 mg, 20 μmol

Scheme XXXI: *attempts to synthesise a catalyst using Heiser's method also failed*

Ru(DPPF)(allyl)(acac)

Up to now, attempts to reduce the steric bulk around the metal and hence facilitate approach of alkenes towards ruthenium had concentrated on varying the secondary groups attached to the ruthenium, whilst maintaining the identity of the bisphosphine, BINAP. Finally, it was decided to change the steric bulk of the ligand to a less demanding bisphosphine. The most 'successful' catalyst in terms of both hydrogenations and attempted binding studies had been Brown's Ru(BINAP)(allyl)(acac). Thus an analogue of this catalyst was synthesised using the ligand dppf (1.1'-bis(diphenylphosphino)ferrocene), ***Scheme XXXII***. The catalyst was prepared by refluxing DPPF and (η^4-bicyclo[2.2.1]hepta-2,5-dienyl(η^3-2-propenyl)acetylacetonatoRu^{II} under argon in THF overnight[38]. Removal of the solvent *in vacuo* yielded the product as a yellow powder (δ 62.6, 27.0, d, J = 35 Hz).



60 mg, 0.18 mmol 100 mg, 0.18 mmol

Scheme XXXII: *Ru(DPPF)(allyl)(acac) was synthesised as a catalyst with less steric bulk around the ruthenium*

Firstly its behaviour in binding studies under argon was investigated using an excess of substrate over catalyst. The activated catalyst (activation being achieved by treatment with TMSTfO) displayed two doublets in its ^{31}P NMR at 233K, δ 63.1, 41.9 ppm, J = 40 Hz (202.46 MHz, CD_3OD). Substrate 3 (***Figure 69***) was very weakly bound to this catalyst at 233K; the spectrum obtained was essentially that of free activated catalyst. The solution was yellow throughout the binding experiment - once again a visual indication of complex formation was lacking. The spectrum from substrate 1 (***Figure 69***) is shown in ***Figure 71***. The catalyst is achiral and so only one diastereomer would be expected, yet four doublets were observed at 233K. This meant either that two species were present or that maybe some dimeric species had been formed. As the spectrum from this

compound was quite clean, it was decided to concentrate future investigations on this catalyst / substrate system. Notice that the substrate appeared to be bound through both its alkene (in the region of 40 ppm) and carbonyl (in the region of 70 ppm) moities. A binding study using N,N-dimethyl acetamide did not yield a clean, informative spectrum.

^{19}F NMR (49.69 MHz, CD_3OD) was carried out to determine whether the triflate was covalently or ionically bound to ruthenium. All three substrates (***Figure 69***) gave rise to singlets at -81.9 ppm. Ionic sodium triflate gave rise to a singlet at -93.6 ppm *ie* the triflate in these intermediates is covalently bound.

Next, it was decided to 'titrate' the mac / ruthenium dppf system at 233K and see if more enamide became bound as the concentration of substrate was increased and whether the relationship between amount of bound species and concentration was linear. The titrations began with a binding sample (prepared in the normal fashion) containing a five molar excess of mac over catalyst. As the ^{31}P NMR shows, there was no trace of 'bound' species , despite the excess amount of substrate, so an additional five moles of substrate were added. Following this addition, subsequent additions increased the amount of substrate by ten mol equivalents each time. Measurement of the integrals corresponding to bound species indicated that the relationship between bound species and substrate concentration was approximately linear. The results are shown in ***Figure 72***.

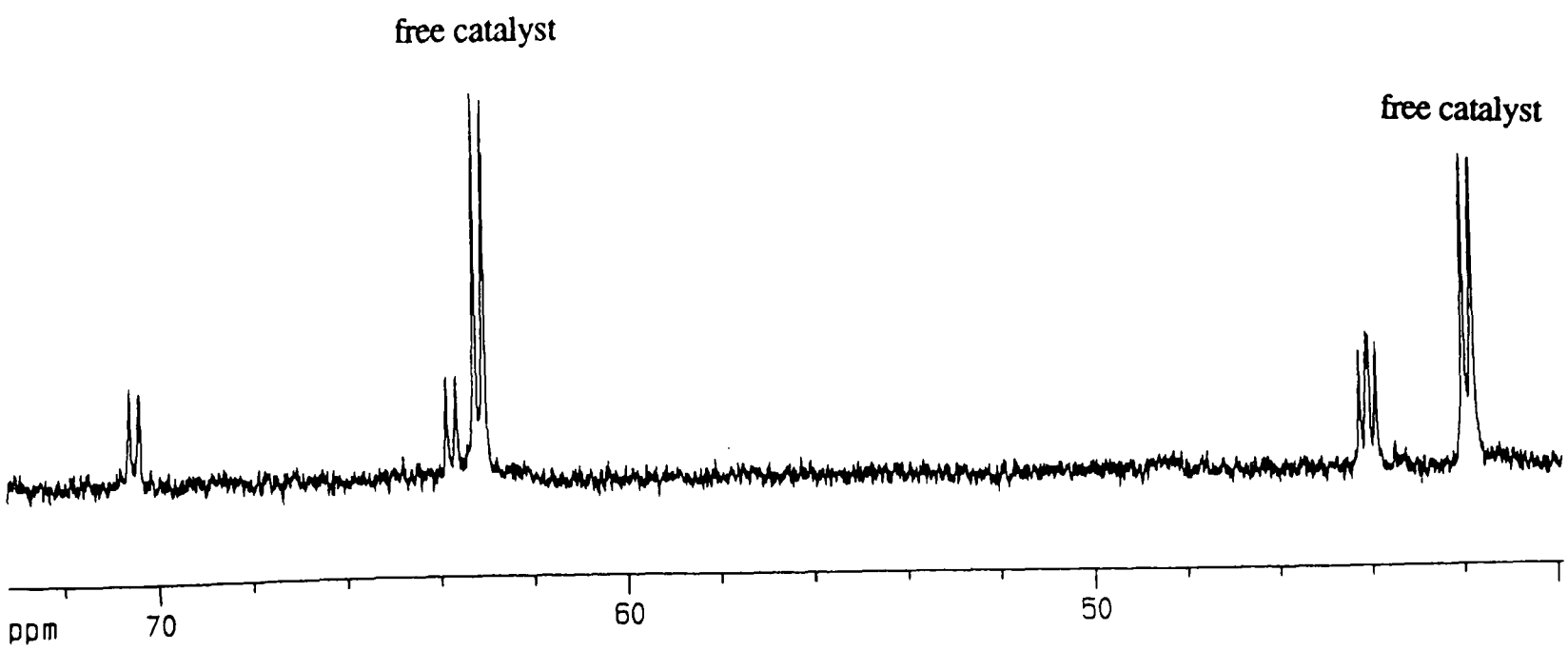


***Figure 71**: a binding study using mac and Ru(DPPF)(allyl)(acac)*

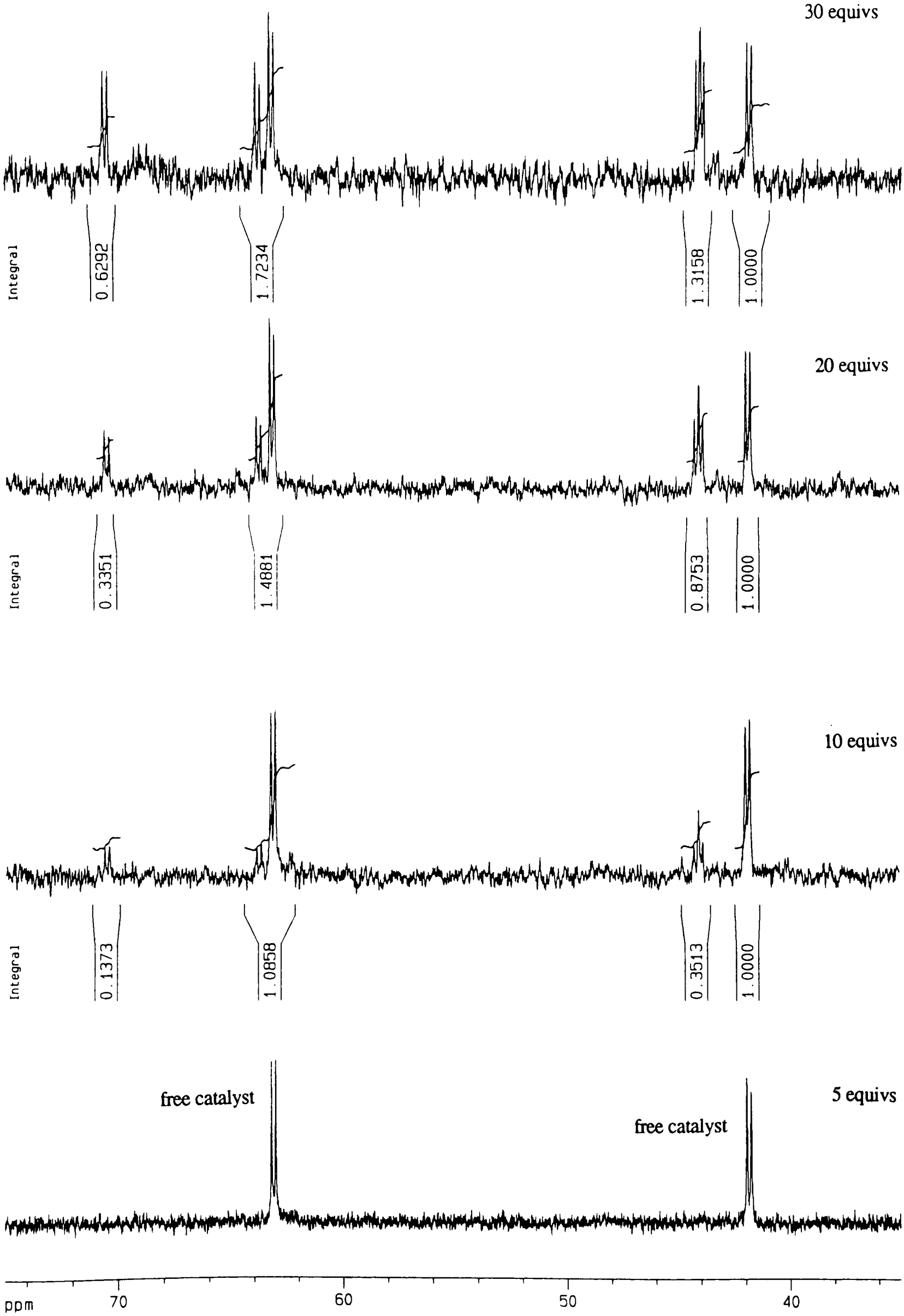


***Figure 72**: titrating the mac/Ru(DPPF)(allyl)(acac) system at 233K*

To check the reproducibility of the titration results, the process was repeated using labelled mac as the substrate and monitored using both ^{31}P and ^{13}C NMR. Phosphorus spectra obtained were the same as those shown in ***Figure 72*** underlining the reproducibility of the titration exercise. However the carbon spectra did not show any evidence of the alkene being bound to the metal (the chemical shift of the labelled carbon atom did not change) indicating that ruthenium is so electrophilic (in comparison with rhodium) that oxygen always binds to it in preference to any other moities present in the substrate. But an examination of the ^{13}C NMR spectra showed that the chemical shifts of the ester and amide carbonyls had not shifted either - if they had it could have provided evidence that the enamide was bound through the oxygen atom.

The NMR sample was left at -78°C for one week to check whether the species observed with thirty equivalents of substrate collapsed with time down to a single species. ^{31}P NMR acquired at 233K after this time period showed additional species at 41.8, 31.5, 12.5 and 10.4 ppm. These double doublets were probably due to bridged ruthenium dimers. They seemed to have been formed at the expense of 'free' catalyst. On warming through to 253, 273 and 298K, the spectra broadened to finally display a major broad peak at 43 ppm.

Electrospray mass spectrometry on mixtures of catalyst and mac or N,N-dimethyl acetamide were inconclusive and did not really point to the substrates being bound to the metal.

When tested as a hydrogenation catalyst, this catalyst was found to be very effective (***Figure 77***, using catalyst loadings of between 1 and 2 mol %). Consistently reproducible kinetics were obtained for hydrogenations carried out on mac (**1**, ***Figure 69***). Solutions were pale yellow throughout the hydrogenation procedure *ie* as usual with these ruthenium catalysts, there was no visual evidence of catalyst activation, formation of a complex between the substrate and catalyst, or completion of the reaction.

The next stage in investigating this catalytic system was to perform binding studies under hydrogen. When a sample of catalyst on its own was 'whirlimixed' under hydrogen and observed by ^{31}P NMR, no change was observed from the spectrum of free catalyst under argon (doublets at 63.1 and 41.9 ppm). No evidence of bound species was seen on adding ten equivalents of mac to this tube.

However when a sample of catalyst that had been whirlimixed and kept under hydrogen was left for three weeks at -20°C, the spectrum changed and was a broad dynamic peak around 60-70 ppm at 213, 223 and 233K. At 300K the spectrum sharpened up, as shown in ***Figure 73***.

These results were interpreted as indicating that there was an induction period for catalyst 'activation' which was very long at 233K. This was why there was no evidence of bound species on immediately adding ten equivalents of mac to 'activated' catalyst. It was decided to test this inference out in three ways:

(i) by adding substrate to the sample of catalyst that had been left under hydrogen for three weeks.

(ii) by whirlimixing an NMR tube of catalyst under hydrogen and then adding excess substrate at room temperature (when any induction period would be much shorter than at 233K). The sample would then be cooled and spectra acquired at 233K.

(iii) by carrying out hydrogenations at temperatures between 0°C and 25°C to see (from plots of pressure against time) whether there was an induction period and how it varied with temperature.

(i) Adding excess substrate to the NMR tube that had been left for three weeks resulted in a phosphorus spectrum that was not very well resolved at 233K (***Figure 74***). A series of blocked spectra (of approximately 30 minutes acquisition time each) were acquired to see if the system changed with time. No changes from the initial spectrum were observed.

(ii) Mixing the catalyst and substrate at room temperature before cooling and beginning the NMR acquisition led to new peaks besides those corresponding to free catalyst (***Figure 75***). Once again, blocked spectra showed no change of this system with time.

iii) A series of hydrogenations were performed on mac at various catalyst concentrations (between 0.5 and 2.5 mol%) corresponding to reductions carried out at 25°C, thus allowing a direct correlation of reaction rates. Reductions were performed at 18.4, 14.2, 8.9, 0.7 and 0°C. The reactions were obviously considerably slower at lower temperatures but induction periods, of 100s, were only observed at 0.7°C and 0°C and were not apparent at any of the other temperatures. An induction period of 100s at around 273K would be expected to extrapolate to a much longer induction period at 233K, the temperature of acquisition for most of the NMR work to date.

Thus all three investigations pointed towards an induction period, adding weight to the reasoning why binding investigations had proved unsuccessful. Although the NMR work had not yielded conclusive results due to the apparent inability to break into the catalytic cycle, the small inroads and conclusions that were made provide the most substantial set of results reported to date on investigations, using NMR techniques, into the ruthenium complex catalysed reduction of alkenes.

Allowing for the constraints imposed by the techniques and machinery available, all possible routes towards gaining an insight into the mechanism from NMR studies were exhausted. It had been hoped to conduct binding studies at high hydrogen pressures, but it was not possible for such studies to be pursued.

In a final attempt to obtain solid evidence of the substrate (and possibly a hydrogen containing intermediate) coordinated to ruthenium, it was decided to monitor hydrogenations by electrospray mass spectrometry. The first system to be looked at was the Ru(DPPF)(allyl)(acac) and mac. Using a catalyst loading of 1.5 mol% led to a reaction time of 500s. Thus, in the electrospray reaction, the reaction was allowed to proceed for 150s before being quenched (by cooling to -78°C, evacuating the hydrogen

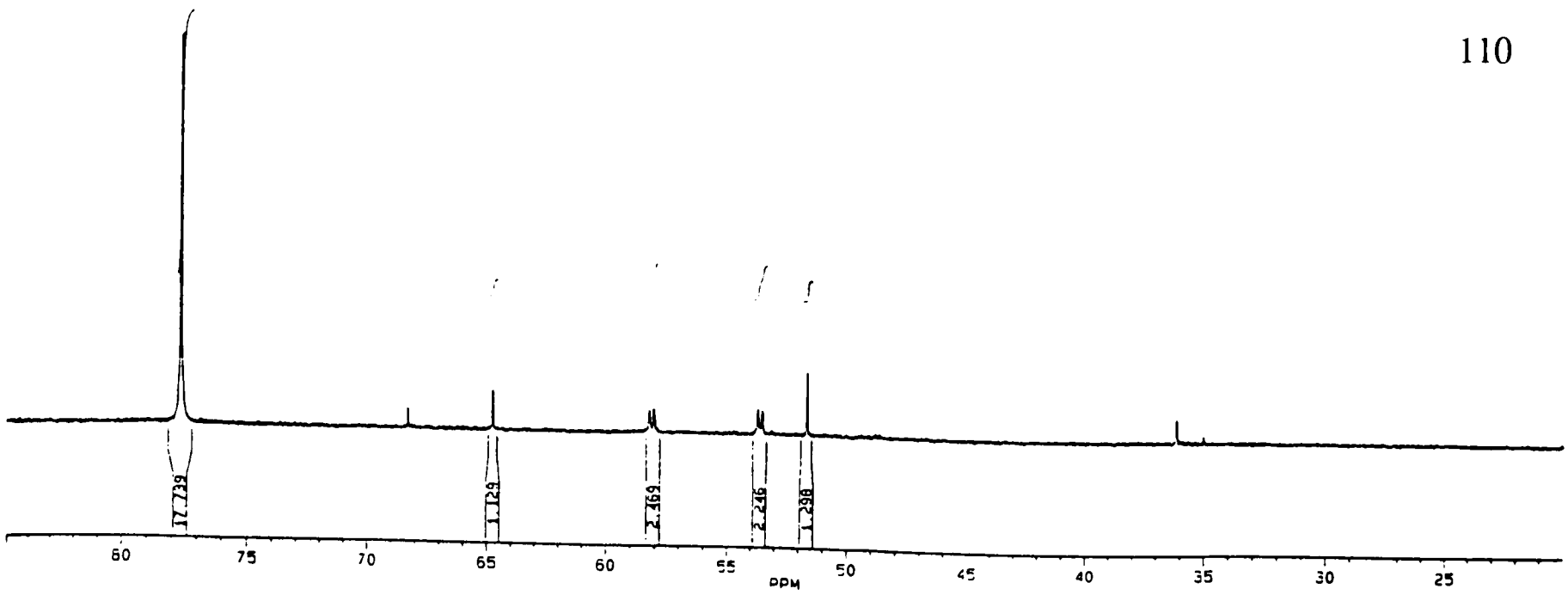


***Figure 73**: a catalyst sample prepared under hydrogen and kept at 253K for three weeks had the structure shown above at 300K*

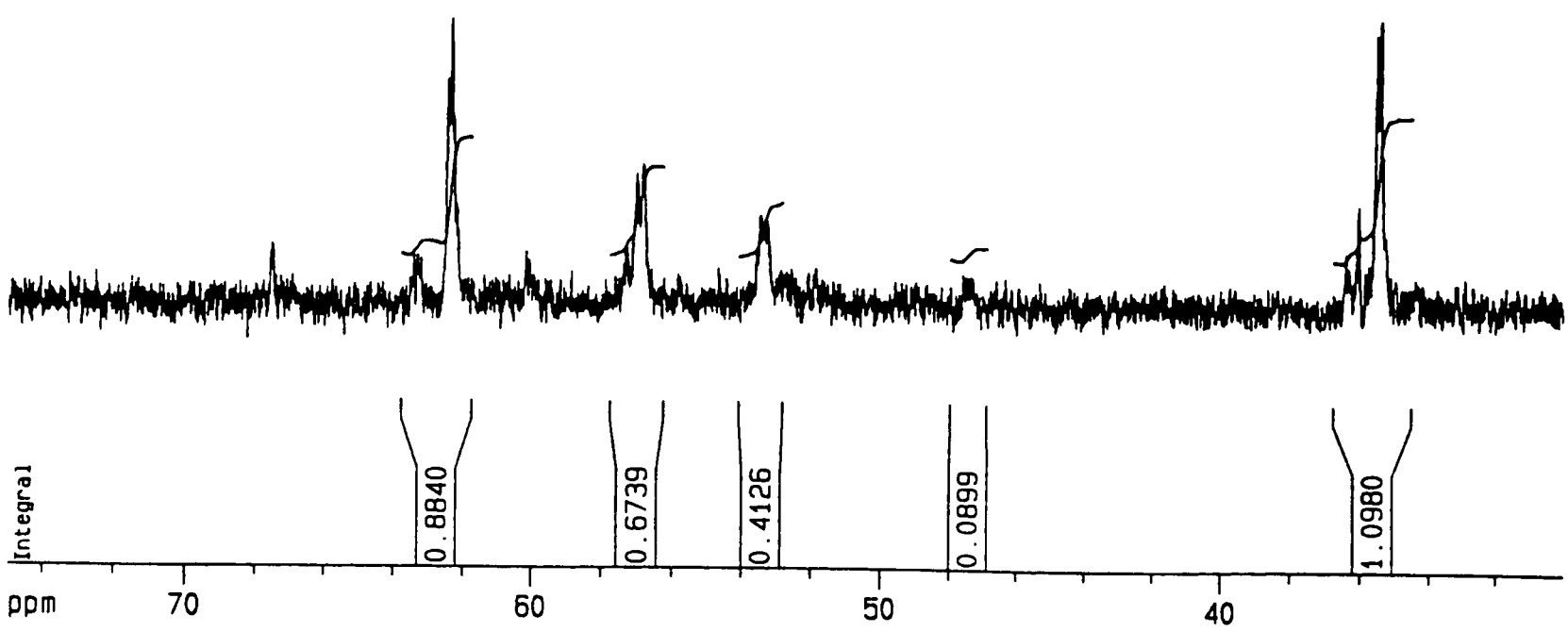


Figure 74**: an unresolved spectrum was obtained on the addition of substrate to the NMR sample used in **Figure 73

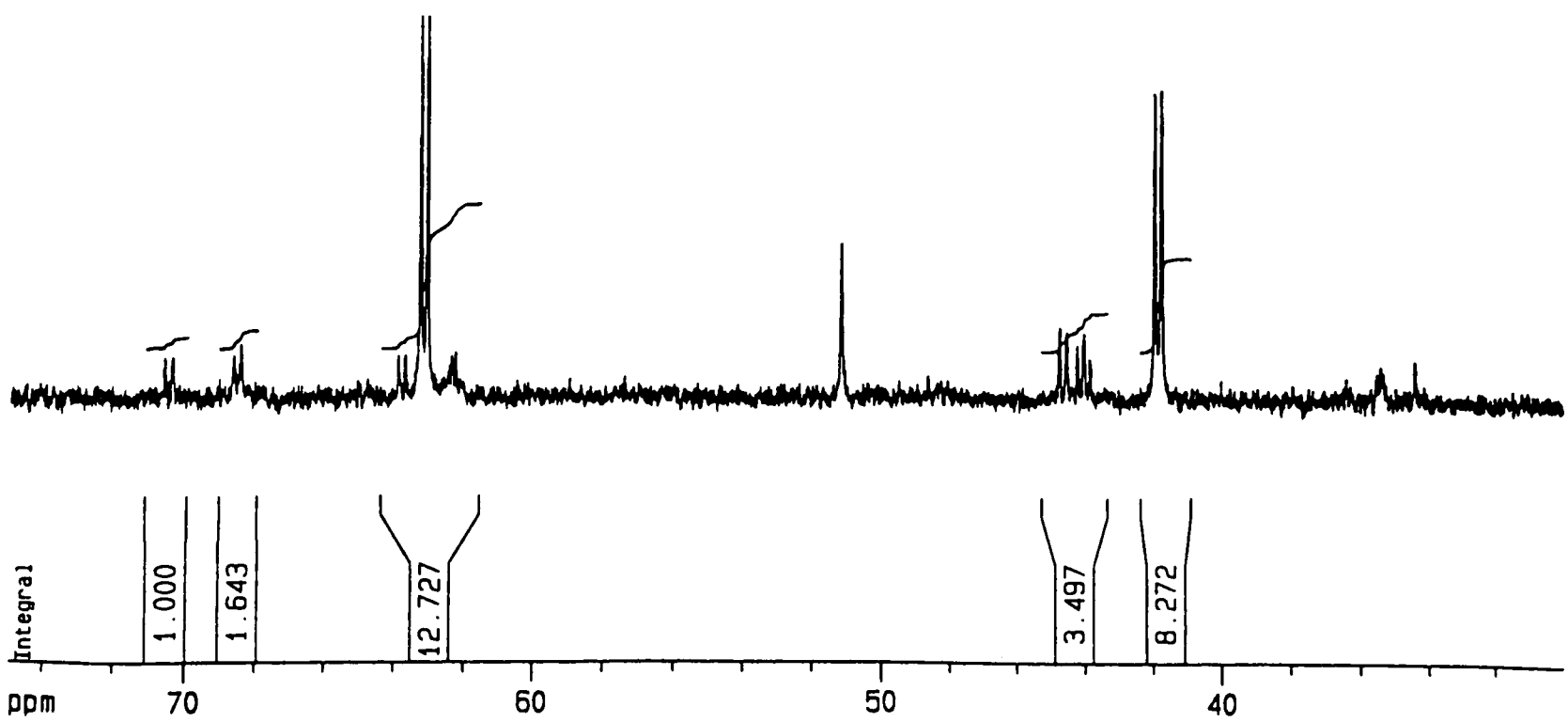


***Figure 75**: above is the spectrum obtained from a system prepared under hydrogen at room temperature and then subsequently cooled*

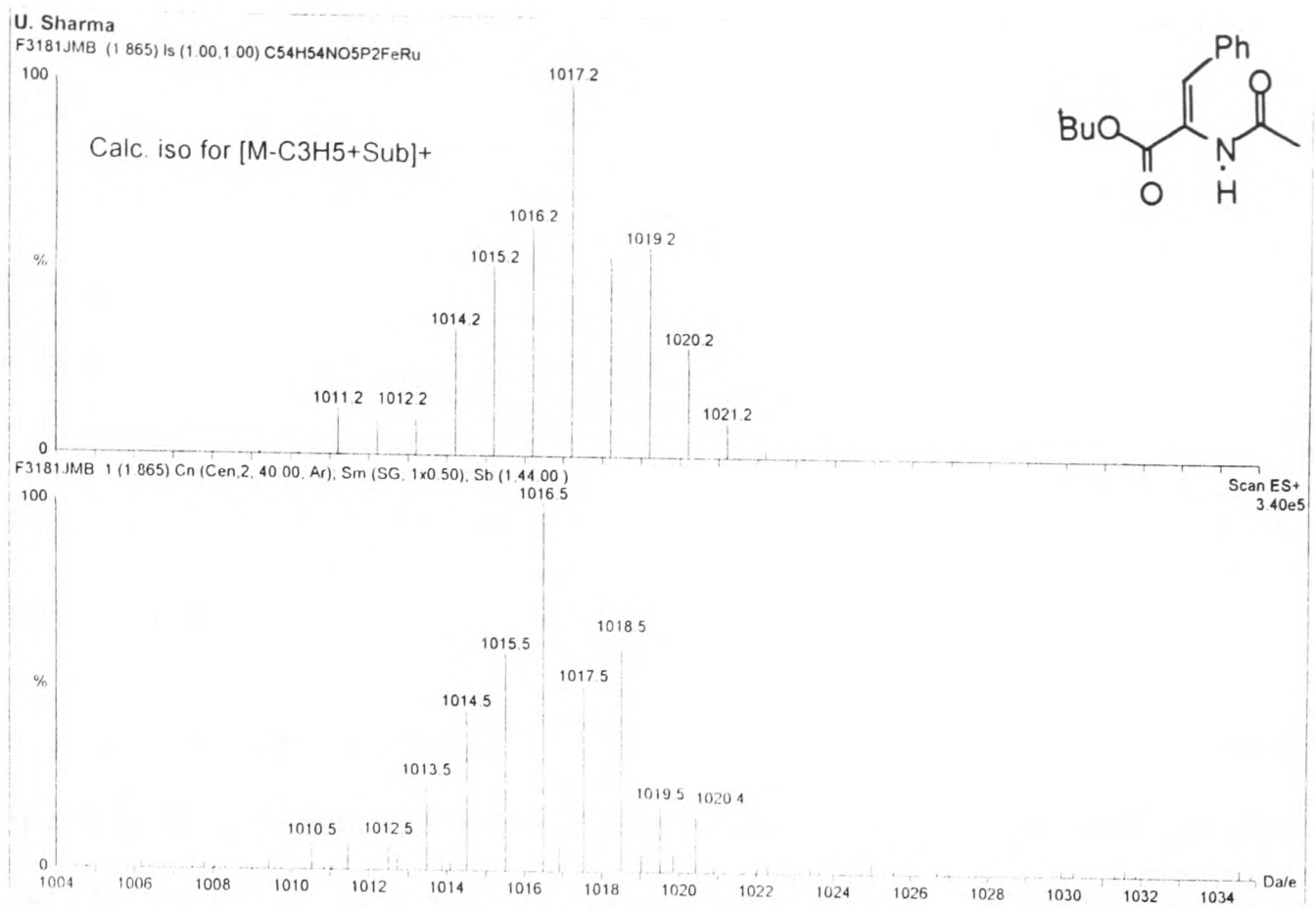
atmosphere and replacing it with argon). An aliquot was extracted from the reaction mixture and analysed by mass spectrometry. Previous electrospray mass spectrometry investigations (p107) had failed to conclusively show any bound species. This time a peak was observed at 974 which corresponded to [M-allyl+mac]$^+$. There was no evidence of a hydrogen containing species, ***Figure 76***.

The process was repeated using deuterium instead of hydrogen. Identical results were obtained to the reaction under hydrogen *ie* there was no evidence of an intermediate containing deuterium. Both spectra showed a weighting in the isotope pattern indicating there was an additional peak in the [M-allyl+mac]$^+$ isotope range, corresponding to [M-allyl+reduced mac]$^+$, which was about 5% the intensity of the [M-allyl+mac]$^+$ peak.

As verification, an *in situ* 'hydrogenation' on the ruthenium catalyst and reduced mac was carried out. The electrospray mass spectrometry did indeed show a peak corresponding to [M-allyl+reduced mac]$^+$. These results were backed up by carrying out an electrospray monitored hydrogenation of the ^{t}butyl amide (**2**, ***Figure 70***). Once again a peak for [M-allyl+sub]$^+$ was observed, with a weighting in the isotope pattern towards [M-allyl+reduced substrate]$^+$, ***Figure 76***. So, although the reduced product appeared bound to the ruthenium, the extent to which it was bound was minimal in the presence of non reduced substrate.

Finally, this procedure was carried out using DMA as the substrate to confirm binding occurred through oxygen to the oxophilic ruthenium centre (this was the only way that the reduced products could have coordinated to ruthenium). As expected, the electrospray confirmed the presence of a peak at 842 corresponding to [M-allyl+DMA]$^+$.

Following the success of electrospray monitored hydrogenations using Ru(DPPF)(allyl)(acac), it was decided to investigate the behaviour of Heiser's catalyst in such experiments. A reaction was conducted using a catalyst loading of 1.6 mol%, quenched after 80s and an aliquot extracted for observation by electrospray mass spectrometry. A peak, believed to correspond to [M-$CF_3CO_2^-$+substrate+MeCN]$^+$, was



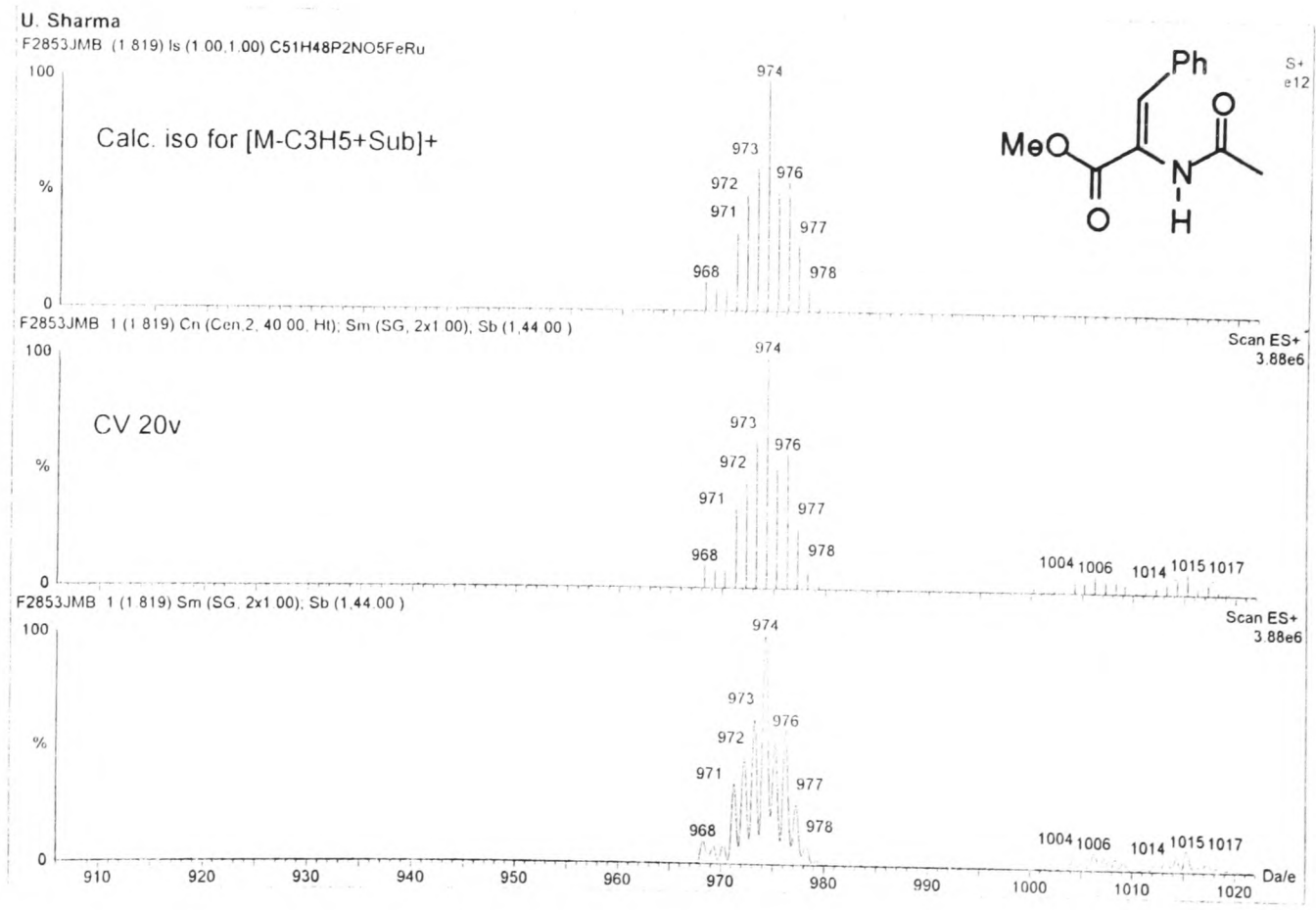
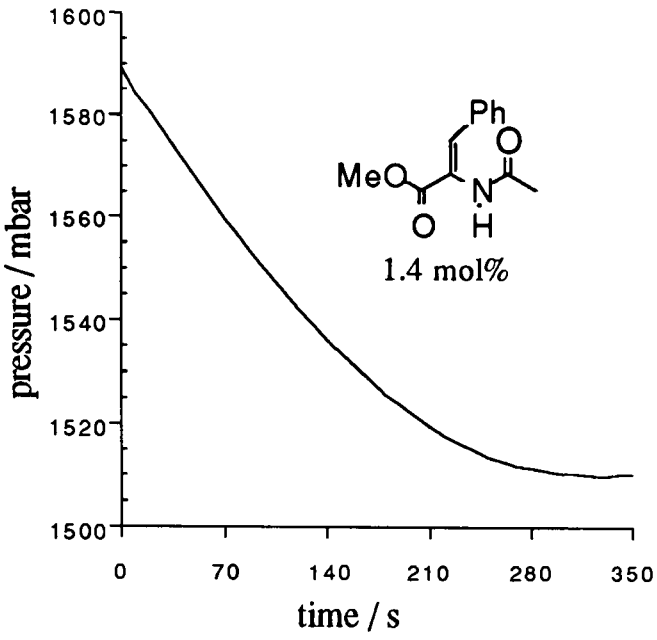


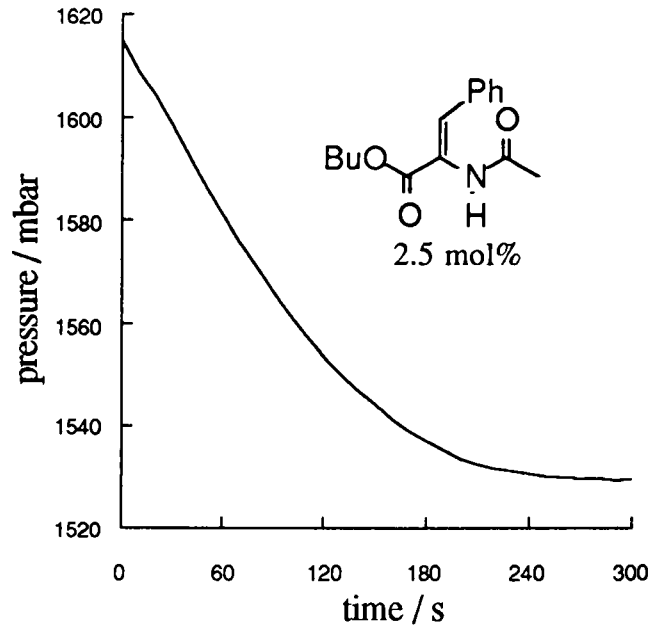
***Figure 76**: in situ hydrogenations monitored by electrospray showed peaks corresponding to [M-allyl+sub]$^+$*

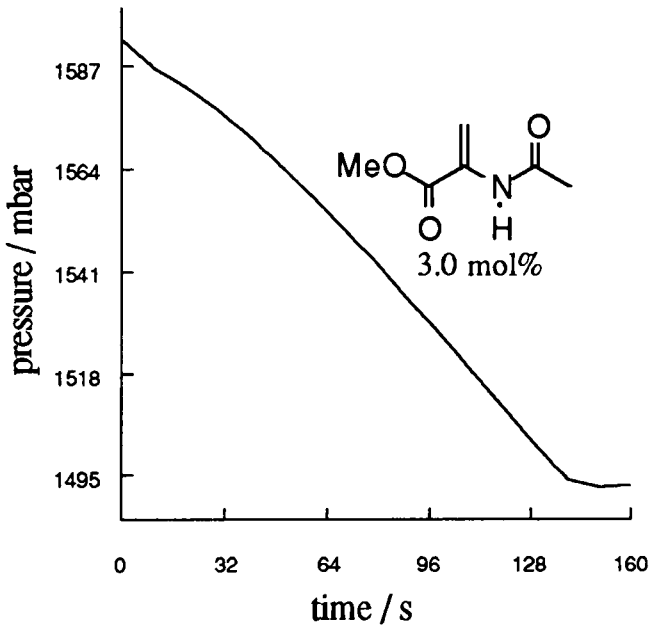
observed at 1124. Once again, there was a small weighting in the isotope pattern towards a trace of reduced product also being coordinated to the metal.

Having exhausted all of the possible options available for conducting NMR studies, it was decided to return to the kinetic side of this study. As mentioned previously (p19, introduction) the most extensive mechanistic work carried out on ruthenium chemistry has been by Halpern on tiglic acid[37]. He obtained a rate law for the reduction of this substrate which featured both product inhibition and an inverse dependence of reaction rate on the initial concentration of substrate. Firstly, the Ru(DPPF)(allyl)(acac) catalyst's activity was investigated with respect to hydrogenating other enamides. The results are shown in ***Figure 77***. No reduction of **3** (***Figure 69***) was observed.

It is surprising that the reaction rates observed with Ru(DPPF)(allyl)(acac) were comparable to those obtained with Ru(BINAP)(allyl)(acac). It would be expected (and is indeed observed in rhodium chemistry) that achiral catalysts are capable of hydrogenating substrates much faster than their chiral counterparts, due to the lack of competing major/minor diastereomeric interconversion.







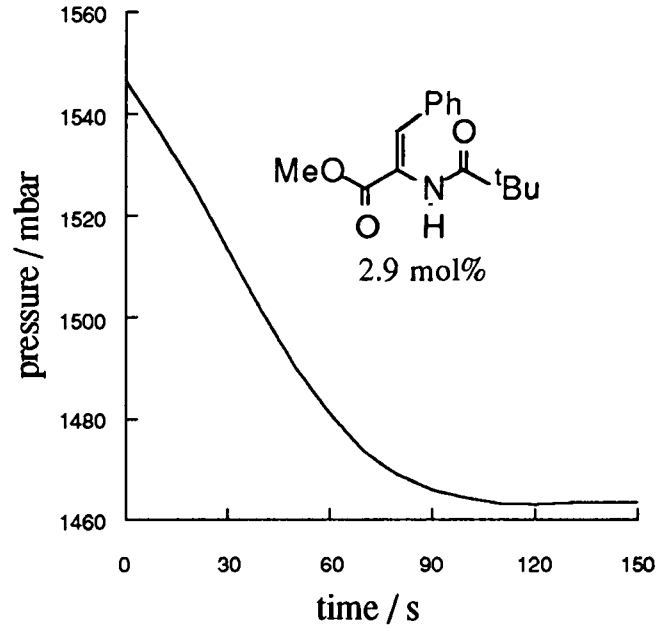


Figure 77: *Ru(DPPF)(allyl)(acac) catalysed the reduction of four of the five enamides it was tested on*

Kinetics

Hydrogenations using Ru(DPPF)(allyl)(acac) were clean and quick with no appparent secondary processes occurring. Thus, it was decided to next concentrate on a detailed kinetic analysis of this catalyst (with mac) and its dependence of reaction rate on classic variables such as hydrogen pressure, catalyst concentration and substrate concentration.

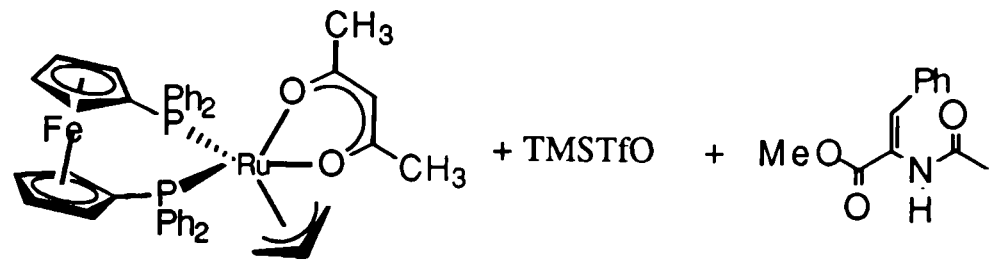
Care was taken to ensure reactions were carried out at catalyst concentrations far enough away from diffusion control to allow the results of modelling the data to be meaningful (and not overshadowed by the dependency on hydrogen diffusing into the methanol).

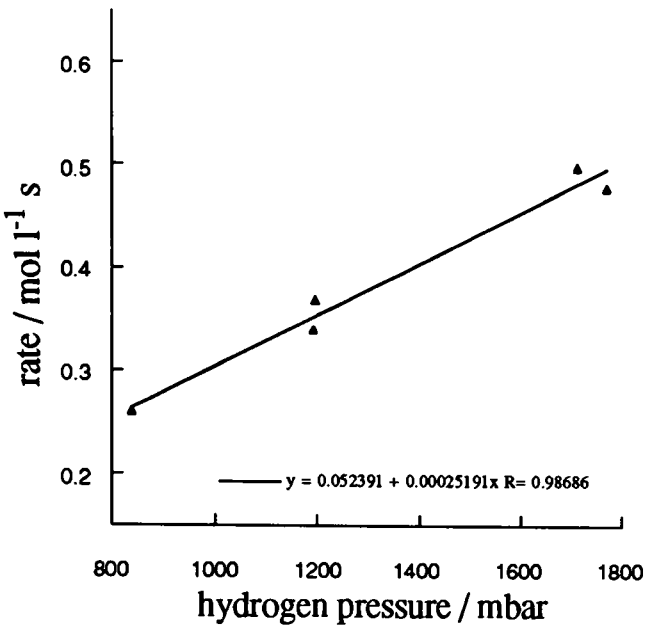
Variations on catalyst concentration were carried out between 1.0 and 2.5 mol%. Substrate concentration experiments used between one and four equivalents of substrate at a catalyst concentration of 1.5 mol%. Pressure dependencies were looked at between 800 and 1800 mbar, again using a catalyst loading of 1.5 mol%. The temperature was consistently 25.5°C. Reactions were repeated until consistent results were obtained. The results obtained are shown in ***Figure 78***. The reaction rate showed the expected linear dependence on catalyst concentation and hydrogen pressure but, surprisingly, an inverse dependence of rate on substrate concentration was found.

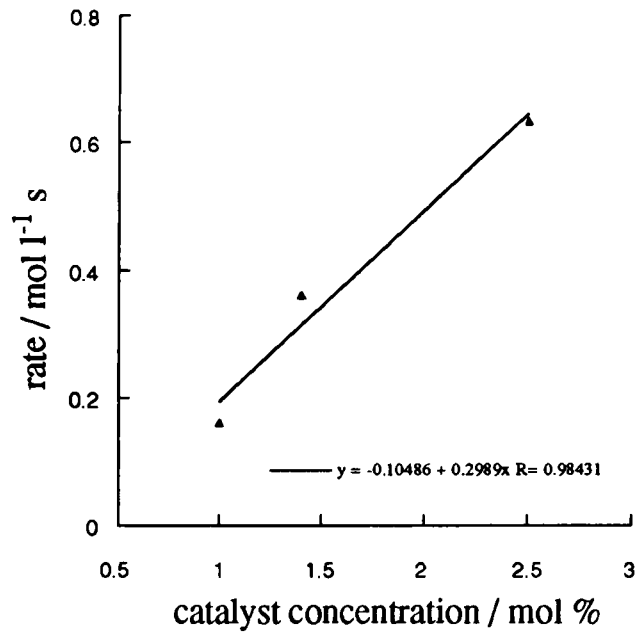
As Halpern's tiglic acid work found product inhibition in the reduction of α,β unsaturated acids (p19, introduction), it was decided to investigate the effect of externally added reduced mac on reaction rate. In keeping with Halpern's findings, apparent product inhibition was observed.

The next catalyst to undergo a detailed kinetic study was Heiser's.

Investigations were carried out using both substrates shown in ***Figure 79***. Once again, the dependency of the reaction rate on hydrogen pressure, catalyst concentration and substrate concentration was investigated at catalyst concentrations far enough away from diffusion control for the interpretation of the results to be meaningful.







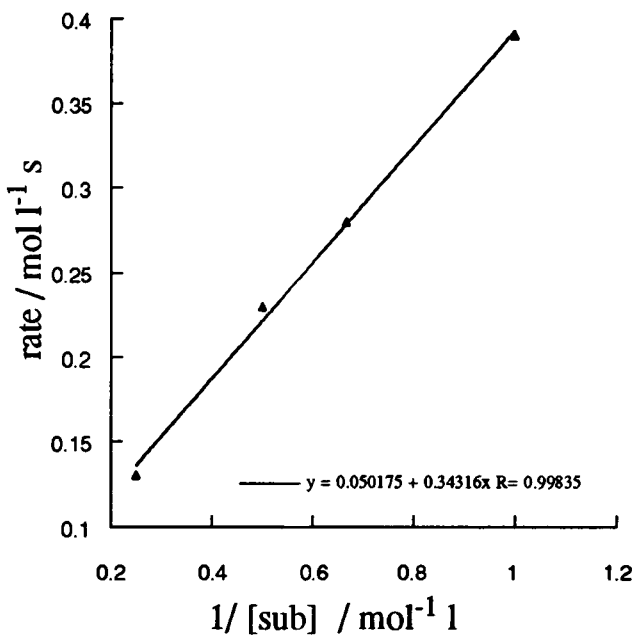


Figure 78: *the reaction rate for Ru(DPPF)(allyl)(acac) showed a first order dependence on catalyst concentration and hydrogen pressure yet an inverse dependence on substrate concentration*

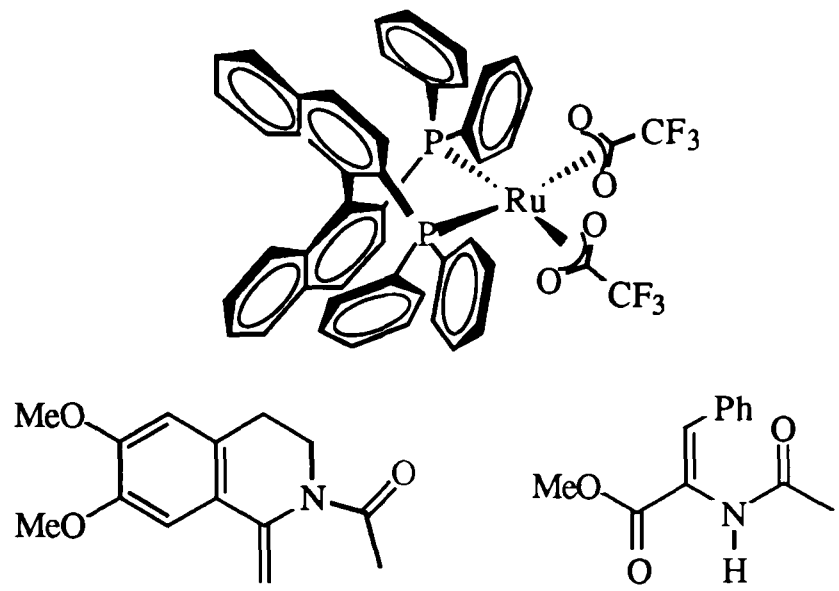
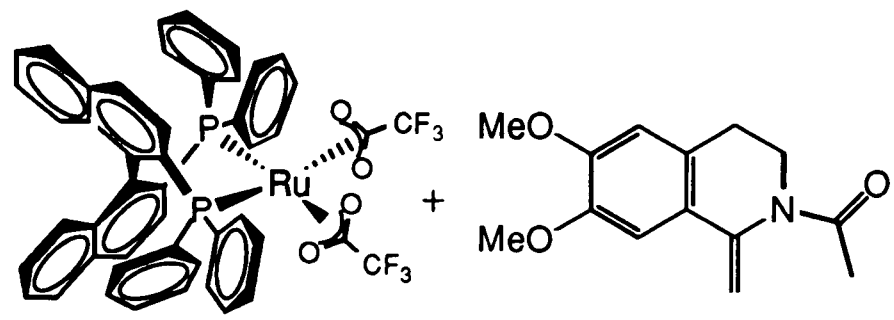
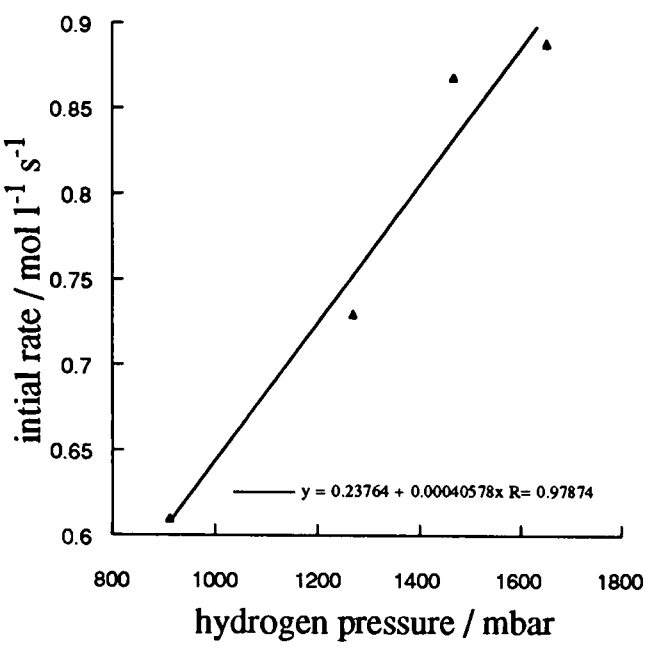
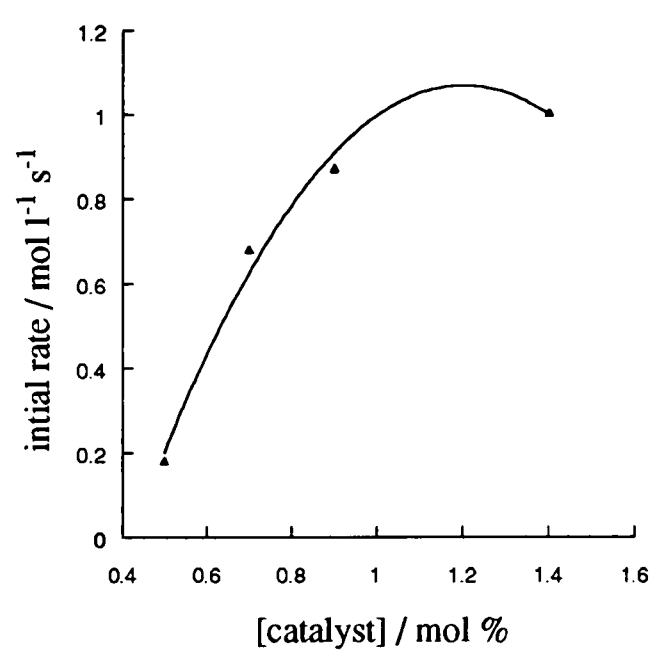


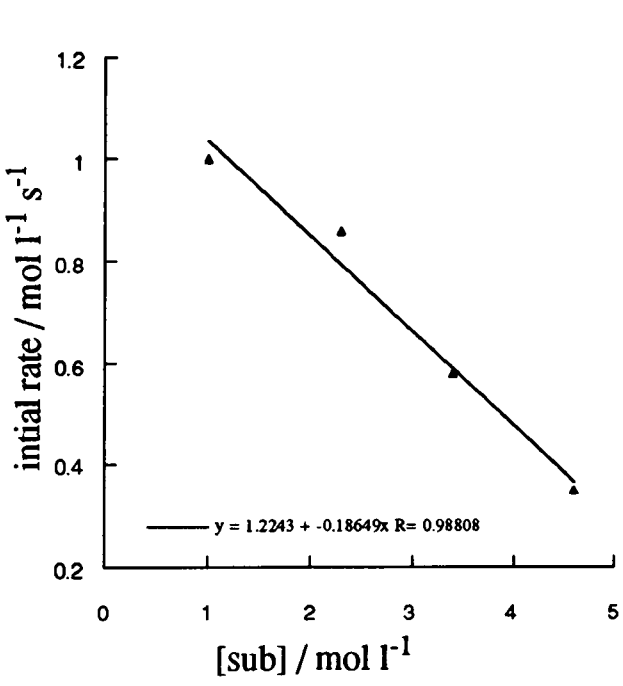
Figure 79: *experiments were conducted to determine the rate law for hydrogenation of the two substrates above catalysed by Heiser's complex*

The first substrate to be looked at was the isoquinoline derivative. Variations on catalyst concentration were carried out between 0.5 and 1.0 mol%. Substrate concentration experiments used between one and four equivalents of substrate at a catalyst concentration of 1.5 mol%. Pressure dependencies were looked at between 800 and 1700 mbar, again using a catalyst loading of 1.5 mol%. The temperature was consistently 25.5°C. Reactions were repeated until consistent results were obtained. The results obtained are showed in ***Figure 80***. The reaction rate showed the expected linear dependence on hydrogen pressure and a positive dependence on catalyst concentration. Increasing the amount of substrate was found to slow the reactions down, but the results did not fit an inverse dependence on substrate. The order with respect to substrate was therefore a negative fractional value. This negative dependence of reaction rate on substrate concentration could explain why previous binding studies and attempts to monitor hydrogenations *via* NMR, almost always conducted in the presence of excess substrate, had failed to isolate any reaction intermediates. A ten fold excess of substrate would slow the reaction down considerably at 298K; most of the NMR studies were conducted at 233K.









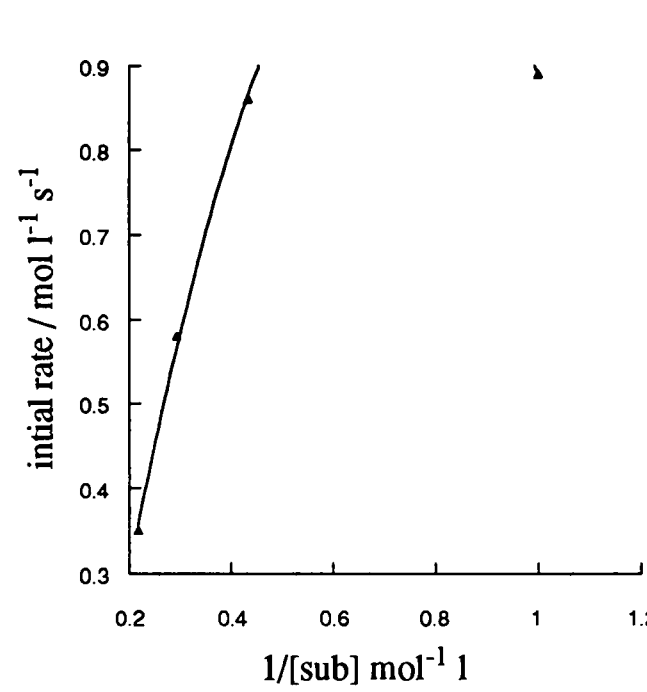


Figure 80: *attempts to find a rate law for the Heiser/isoquinoline system indicated that the reaction had a negative fractional order with respect to substrate concentration*

Heiser's catalyst was next investigated with mac as the substrate, to verify the negative fractional dependence of reaction rate on substrate concentration. Reductions carried out on this substrate exhibited an induction period which varied from 150s at a catalyst concentration of 2.5 mol% to 500s at 0.5 mol% catalyst. Due to the longer reaction times of mac in comparison with the isoquinoline derivative and the fact that reductions of this

substrate displayed an induction period, variations on substrate concentration and initial hydrogen pressure were conducted using catalyst loadings of 2.2 mol%. The results of these investigations were *not* the same as in the case of the isoquinoline derivative (***Figure 82***). The system showed a first order dependence of reaction rate on catalyst concentration, an inverse dependence on substrate concentration and a *zero* order dependence on the initial hydrogen pressure. A rate equation that was hydrogen independent could arise either because the resting state and rate determining transition state had the same hydrogen concentration, or because hydrogen was not involved at all in the rate determining step.

In view of these interesting results, detailed kinetic analyses were extended to other catalyst/substrate systems. The next system to be investigated was the Ru(BINAP)(allyl)(acac) catalysed reduction of mac, ***Figure 81***.

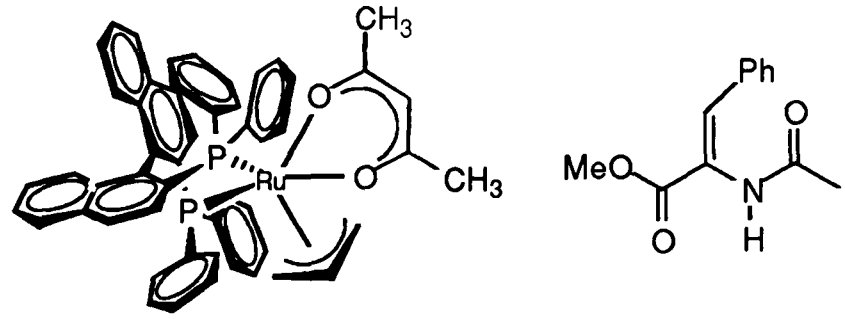
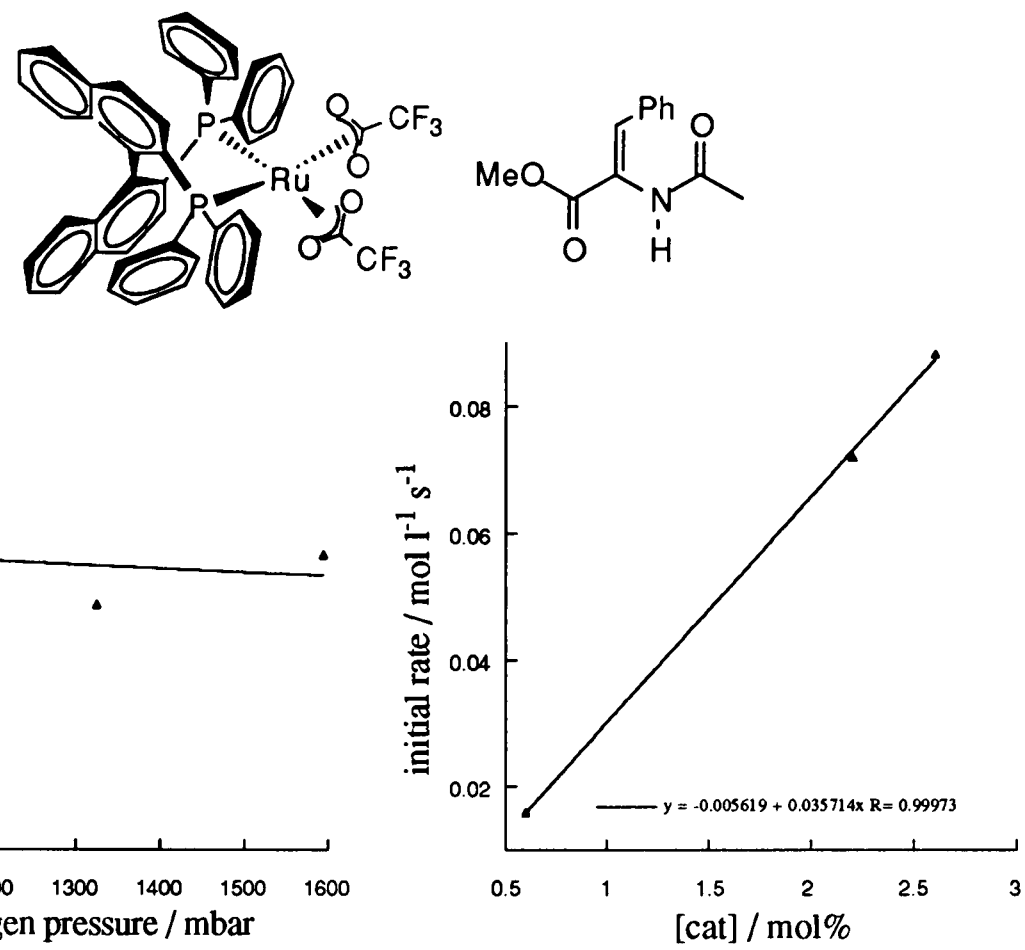


Figure 81: *the hydrogenation of mac catalysed by Ru(BINAP)(allyl)(acac) was the next system to be studied*

It had been previously been found that reductions using this catalyst were still diffusion controlled at catalyst concentrations as low as 1 mol% (p82). Hence, investigations into the order of reaction with respect to catalyst concentration used loadings between 0.4 and 0.8 mol%. Pressure variations (between 800 and 1700 mbar) and substrate variations were conducted using 0.6 mol% catalyst.

The plots obtained from these investigations showed that the data on this system was slightly more erratic than data obtained from previously studied systems (***Figure 83***). The results showed the reaction rate to be first order with respect to catalyst concentration, zero order with respect to initial hydrogen pressure and, as with the

Heiser/isoquinoline derivative system, the dependency on substrate concentration appeared to have a negative fractional value.



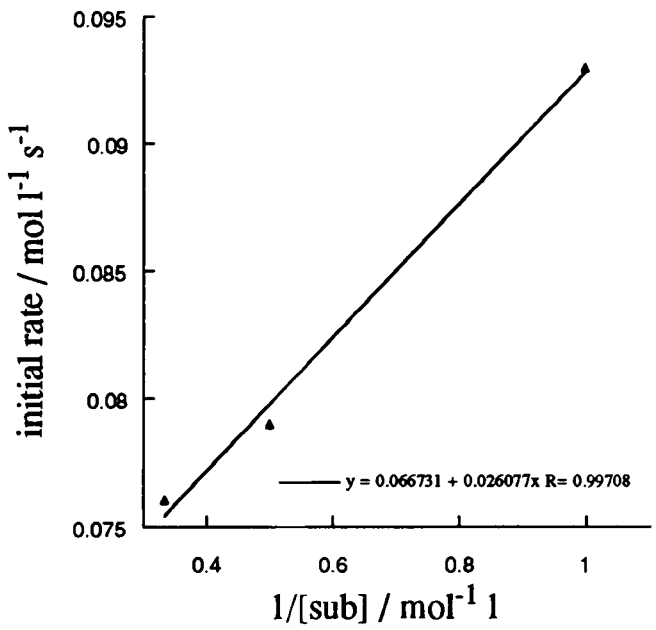
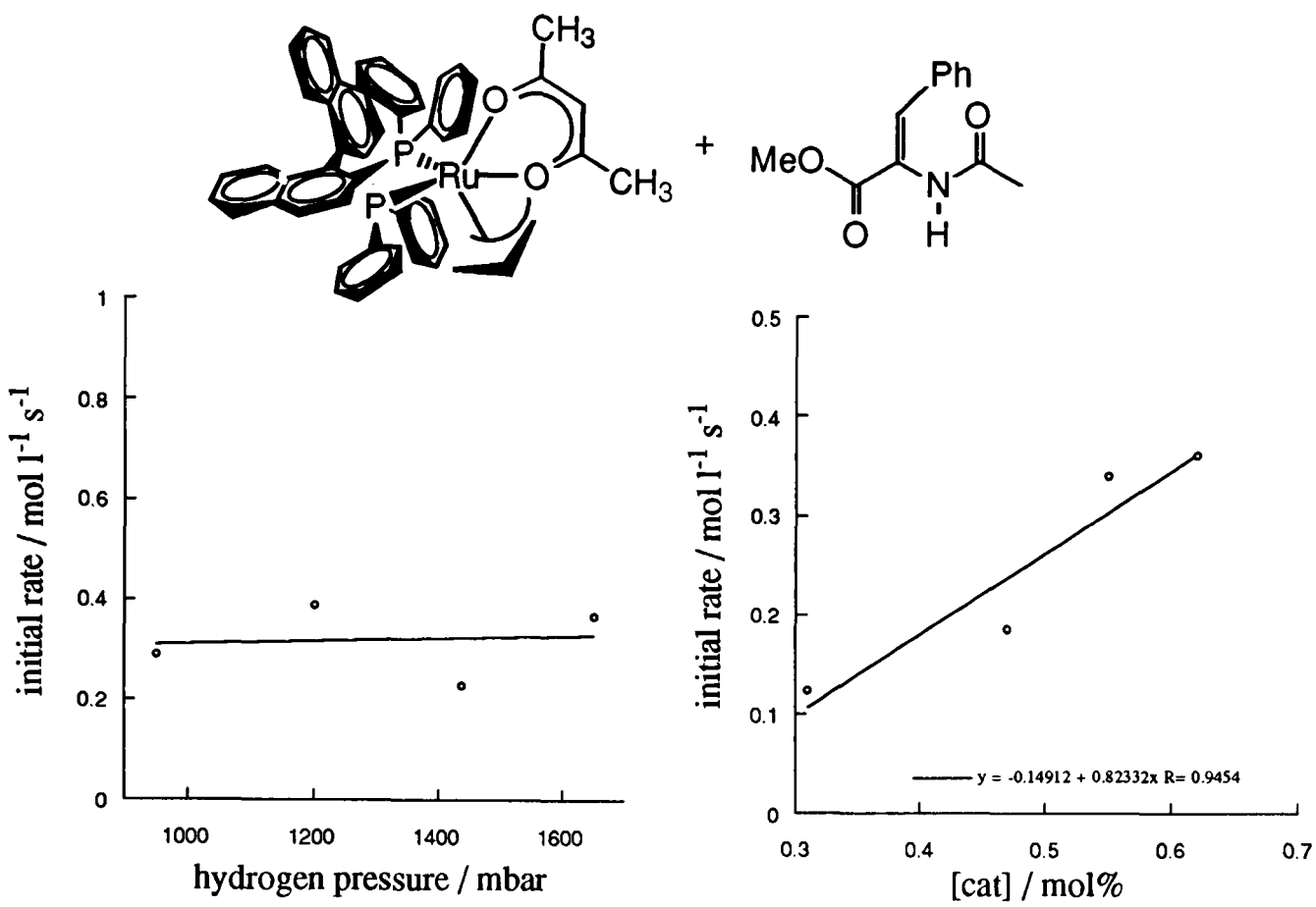


Figure 82: *the Heiser catalysed reduction of mac did not give rise to the same form of rate law as the reduction of the isoquinoline derivative*

Finally, it was decided to synthesise the last in the series of this 'family' of catalysts, namely the DPPF analogue of Heiser's catalyst. Conducting kinetic analyses on hydrogenations using this catalyst would result in the whole range of varying the bisphosphine ligand and/or other moities attached to ruthenium having been investigated. The catalyst synthesis was performed using Heiser's standard method[69] (***Scheme***

XXXIII) and yielded the product as a yellow powder (δ 56.94 ppm, 101.23 MHz, CH_2Cl_2).



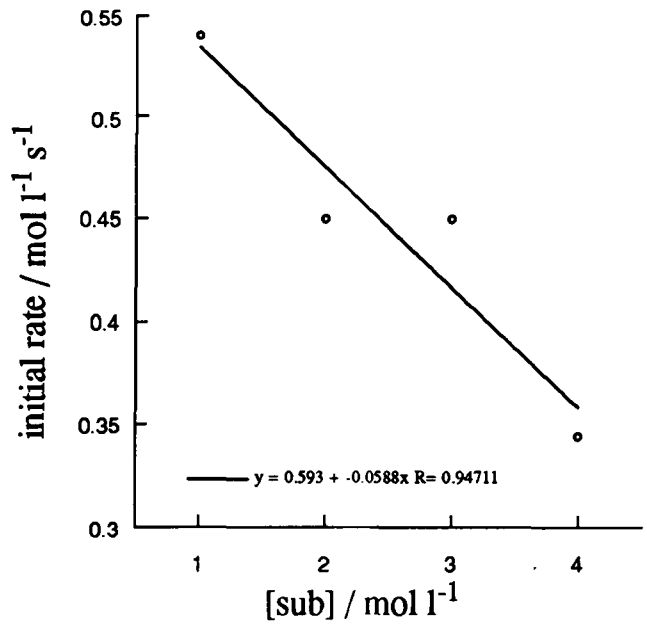
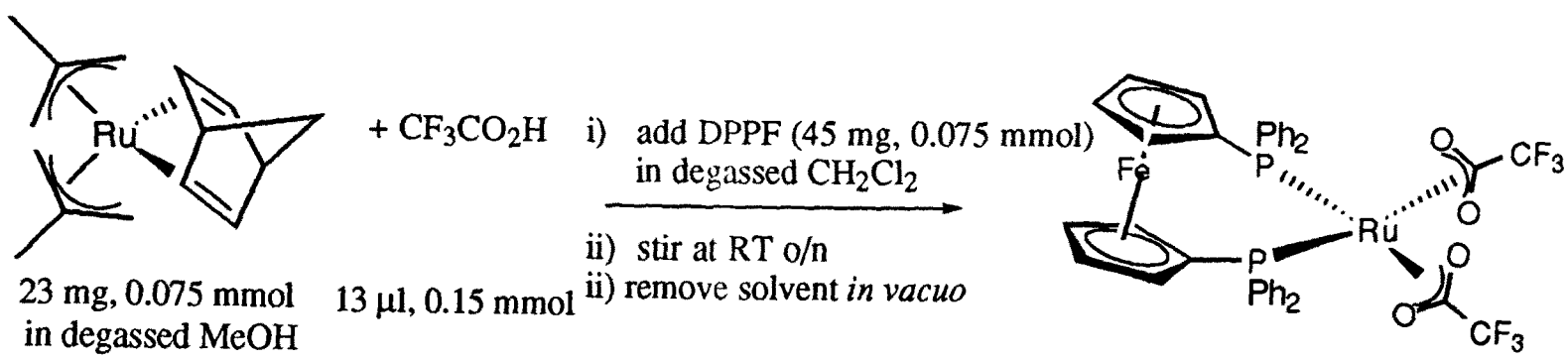


Figure 83: *the system above was first order only with respect to catalyst concentration. The reaction rate was zero order with respect to hydrogen pressure and the dependency on substrate concentration was a negative fractional value*

Unfortunately, when the activity of this catalyst towards enamide reductions was investigated, it was found that the catalyst was effective at hydrogenating only the isoquinoline derivative (***Figure 83***). As usual with these ruthenium catalysts, there was no visual indication of catalyst activation, complex formation or completion of the

reaction. The reduction of the isoquinoline derivative using 2.5 mol% catalyst showed an induction period of 100s and required almost 3000s for completion. Thus, it was decided that attempts to obtain good kinetic data on this catalyst/substrate system would not succeed and instead data modelling would only be carried out on the systems already investigated above.



Scheme XXXIII: *the synthesis of a DPPF analogue of Heiser's BINAP catalyst*

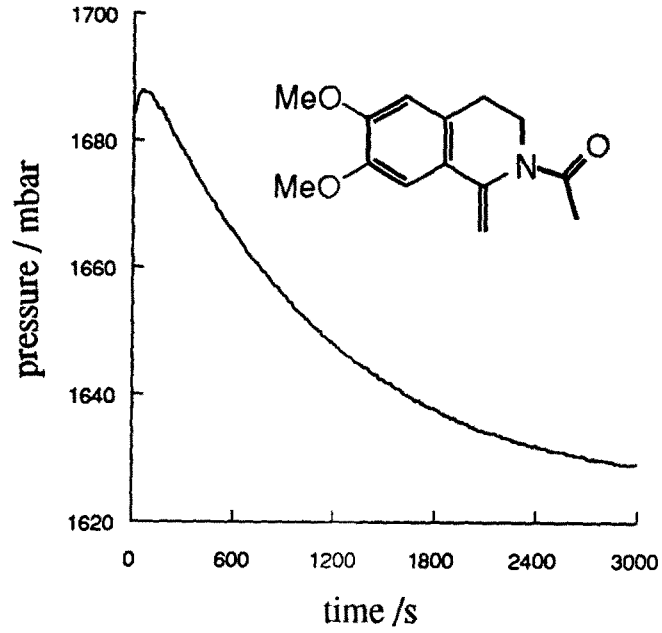


Figure 83: *$Ru(DPPF)(CF_3CO_2)_2$ was only effective at hydrogenating one of the five enamides it was tested out on*

The eventual model of this catalytic cycle would have to be adaptable enough to fit either a zero or a first order dependence of reaction rate on initial hydrogen pressure, a negative dependence (fractional or inverse) on substrate concentation, a first order dependence on catalyst concentration and also include possible product inhibition, as summarised in ***Table VI***. It would also need to include a complex involving substrate and catalyst; justification for this was found from electrospray and NMR studies using Brown's allyl acac catalysts (p88, p106).

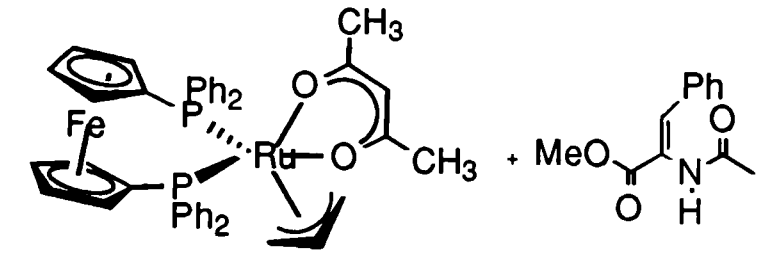
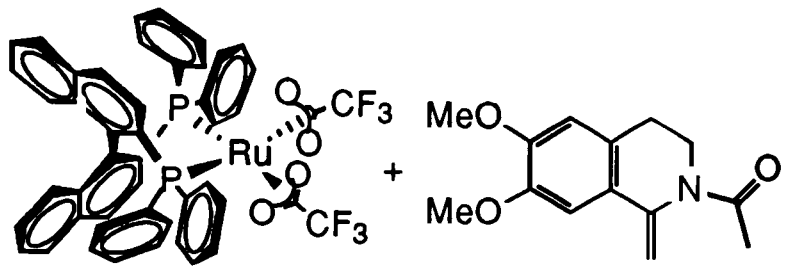
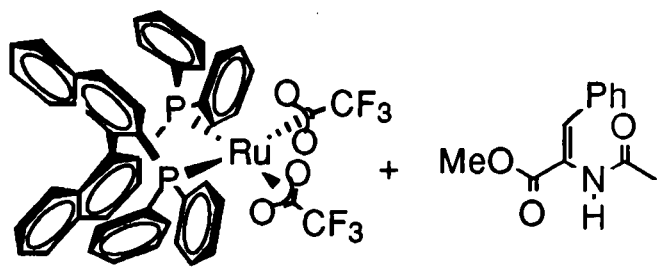
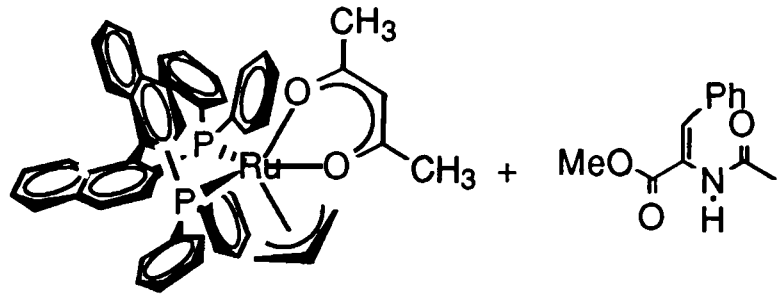
System	Rate law
	$k_{obs} \alpha \frac{[H_2]\,[cat]}{[sub + prod]}$
	$k_{obs} \alpha \frac{[H_2]\,[cat]^x}{[sub + prod]^y}$
	$k_{obs} \alpha \frac{[H_2]^o\,[cat]}{[sub]}$
	$k_{obs} \alpha \frac{[H_2]^o\,[cat]}{[sub]}$

***Table VI**: a summary of the results of accurate kinetic investigations into the rate dependence on the variables, hydrogen pressure, [substrate] and [catalyst]*

Preliminary modelling was carried out on a very simple model, using the results of runs on the Ru(DPPF)(allyl)(acac) catalyst. An achiral catalyst simplified the model considerably due to the omission of major and minor diastereomers and their interconversion.

Initial attempts at constructing a model included both substrate and product inhibition terms. This was in keeping with Halpern's kinetic studies on tiglic acid[37] and also fitted the results of kinetic investigations, electrospray experiments and preliminary modelling (p85). Plausible models were arrived at using GEAR[53] (p45) by attempting to reproduce model plots featuring the same experimentally observed curvature and reaction time.

Plots obtained for faster reactions were only reproduced in GEAR by introducing considerable product inhibition into the model.

Once a satisfactory preliminary model had been constructed using GEAR, a direct comparison between theoretical and experimental data was made using the modelling programme GIT[53] (p47). The first model to be tested is shown below, ***Scheme XXXIV***.

1	**G**	⟶	**H**
2	**H**	⟶	**G**
3	**Ru + S**	⟶	**RuS**
4	**RuS**	⟶	**Ru + S**
5	**Ru + H**	⟶	**RuH**
6	**RuH**	⟶	**Ru + H**
7	**RuH + S**	⟶	**P + Ru**
8	**Ru + P**	⟶	**RuP**
9	**RuP**	⟶	**Ru + P**

Scheme XXXIV: *preliminary models of the catalytic cycle contained significant product inhibition*

Equations **1** and **2** referred to the gas-liquid interfacial transfer of hydrogen, as discussed on p46. Equations **3, 4** and **5, 6** corresponded to formation of a substrate-containing complex and a hydrogen-containing complex respectively. Equations **8, 9** represented product inhibition due to complexation of product to active catalyst, thereby resulting in a reduction of the amount of free catalyst available to the substrate. Equation **7** illustrated the actual reaction between substrate and hydrogen leading to reduced product.

Investigations iterated on the rate constants k_3, k_5 and k_7 and refined the fits as required by changing the importance of substrate inhibition and product inhibition. Although reasonable fits to either the slower reactions or the faster runs using the Ru(DPPF)(allyl)(acac)/mac system could be obtained, the whole set of data could only be fitted to this model on the introduction of unreasonably high rate constants for some of

the steps. This indicated that the model was not correct and further descriptions of the catalytic pathway were sought, with the aid of GEAR.

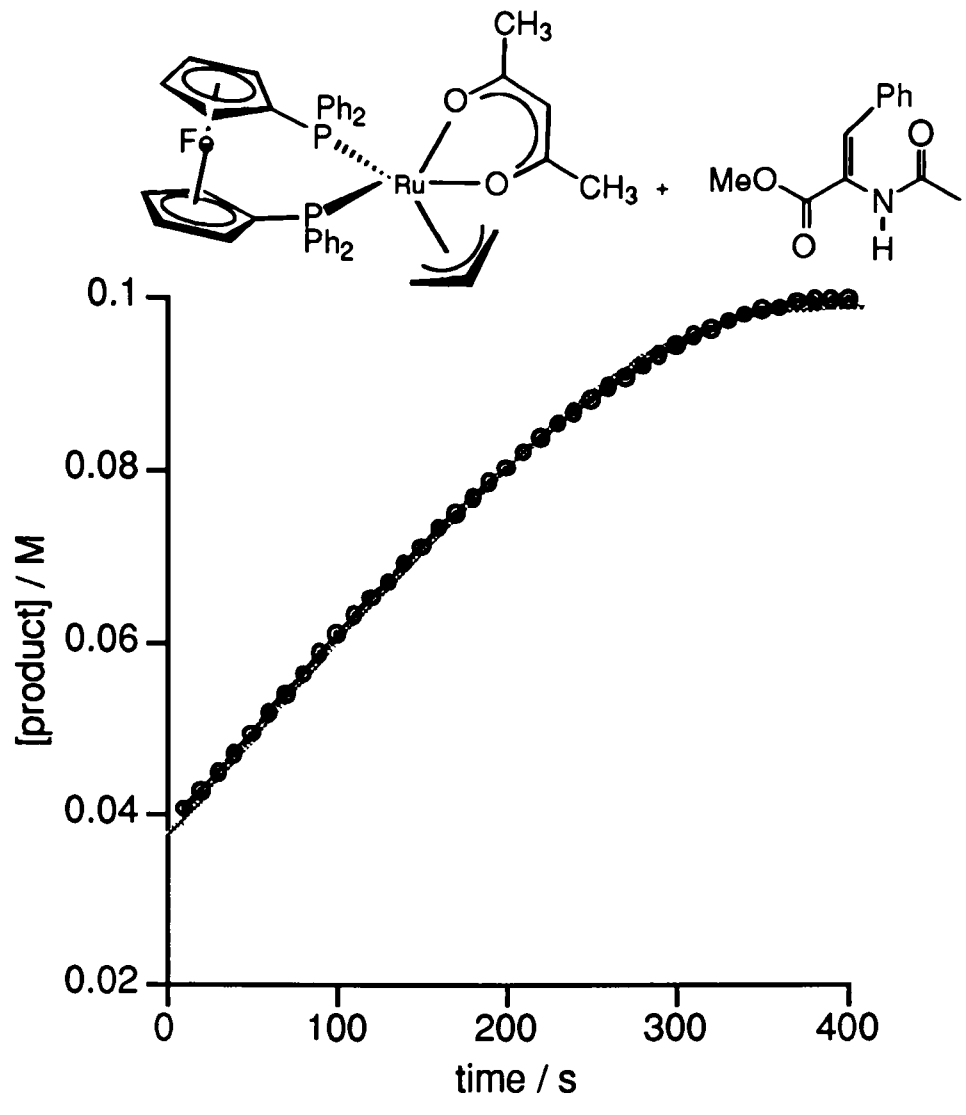
After several unsuccessful attempts which all pointed towards the importance of product inhibition, a model containing a product inhibition step involving *two* molecules of product was arrived at (steps **6, 7** ***Scheme XXXV***).

1	**G**	⟶	**H**
2	**H**	⟶	**G**
3	**Ru + S**	⟶	**RuS**
4	**RuS**	⟶	**Ru + S**
5	**RuS + H**	⟶	**P + Ru**
6	**Ru + P + P**	⟶	**RuP**
7	**RuP**	⟶	**Ru + P + P**

Scheme XXXV: *the best model of the catalytic cycle contained a termolecular product inhibition step*

The modelling programme GIT was run using data from the Ru(DPPF)(allyl)(acac)/mac system, iterating on k_4, k_5 and k_7. Goodness of fit was judged by the value of the least squares deviation (***Table VII***) between the observed and calculated lines and also by eye. All the data from this system fitted the model well (***Figure 84*** and Appendix 2), the values of rate constants and deviations obtained for some of the runs are tabulated below, ***Table VII***. Further plots can be found in Appendix 2.

In order to test the model's credibility, it was used to simulate rate data obtained from the other catalyst/substrate systems studied. The Heiser/mac, Heiser/isoquinoline and Ru(BINAP)(allyl)(acac)/mac systems could all be fitted to this model (***Figure 84***, Appendix 2, ***Table VII***). As ***Table VII*** shows, none of the rate constants required to produce good fits were unreasonable in their magnitude and the results obtained were consistent. Thus, it would appear that the model depicted in ***Scheme XXXV*** could be an accurate representation of the catalytic pathway for ruthenium complex catalysed alkene hydrogenation.



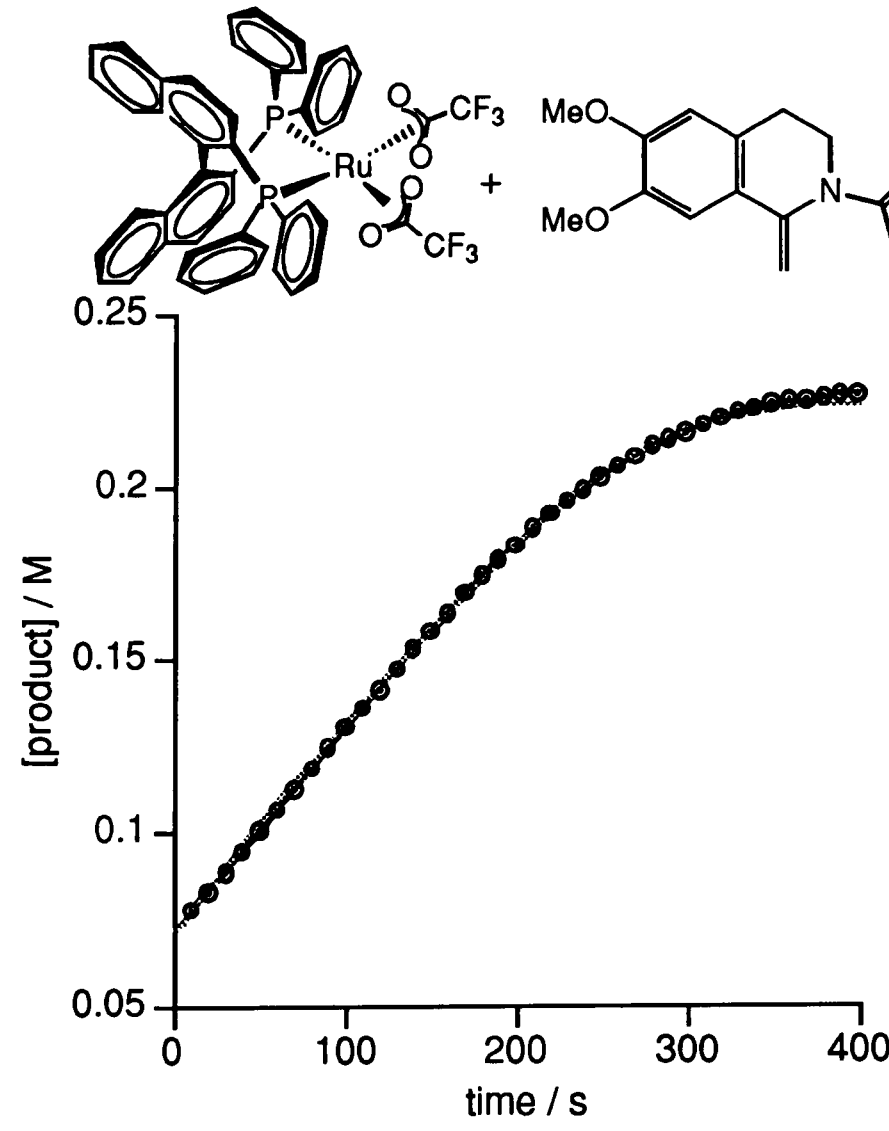


Figure 84**: plots comparing experimental data (circles on a line) with theoretical data (light grey line) predicted by the model in **Scheme XXXV

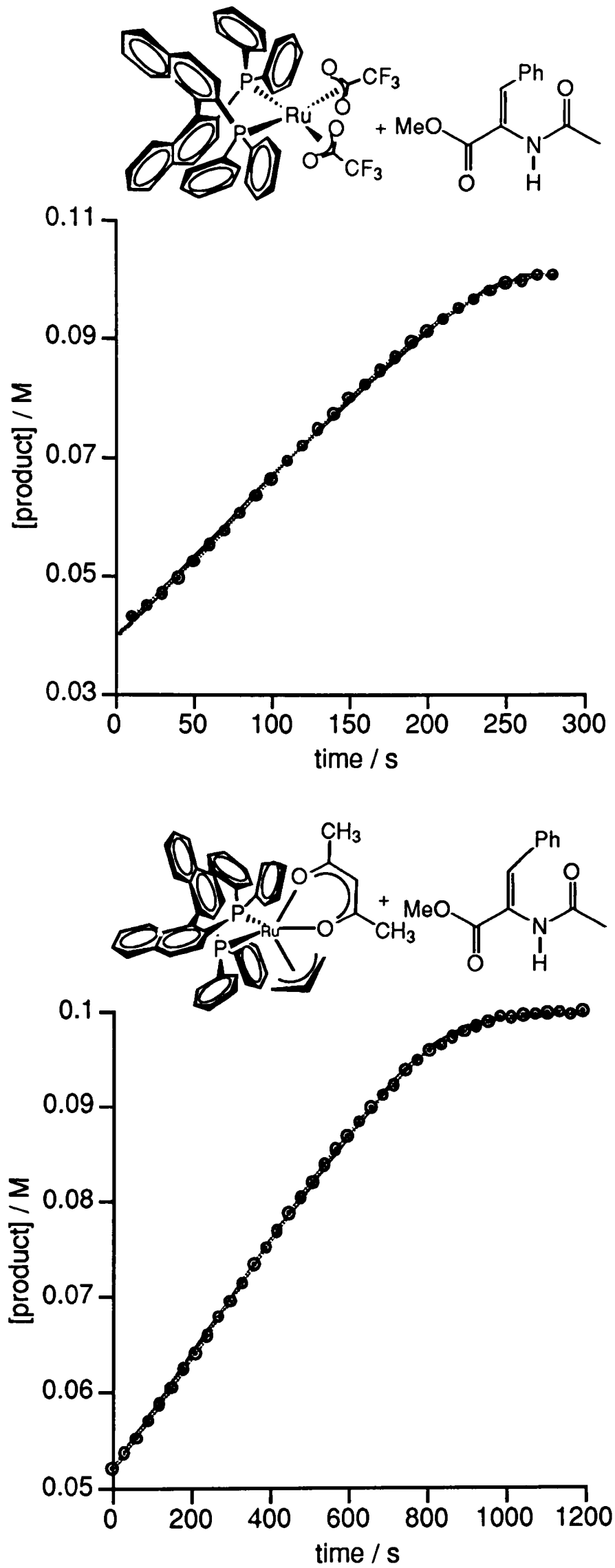
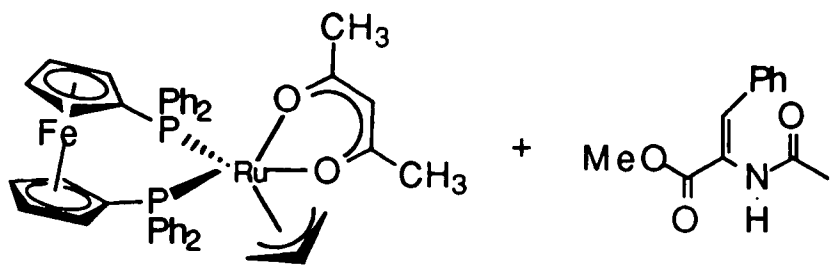
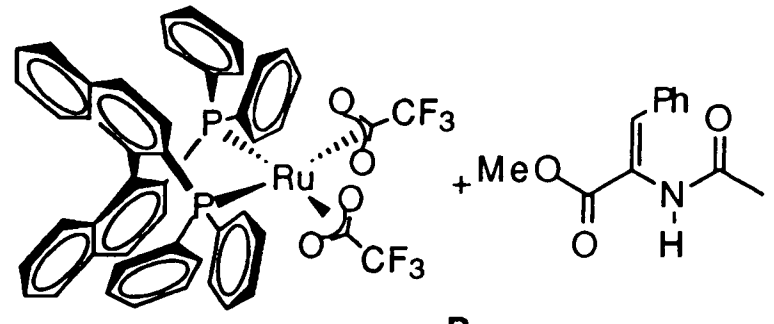


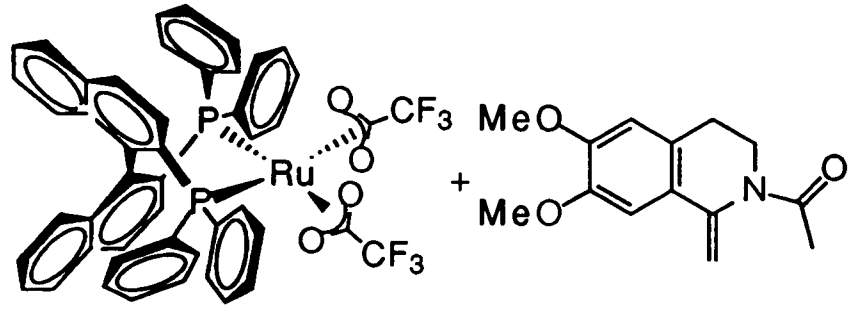
Figure 84**: plots comparing experimental data with theoretical data predicted by the model in **Scheme XXXV



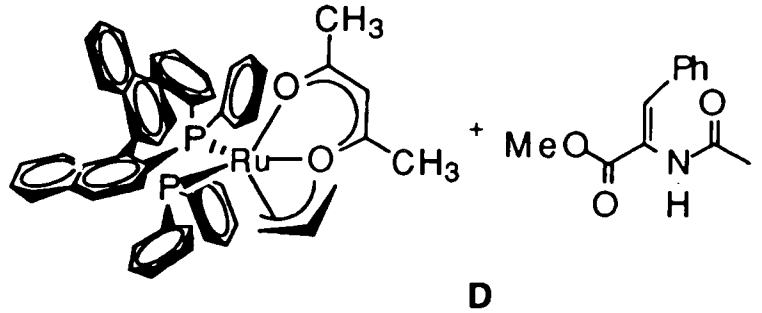
A



B



C



D

system	equivalents of substrate	[catalyst] / mol%	initial hydrogen pressure / mbar	k_4 / s^{-1}	k_5 / $mol^{-1}ls^{-1}$	k_7 / s^{-1}	*deviation
A	1	1.48	1191	6.15	50.3	69.0	$0.752x10^{-3}$
	2	1.53	1641	"	"	"	$0.216x10^{-2}$
	1	1.48	877	"	"	"	$0.405x10^{-3}$
	1	1.40	1615	"	"	"	$0.712x10^{-3}$

system	equivalents of substrate	[catalyst] / mol%	initial hydrogen pressure / mbar	k_4 / s^{-1}	k_5 / $mol^{-1}ls^{-1}$	k_7 / s^{-1}	*deviation
A	1	1.53	1768	6.15	50.3	69.0	$0.139x10^{-2}$
B	1	2.6	1640	6.46	8.48	243	$0.214x10^{-2}$
	1	1.40	1320	"	"	"	$0.934x10^{-3}$
	1	1.40	1024	"	"	"	$0.830x10^{-3}$
	2	2.20	1646	"	"	"	$0.125x10^{-2}$
C	2.3	1.5	1658	1.02	119	1.83	$0.168x10^{-2}$
	1	1.5	912	"	"	"	$0.985x10^{-3}$
	1	0.9	1648	"	"	"	$0.136x10^{-2}$
	1	1.5	1268	"	"	"	$0.174x10^{-2}$
D	1	0.68	1202	1.04	104	1.58	$0.657x10^{-3}$
	1	0.68	951	"	"	"	$0.530x10^{-3}$
	1	0.68	1624	"	"	"	$0.641x10^{-3}$

*indicates the least squares deviation between the calculated and observed plots. For files containing up to 50 observation points, deviations of the order of 10^{-2}, coupled with plots whose fit was also judged acceptable by eye were deemed acceptable deviations

Table VII**: illustrated in the table above are some of the runs used in modelling the catalytic cycle depicted in **Scheme X

On examining the rate constants in ***Table VII***, the following points emerge:

i) a comparison of systems A and D shows the effect of changing the ligand. Reaction rate k_5 is faster when using BINAP as the ligand than when using DPPF; both the substrate and product binding to the BINAP containing catalyst appear to be stronger. The difference between the two systems is significant enough to indicate that the ligand has considerable influence in the catalytic cycle.

ii) Systems Band C show the effect of varying the substrate. The reaction rate is faster for mac than with the bulkier isoquinoline substrate. The isoquinoline is bound less strongly to the metal centre, as is its product.

iii) a comparison of systems Band D indicates the effect of secondary groups on the catalytic cycle. Trifluoroacetate groups apparently lead to much slower rates of reaction and weaker binding to the metal centre. As the difference in rates between the two systems is quite marked, one can surmise that the catalytic cycle must contain an entity other than the ligand, substrate or hydrogen bound to the metal centre.

The trends in k_5 values between the different systems match those originally obtained from preliminary modelling work (p85). As found initially in that chapter and later in the more detailed kinetic work, system D underwent much faster reactions than system B. This matches modelling results. But system C actually reacted significantly faster than system D in reality (primarily due to the short induction period observed with system D). It was also found that system A was twice as slow as system D (in good agreement with modelling results) yet considerably faster than system B.

The most successful catalyst systems, in terms of their ability to reduce most of the substrates employed quickly and effectively, were those containing heavily electron withdrawing groups (contrast the success of Heiser's catalyst with the failure of Noyori's catalyst under the conditions employed in this work).

The fact that, in reality, system C underwent faster reductions than system B could indicate that the requirement of an electron withdrawing group such as the ester is not as stringent in ruthenium work as it is in rhodium.

Systems C and D give the fastest values for k_5 and show the strongest binding to the metal. From the kinetic work carried out on these systems, a zero order dependence of reaction rate on hydrogen pressure was observed (***Table VI***, p123). This could possibly mean that with substrates which bind strongly to the metal, as soon as hydrogen approaches the catalyst, it reacts very quickly so that the actual rate determining step is not in fact reaction with hydrogen, but binding of the substrate to the metal; substrate binding is therefore not an equilibrium step in this case. If the binding with system B was considerably weaker than with system C, it could be possible to imagine the existence of a slight induction period, as is observed.

In conclusion, there is a considerable difference between the mechanisms of rhodium complex and ruthenium complex catalysed alkene hydrogenation. Ruthenium appears (from NMR and electrospray work) to be a much more oxophilic centre. Whereas the resting state in the rhodium catalytic cycle contains the olefin bound to the metal, the species occasionally observed in ruthenium NMR work did not appear to be involved in the catalytic cycle; NMR work carried out under hydrogen failed to show the existence of any species other than the catalyst.

From the kinetic work, it can be deduced that the mechanism involves a negative dependence of reaction rate on substrate concentration and product concentration, the catalytic cycle contains an entity other than ligand, substrate and hydrogen bound to the metal and that the more electron withdrawing the secondary groups attached to the metal centre, the faster hydrogenations are. The nature of the ligand itself is also influential; BINAP is observed to be more effective than DPPF.

Directed Hydrogenation

It has already been explained (p27) how, in the reduction of alkenes, proximal polar functional groups can coordinate to metal centres and lead to enhanced diastereoselectivity in the hydrogenated product. The coordinating atom in the polar functional group is usually oxygen; it was decided to see if fluorine could be effective as a coordinating atom in directed hydrogenation.

Compounds **1** and **2** (***Figure 85***) were prepared by reacting the alcohol precursors with DAST[71].

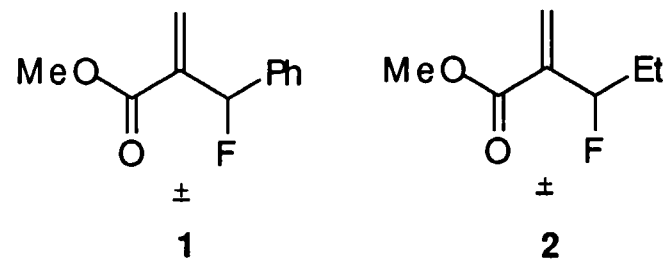


Figure 85: *allylic fluorides used in directed hydrogenation investigations*

Attempted reductions of these compounds were then carried out using ruthenium BINAP catalysts and the products were analysed to determine whether any diastereoselection occurred. The diastereomers (**3, 4** ***Figure 86***) were assigned by ^{1}H NMR, following an independent synthesis of **3** by fluorination of the *anti* alcohol with DAST (DAST fluorinations usually proceed with inversion of configuration; in this particular case the reaction occurred with retention, as verified by existing data on this compound)[72]: compound **4** δH_a 5.75 ppm, $^{2}J_{H\text{-}F}$ = 46 Hz, $^{3}J_{H\text{-}H}$ = 7 Hz, δH_b 2.92, $^{3}J_{H\text{-}F}$ = 23 Hz; compound **3** δH_a 5.55 ppm, $^{2}J_{H\text{-}F}$ = 46 Hz, $^{3}J_{H\text{-}H}$ = 9 Hz, δH_b 3.04 ppm, $^{3}J_{H\text{-}F}$ = 9 Hz. MMX molecular modelling also reinforced this diastereomeric assignment.

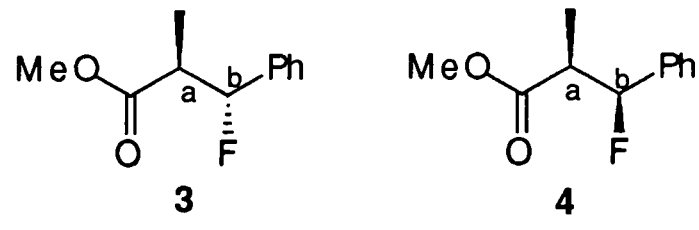


Figure 86: *the possible diastereomeric reduced products were distinguished by ^{1}H NMR and MMX molecular modelling*

Ruthenium BINAP catalysts do not normally catalyse the reduction of α,β unsaturated esters unless a directing group is present[73]. Reductions were carried out in a Fischer Porter bottle or an autoclave, using 2-5 mol% catalyst and taking the usual precautions to exclude the presence of air. No colour changes were observed during the reaction. Reactions performed using Heiser's catalyst (***Figure 87***) were quite slow at elevated temperatures, but consistently produced an excess of the *syn*isomer, **4**. Repeating the reactions using a racemic BINAP catalyst led to the *syn*diastereomer being produced as 90% of the reduced product, ***Table XI***. This would be expected from MMX molecular modelling if the hydrogenation was controlled by the interacition of C-F with ruthenium.

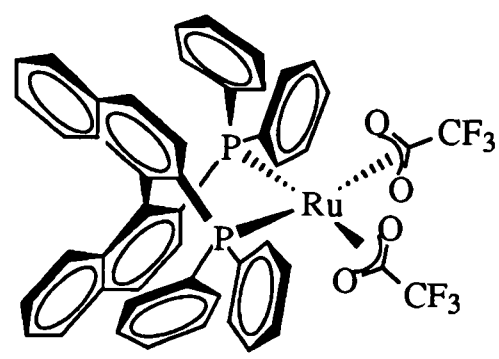


Figure 87: *Heiser's catalyst was the catalyst chosen to carry out reductions on the allylic halides*

The ethyl analogue **2**, ***Figure 85*** could not be reduced under these conditions. The results shown in ***Table XI*** indicate the achievement of the first example of a diastereoselective hydrogenation of an allylic fluoride with fluorine participation during the catalytic cycle.

catalyst	**conditions**	**% reduction**	**diastereomeric ratio 4:3**
$Cy_3P(py)IrCOD\ PF_6$	25°C, 21h, 3 atm	92	30:70
(+/-) heiser	20°C, 14h, 6 atm	30	89:11
heiser	25°C, 40h, 3 atm	48	93:7

Table XI: *diastereomeric ratios obtained on the reduction of racemic **1***

Experimental

General procedures: Reactions were carried out in solvents distilled from standard drying agents[65]. Reactions of air sensitive compounds were conducted under a dry argon atmosphere, using standard vacuum line techniques[66] in Schlenk glassware. Unless otherwise stated, solvents were deoxygenated by three freeze-thaw cycles in which the solvent was first cooled at -78°C (CO_2/acetone), warmed up *in vacuo* and subsequently flushed with argon. Solid reagents were degassed as necessary by evacuation and flushing with argon at room temperature. Transfers and filtrations were carried out using stainless steel cannula wires.

Analytical thin layer chromatography (t.l.c.) was performed on Merck plastic-backed plates precoated with 0.2 mm silica 60 F_{254}. Column chromatography was performed on Merck silica gel 60H, 230-300 mesh using the flash chromatographic method of Still[74]. Preparative t.l.c. was performed on glass plates coated with silica gel HF_{254}.

Solvents were purchased from Rhône-Poulenc, Fisons, Rathburns or the Aldrich Chemical Co. Reagents were purchased form the Aldrich Chemical Co., Rose Chemicals, Lancaster or Strem. Precious metal salts were on loan from Johnson-Matthey.

Melting points were determined using a Riechert-Koffler block and are uncorrected.

NMR Spectra: All NMR spectra were recorded by the author. Dr Tim Claridge carried out the inversion experiments on rhodium oxpamp and dipamp.

^1H NMR spectra were recorded on a Varian Gemini 200 (200 MHz), Bruker WH 300 (300 MHz), Bruker AM 500 (500 MHz) or a Bruker AMX 500 (500 MHz) spectrometer. The spectra are internally referenced to one residual solvent peak: $CDCl_3$ δ 7.27, C_6D_6 δ 7.16, C_7D_8 δ 2.09, CD_2Cl_2 δ 5.32, CD_3OD δ 3.31, CD_3CN δ 1.95.

^{13}C NMR spectra were recorded on a Varian Gemini 200 (50.31 MHz), Bruker AM 250 (62.89 MHz) or a Bruker AMX 500 (125.80 MHz) spectrometer. The spectra are

internally referenced to the solvent: $CDCl_3$ δ 77.0, C_7D_8 δ 20.4, CD_2Cl_2 δ 53.8, CD_3OD δ 49.0.

^{31}P NMR spectra were recorded on a Bruker AM 250 (101.3 MHz, referenced to 85% aqueous phosphoric acid, H_3PO_4 δ 0.0), Bruker AM 500 (202.6 MHz, referenced to phosphoric acid δ 0.0) or a Bruker AMX 500 (202.6 MHz, referenced to phosphoric acid δ 0.0) spectrometer.

^{11}B NMR spectra were recorded on a Bruker AM 250 (80.21 MHz) and are externally referenced to $BF_3.Et_2O$ (δ 0.0).

^{19}F NMR spectra were recorded on a Bruker AM 250 (49.69 MHz) and are externally referenced to $CFCl_3$ (δ 0.0).

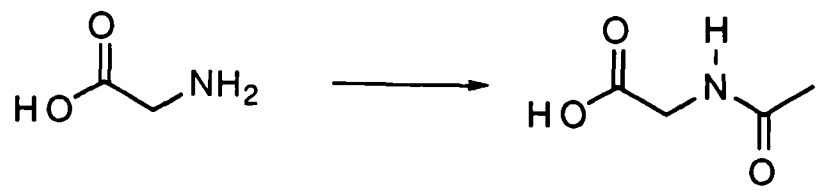
Chemical shifts are quoted as parts per million (ppm). Abbreviations used in the description of spectra are: s = singlet, d = doublet, t = triplet, dd = doublet of doublets, dq = doublet of quartets, m = multiplet, br = broad, J = coupling constant.

Infrared Spectra were recorded on a Perkin-Elmer 1750 Fourier Transform spectrometer either using NaCl plates or as a KBr disc. Abbreviations used in the description of spectra are: s = strong, br = broad.

Mass spectra were recorded on a V.G. Trio-1 spectrometer, V.G. Masslab 20-250 or ZAB 1F spectrometer. G.C. conditions: BP 1 column, 60-260°C at 25°C min^{-1} temperature ramp. Values are followed in parentheses by the intensity as a percentage of the base peak. Electrosprays were recorded Dr Robin Aplin and Dr Henry Matimba.

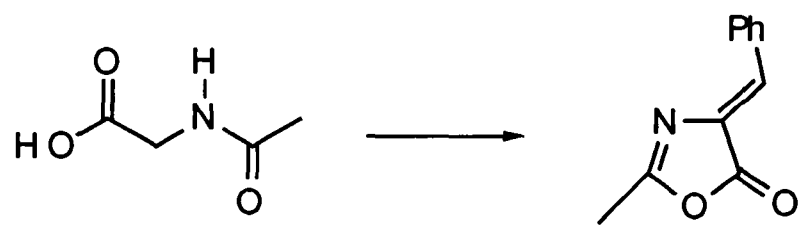
Synthesis of substrates

N-Acetylglycine



Acetic anhydride (26 ml, 0.15 mol) was added to a solution of glycine (9.21 g, 0.121 mol) in water (36 ml). After stirring for 5 min, the mixture was left overnight at 0°C and the precipitate which formed was collected by suction filtration, washed with water (15 ml) and dried *in vacuo* to yield the product as a white powder (9.30 g, 66%); m.p. 214-216°C (lit.[49], 207-208°C); υ_{max}/cm^{-1} (nujol) 2960(N-H), 2400-2700(br. OH), 1720(C=O acid) and 1600, 1425(C=O amide); δ_H(200 MHz, D_2O) 1.82 (3H, s, CH_3) and 3.74 (2H, s, CH_2); δ_C(50.3 MHz, D_2O) 21.23(CH_3), 40.85(CH_2), 173.69(amide C=O) and 174.91(ester C=O); *m/z* (CI) 135(M^++18, 45%), 118(M^++1, 100), 100(M^+-OH, 7) and 74(M^+-CH_3CO, 5).

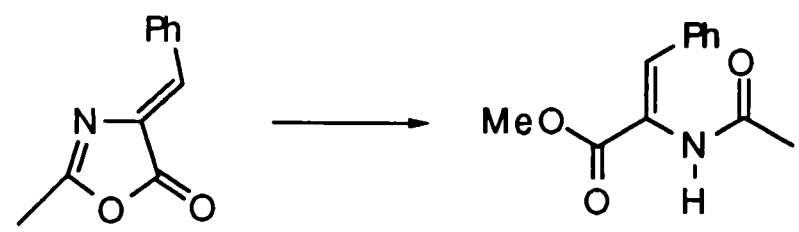
(Z)-Methyl-4-phenylmethylene-5-oxazolone



A mixture of N-acetylglycine (4.95 g, 0.042 mol), acetic anhydride (11.5 ml, 0.122 mol) and anhydrous sodium acetate (2.60 g, 0.064 mol) was heated together with benzaldehyde (6.52 ml, 0.064 mol) at 120°C until homogeneous (about 20 min). The resulting solution was then refluxed for 1h and left overnight at -36°C to effect crystallisation. The resulting crystals were filtered, washed with water (15 ml) and dried *in vacuo* to yield the title compound as yellow/orange crystals (5.19 g, 75%); m.p. 158-160°C (lit.[49], 148-150°C); υ_{max}/cm^{-1}(KBr) 1755(C=O) and 1656(C=C); δ_H(200 MHz, $CDCl_3$) 2.42(3H, s, Me) and 7.42-8.07(6H, m, Ph & vinyl); δ_C(50.3 MHz, $CDCl_3$)

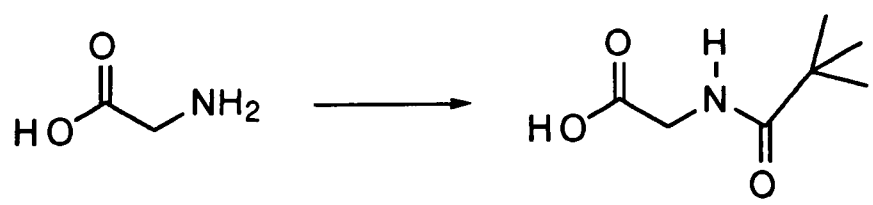
15.3(CH_3), 128.33(*C*=CH), 129.07 (*m*), 131.33(C=*C*H), 131.65(*p*), 132.38(*o*), 133.33(*ipso*), 166.45(C=N) and 168.13(C=O); *m/z* (CI) 188(M^++1, 100%).

Z-Methyl-2-acetylamino-3-phenylpropenoate



A mixture of Z-methyl-4-(phenylmethylene)-5-oxazolone (2.624 g, 0.014 mol) and anhydrous sodium acetate (0.05 g, 0.625 mol) was refluxed for 3h in methanol (62.5 ml). The solvent was then removed *in vacuo* and the gummy residue purified by column chromatography (eluant: ethyl acetate) to yield the product as an off-white solid (2.51 g, 82%); m.p. 134-136°C (lit.[49], 122-124°C); υ_{max}/cm^{-1}(KBr) 3152(N-H), 1728(ester C=O), 1656(C=C) and 1528(amide C=O); δ_H(200 MHz, $CDCl_3$) 1.98(3H, s, CH_3CO), 3.87(3H, s, CH_3O), 6.95(1H, br s, NH), 7.37-7.41(5H, m, Ph) and 7.46(C=CH); δ_C(50.3 MHz, $CDCl_3$) 22.75(*C*H_3CO), 52.46(CH_3O), 124.89(*C*=CH), 128.68(*m*), 129.61(C=*C*H), 129.94(*o*), 132.93(*p*), 133.73(*ipso*), 166.09(amide C=O) and 170.15(ester C=O); *m/z* (CI) 220(M^++1, 100%), 190(92), 188(M^+-CH_3O, 95), 178(67), 177(M^+ - O=C=CH_2, 78), 169(88), 159(62) and 116(67).

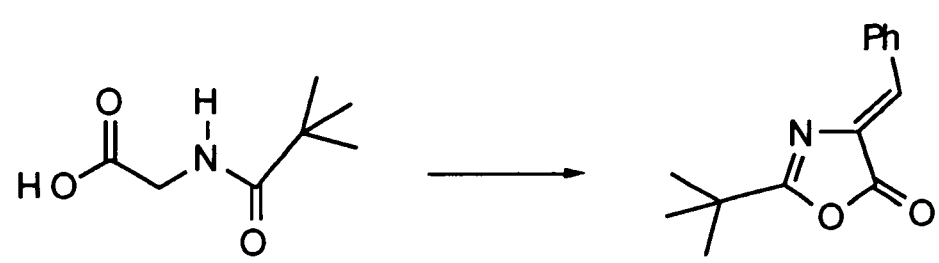
N-Trimethylacetylglycine



Glycine (10.00 g, 0.133 mol) was dissolved in 10% sodium hydroxide solution (100 ml) and pivaloyl chloride (17 ml, 0.14 mol) was then added in small portions with vigorous stirring after each addition to ensure all the chloride had reacted[75]. After the addition of crushed ice, 5M hydrochloric acid was slowly added until the acidity of the solution was

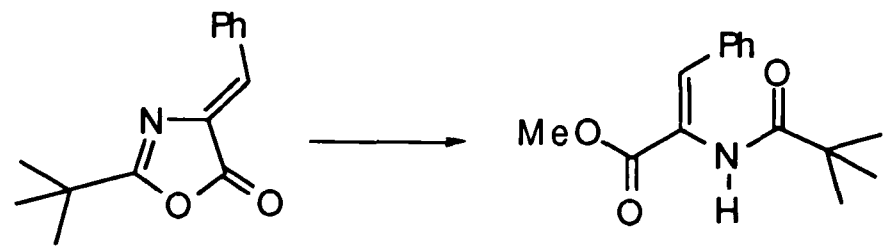
pH 3. The solution was then extracted with ether (3x50 ml), dried ($MgSO_4$), and the ether removed *in vacuo* to yield a residue which was recrystallised using ethyl acetate/60-80 petrol, giving the product as pale yellow crystals (12.3 g, 61%); m.p. 148-150°C; υ_{max}/cm^{-1} (KBr) 3408(N-H), 2800(br. OH), 1747(C=O acid), and 1614, 1542(C=O amide); δ_H(200 MHz, $CDCl_3$) 1.24(9H, s, ^tBu), 4.07(2H, d, J=5.13 Hz, CH_2) and 6.45(1H, s, NH); δ_C(50.3 MHz, $CDCl_3$) 26.12($C(CH_3)_3$), 38.05($C(CH_3)_3$), 40.95(CH_2), 173.70(C=O amide) and 183.21(C=O acid); *m/z* (CI) 177(M^++18, 12%), 160(M^++1, 100), 142(M^+-OH, 14) and 102(M^+-^tBu, 8).

Z-Tert-butyl-4-phenylmethylene-5-oxazolone



A mixture of trimethylacetylglycine (2.00 g, 0.013 mol), acetic anhydride (10 ml, 0.11 mol) and anhydrous sodium acetate (0.82 g, 0.01 mol) was heated together with benzaldehyde (2.03 ml, 0.02 mol) at 120°C until homogeneous[49]. The resulting solution was then refluxed for 1h and left overnight at -36°C to effect crystallisation. The resulting crystals were filtered, washed with water (15 ml) and dried *in vacuo* to yield the title compound as a yellow powder (2.20 g, 74%); m.p. 85-87°C ; υ_{max}/cm^{-1}(KBr) 1796(C=O), 1656(C=N) and 1600(C=C); δ_H(200 MHz, $CDCl_3$) 1.40(9H, s, ^tBu), 7.16(1H, s, C=CH) and 7.46-8.11(5H, m, Ph); δ_C(50.3 MHz, $CDCl_3$) 26.91($C(CH_3)_3$), 34.33($C(CH_3)_3$), 129.03(*m*), 131.26(*C*=CH), 131.69(*p*), 132.53(*o*), 133.35(*ipso*), 133.35(*C*=CH), 168.57(C=N) and 175.15(C=O); *m/z* (CI) 230(M^++1, 100), 116(23), 85(57) and 57(^tBu, 100).

Z-Methyl-2-trimethylacetyl-3-phenylpropenoate



A mixture of Z-*tert*-butyl-4-phenylmethylene-5-oxazolone (0.50 g, 2.18 mmol) and anhydrous sodium acetate (0.008 g, 1mmol) was refluxed for 4h in methanol (15 ml, 0.37 mol)[49]. The solvent was removed *in vacuo* and the residue purified by column chromatography (eluant: ethyl acetate). Removal of the solvent yielded the title compound as a white powder (0.45 g, 75%); m.p. 104-106°C; υ_{max}/cm^{-1}(KBr) 3273(N-H), 1725(ester C=O), 1658, 1505(amide C=O) and 1640(C=C); δ_H(200 MHz, $CDCl_3$) 1.303(9H, s, ^tBu), 3.86(3H, s, CH_3), 7.25(1H, br s, NH), 7.38(C=CH) and 7.40-7.43(5H, m, ArH); δ_C(50.3 MHz, $CDCl_3$) 27.12($C(CH_3)_3$), 39.21($C(CH_3)_3$), 52.06(CH_3O), 128.67(*m*), 129.48(C=*C*H), 129.73(*o*), 131.66*p*), 134.22(*ipso*), 166.19(amide C=O) and 176.90(ester C=O); *m/z* (CI) 262(M^++1, 100%), 230(M^+-CH_3O, 5), 85(^tBuCO, 7) and 57(^tBu, 5).

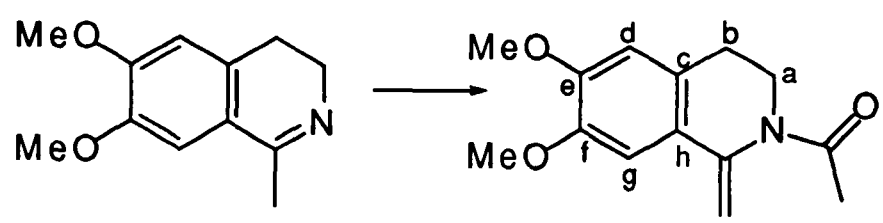
Z-Tert-butyl-2-acetylamino-3-phenylpropenoate



Iso-butene (15 ml) was condensed at -78°C into a suspension of α-acetamidocinnamic acid (1.03 g, 5 mmol) in dry, degassed dichloromethane (6 ml) contained in a Fischer-Porter bottle. After the addition of concentrated sulphuric acid (12 drops), the bottle was sealed and stirred at room temperature for 6 days, by which time the solution was clear. The bottle was then cooled in an ice/salt bath, excess *iso*butene was vented and after the addition of saturated aqueous sodium hydrogen carbonate (20 ml), the aqueous layer was extracted with dichloromethane (3x10 ml). The combined organic layers were washed

with brine (25 ml), dried (Na_2SO_4) and the solvent removed *in vacuo* to yield the title compound which was recrystallised from ether/hexane giving white crystals (1.06 g, 81%); m.p. 147-149°C (lit.[23], 142-144°C); υ_{max}/cm^{-1}(KBr) 3236(N-H), 1714(ester C=O), 1663(C=C), 1643, 1522(amide C=O) and 1294(^tBu CH); δ_H(500 MHz, $CDCl_3$) 1.54(9H, s, ^tBu), 2.12(3H, s, CH_3), 6.98(1H, s, NH) and 7.26-7.43(6H, m, Ph & C=CH); δ_C(50.3MHz, $CDCl_3$) 28.16(C(CH_3)$_3$), 23.43(CH_3), 82.28(*C*(CH_3)$_3$), 128.62(*m*), 129.20(C=*C*H), 129.61(*o*), 130.69(*p*), 134.56(*ipso*), 164.48(amide C=O) and 168.51(ester C=O); *m/z* (CI) 262(M^++1, 75%), 206(100), 163(38), 188(M^+-^tBuO, 5) and 57(^tBu, 4).

2-Acetyl-6,7-dimethoxy-1-methylene-1,2,3,4-tetrahydroisoquinoline

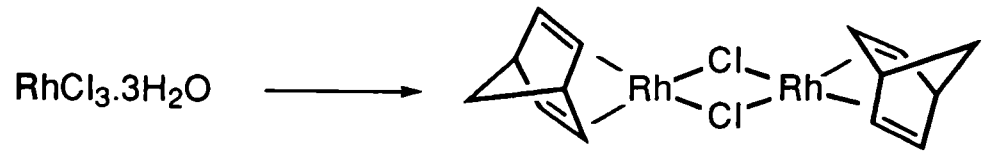


6,7-dimethoxy-1-methyl-3,4-dihydroisoquinoline (4 g, 0.02 mol) was placed under argon into a two necked round bottomed flask fitted with a reflux condenser and thermometer. Freshly distilled acetic anhydride (10 ml) and pyridine (10 ml) were added under argon to the flask and the contents were heated at 95°C for 30 min to yield a brown solution[70]. The flask was left overnight at room temperature and then the solvents were removed by reduced pressure distillation at 50°C. The residue was diluted with distilled ethyl acetate (4 ml) and further removal of the solvent *in vacuo* yielded a brown solid which was recrystallised from distilled ethyl acetate to yield the title compound as a yellow powder (3.5 g, 70%); m.p. 111-114°C (lit., 106-107°C); δ_H(500 MHz, $CDCl_3$) 2.23(3H, s, CH_3CO), 2.83(2H, t, J=6.03 Hz, H_b), 3.88(3H, s, CH_3O), 3.92(3H, s, CH_3O), 3.98(2H, t, J=6.00 Hz, H_a), 4.96(1H, br s, C=CH), 5.60(1H, s, C=CH), 6.60(1H, s, H_d) and 7.08(1H, s, H_g); δ_C(125.80MHz, $CDCl_3$) 22.88(*C*H_3CO), 29.00(b), 42.06(a), 56.34(CH_3O), 56.47(CH_3O), 104.65(C=*C*H_2), 107.10(d),

111.65(g), 124.10(h), 128.46(c), 144.20(*C*=CH_2), 148.14(f), 150.26(e) and 169.80(amide C=O).

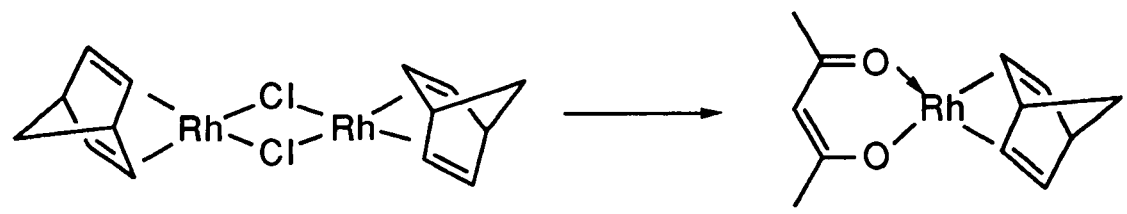
Synthesis of rhodium catalysts

Bis-bicyclo[2.2.1]hepta-2,5-diene chloro-μ-chloro dirhodium



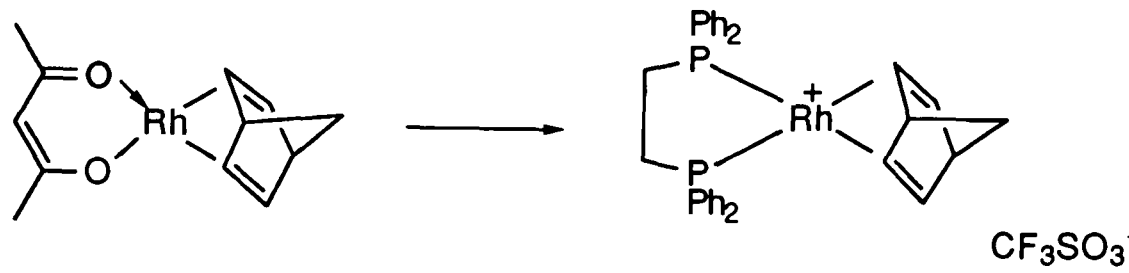
Freshly distilled bicyclo[2.2.1]hepta-2,5-diene (7.8 ml, 0.07 mol) was added to a stirred solution of rhodium (III) chloride (2.72 g, 13 mmol) in dry ethanol (40 ml). The red solution was stirred under argon for 48h and slowly produced the product as a yellow precipitate which was filtered and dried (2.12 g, 52%); m.p. 237-239°C (lit.[50], 240°C); δ_H(300 MHz, $CDCl_3$) 1.19(2H, t, $J_{CH\text{-}CH_2}$=1.53 Hz, C*H*$_2$CH), 3.83(2H, s, C*H*CH=CH) and 3.94(14H, dd, $J_{Rh\text{-}CH}$=2.54 Hz, $J_{CH\text{-}CH}$=4.66 Hz, CHC*H*=C*H*).

Bicyclo-[2.2.1]-hepta-2,5-diene rhodium 2,5-pentanedionate



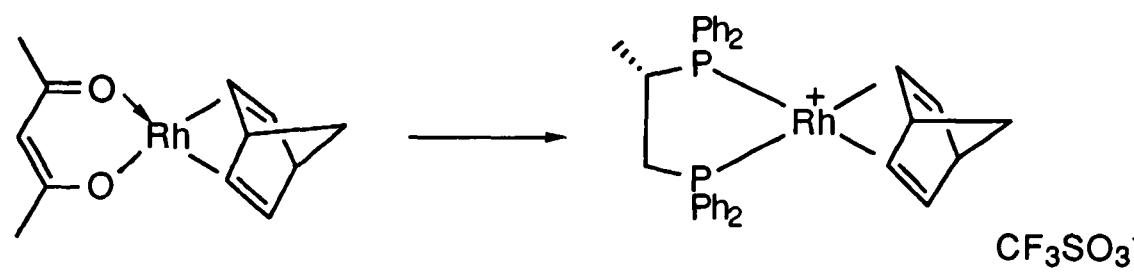
Potassium acetylacetonate (1.52 g, 27.3 mmol) was added to a solution of bis-bicyclo[2.2.1]hepta-2,5-diene chloro-μ-chloro dirhodium (1.58 g, 3.5 mmol) in dry tetrahydrofuran (40 ml). The suspension was vigorously stirred for 4h, filtered and the solvent removed *in vacuo*. The residue was purified by sublimation under reduced pressure (125°C at 0.1 mbar) to yield the product as a bright yellow powder (1.42 g, 71%); m.p. 182-184°C (lit.[50], 176-177°C); δ_H(300 MHz, $CDCl_3$) 1.24(2H, t, $J_{CH\text{-}CH_2}$=1.64 Hz, C*H*$_2$CH), 1.92(6H, s, CH_3), 3.95(4H, dd, $J_{Rh\text{-}CH}$=4.73 Hz, $J_{CH\text{-}CH=C}$=2.55 Hz, CHC*H*=C*H*), 3.98(2H, s, C*H*CH=CH) and 5.31 (1H, s, COCHCO).

1,2-Bis-(diphenylphosphino)ethane rhodium(I) bicyclo[2.2.1]-hepta-2,5-diene trifluoromethane sulphonate



Trimethylsilyl trifluoromethanesulphonate (210 µl, 1.09 mmol) was added to a solution of bicyclo-[2.2.1]-hepta-2,5-diene rhodium 2,5-pentanedionate (0.20 g, 0.68 mmol) in degassed tetrahydrofuran (4 ml) stirred under argon. The yellow/orange solution was stirred for 5 min, 1,2-bis-(diphenylphosphino)ethane (0.32 g, 0.8 mmol) was added and the resultant cherry red solution was stirred for another 15 min[50]. Then degassed pentane (20 ml) was added and the precipitate which slowly formed was collected by removal of the solvent *in vacuo* and washing with degassed pentane (3x5 ml), yielding the title compound as an orange powder (0.48 g, 93%); m.p. 195-197°C (lit., 200°C); δ_H(300 MHz $CDCl_3$) 1.82(2H, s, C*H*$_2$CH), 2.29(4H, d, $J_{CH\text{-}P}$=19.60 Hz, CH_2P), 4.24(2H, s, C*H*CH=CH), 5.33(4H, m, CHC*H*=C*H*) and 7.52(20H, m, Ar); δ_P(101.23 MHz, THF) 53.5(d, $J_{Rh\text{-}P}$=157.2 Hz); *m/z* (ES) 593(M^+, 100%).

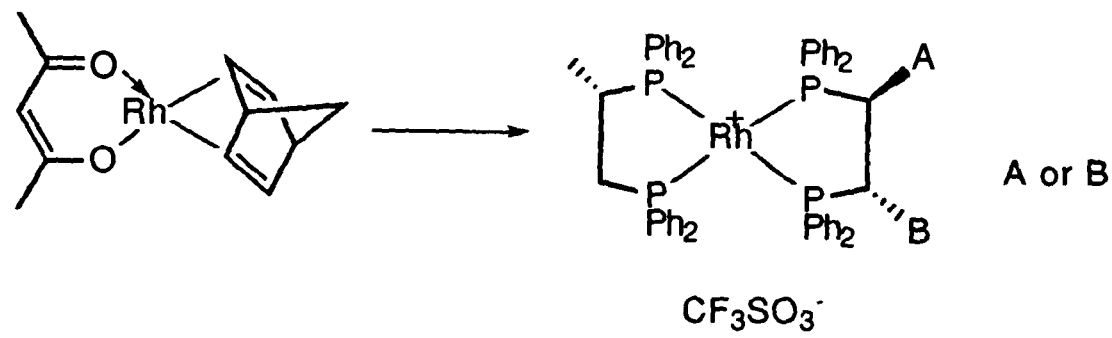
(R)-1,2-Bis-(diphenylphosphino)propane rhodium(I) bicyclo[2.2.1]-hepta-2,5-diene trifluoromethane sulphonate



Trimethylsilyl trifluoromethanesulphonate (22 µl, 0.11 mmol) was added to a solution of bicyclo-[2.2.1]-hepta-2,5-diene rhodium 2,5-pentanedionate (30 mg, 0.1 mmol) in degassed tetrahydrofuran (1 ml) stirred under argon. The yellow/orange solution was stirred for 5 min, (R)-1,2-bis-(diphenylphosphino)propane (42 mg, 0.1 mmol) was

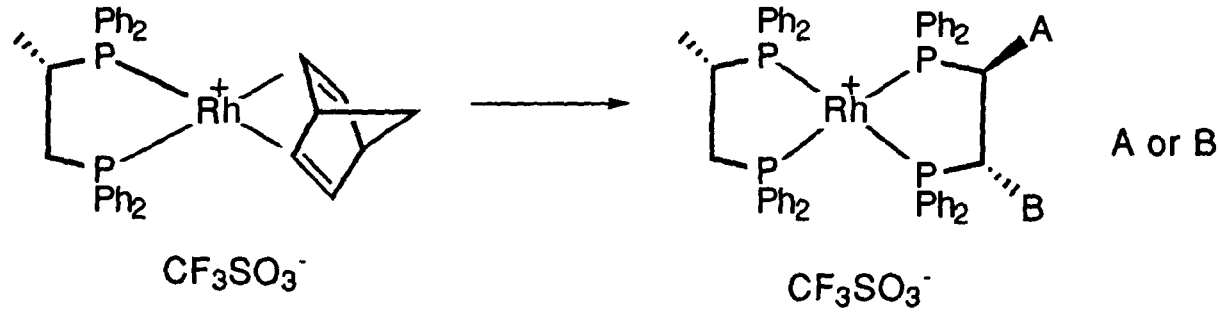
added and the resultant cherry red solution was stirred for another 15 min[50]. Then degassed ether (15 ml) was added and the precipitate which slowly formed was collected by removal of the solvent *in vacuo* and washing with degassed ether (3x2.5 ml), yielding the title compound as an orange powder (68 mg, 91%); δ_P(202.46 MHz, THF) 62.51 and 43.97(dd, $J_{Rh\text{-}P}$=156.0 Hz, $J_{P\text{-}P}$=35.2 Hz); *m/z* (ES) 607(M^+, 100%).

Bis[(R)-1,2-bis-(diphenylphosphino)propane] rhodium trifluoromethane sulphonate



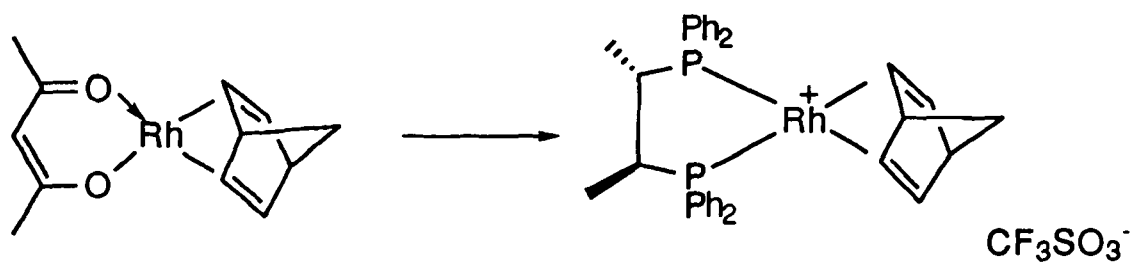
Trimethylsilyl trifluoromethanesulphonate (4 µl, 17 µmol) was added to a solution of bicyclo-[2.2.1]-hepta-2,5-diene rhodium 2,5-pentanedionate (5 mg, 17 µmol) in degassed tetrahydrofuran (0.5 ml) stirred under argon[50]. The yellow/orange solution was stirred for 5 min, (R)-1,2-bis-(diphenylphosphino)propane (14 mg, 34 µmol) was added and the resultant cherry red solution was stirred for another 15 min. Then degassed ether (5 ml) was added and the precipitate which slowly formed was collected by removal of the solvent *in vacuo* and washing with degassed ether (3x0.5 ml), yielding a product which was not clean by ^{31}P NMR.

Bis[(R)-1,2-bis-(diphenylphosphino)propane] rhodium trifluoromethane sulphonate



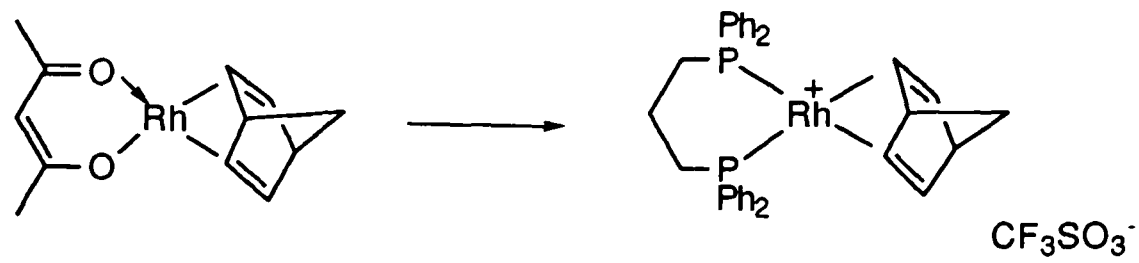
A solution of (R)-1,2-bis-(diphenylphosphino)propane rhodium(I) bicyclo[2.2.1]-hepta-2,5-diene trifluoromethane sulphonate (10 mg, 0.013 mmol) in degassed tetrahydrofuran (2.5 ml) was added to an 8 mm NMR tube containing degassed (R)-1,2-bis-(diphenylphosphino)propane (5.5 mg, mmol). The NMR tube was sealed under argon, 'whirlimixed' until all the solid had dissolved and then placed in a 10 mm NMR tube with D_2O in the interannular space (to obtain the external lock signal). ^{31}P NMR (101.26 MHz) showed a predominance of two doublets of triplets, δ_P(202.46 MHz, THF) 61.80 and 45.13(dt, J_{Rh-P}=132.0 Hz, J_{P-P}=35.1 Hz).

(2R,3R-Bis-(diphenylphosphino)butane rhodium(I) bicyclo[2.2.1]-hepta-2,5-diene trifluoromethane sulphonate



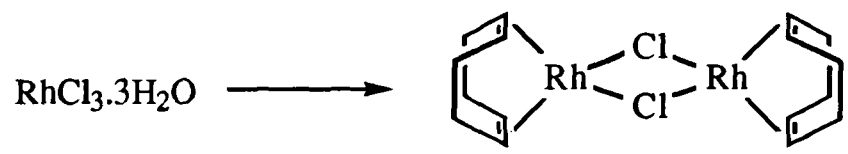
Trimethylsilyl trifluoromethanesulphonate (22 µl, 0.11 mmol) was added to a solution of bicyclo-[2.2.1]-hepta-2,5-diene rhodium 2,5-pentanedionate (30 mg, 0.1 mmol) in degassed tetrahydrofuran (1 ml) stirred under argon. The yellow/orange solution was stirred for 5 min, (2R,3R)-bis-(diphenylphosphino)butane (43 mg, 0.1 mmol) was added and the resultant orange solution was stirred for another 15 min[50]. Then degassed ether (15 ml) was added and the precipitate which slowly formed was collected by removal of the solvent *in vacuo* and recrystallised from degassed tetrahydrofuran and ether (3x2.5 ml), yielding the title compound as an orange powder (66 mg, 86%); δ_P(202.46 MHz, THF) 59.21(d, J_{Rh-P}=153.8 Hz); *m/z* (ES) 621(M^+, 100%).

1,3-Bis-(diphenylphosphino)propane rhodium(I) bicyclo[2.2.1]-hepta-2,5-diene trifluoromethane sulphonate



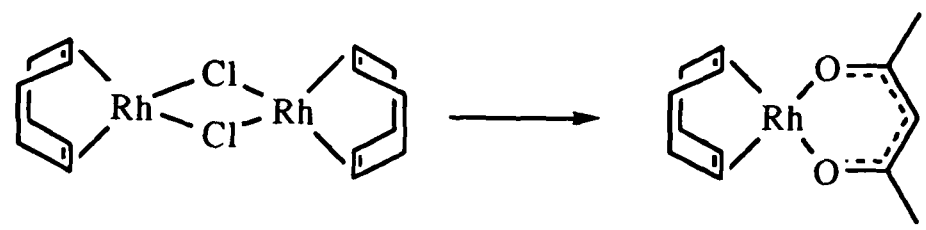
Trimethylsilyl trifluoromethanesulphonate (22 µl, 0.11 mmol) was added to a solution of bicyclo-[2.2.1]-hepta-2,5-diene rhodium 2,5-pentanedionate (30 mg, 0.1 mmol) in degassed tetrahydrofuran (1 ml) stirred under argon. The yellow/orange solution was stirred for 5 min, (R)-1,2-bis-(diphenylphosphino)propane (42 mg, 0.1 mmol) was added and the resultant orange solution was stirred for another 15 min[50]. Then degassed ether (15 ml) was added and the precipitate which slowly formed was collected by removal of the solvent *in vacuo* and washing with degassed ether (3x2.5 ml), yielding the title compound as an orange powder (75 mg, 100%); δ_P(202.46 MHz, THF) 12.80(d, $J_{Rh\text{-}P}$=149.0 Hz); *m/z* (ES) 607(M^+, 100%).

Di-µ-chloro-bis(1,5-cyclooctadiene) dirhodium



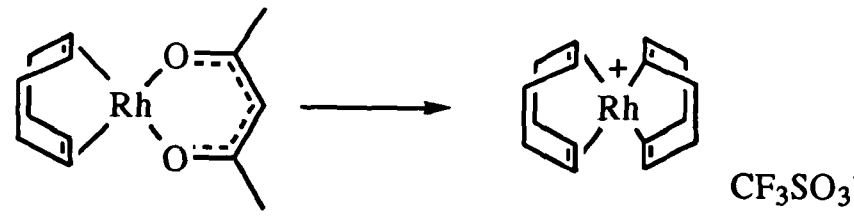
Freshly distilled 1,5-cyclooctadiene (1.5 ml, 12 mmol) was added to a stirred solution of rhodium (III) chloride (0.75 g, 3.6 mmol) in dry ethanol (20 ml) and the solution was refluxed under argon for 2h[76]. The orange precipitate was filtered and washed with ethanol to yield the title compound (583 mg, 83%).

(1,5-Cyclooctadiene)(2,4-pentanedionato)dirhodium



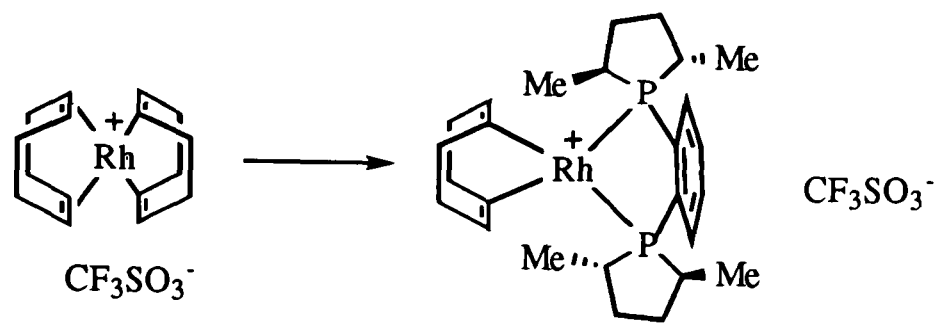
Potassium acetylacetonate (150 mg, 1.23 mmol) was added to a solution of (1,5-cyclooctadiene)(2,4-pentanedionato)dirhodium (300 mg, 0.61 mmol) in dry tetrahydrofuran (4 ml)[50]. The suspension was vigorously stirred overnight, the solid removed by cannula filtration and the solvent removed *in vacuo* to yield the product as a bright yellow powder (346 mg, 92%); δ_H(200 MHz, $CDCl_3$) 1.80-1.84(4H, m, CH_2), 2.40-2.52(4H, m, CH_2), 1.94(6H, s, CH_3), 4.07(4H, br s, CH=CH) and 5.33(1H, s, COCHCO).

Bis(1,5-cyclooctadiene)rhodium trifluoromethane sulphonate



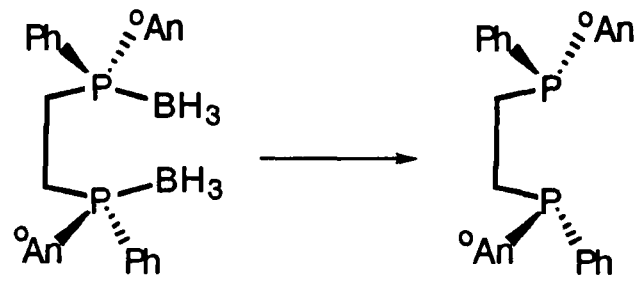
Freshly distilled, degassed cyclooctadiene (450 µl) was added to a solution of (1,5-cyclooctadiene)(2,4-pentanedionato)dirhodium (250 mg, 0.75 mmol) in degassed dichloromethane (1.25 ml)[77]. The solution was stirred rapidly whilst trimethylsilyl trifluoromethanesulphonate (313 µl, 0.75 mmol) was added dropwise. Stirring was continued for 10 min before the dropwise addition of degassed diethyl ether was begun. This resulted in the formation of dark red crystals which were obtained by removal of the solvent *in vacuo* followed by washing with degassed diethyl ether (350 mg, 100%); δ_H(300 MHz, CD_3OD) 1.73(4H, d, J_{Rh-H}=7.3 Hz, CH_2), 2.46(4H, br s, CH_2), and 3.99(4H, br s, CH=CH); *m/z* (ES) 293([M - C_8H_{18} + 2MeCN]$^+$, 100%) and 252([M - C_8H_{18} + MeCN]$^+$, 60).

1,2-Bis((2R,5R)-2,5-dimethylphospholano)benzene rhodium (I) 1,5-cyclooctadiene trifluoromethane sulphonate



A solution of bis(1,5-cyclooctadiene)rhodium trifluoromethane sulphonate in degassed tetrahydrofuran (30 mg in 1.5 ml, 0.06 mmol) was added dropwise *via* cannula to a solution of 1,2-bis((2R,5R)-2,5-dimethylphospholano)benzene in degassed tetrahydrofuran (19 mg in 0.5 ml, 0.06 mmol). The resultant orange solution was stirred for 15 min and then degassed diethyl ether (10 ml) was added[15]. The precipitate which slowly formed was collected by removal of the solvent *in vacuo* and washing with degassed diethyl ether (3 x 5 ml), yielding the title compound as a bright orange solid (40 mg, 100%); δ_P(202.46 MHz, $CDCl_3$) 77.24(d, J_{Rh-P}=148.4 Hz); *m/z* (ES) 517(M^+, 100%).

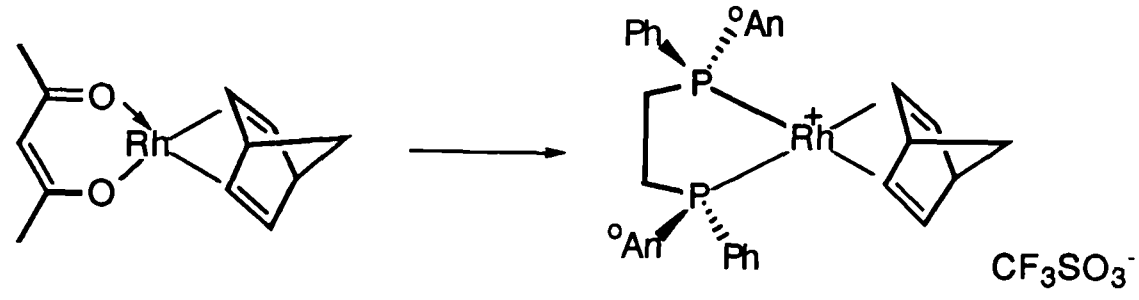
(S,S)-1,2-Bis-(orthoanisylphenylphosphino)ethane



Freshly distilled, degassed diethylamine (3 ml) was added to an 8 mm NMR tube containing degassed (S,S)-1,2-bis-(*ortho*anisylphenylphosphino)ethane diborane (105 mg, 0.23 mmol) and the tube was then heated at 50°C for 10h. After this time, ^{31}P NMR (101.23 MHz) showed the reaction to be complete, so the solvent was removed *in vacuo* and the residue dissolved in distilled, degassed toluene before filtration under argon through a pad of basic alumina. Removal of the solvent once more left a grainy oil

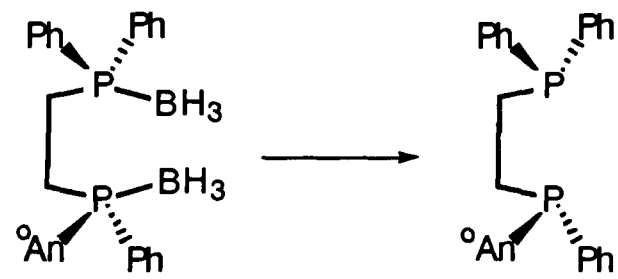
which was crystallised under argon from degassed methanol to give a white powder[60] (57 mg, 54%); δ_P(202.46 MHz, CD_3OD) -20.71.

(S,S)-1,2-Bis-(orthoanisylphenylphosphino)ethane rhodium(I) bicyclo[2.2.1]-hepta-2,5-diene trifluoromethane sulphonate



Trimethylsilyl trifluoromethanesulphonate (24 µl, 0.12 mmol) was added to a solution of bicyclo-[2.2.1]-hepta-2,5-diene rhodium 2,5-pentanedionate (32 mg, 0.11 mmol) in degassed tetrahydrofuran (1 ml) stirred under argon. The yellow/orange solution was stirred for 5 min, (S,S)-1,2-bis-(*ortho*anisylphenylphosphino)ethane (50 mg, 0.11 mmol) was added and the resultant orange solution was stirred for another 15 min[50]. Then degassed pentane (15 ml) was added and the precipitate which slowly formed was collected by removal of the solvent *in vacuo* and recrystallised from degassed tetrahydrofuran and ether (3x2.5 ml), yielding the title compound as an orange powder (64 mg, 73%); δ_P(202.46 MHz, CD_3OD) 51.04(d, J_{Rh-P}=158.7 Hz).

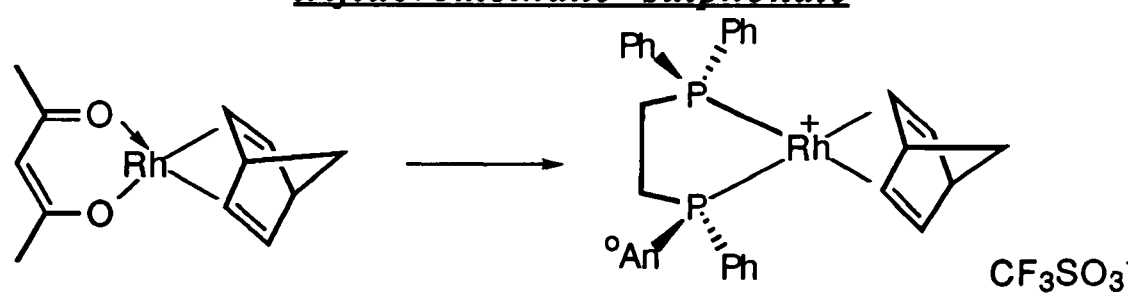
(S)-(2-Methoxyphenyl)-P-phenyl-P-(2'-diphenylphosphino)ethylphosphine



Freshly distilled, degassed diethylamine (4.5 ml) was added to an 8 mm NMR tube containing degassed (S)-(2-methoxyphenyl)-P-phenyl-P-(2'-diphenylphosphino) ethylphosphine diborane (123 mg, 0.3 mmol) and the tube was then heated overnight at 50°C. After this time, ^{31}P NMR (101.23 MHz) showed the reaction to be complete, so

the solvent was removed *in vacuo* and the residue dissolved in distilled, degassed toluene before filtration under argon through a pad of basic alumina. Removal of the solvent once more left a grainy oil which was crystallised under argon from degassed methanol to give a white powder[58] (103 mg, 84%); δ_P(202.46 MHz, $CDCl_3$) -11.19 and -20.71(d, J_{P-P}=34.8 Hz).

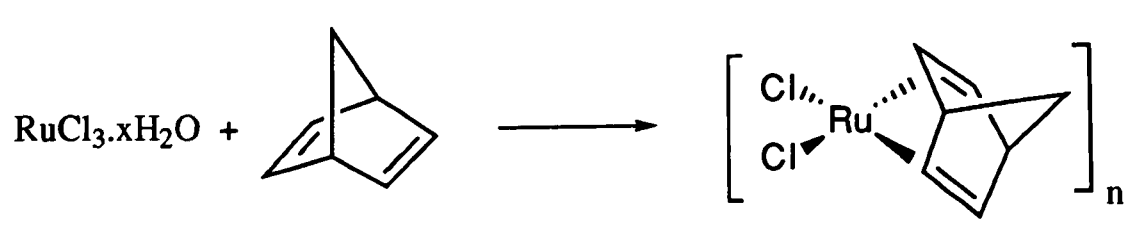
(S)-(2-Methoxyphenyl)-P-phenyl-P-(2'-diphenylphosphino) ethylphosphine rhodium(I) bicyclo[2.2.1]-hepta-2,5-diene trifluoromethane sulphonate



Trimethylsilyl trifluoromethanesulphonate (26 µl, 0.13 mmol) was added to a solution of bicyclo-[2.2.1]-hepta-2,5-diene rhodium 2,5-pentanedionate (34 mg, 0.12 mmol) in degassed tetrahydrofuran (1 ml) stirred under argon. The yellow/orange solution was stirred for 5 min and then a solution of (S)-(2-methoxyphenyl)-P-phenyl-P-(2'-diphenylphosphino)ethylphosphine in degassed THF (50 mg, 0.12 mmol in 2 ml) was added dropwise over a 15 min period. After the addition was complete, the orange/red solution was added dropwise to rapidly stirred, degassed pentane (30 ml). The resultant solid was allowed to settle and the solvent removed *in vacuo*, yielding the title compound as a light orange powder (75 mg, 83%); δ_P(202.46 MHz, CD_3OD) 56.54 and 51.27(dd, J_{Rh-P}=158.3 Hz, J_{P-P}=29.7 Hz).

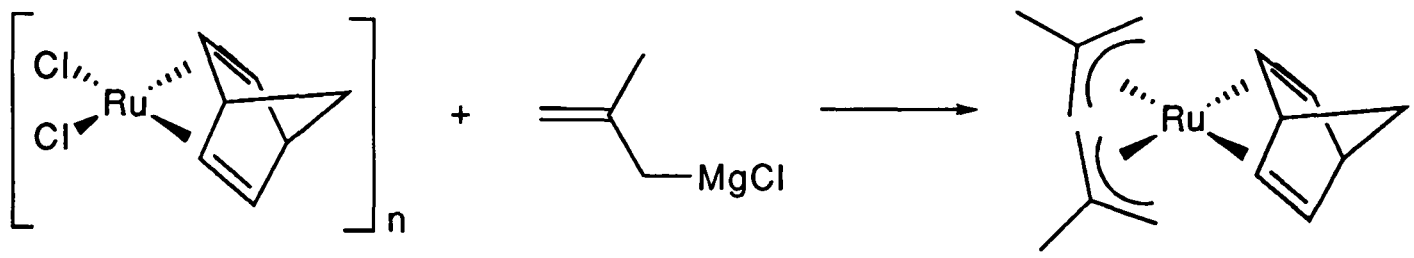
Synthesis of ruthenium catalysts

Di-µ-chloro-(η^4-bicyclo[2.2.1]hepta-2,5-dienyl) ruthenium II polymer



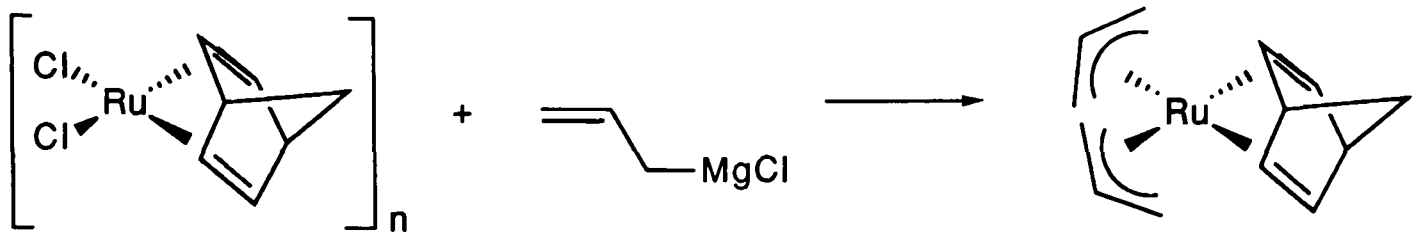
Freshly distilled, degassed bicyclo[2.2.1]hepta-2,5-diene (6.5 ml, excess) was added to a Schlenk containing ruthenium chloride (2 g, 10 mmol) and distilled, degassed ethanol (65 ml). The brown suspension was stirred overnight at 45°C and then filtered to yield a brown solid[78] (2.34 g, 92%).

(η⁴-Bicyclo[2.2.1]hepta-2,5-diene) bis-(η³-2-methylpropenyl)ruthenium II



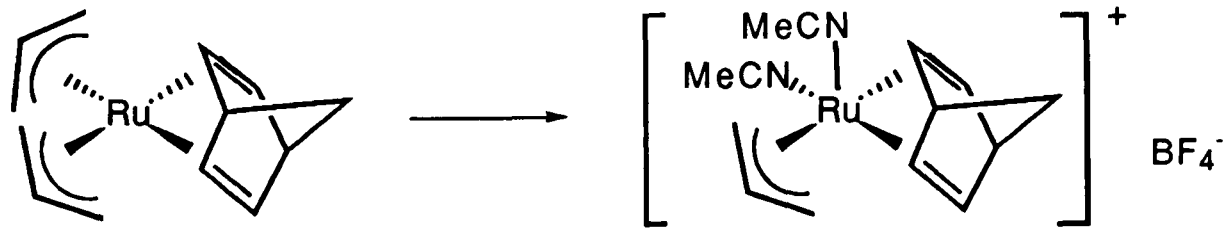
The ruthenium oligomer (1.4 g, 5.3 mmol) was ground up in a mortar and pestle and placed in a 250 ml two-necked round bottomed flask. The contents of the flask were degassed and then distilled, degassed diethyl ether (30 ml) was added. The mixture was stirred rapidly and a solution of 2-methylpropenemagnesium chloride[67] (75 ml of 0.65M solution, excess) was added *via* cannula over 0.5h[79]. The resultant dark brown suspension was stirred at room temperature for 12h and then filtered under argon through a porous frit. The filtrate was cooled to 0°C and then 20 ml distilled, degassed water (degassed by purging with argon) was added in 5 ml portions over 15 min. The aqueous layer was extracted with distilled, degassed diethyl ether (3x15 ml) and the brown organics were dried for 1h over magnesium sulphate. Then the organics were filtered under argon *via* cannula and the solvent removed *in vacuo*. The resultant gum was dissolved in pentane and filtered through a 0.5 cm neutral alumina column. Removal of the pentane *in vacuo* yielded the product as a yellow solid (1.24 g, 76%); δ_H(500 MHz, $CDCl_3$) bicyclo[2.2.1]hepta-2,5-diene: 1.15(2H, m, CH_2), 1.33(2H, m, olefin), 3.63(2H, m, CH) and 4.28(2H, m, olefin); 2 - methylpropenyl: 1.25(2H, m), 1.49(2H, m), 1.73(6H, s, CH_3), 3.38(2H, s) and 3.66(2H, s).

(η⁴-Bicyclo[2.2.1]hepta-2,5-diene) bis-(η³propenyl) ruthenium II



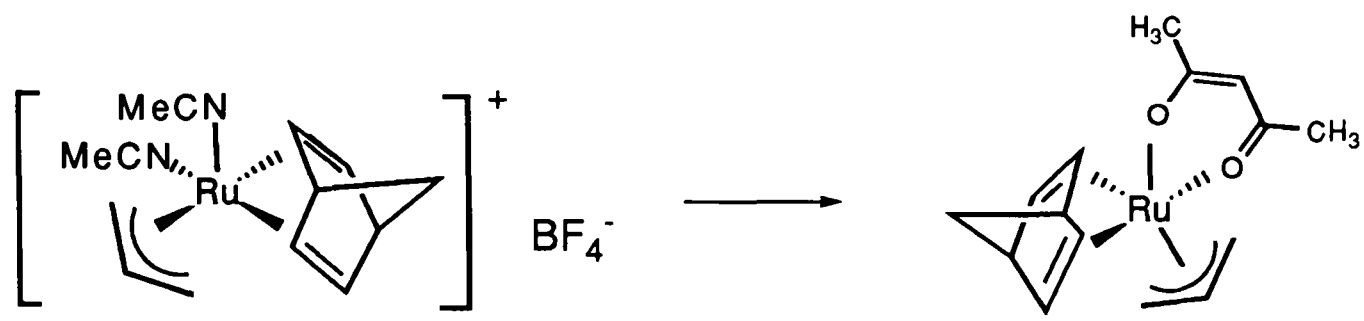
This compound was prepared by method described above, using commercial allylmagnesium chloride (1.03 g, 71%); δ_H(300 MHz, C_6D_6) bicyclo[2.2.1]hepta-2,5-diene: 1.28(2H, m, CH_2), 1.33(2H, m, olefin), 3.43(2H, m, CH) and 4.05(2H, m, olefin); propenyl: 0.10(2H, m), 1.62(2H, m), 3.06(2H, m), 2.9-3.2(2H, m) and 3.70(2H, m).

(η⁴-Bicyclo[2.2.1]hepta-2,5-dienyl) (η³propenyl) bis-(η¹-acetonitrilo) ruthenium II tetrafluoroborate



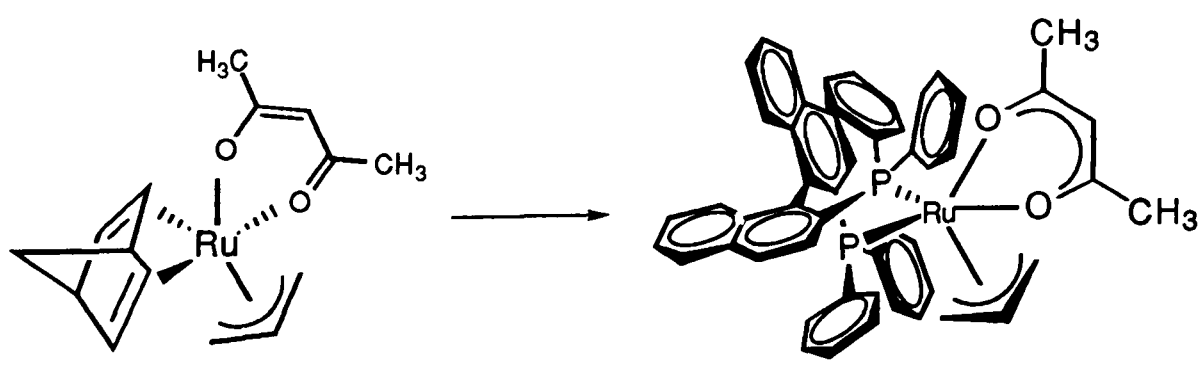
Triphenylcarbenium tetrafluoroborate[80] (240 mg, 0.73 mmol) was added to a Schlenk containing a degassed solution of (η^4-bicyclo[2.2.1]hepta-2,5-dienyl) bis-(η^3propenyl) ruthenium II (200 mg, 0.73 mmol) and acetonitrile (275 µl, 5.3 mmol) in dichloromethane (0.73 ml). The red/brown solution was stirred at room temperature for 2h and then a large excess of degassed diethyl ether (7.3 ml) was added to yield the product as a yellow powder[81] (288 mg, 82%); δ_H(300 MHz, $CDCl_3$) bicyclo[2.2.1]hepta-2,5-diene: 1.31(2H, m, CH_2), 2.37-3.93(2H, m, olefin), 3.64-3.87(2H, m, CH) and 4.13-4.24(2H, m, olefin); propenyl: 1.79(1H, m), 3.01(1H, m), 3.18(1H, m), 3.76(1H, m) and 5.10(1H, m).

(η4-Bicyclo[2.2.1]hepta-2,5-dienyl) (η32-propenyl)(acetylacetonato) ruthenium II



A solution of sodium acetylacetonate in distilled, degassed acetone (226 mg, 1.85 mmol) was added to a Schlenk containing (η^4-bicyclo[2.2.1]hepta-2,5-dienyl) (η^3propenyl) bis-(η^1-acetonitrilo) ruthenium II tetrafluoroborate in distilled, degassed acetone (747 mg, 1.85 mmol). The resultant yellow solution was stirred at room tempertature for 12h[81]. The solvent was then removed *in vacuo* and the residue was dissolved in distilled, degassed pentane (5 ml) and filtered through 0.5 cm celite. Further removal of solvent led to a brown oil which was purified by short path distillation (115°C at 0.04 mmHg) to yield the title compound as a yellow powder (153 mg, 62%); δ_H(300 MHz, $CDCl_3$) acetylacetonate: 1.27(3H, s, CH_3), 2.12(3H, s, CH_3), and 5.25(1H, s, olefin); propenyl: 1.36(1H, m), 1.67-1.72(1H, m), 2.68(1H, m), 3.45(1H, m) and 4.65-4.75(1H, m); bicyclo[2.2.1]hepta-2,5-diene: 1.31(2H, m, CH_2), 1.59-2.03(2H, m, olefin), 3.32-3.80(2H, m, CH) and 3.29-4.12(2H, m, olefin).

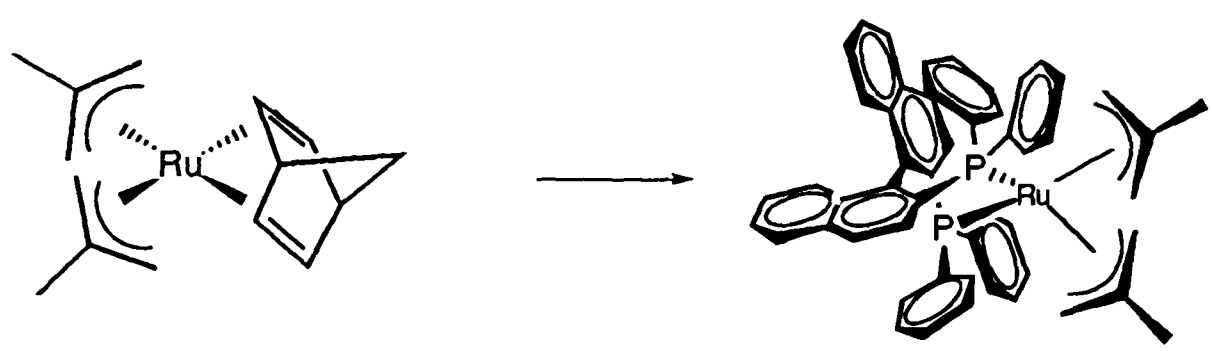
(S)-2,2-Bis(diphenylphosphino)-1,1-binaphthyl(η3-propenyl)(acetylacetonato)ruthenium II



(η^4-Bicyclo[2.2.1]hepta-2,5-dienyl) ($\eta^3$2-propenyl)(acetylacetonato) ruthenium II (20 mg, 0.06 mmol) and (R)-2,2'-bis(diphenylphosphino)-1,1'-binaphthyl (37 mg, 0.06

mmol) were degassed in a two-necked Schlenk fitted with a cold finger. The minimum amount of freshly distilled, degassed toluene was added *via* cannula (1 ml) and then the contents of the Schlenk were degassed again. The yellow mixture was refluxed overnight to yield a red/brown solution[38]. The toluene was removed *in vacuo* and the residue washed with degassed pentane to give the title compound as a yellow powder (46 mg, 89%); δ_P(202.46 MHz, toluene) 64.42(d, J=37.1 Hz), 37.20(d, J=37.1 Hz); *m/z* (ES) 864($M+H^+$, 100%) correct isotope pattern for ruthenium.

Attempted preparation of (R)-2,2'-bis(diphenylphosphino)-1,1'-binaphthyl bis(n3-2-methylpropenyl)ruthenium II

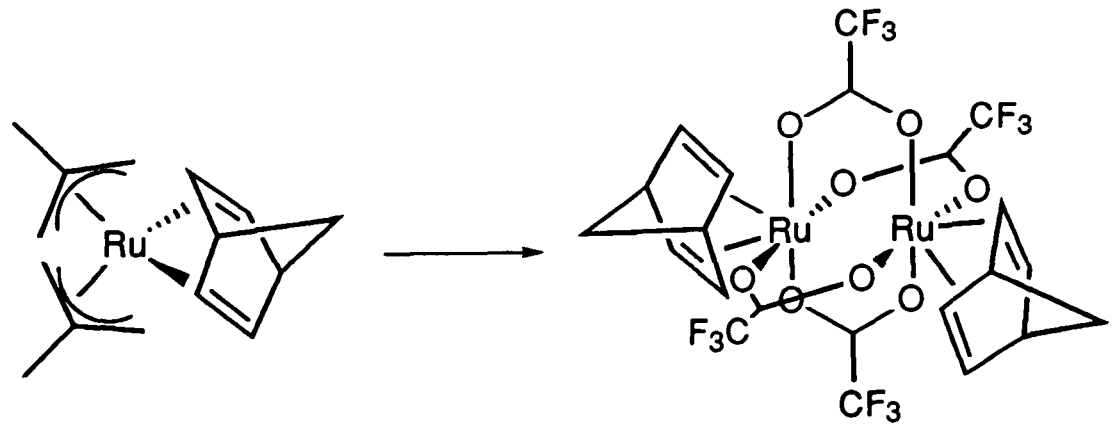


The next synthesis to be attempted was Genet's bis(methylallyl) catalyst. Initial attempts were made using the bis(allyl) system. Ruthenium bis(allyl)(bicyclo[2.2.1]hepta-2,5-dienyl) (25 mg, 0.08 mmol) and (R)-2,2'-bis(diphenylphosphino)-1,1'-binaphthyl (50 mg, 0.08 mmol) were stirred at 100°C in toluene for five hours in accordance with the literature procedure[63]. Very little product was observed (by ^{31}P NMR) and the reaction mixture contained mostly starting material. The reaction was repeated and monitored by ^{31}P NMR (101.23 MHz). After 48 hours two doublets at 70 ppm and 58 ppm (J = 52 Hz) were observable in the NMR, along with a peak corresponding to unreacted (R)-2,2'-bis(diphenylphosphino)-1,1'-binaphthyl at -14 ppm. The starting material peak diminished over the next three days but the reaction was not a clean one, as observed by the NMR.

Attempts to reflux the reaction mixture led to a much messier NMR and purification of the reaction mixture by conducting columns under argon (eluting with ethyl acetate) enabled

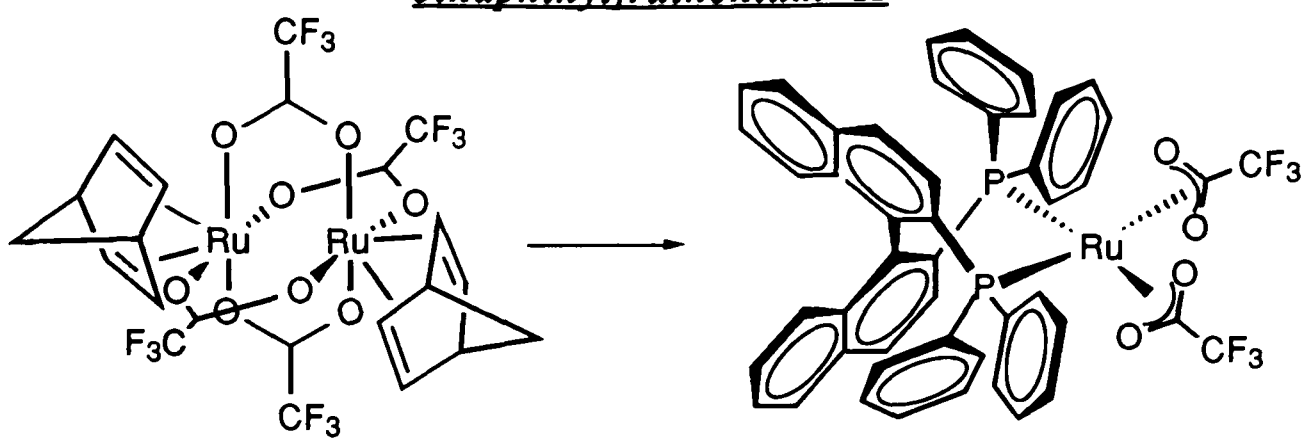
the species showing two doublets in its ^{31}P NMR to be obtained. However the literature claims that the methyl allyl system leads to a product with a chemical shift at 40 ppm. Thus, it was decided to move onto a synthesis starting with (η^4-bicyclo[2.2.1]hepta-2,5-dienyl) bis-(η^3-2-methylpropenyl) ruthenium II. The reaction mixture was stirred at 100°C and monitored by ^{31}P NMR once more. A peak at 40 ppm was observable after 12 hours, though after several days two doublets at 56 ppm and 69 ppm could also be seen. These grew in intensity with respect to the reported peak at 40 ppm over the next few days. The refluxed reaction mixture was once more a much dirtier reaction than the reaction stirred at 100°C.

(η^4-Bicyclo[2.2.1]hepta-2,5-dienyl) tetrakis (μ trifluoroacetato)ruthenium II



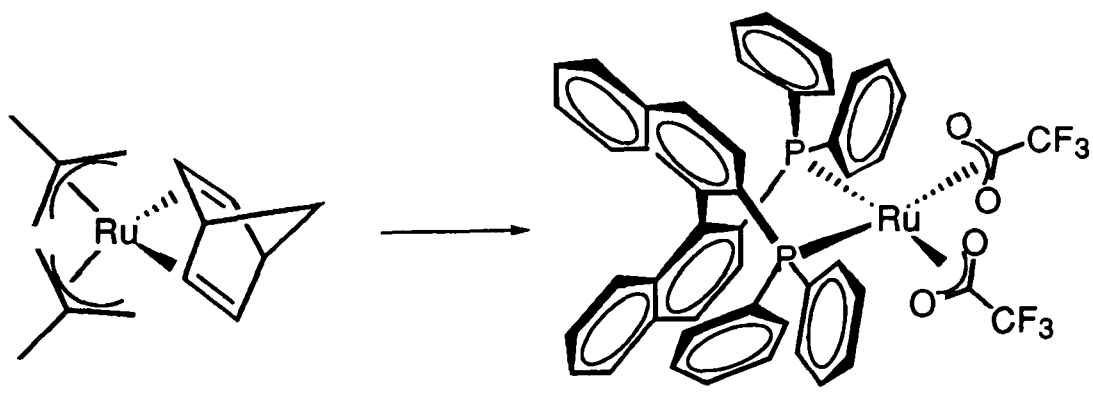
Freshly distilled, degassed trifluoroacetic acid (128 μl, 1.66 mmol, degassed by purging with nitrogen) was added dropwise to a stirred solution of (η^4-bicyclo[2.2.1]hepta-2,5-dienyl) bis-(η^3-2-methylpropenyl) ruthenium II in diethyl ether (225 mg, 0.81 mmol in 2.7 ml) and the orange solution was then stirred for 2h[69]. The solvent was removed *in vacuo* to yield a brown oil which was washed with degassed ether at -5°C to give the title compound as a yellow/brown powder (508 mg, 72%); *m/z* (ES) 359(100%) and 318(30%) correct isotope pattern for ruthenium.

Bis(trifluoroacetato)[(R)-2,2'-bis(diphenylphosphino)-1,1'-binaphthyl]ruthenium II



A solution of (η^4-bicyclo[2.2.1]hepta-2,5-dienyl) tetrakis (μ trifluoroacetato)ruthenium II (35 mg, 0.04 mmol) and (R)-2,2'-bis(diphenylphosphino)-1,1'-binaphthyl (50 mg, 0.08 mmol) in degassed diethyl ether (530 μl) and degassed tetrahydrofuran (200 μl) was heated overnight at 40°C in a Schlenk fitted with a cold finger[69]. Removal of the solvent *in vacuo* from the dark orange solution followed by crystallisation with degassed ether and pentane led to the title compound as a yellow solid (33 mg, 87%); δ_P(202.46 MHz, $CDCl_3$) 57.50; *m/z* (ES) 864($M+H^+$, 100%) correct isotope pattern for ruthenium.

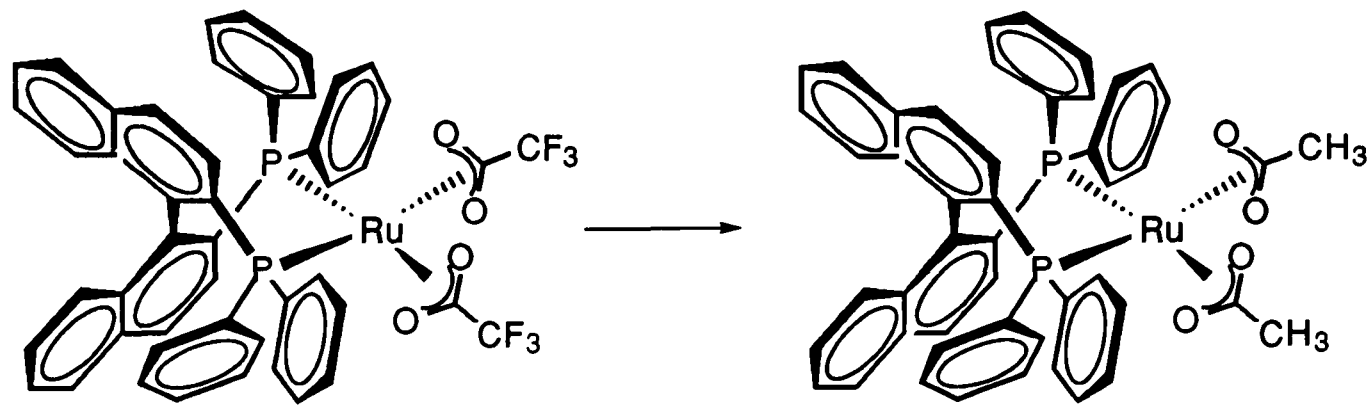
Bis(trifluoroacetato)[(R)-2,2'-bis(diphenylphosphino)-1,1'-binaphthyl]ruthenium II



A solution of (R)-2,2'-bis(diphenylphosphino)-1,1'-binaphthyl (150 mg, 0.24 mmol) in the minimum amount of degassed dichloromethane was added, *via* cannula, to a Schlenk containing a yellow solution of (η^4-bicyclo[2.2.1]hepta-2,5-dienyl) bis-(η^3-2-methylpropenyl) ruthenium II (88 mg, 0.29 mmol) and freshly distilled, degassed trifluoroacetic acid (54 μl, 0.7 mmol, degassed by purging with nitrogen) in the minimum amount of degassed methanol. The contents of the Schlenk were degassed again and then stirred at room temperature overnight[69]. Removal of the solvent *in vacuo*

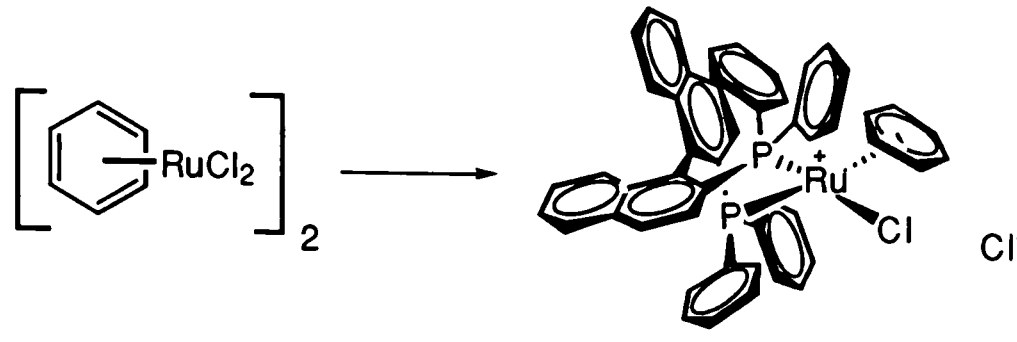
led to the product as a yellow solid. Note that the product was extremely sensitive to traces of water (even in $CDCl_3$) and on contact with water, water bridged dimeric species were formed. Adding trifluoroacetic anhydride to such a solution resulted in reconversion of the bridged species into the trifluoroacetate monomer (211 mg, 93%); δ_P(202.46 MHz, $CDCl_3$) 57.50; *m/z* (ES) 864($M+H^+$, 100%) correct isotope pattern for ruthenium.

Bis(acetato)[(R)-2,2'-bis(diphenylphosphino)-1,1'-binaphthyl]ruthenium II



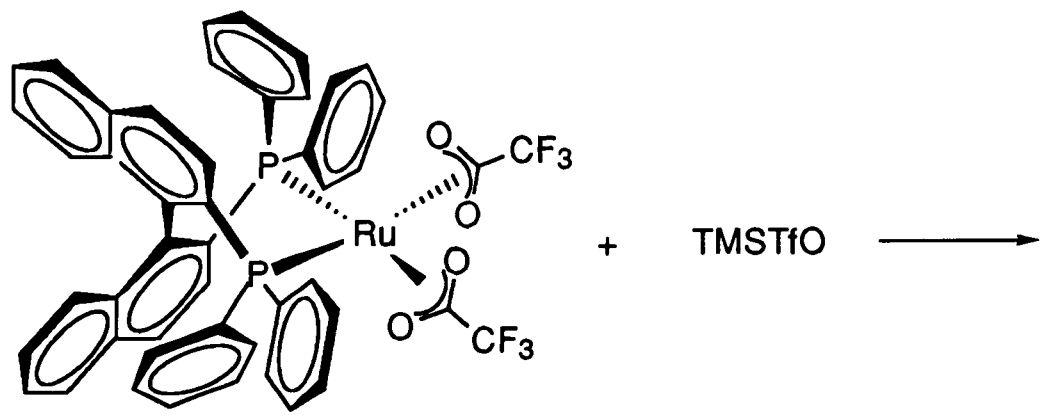
A thoroughly degassed suspension of bis(trifluoroacetato)[(R)-2,2'-bis(diphenylphosphino)-1,1'-binaphthyl]ruthenium II (22 mg, 0.023 mmol) and sodium acetate (25 mg, 0.23 mmol) in methanol (500 µl) was stirred at 40°C for 2h[69]. The solvent was removed *in vacuo* and the residue extracted with degassed dichloromethane (1 ml). Removal of the dichloromethane *in vacuo* yielded the title compound as a yellow powder (20 mg, 84%); δ_P(202.46 MHz, $CDCl_3$) 65.84; *m/z* (ES) 865($M+Na^+$, 90%), 824 ($[M - CH_3CO_2^- + MeCN]^+$, 100), correct isotope pattern for ruthenium.

(R)-2,2'-Bis(diphenylphosphino)-1,1'-binaphthyl benzeneruthenium chloride



A mixture of benzeneruthenium (II) chloride dimer (13 mg, 0.02 mmol) and (R)-2,2'-bis(diphenylphosphino)-1,1'-binaphthyl (25 mg, 0.04 mmol) was placed in an 8 mm NMR tube and degassed. An 8:1 mixture of distilled, degassed ethanol and toluene (2.8:0.3 ml) was added *via* cannula and the contents of the NMR tube were heated at 50-55°C in blocks of 15 min. Every 15 min, the NMR tube was allowed to cool, placed in a 10 mm NMR tube with D_2O in the interannular space and a ^{31}P NMR was obtained (101.23 MHz). The process was continued until the first traces of impurity started to form (doublets at 55.4, 60.3 J=42 Hz which appeared after 1.5h). The solution was then filtered through a celite pad and the solvent removed *in vacuo* to yield the product as a brown powder[64] (12 mg, 69%); δ_P(202.46 MHz, $CDCl_3$) 31.0(d, J=63 Hz) and 39.1(d, J=63 Hz); *m/z* (ES) 837(M^+, 100%), correct isotope pattern for ruthenium.

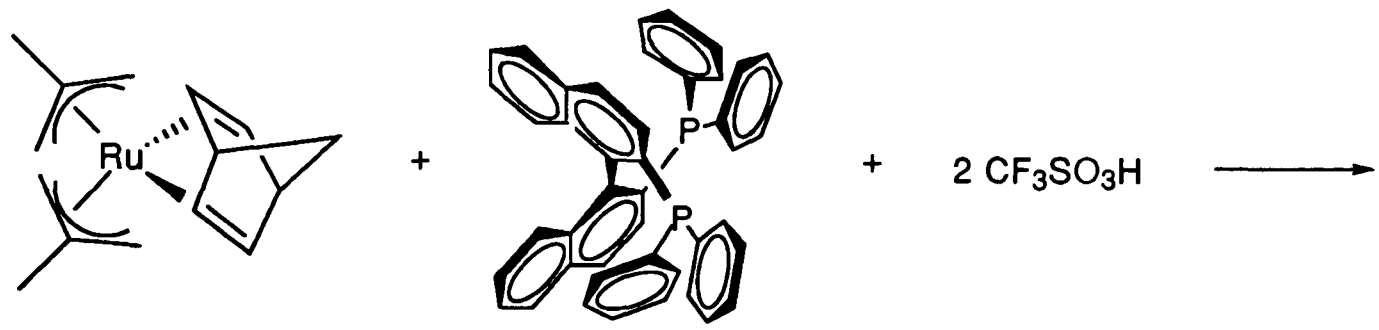
Modification of bis(trifluoroacetato)[(R)-2,2'-bis(diphenylphosphino)-1,1'-binaphthyl]ruthenium II



Trimethylsilyl trifluoromethanesulphonate (30 µl, excess) was added to a 5 mm NMR tube containing a thoroughly degassed solution of bis(trifluoroacetato)[(R)-2,2'-bis(diphenylphosphino)-1,1'-binaphthyl]ruthenium II (15 mg, 0.016 mmol) in $CDCl_3$.

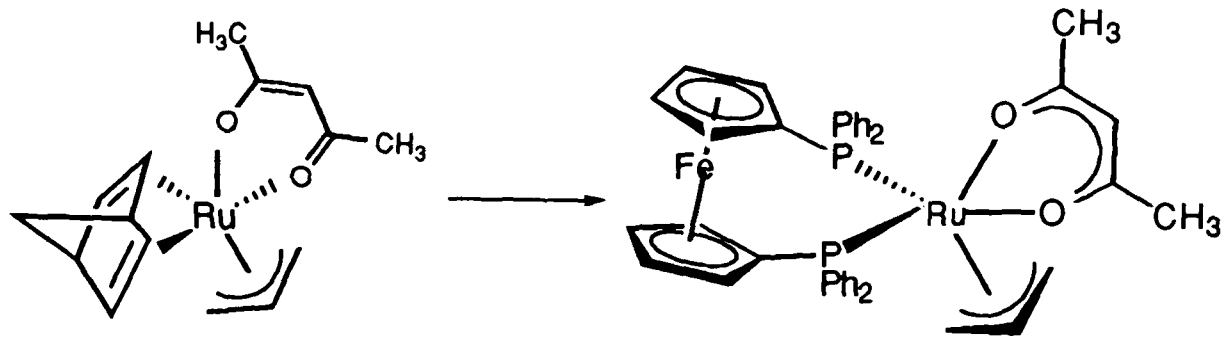
The initially yellow coloured solution immediately turned dark red on the addition of the trimethylsilyl trifluoromethanesulphonate. ^{31}P NMR (202.46 MHZ) showed four broad signals (δ 81.4, 75.9, 7.4, 0.8 ppm) and one narrow singlet (δ 54.3 ppm). When the reaction was carried out using two equivalents of TMSTfO, it was found that there were two broad peaks in the ^{31}P NMR spectrum, δ 75.1 and 7.9 ppm, which were accompanied by an intense singlet at -2.1 ppm. The structure of this catalyst is unknown; mass spectrometry investigations yielded a peak corresponding to RuP_2TfO.

Modification of bis(trifluoroacetato)[(R)-2,2'-bis(diphenylphosphino)-1,1'-binaphthyl]ruthenium II



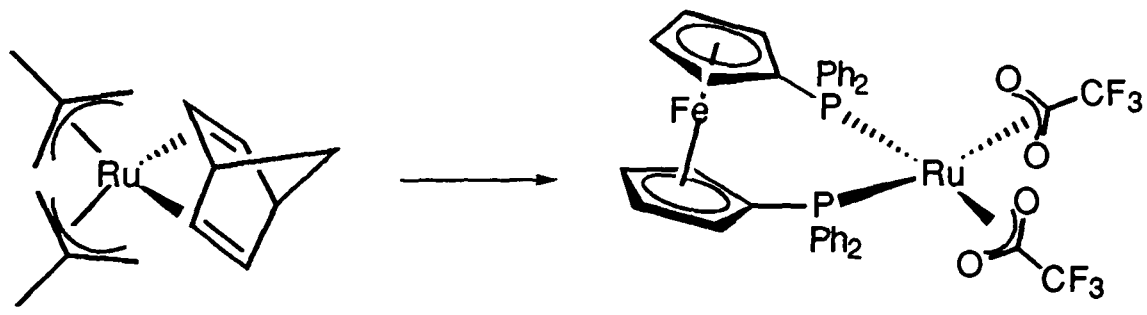
(R)-2,2'-Bis(diphenylphosphino)-1,1'-binaphthyl (25 mg, 0.4 mmol) in the minimum amount of distilled, degassed dichloromethane was added *via* cannula to an 8 mm NMR tube containing thoroughly degassed (η^4-bicyclo[2.2.1]hepta-2,5-dienyl) bis-(η^3-2-methylpropenyl) ruthenium II (12 mg, 0.4 mmol), methanol and triflic acid (70 µl, 0.8 mmol). The initially yellow solution turned dark red immediately and ^{31}P NMR (101.23 MHz) showed the existence of two pairs of double doublets (δ 74.5, 1.5 ppm, J=52 Hz and δ 38.7, 37.6 ppm, J=34 Hz). Once again, the structure of this catalyst is unknown. Electrospray mass spectrometry showed a peak corresponding to RuP_2TfO.

1,1'-Bis(diphenylphosphino)ferrocene (η³-propenyl)(acetylacetonato)ruthenium II



(η⁴-Bicyclo[2.2.1]hepta-2,5-dienyl) (η³2-propenyl)(acetylacetonato) ruthenium II (60 mg, 0.18 mmol) and 1,1'-bis(diphenylphosphino)ferrocene (100 mg, 0.18 mmol) were degassed in a two-necked Schlenk fitted with a cold finger. The minimum amount of freshly distilled, degassed tetrahydrofuran was added *via* cannula (1 ml) and then the contents of the Schlenk were degassed again. The orange mixture was refluxed overnight to yield a dark orange solution[38]. The toluene was removed *in vacuo* and the residue washed with degassed pentane to give the title compound as a yellow powder (143 mg, 100%); δ_P(101.23 MHz, THF) 62.6(d, J=35.0 Hz), 27.0(d, J=35.0 Hz); *m/z* (ES) 796($M+H^+$, 100%), correct isotope pattern for ruthenium.

Bis(trifluoroacetato)[1,1'-Bis(diphenylphosphino)ferrocene] ruthenium II



A solution of 1,1'-bis(diphenylphosphino)ferrocene (45 mg, 0.08 mmol) in the minimum amount of degassed dichloromethane was added, *via* cannula, to a Schlenk containing a yellow solution of (η⁴-bicyclo[2.2.1]hepta-2,5-dienyl) bis-(η³-2-methylpropenyl) ruthenium II (23 mg, 0.08 mmol) and freshly distilled, degassed trifluoroacetic acid (13 μl, 0.17 mmol, degassed by purging with nitrogen) in the minimum amount of degassed

methanol. The contents of the Schlenk were degassed again and then stirred at room temperature overnight[69]. Removal of the solvent *in vacuo* led to the product as a yellow solid (70 mg, 100%); δ_P(101.23 MHz, CH_2Cl_2) 56.94; *m/z* (ES) 820($M+H^+$ - $2CF_3CO_2^-$ + 4 MeCN, 100%) correct isotope pattern for ruthenium.

General method for hydrogenations using the constant volume apparatus, exemplified by Ru(BINAP)(allyl)(acac) catalysed reductions.

The required amount of catalyst (10 μmol) was weighed out and degassed in a small schlenk. The solid was then dissolved in freshly distilled, degassed CH_2Cl_2 (1 ml) and activated by the addition of two equivalents of TMSTfO under argon. Activation was achieved by stirring for 15 mins, during which time a colour change from yellow to orange was observed. Removal of the CH_2Cl_2 *in vacuo*, yielded the activated catalyst as a yellow/brown oil. This was then dissolved in freshly distilled, degassed methanol to form a stock solution of catalyst and kept under argon at -78°C until required.

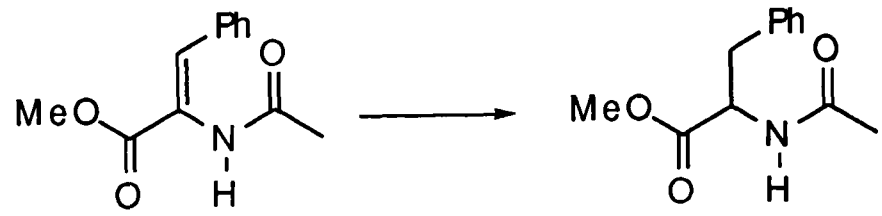
A stock solution of substrate (0.5 mmol) in degassed methanol (2.5 ml) was also prepared and then 500 μl substrate solution (0.1 mmol), a known volume of catalyst solution (usually between 0.5 and 2.5 mol%) and enough degassed methanol to make the total volume up to 1.0 ml were placed in the reaction vessel of the constant volume apparatus (described earlier) under a stream of argon. The reaction vessel was cooled to -78°C (CO_2/acetone) and the apparatus was evacuated to below 0.1 mbar. It was then filled with argon to a pressure of approximately 1100 mbar (recording pressures on the microcomputer using ADDH2) and the freeze-pump-thaw technique was repeated a further five times before the entire apparatus was filled with hydrogen to a pressure of approximately 1000 mbar.

The reaction mixture was then subjected to another six freeze-pump-thaw degas cycles using hydrogen in place of argon and at the end of the final cycle the hydrogen pressure was set to approximately 150 mbar below the required pressure (i.e. usually set to 1450 mbar) and the apparatus sealed.

The reaction vessel was warmed to the required temperature (25°C or 0°C) and kept at that temperature with the aid of a water circulator fitted with a thermostat. When the pressure in the apparatus had stabilised to within 0.5 mbar (over approximately a 2 min period), a magnetic stirrer, which was preset to a constant speed, was placed under the reaction vessel and sampling of the reaction vessel pressure (at 5s intervals for fast reactions and longer times for slower reactions) was commenced with the computer programme $ADDH_2$. Sampling was continued until the pressure in the reaction vessel had stabilised to within 0.5 mbar.

The hydrogenation procedure was then repeated for each substrate, using different catalyst concentrations, substrate concentrations and variations in the initial pressure of hydrogen.

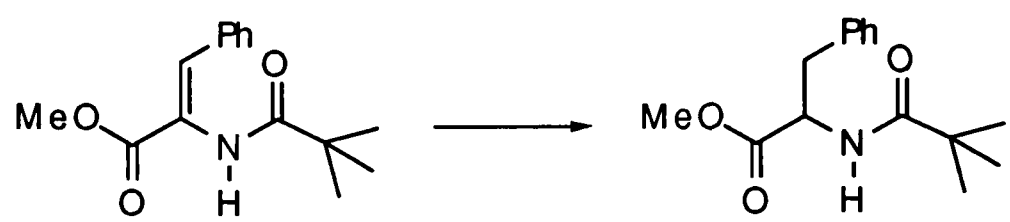
Hydrogenation of Z-methyl-2-acetylamino-3-phenylpropenoate.



Samples of Z-methyl-2-acetylamino-3-phenylpropenoate (21.9 mg, 0.10 mmol) were hydrogenated under the conditions described above using different amounts of catalyst (0.5-2.5 mol%). The dark red enamide complex went pale yellow on hydrogenation. The work-up procedure involved filtering through celite and purification *via* preparative T.L.C (eluant: hexane/ethyl acetate 3:1) to yield methyl-2-acetylamino-3-phenylpropanoate as a white powder, m.p. 83-85°C; υ_{max}/cm^{-1}(KBr) 3336(N-H), 1755(ester C=O) and 1651, 1537(amide C=O); δ_H(500 MHz, $CDCl_3$) 1.98(3H, s, CH_3), 3.10(1H, dd, J_1=13.84, J_2=5.65 Hz, CH_2), 3.15(1H, dd, J_1=13.88, J_2=5.86 Hz, CH_2), 3.73(3H, s, CH_3O), 4.89(1H, dt, J_1=4.58, J_2=6.66 Hz, CH), 5.93(1H, d, J=6.31 Hz, NH) and 7.10-7.31(5H, m, Ph); δ_C(50.3 MHz, $CDCl_3$) 23.00(CH_3CO), 37.83(CH_2), 52.18(CH_3O), 53.09(CH), 127.05(*p*), 128.52(*m*), 129.17(*o*), 135.85(*ipso*), 169.54(amide C=O) and 172.07(ester C=O); *m/z* (CI) 222(M^++1, 88%),

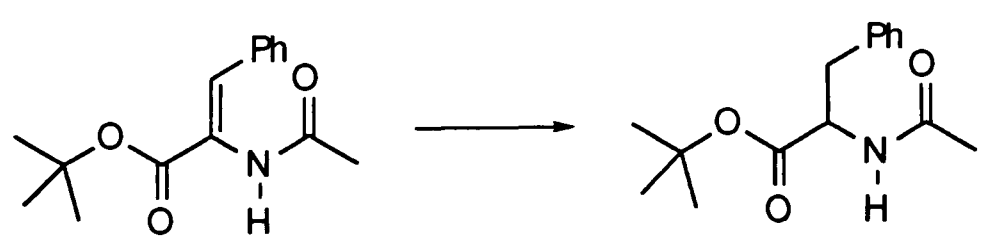
135.85(*ipso*), 169.54(amide C=O) and 172.07(ester C=O); *m/z* (CI) 222(M^++1, 88%), 190(M^+-CH_3O, 12), 163(M^+-CH_3CONH, 17), 162(M^+-CO_2CH_3, M^+-$CH_3C(OH)NH$, 100), (120, 35), 91($C_7H_7^+$, 93), 88(43) and 65($C_5H_5^+$, 22).

Hydrogenation of Z-methyl-2-trimethylacetyl-3-phenylpropenoate.



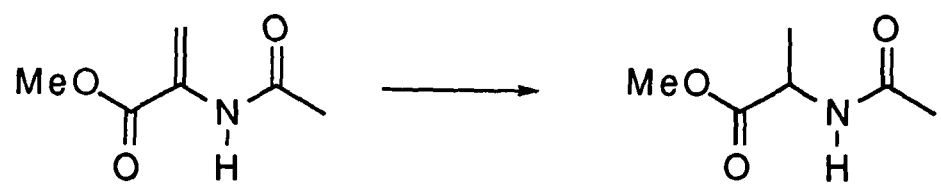
Samples of Z-methyl-2-trimethylacetylamino-3-phenylpropenoate (26.1 mg, 0.10 mmol) were hydrogenated under the conditions described earlier using different amounts of catalyst (0.5-2.5 mol%). The dark red enamide complex went pale yellow on hydrogenation. The work-up procedure involved filtering through celite and purification *via* preparative T.L.C (eluant: hexane/ethyl acetate 3:1) to yield methyl-2-trimethylacetylamino-3-phenylpropanoate as a white powder, m.p. 87-90°C; υ_{max}/cm^{-1}(KBr) 3326(N-H), 1748(ester C=O) and 1606, 1541(amide C=O); δ_H(500 MHz, $CDCl_3$) 1.15(9H, s, ^tBu), 3.10(1H, dd, J_1=13.82, J_2=5.76 Hz, CH_2), 3.18(1H, dd, J_1=13.83, J_2=5.83 Hz, CH_2), 3.74(3H, s, CH_3), 4.86(1H, ddd, J_1=5.80, J_2=5.80, J_3=7.63 Hz, CH), 6.04(1H, d, J=5.06 Hz, NH), 7.09(2H, m, *m*) and 7.27-7.30(3H, m, *o&p*); δ_C(50.3 MHz, $CDCl_3$) 27.62($C(CH_3)_3$), 38.09($C(CH_3)_3$), 52.50(CH_2), 53.15(CH_3), 76.78(CH), 127.40(*o*), 128.77(*m*), 129.60(*p*), 136.28(*ipso*), 172.61(amide C=O) and 178.16(ester C=O); *m/z* (CI) 264(M^++1, 100%), 232(M^+-CH_3O, 11), 204(M^+-CO_2CH_3, 13), 162(M^+-$^tBuC(OH)NH$, 82), 91($C_7H_7^+$, 53), 85(^tBuCO, 27), 65($C_5H_5^+$, 8) and 57(^tBu, 95).

Hydrogenation of Z-tertbutyl-2-acetylamino-3-phenylpropenoate.



Samples of Z-*tert*-butyl-2-acetylamino-3-phenylpropenoate (26.1 mg, 0.10 mmol) were hydrogenated under the conditions described earlier using different amounts of catalyst (0.5-2.5 mol%). The dark red enamide complex went pale yellow on hydrogenation. The work-up procedure involved filtering through celite and purification *via* preparative T.L.C (eluant: hexane/ethyl acetate 3:1) to yield *tert*butyl-2-acetylamino-3-phenylpropanoate as a colourless oil; υ_{max}/cm^{-1}(NaCl) 3294(N-H), 1733(ester C=O) and 1653, 1541(amide C=O); δ_H(500 MHz, $CDCl_3$) 1.41(9H, s, ^tBu), 1.98(3H, s, CH_3), 3.09(2H, d, J=5.98 Hz, CH_2), 4.76(1H, dt, J_1=6.53, J_2=7.68 Hz, CH), 5.97(1H, d, J=7.12 Hz, NH) and 7.14-7.30(5H, m, Ph); δ_C(50.3 MHz, $CDCl_3$) 23.10(CH_3), 27.89(C(CH_3)$_3$), 38.07(CH_2), 53.51(CH), 82.26(C(CH_3)$_3$), 126.88(*p*), 128.28(*m*), 129.43(*o*), 136.22(*ipso*), 169.39(amide C=O) and 170.81(ester C=O); *m/z* (CI) 264(M^++1, 40%), 208(100), 207(M^+-CH_2C=C(CH_3)$_2$, 22), 162(M^+-$CO_2{}^tBu$, 18), 148(30), 120(42), 91($C_7H_7^+$, 30), 65($C_5H_5^+$, 5) and 57(^tBu, 27).

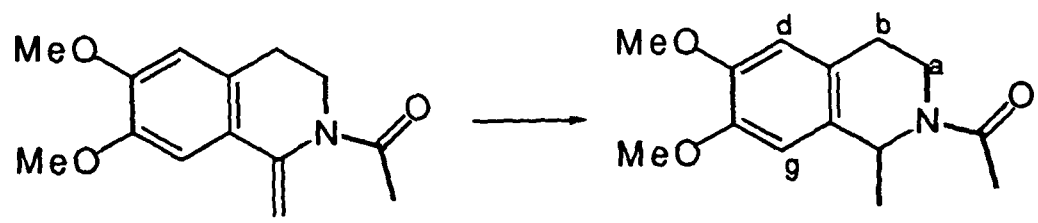
Hydrogenation of methyl-2-acetylaminopropenoate.



Samples of methyl-2-acetylaminopropenoate (14.3 mg, 0.10 mmol) were hydrogenated under the conditions described earlier using different amounts of catalyst (0.2-0.3 mol%). The enamide complex was a very pale yellow and there was no observable colour change on hydrogenation. The work-up procedure involved filtering through celite and purification *via* preparative T.L.C (eluant: hexane/ethyl acetate 3:1) to yield methyl-2-amino-3-phenylpropanoate as a yellow solid, m.p. 35°C; υ_{max}/cm^{-1}(NaCl) 3292(N-H), 1740(ester C=O), and 1652, 1541(amide C=O); δ_H(500 MHz, $CDCl_3$) 1.34(3H, d, J=7.24 Hz, CH_3CH), 1.95(3H, s, CH_3C=O), 3.68(3H, s, CH_3O), 4.52(1H, dq, J_1= 7.28, J_2=7.28 Hz, CH) and 6.45(1H, br. s, NH); δ_C(50.3 MHz, $CDCl_3$) 17.81(CH_3CH), 22.65(CH_3C=O), 47.91(CH_3O), 52.23(CH), 170.38(amide C=O) and

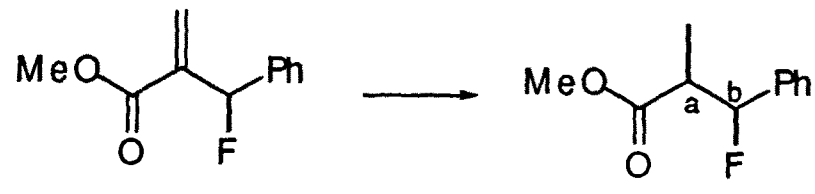
173.95(ester C=O); *m/z* (CI) 146(M^++1, 100%), 104(22), 102(M^+-CH_3O, 4), 87(M^+-CH_3CONH, 7) and 86(M^+-CO_2CH_3, M^+-$CH_3C(OH)NH$, 87).

Hydrogenation of 2-acetyl-6,7-dimethoxy-1-methylene-1,2,3,4-tetrahydroisoquinoline



Samples of 2-acetyl-6,7-dimethoxy-1-methylene-1,2,3,4-tetrahydroisoquinoline (24.7 mg, 0.10 mmol) were hydrogenated under the conditions described earlier using different amounts of catalyst (0.2-0.3 mol%). The solution was pale yellow both before and after hydrogenation. The work-up procedure involved filtering through celite and purification *via* preparative T.L.C (eluant: pentane/ethyl acetate 3:1) to yield 2-acetyl-6,7-dimethoxy-1-methyl-1,2,3,4-tetrahydroisoquinoline as a yellow solid, δ_H(500 MHz, $CDCl_3$) 1.49 and 1.53(3H, d, J=6.8 Hz, CH_3CH), 2.14 and 2.23(3H, s, CH_3CO), 2.61-3.04(2H, m, H_b), 3.50-3.58 and 3.82-3.85(2H, m, H_a), 3.88(3H, s, CH_3O), 3.92(3H, s, CH_3O), 4.62-4.93 and 5.57(1H, m, q, J=6.8 Hz, methyne), 6.60(1H, s, H_d) and 6.72(1H, s, H_g).

Hydrogenation of methyl-2-fluorophenylmethyl propenoate



Samples of methyl-2-fluorophenylmethyl propenoate (19.4 mg, 0.10 mmol) in degassed 1,2-dichloroethane (1-2 ml) were hydrogenated using different amounts of ruthenium catalyst (2.5-5 mol%) in an autoclave or Fischer Porter bottle with starting pressures of 7-10 atm. The solution was pale yellow both before and after hydrogenation. The percentage conversion and the *anti/syn* product ratio was determined by NMR (AMX

500MHz) anti δH_a 5.75 ppm, $^2J_{H\text{-}F}$ = 46 Hz, $^3J_{H\text{-}H}$ = 7 Hz, δH_b 2.92, $^3J_{H\text{-}F}$ = 23 Hz; syn δH_a 5.55 ppm, $^2J_{H\text{-}F}$ = 46 Hz, $^3J_{H\text{-}H}$ = 9 Hz, δH_b 3.04 ppm, $^3J_{H\text{-}F}$ = 9 Hz.

Kinetic analysis of hydrogenation reactions.

Data from hydrogenations was stored as *pt* data using the programme $ADDH_2$[51]. ITR files were then created using the computer programmme MAKEITR[54]. This file contained initial concentrations of the model species together with the experimental data, which was converted into concentrations of product with time. The files were then reduced in size to about fifty points by removing points from the less important straight-line region of the plots, whilst keeping all the data which corresponded to the curved region of the plots.

Next the modelling programme GIT was run, using a GEAR file containing the model rate constants (with rates of interest marked as variable) for each of the runs from the set of five obtained from hydrogenating each substrate. GIT modelled the experimental data against the theoretical data and gave a value for the optimum deviation between the two. The best values for the rate constants were found by initially guessing their values and running GIT. Guesses were deliberately set low because the iterating programme altered rate constants by a percentage of their value and thus a larger change in these constants could be achieved. This allowed the programme to 'escape' from local minima. GIT was allowed to optimise the variable rate constants to produce a best fit and the value for the average deviation was noted. The process was then repeated with different initial values for the variable rate constants until the lowest average deviation was obtained. Values of k were then obtained for the sets of data combined, keeping all other rates constant and iterating on k only.

^{31}P NMR studies: observation of bound enamide complexes.

A sample of catalyst (10 μmol) was weighed out and degassed. 300μl freshly distilled, degassed CD_3OD was added under argon, using a 500 μl syringe, to the catalyst sample

and once dissolution was complete, the catalyst solution was transferred, *via* cannula, to an NMR tube.

The required amount of degassed substrate in 300 μl degassed CD_3OD was then added to the NMR tube which was sealed under argon and transferred to a precooled NMR probe (202.46 MHz). Cooling was achieved using liquid nitrogen; at observation temperatures below the dewpoint (roughly -60°C), nitrogen gas was used to spin the sample.

After allowing 10 minutes for the NMR tube and its contents to equilibrate, the sample was shimmed and acquisition was begun.

References

1. R. M. Hanson, J. M. Klunder, S. Y. Ko and K. B. Sharpless, *J. Am. Chem. Soc.*, 1987, **109**, 5765; W. Zhang, J. L. Loebach, S. R. Wilson and E. N. Jacobsen, *J. Am. Chem. Soc.*, 1990, **112**, 2801.
2. J. S. M. Wai, I. Markó, J. S. Svensden, E. N. Jacobsen and K. B. Sharpless, *J. Am. Chem. Soc.*, 1989, **111**, 1123; 1988, **110**, 1968.
3. S. Inoue, H. Takaya, K. Tani, S. Otsuka, T. Sato and R. Noyori, *J. Am. Chem. Soc.*, 1990, **112**, 4897; *J. Chem. Soc., Chem. Commun.*, 1982, 600.
4. J. M. Brown, *Angew. Chem., Int. Ed. Engl.*, 1987, **26**, 190.
5. L. Horner, H. Siegel and H. Büthe, *Angew. Chem.*, 1968, **80**, 1034.
6. W. S. Knowles and M. J. Sabaky, *J. Chem. Soc., Chem. Commun.*, 1968, 1445.
7. J. A. Osborne, F. H. Jardine, Y. F. Yang and G. Wilkinson, *J. Chem. Soc.*, 1966, 1711.
8. H. B. Kagan, *Bull. Soc. Chim. Fr.*, 1988, 846.
9. a) W. S. Knowles, M. J. Sabaky and B. D. Vineyard, *J. Am. Chem. Soc.*, 1976, **98**, 2134; 3143.
   b) J. M. Brown and P. A. Chaloner, *J. Am. Chem. Soc.*, 1980, **102**, 3040.
   c) H. Brunner, Top. Stereochem., 1988, **18**, 129.
10. J. Halpern, *Asymmetric Synthesis Vol 5*, Academic Press, Orlando USA, 1985.
11. a) T. P. Dang and H. B. Kagan, *J. Chem. Soc., Chem. Commun.*, 1971, 481.
    b) T. P. Dang and H. B. Kagan, *J. Am. Chem. Soc.*, 1972, **94**, 6429.
12. M. Nógrádi, *Stereoselective Synthesis*, VCH, Weinheim, 1986, p.53.
13. K. E. Koenig, G. L. Bachman and B. D. Vineyard, *J. Org. Chem.*, 1980, **45**, 2362.
14. J. M. Brown, R. Glaser, P. A. Chaloner and S. Geresch, *Tetrahedron*, 1980, **36**, 815; J. M. Brown and D. Parker, *J. Org. Chem.*, 1982, **47**, 2722.

15. C. Detellier, G. Gelbard and H. B. Kagan, *J. Am. Chem. Soc.*, 1978, **100**, 7556; K. Koenig and W. S. Knowles, *J. Am. Chem. Soc.*, 1978, **100**, 7561; M. J. Burke, J. E Feaster, W. A. Nugent and R. L. Harlow, *J. Am. Chem. Soc.*, 1993, **115**, 10125.

16. C. R. Landis and J. Halpern, *J. Am. Chem. Soc.*, 1987, **109**, 1746.

17. J. M. Brown and P. A. Chaloner, *J. Chem. Soc., Perkin Trans. II*, 1987, 1583; *J. Chem. Soc., Chem. Commun.*, 1983, 644.

18. M. D. Fyzuk and B. Bosnich, *J. Am. Chem. Soc.*, 1977, **99**, 6262.

19. J. M. Brown and P. A. Chaloner, *J. Chem. Soc., Chem. Commun.*, 1980, 344.

20. B. Bosnich and J. Halpern, *J. Chem. Soc., Chem. Commun.*, 1981, 1278.

21. A. S. C. Chan, J. J. Pluth and J Halpern, *Inorg. Chim. Acta*, 1979, **37**, L477.

22. J Halpern, *Organometallics*, 1990, **9**, 1392.

23. B. R. Bender, personal communication.

24. H. Bircher, B. R. Bender, W Von Phillipsborn, *Magn. Res. in Chem.*, 1993, **31**, 293.

25. a) J. M. Brown, L. R. Canning, A. J. Downs and A. M. Forster., *J. Organomet. Chem.*, 1983, **255**, 103.
b) M. S. Chinn and R. Eisenberg, *J. Am. Chem. Soc.*, 1992, **114**, 1908; S. B. Duckett, C. L. Newell and R. Eisenberg, *J. Am. Chem. Soc.*, 1993, **115**, 1156; 1994, **116**, 10548.

26. J. S. Giovannetti, C. M. Kelly and C. R. Landis, *J. Am. Chem. Soc.*, 1993, **115**, 4040.

27. G. J. Kubas, *Acc. Chem. Res.*, 1988, **21**, 120 and references cited therein.

28. A. S. C. Chan and J. Halpern, *J. Am. Chem. Soc.*, 1980, **102**, 836; 5952.

29. J. M. Brown and P. J. Maddox, *J. Chem. Soc., Chem. Commun.*, 1987, 1276.

30. A. L. Sargent, M. B. Hall and M. F. Guest, *J. Am. Chem. Soc.*, 1992, **114**, 517.

31. U. D. Sharma, Part II Thesis, University of Oxford, 1993.

32. J. A. Osborn and R. R. Schrock, *J. Chem. Soc., Chem. Commun.*, 1970, 567.

33. S. Otsuka, K. Tani and Y. Tatsuno, *Chem. Lett.*, 1986, 737.

34a. S. Otsuka, K. Tani and Y. Tatsuno, *J. Organomet. Chem.*, 1985, **279**, 87.

34b. C. Hatat, A. Karim, N. Kokel, A. Mortreux and F. Petit, *New J. Chem.*, 1990, **14**, 141.

35. R. Noyori, T Ohta and H. Takaya, *Inorg. Chem.*, 1988, **27**, 566 and references therein.

36. Y. Hsiao, R. Noyori, T Ohta and H. Takaya, *J. Am. Chem. Soc.*, 1986, **108**, 7117.

37. a) A. Curra, A. Macchioni, R. Nesper and P. Pregosin, *Helv. Chim. Acta*, 1996, **79**, 1587.

b) M. T. Ashby and J. Halpern, *J. Am. Chem. Soc.*, 1991, **113**, 589.

38. N. W. Alcock, J. M. Brown, M. Rose and A. Wienand, *Tet. Asymm.*, 1991, **2**, 47; J. M. Brown, F. I. Knight, M. Rose and A. Wienand, *Recueil Des Travaux Chimiques Des Pay Bas*, 1995, **114**, 242.

39. Y. Amrani, J. Bakos, B. Heil, L. Lecomte, D. Sinon and I. Toth, *Organometallics*, 1989, **8**, 542.

40. a) R. Noyori, T. Ohta and H. Takaya, *Tet. Lett.*, 1990, **31**, 7189.

b) C. L. Newell and R. Eisenberg, *Abstacts. Am. Chem. Soc.*, 1994, **208**, 604INOR;1995, **210**, 148INOR.

41. M. Kitamura, R. Noyori, T. Okhuma, T Ohta and H. Takaya, *J. Am. Chem. Soc.*, 1988, **110**, 629.

42. M. Kitamura, R. Noyori and T. Okhuma, *J. Am. Chem. Soc.*, 1987, **109**, 5856.

43. S. A. King, A. S. Thompson and T. R. Verheoven, *J. Org. Chem.*, 1992, **57**, 6689.

44. T. Ikariya, R. Noyori and T. Okhuma, *J. Am. Chem. Soc.*, 1995, **117**, 2675.

45. M. Kitamura, R. Noyori and H. Takaya, *J. Am. Chem. Soc.*, 1989, **111**, 9143.

46. R. Noyori and H. Takaya, *Acc. Chem. Res.*, 1990, **23**, 345.

47. S. J. Danishefsky and A. Villalobos, *J. Org. Chem.*, 1990, **55**, 2776.

48. M. Kitamura, I. Kasahara, K. Manabe, R. Noyori and H. Takaya, *J. Org. Chem.*, 1988, **53**, 708.

49. *Organic Syntheses Collective Vol II,* Wiley, New York, 1946, p.1 and p.11.

50. J. M. Brown, P. L. Evans and A. P. James, *Organic Syntheses,* 1990, **68**, 64.

51. D. W. Price, D. Phil Thesis, University of Oxford, 1992.

52. H. C. Yao and P. H. Emmett, *J. Am. Chem. Soc.*, 1959, **81**, 4125.

53. N. Stabler and J. Chesick, *Int. J. Chem. Kinet.*, 1978, **10**, 461; F. Weigert, *Comput. Chem.*, 1987, **11**, 273.

54. T. Katayama and T. Nitta, *J. Chem. Eng. Data*, 1976, **21**, 194; C. L. Young, *Solubility Data Series*, Ed Permagon Press, Oxford, 1981.

55. U. Berens and R. Selke, *Tet. Asymm.*, 1996, **7**, 2055.

56. J. M. Brown and P. A. Chaloner, *J. Chem. Soc., Perkin Trans. II*, 1987, 1583.

57. J. M. Brown and P. J. Maddox, *J. Chem. Soc., Chem. Commun.*, 1987, 1276.

58. J. M. Brown, M. B. Hursthouse, A. I. Karalulov and J. A. Ramsden, *Tet. Asymm.*, 1994, **5**, 2033.

59. J. M. Brown, T. W. Claridge and J. A. Ramsden, *J. Chem. Soc., Chem. Commun.*, 1995, 2469.

60. T. Imamoto, T. Kusumoto, T. Oshiki and K. Sato, *J. Am. Chem. Soc.*, 1990, **112**, 5244.

61. A. Karim, A. Mortreux and F. Petit, *J. Organomet. Chem.*, 1986, **317**, 93.

62. M. J. Burke, G. P. Harper and C. S. Calberg, *J. Am. Chem. Soc.*, 1995, **117**, 4423; E. Cesarotti, F. Demartin, T. Pilati and F. Sannicolo, *J. Org. Chem.*, 1996, **61**, 6244

63. J. P. Genet, C. Pinel and J. A. Laffitte, *Tet. Asymm.*, 1994, **5**, 665.

64. K. Mashima, N. Sato and H. Takaya, *J. Org. Chem.*, 1994, **59**, 3064.

65. D. D. Perrin and W. L. F. Armarego, *Purification of Laboratory Chemicals,* Pergamon Press, Oxford, 3rd Ed.

66. D. F. Shriver, *The Manipulation of Air Sensitive Compounds*, McGraw-Hill, London, 1969.

67. K. V. Baker, J. M. Brown, N. Hughes, A. J. Skarnulis and A. Sexton, *J. Org. Chem.*, 1991, **56**, 698.

68. A. S. C. Chan and S. Laneman, *Inorg. Chimica Acta,* 1994, **223**, 165.

69. B. Heiser, E. A. Broger and Y. Crameri, *Tet. Asymm.*, 1991, **2**, 51.

70 G. A. Brossi, L. A. Dolan and S. Teitel, *Organic Syntheses,* **56**, 3.

71. D. Parker, D. Phil. Thesis, University of Oxford, 1980.

72. J. M.Brown, M. Comes Franchinni and U. D. Sharma, in press; R. Batra, B. Giese and C. Hassler, *Tet. Lett.*, 1995, **36**, 7639.

73. M. Kitamura, R. Noyori, T. Okhuma, T Ohta and H. Takaya, *J. Org. Chem.*, 1987, **50**, 3174.

74. W. L. Still, M. Kahn and A. Mitra, *J. Org. Chem.*, 1978, **43**, 2923.

75. A. T. Vogel, *A Textbook of Practical Organic Chemistry*, VCH, Weinheim, 1956, p.584.

76. J. Chatt and L. M. Venanzi, *J. Chem. Soc.*, 1957, 4735.

77. M. Green, T. A. Kuk and S. H. Taylor, *J. Chem. Soc.(A),* 1971, 2334.

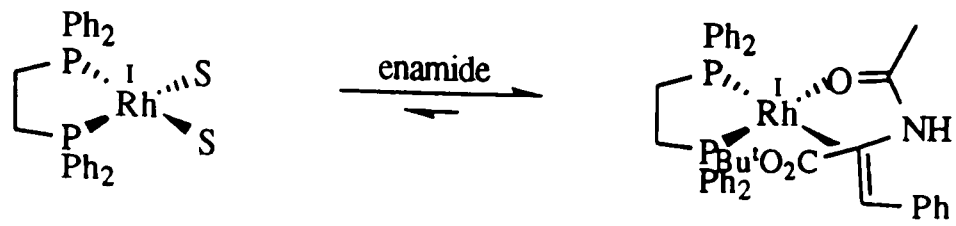
78. E. W. Abel, M. A. Bennett and G. Wilkinson, *J. Chem. Soc.*, 1959, 3178.

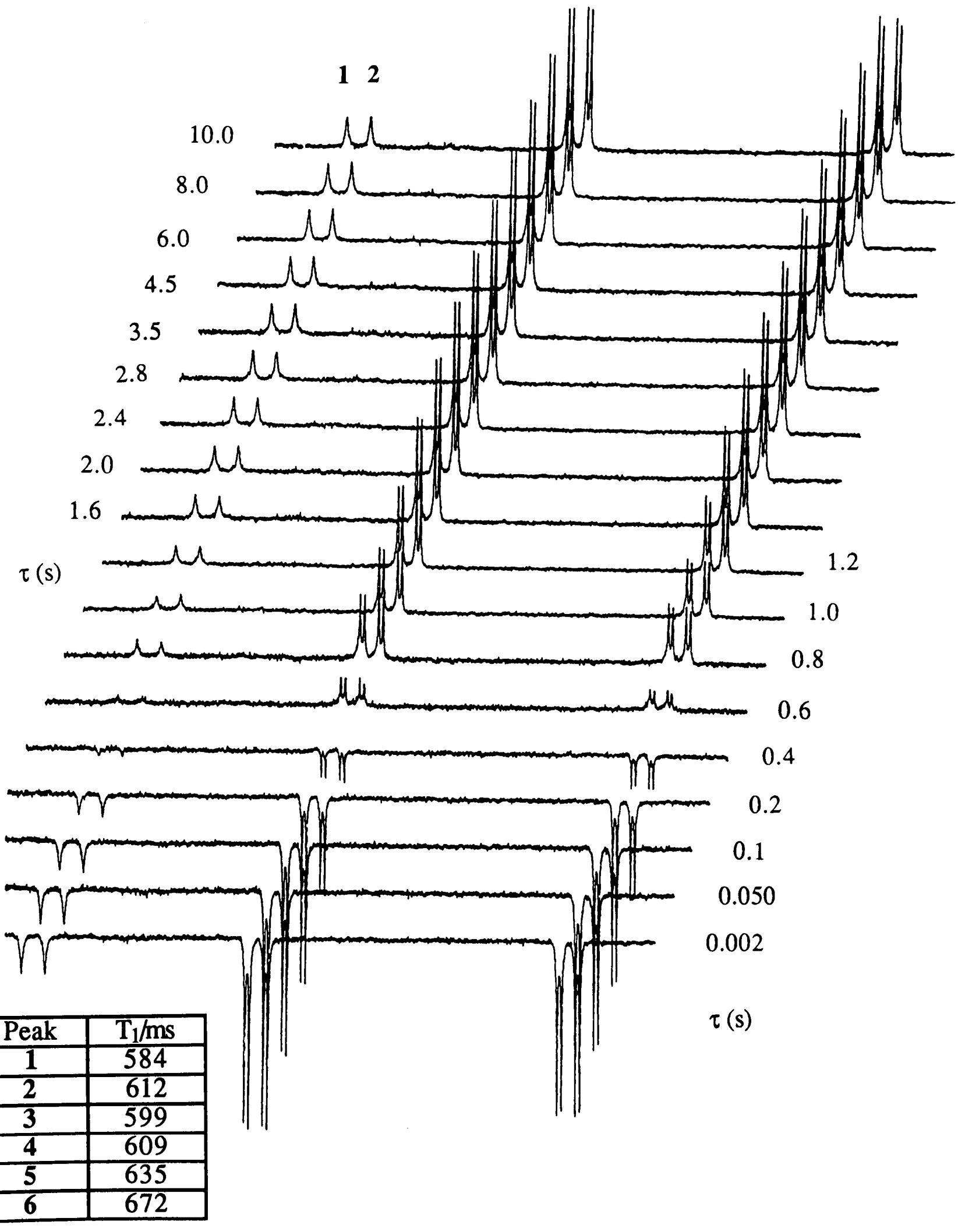
79. M. O. Albers, E. Singleton and J. E. Yates, *Inorganic Syntheses,* 1989, **26**, 249.

80. J. Dauben, L. R. Honnen and K. M. Harmon, *J. Org. Chem.*, 1960, **25**, 1442.

81. R. R. Schrock, B. F. G. Johnson and J. Lewis, *J. Chem. Soc. (Dalton Trans.)*, 1974, 951.

Appendix 1

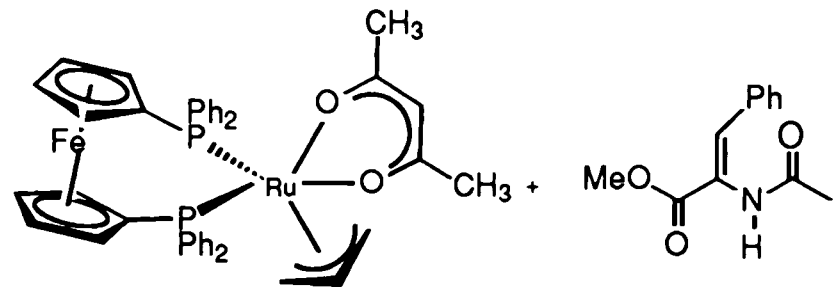


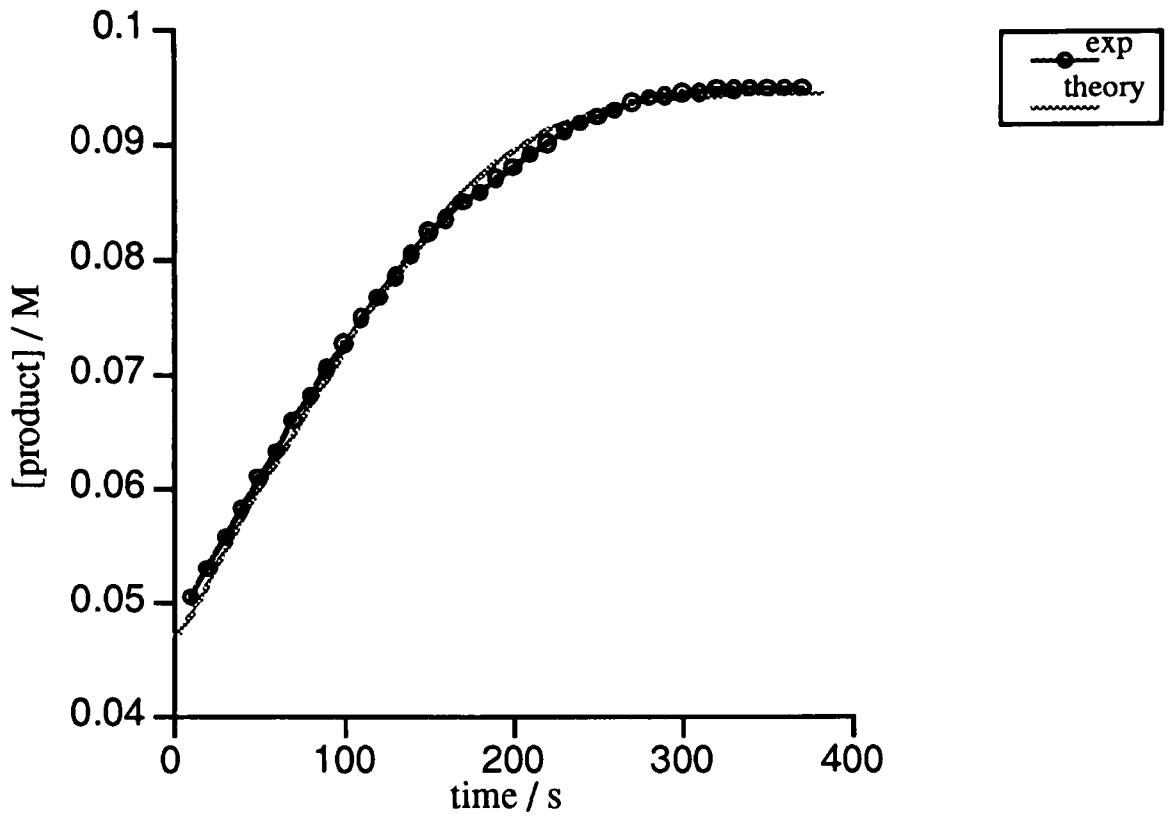


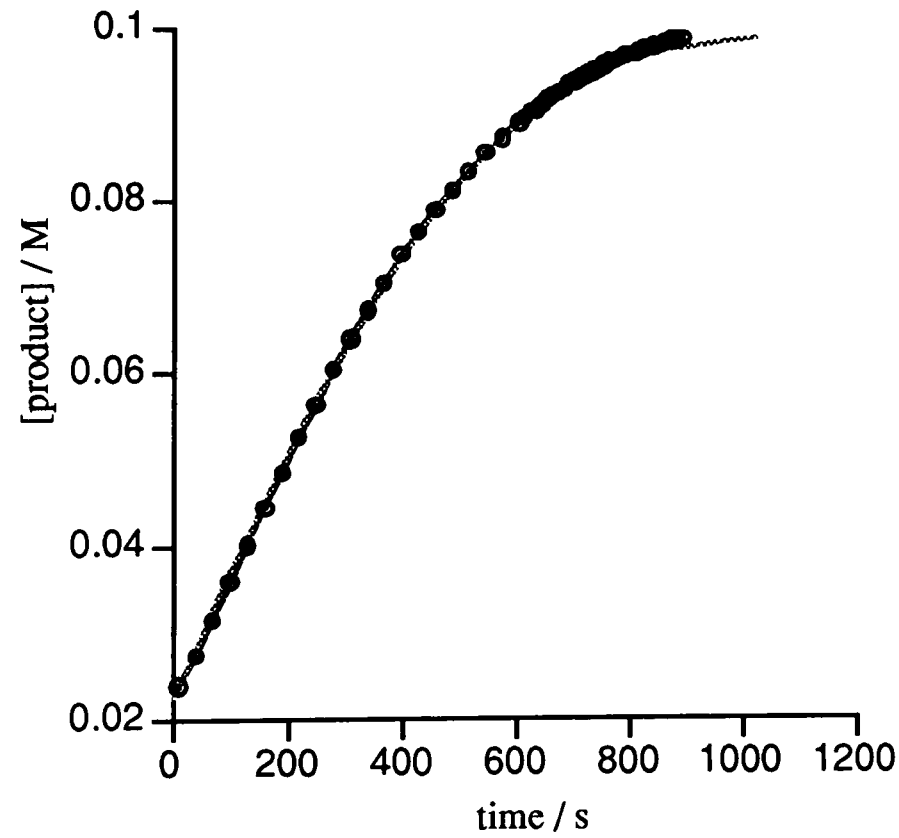
Peak	T_1/ms
1	584
2	612
3	599
4	609
5	635
6	672

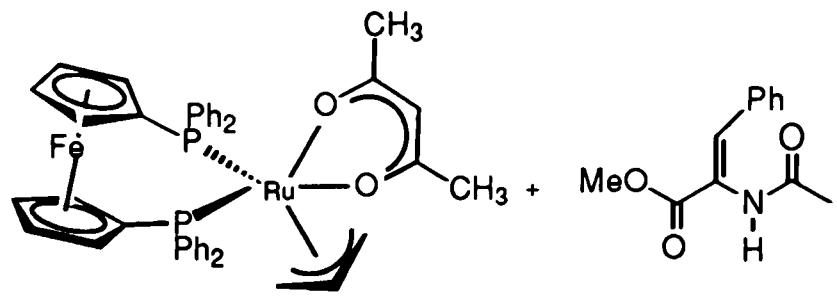
T_1 measurements for the solvate complex and the enamide complex of compound **6**.

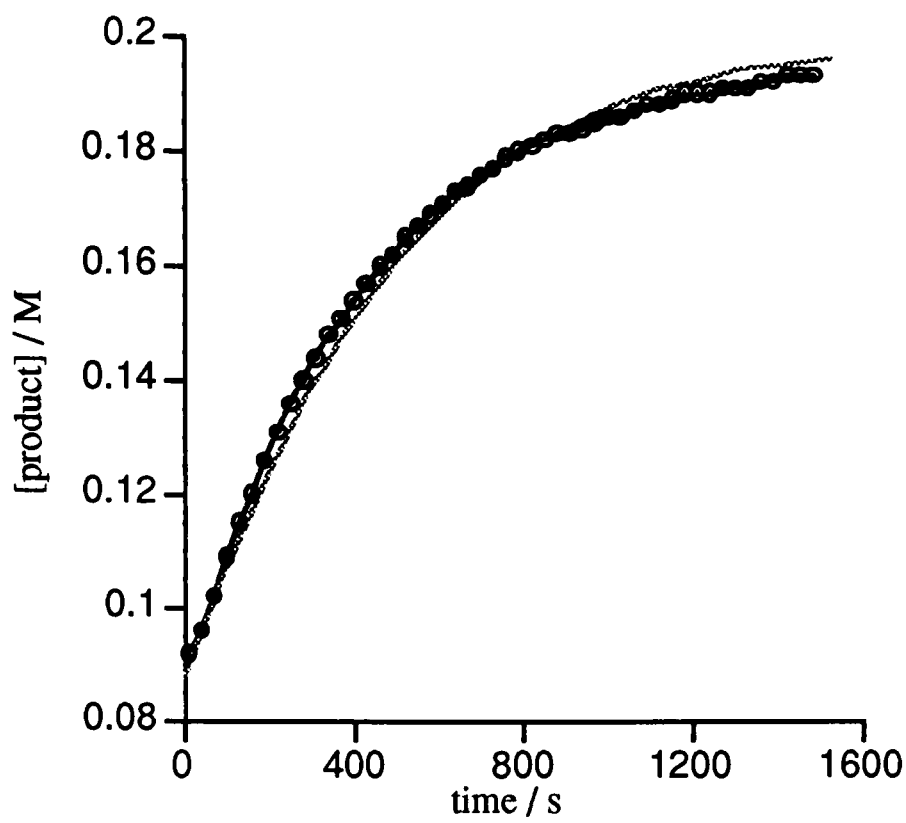
Appendix 2

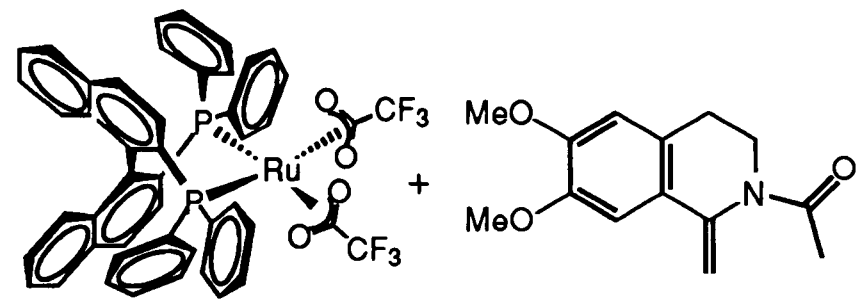

CH3
Ph2
P
Fe
O
Ru
O
CH3
+
Ph
MeO
O
N
H
O
P
Ph2

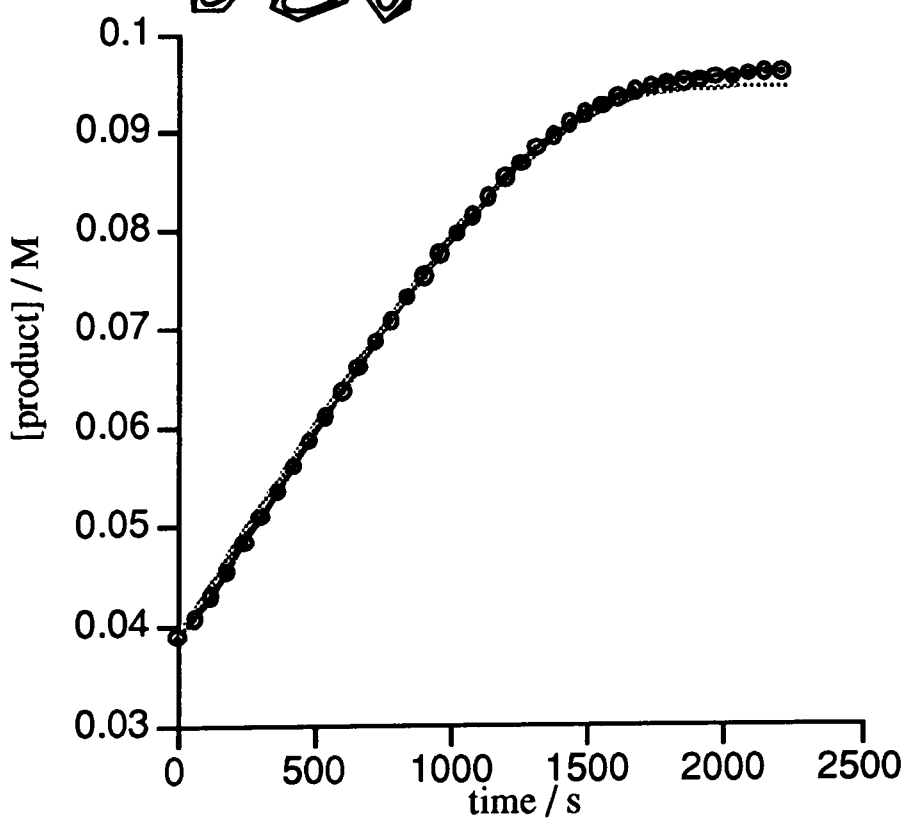

exp
theory
[product] / M
0.1
0.09
0.08
0.07
0.06
0.05
0.04
0
100
200
300
400
time / s

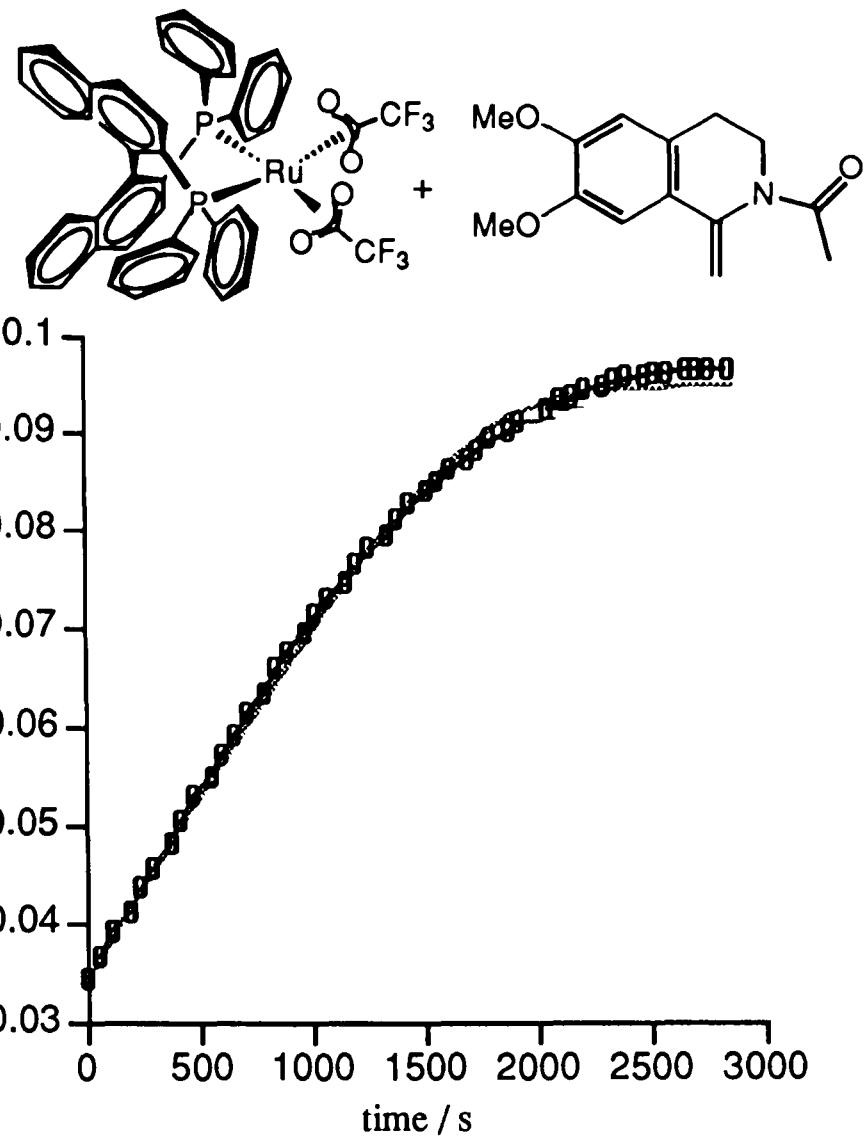

[product] / M
0.1
0.08
0.06
0.04
0.02
0
200
400
600
800
1000
1200
time / s

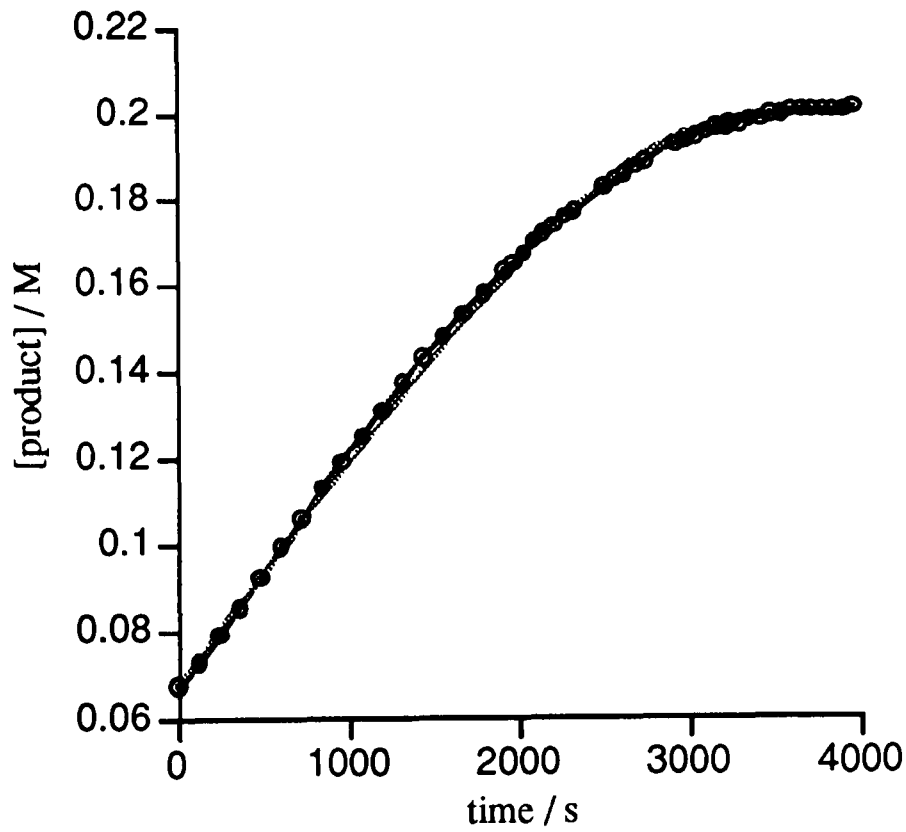

CH3
Ph2
P
Fe
Ru
O
O
CH3
P
Ph2
+
Ph
MeO
O
N
H
O

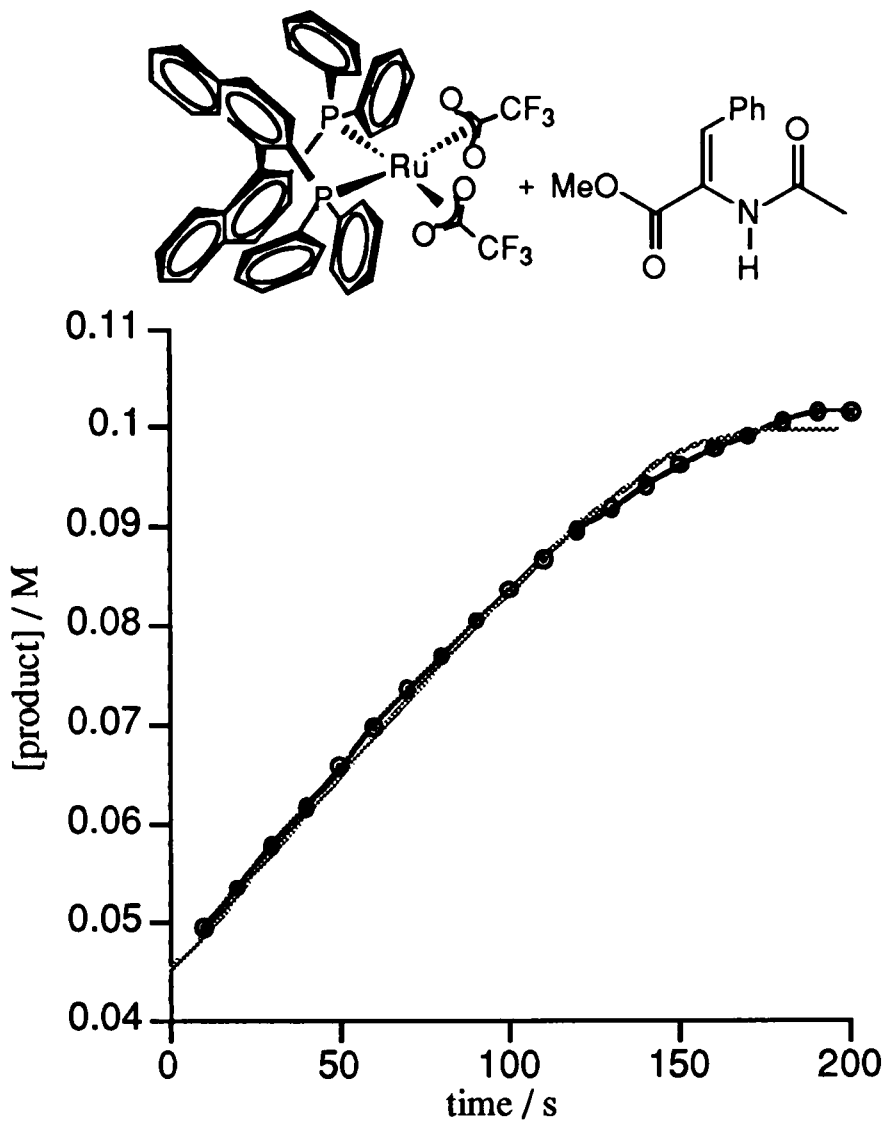

0.2
0.18
0.16
0.14
0.12
0.1
0.08
[product] / M
0
400
800
1200
1600
time / s

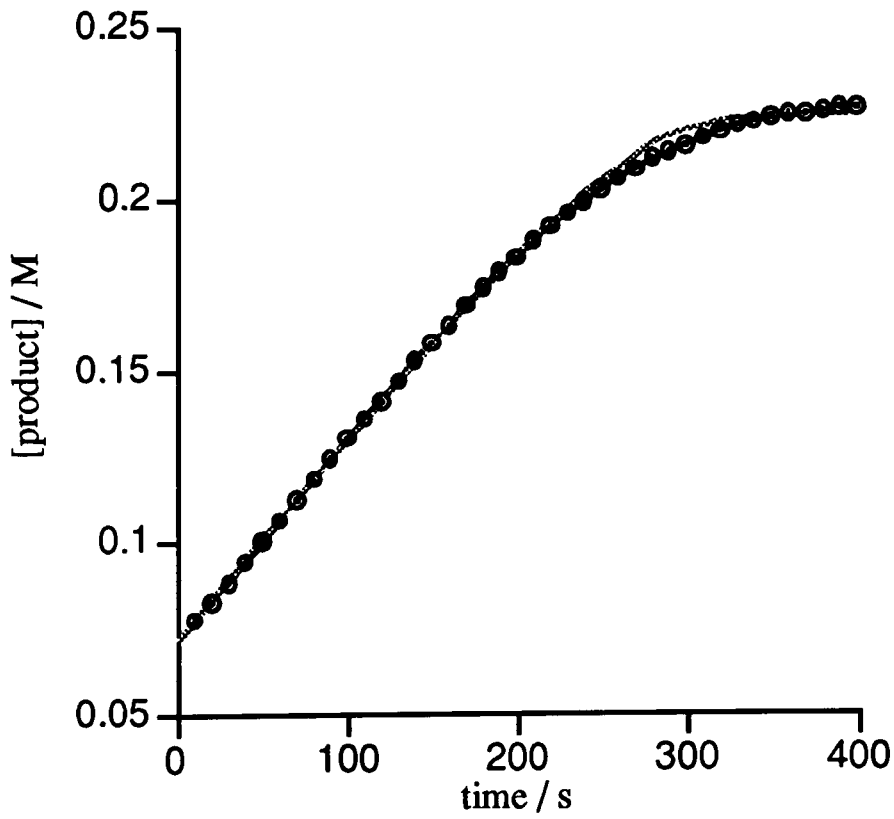

P
Ru
P
O
CF3
O
O
CF3
+
MeO
MeO
N
O

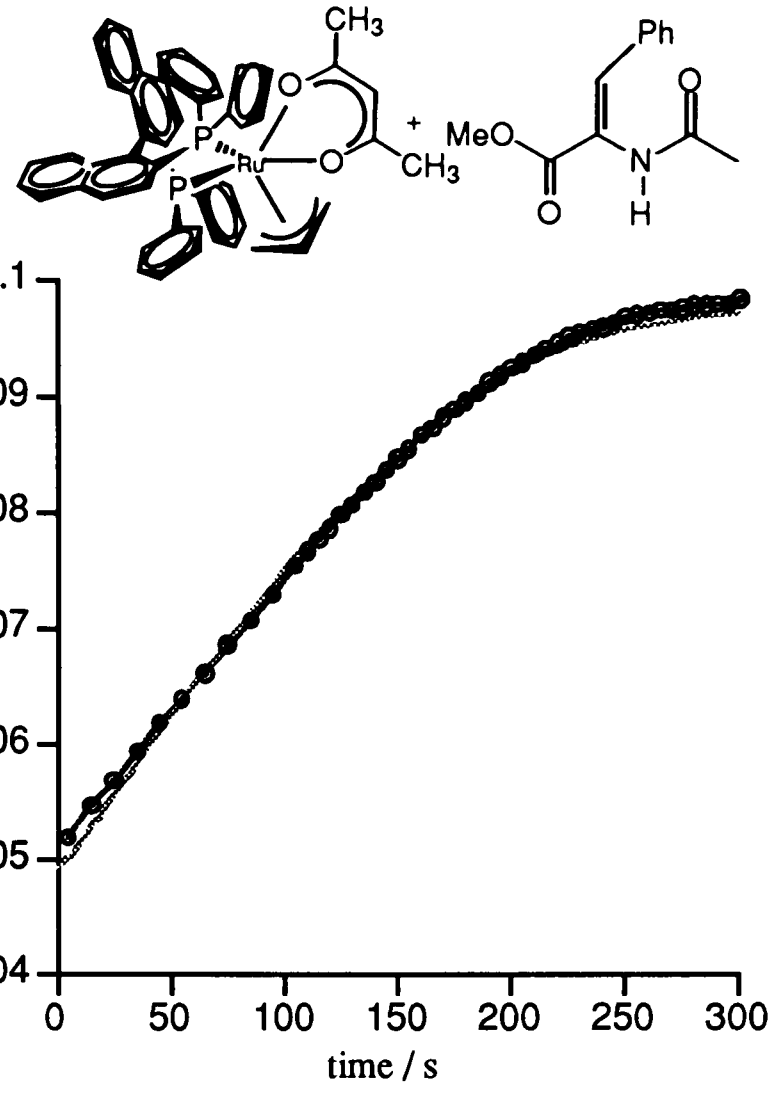

0.1
0.09
0.08
0.07
0.06
0.05
0.04
0.03
[product] / M
0
500
1000
1500
2000
2500
time / s

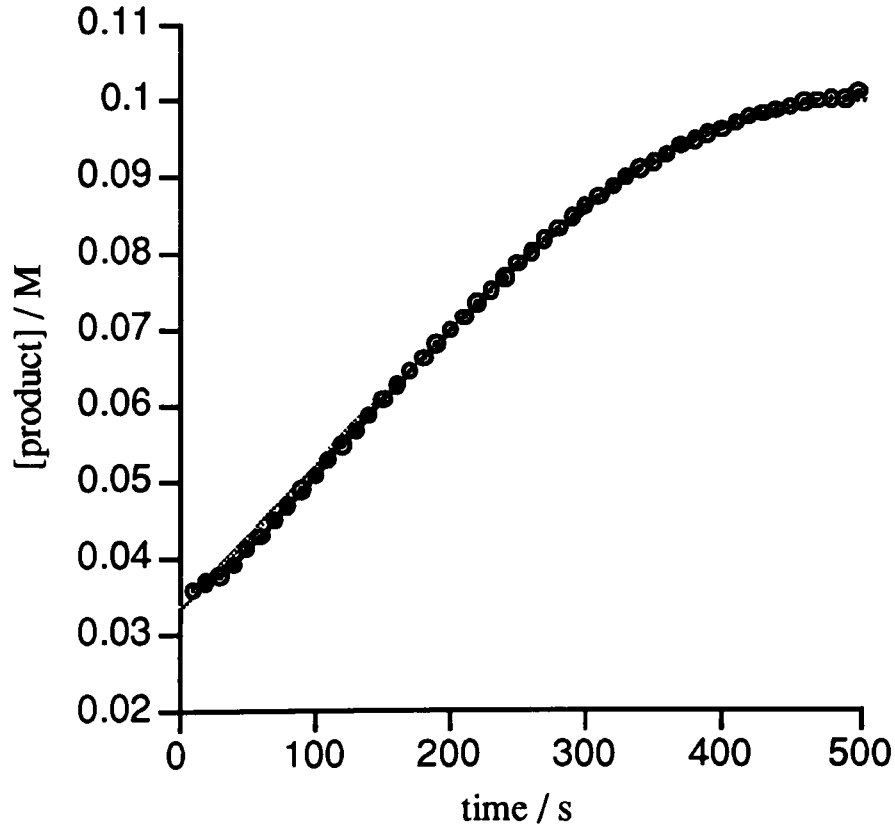

P
Ru
P
O
CF3
O
O
O
CF3
+
MeO
MeO
N
O
0.1
0.09
0.08
0.07
0.06
0.05
0.04
0.03
[product] / M
0
500
1000
1500
2000
2500
3000
time / s


0.22
0.2
0.18
0.16
0.14
0.12
0.1
0.08
0.06
[product] / M
0
1000
2000
3000
4000
time / s


P
Ru
P
O
CF3
O
O
CF3
+ MeO
Ph
O
N
H
O
0.11
0.1
0.09
0.08
0.07
0.06
0.05
0.04
[product] / M
0
50
100
150
200
time / s


0.25
0.2
0.15
0.1
0.05
[product] / M
0
100
200
300
400
time / s


CH3
Ph
O
P
Ru
O
+
MeO
CH3
P
O
N
H
0.1
0.09
0.08
0.07
0.06
0.05
0.04
[product] / M
0
50
100
150
200
250
300
time / s


0.11
0.1
0.09
0.08
0.07
0.06
0.05
0.04
0.03
0.02
[product] / M
0
100
200
300
400
500
time / s